DOCUMENT RESUME

ED 146 694 EA 010 099

AUTHOR Hill, James E.; And Others
TITLE Development of Proposed Standards for Testing Solar Collectors and Thermal Storage Devices. NBS Technical Note 899.
INSTITUTION National Bureau of Standards (DCC), Washington, D.C.
SPONS AGENCY Energy Research and Development Administration, Washington, D.C. Div. of Solar Energy.
REPORT NO NBS-TN-899
PUB DATE Feb 76
NOTE 323p.; Not available in paper copy due to marginal legibility of original document
AVAILABLE FROM Superintendent of Documents, U.S. Government Printing Office, Washington, D.C. 20402 (Stock No. 003-003-01579-2/Catalog No. C13.46:899; $3.10)

EDRS PRICE MF-$0.83 Plus Postage. HC Not Available from EDRS.
DESCRIPTORS Energy Conservation; Evaluation Methods; Graphs; Heating; Heat Recovery; Illustrations; Measurement Instruments; *Performance Specifications; *Solar Radiation; *Standards; *Storage; Technological Advancement; *Thermal Environment.

ABSTRACT

A study has been made at the National Bureau of Standards of the different techniques that are or could be used for testing solar collectors and thermal storage devices that are used in solar heating and cooling systems. This report reviews the various testing methods and outlines a recommended test procedure, including apparatus and instrumentation, for both components. The recommended procedures have been written in the format of a standard of the American Society of Heating, Refrigerating, and Air Conditioning Engineers (ASHRAE) and have been submitted to that organization for consideration. (Author)

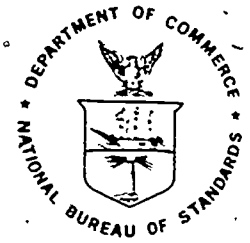


NBS TECHNICAL NOTE 899

U.S. DEPARTMENT OF COMMERCE / National Bureau of Standards

# Development of Proposed Standards for Testing Solar Collectors and Thermal Storage Devices

# NATIONAL BUREAU OF STANDARDS

The National Bureau of Standards[1] was established by an act of Congress March 3, 1901. The Bureau's overall goal is to strengthen and advance the Nation's science and technology and facilitate their effective application for public benefit. To this end, the Bureau conducts research and provides: (1) a basis for the Nation's physical measurement system, (2) scientific and technological services for industry and government, (3) a technical basis for equity in trade, and (4) technical services to promote public safety. The Bureau consists of the Institute for Basic Standards, the Institute for Materials Research, the Institute for Applied Technology, the Institute for Computer Sciences and Technology, and the Office for Information Programs.

**THE INSTITUTE FOR BASIC STANDARDS** provides the central basis within the United States of a complete and consistent system of physical measurement, coordinates that system with measurement systems of other nations, and furnishes essential services leading to accurate and uniform physical measurements throughout the Nation's scientific community, industry, and commerce. The Institute consists of the Office of Measurement Services, the Office of Radiation Measurement and the following Center and divisions:

Applied Mathematics — Electricity — Mechanics — Heat — Optical Physics — Center for Radiation Research: Nuclear Sciences, Applied Radiation — Laboratory Astrophysics[2] — Cryogenics — Electromagnetics — Time and Frequency.

**THE INSTITUTE FOR MATERIALS RESEARCH** conducts materials research leading to improved methods of measurement, standards, and data on the properties of well-characterized materials needed by industry, commerce, educational institutions, and Government; provides advisory and research services to other Government agencies; and develops, produces, and distributes standard reference materials. The Institute consists of the Office of Standard Reference Materials, the Office of Air and Water Measurement, and the following divisions:

Analytical Chemistry — Polymers — Metallurgy — Inorganic Materials — Reactor Radiation — Physical Chemistry.

**THE INSTITUTE FOR APPLIED TECHNOLOGY** provides technical services to promote the use of available technology and to facilitate technological innovation in industry and Government; cooperates with public and private organizations leading to the development of technological standards (including mandatory safety standards), codes and methods of test; and provides technical advice and services to Government agencies upon request. The Institute consists of the following divisions and Centers:

Standards Application and Analysis — Electronic Technology — Center for Consumer Product Technology: Product Systems Analysis, Product Engineering — Center for Building Technology: Structures, Materials, and Life Safety; Building Environment, Technical Evaluation and Application — Center for Fire Research: Fire Science, Fire Safety Engineering.

**THE INSTITUTE FOR COMPUTER SCIENCES AND TECHNOLOGY** conducts research and provides technical services designed to aid Government agencies in improving cost effectiveness in the conduct of their programs through the selection, acquisition, and effective utilization of automatic data processing equipment, and serves as the principal focus within the executive branch for the development of Federal standards for automatic data processing equipment, techniques, and computer languages. The Institute consists of the following divisions:

Computer Services — Systems and Software — Computer Systems Engineering — Information Technology.

**THE OFFICE FOR INFORMATION PROGRAMS** promotes optimum dissemination and accessibility of scientific information generated within NBS and other agencies of the Federal Government; promotes the development of the National Standard Reference Data System and a system of information analysis centers dealing with the broader aspects of the National Measurement System; provides appropriate services to ensure that the NBS staff has optimum accessibility to the scientific information of the world. The Office consists of the following organizational units:

Office of Standard Reference Data — Office of Information Activities — Office of Technical Publications — Library — Office of International Relations — Office of International Standards.

[1] Headquarters and Laboratories at Gaithersburg, Maryland, unless otherwise noted; mailing address Washington, D.C. 20234.
[2] Located at Boulder, Colorado 80302.

# Development of Proposed Standards for Testing Solar Collectors and Thermal Storage Devices

James E. Hill, Elmer R. Streed,
George E. Kelly, Jon C. Geist, and
Tamami Kusuda

Center for Building Technology
Institute for Applied Technology
National Bureau of Standards
Washington, D.C. 20234

Prepared for
The Energy, Research, and Development Administration
Division of Solar Energy, Washington, D.C. 20545

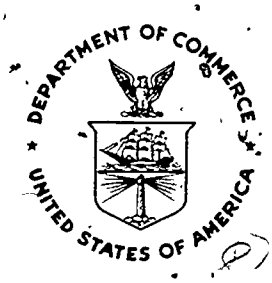


U.S. DEPARTMENT OF COMMERCE, Elliot L. Richardson, *Secretary Designate*
James A. Baker, III, *Under Secretary*
Dr. Betsy Ancker-Johnson, *Assistant Secretary for Science and Technology*
NATIONAL BUREAU OF STANDARDS, Ernest Ambler, *Acting Director*

Issued February 1976

National Bureau of Standards Technical Note 899

Nat. Bur. Stand. (U.S.), Tech. Note 899, 265 pages (Feb. 1976)
CODEN: NBTNAE

For sale by the Superintendent of Documents, U S Government Printing Office
Washington, D C 20402 - Price $3.10
Stock No 003-003-01579-2/Catalog No C13 46.899

## Preface

The use of solar energy for space heating, cooling, and supplying domestic hot water to buildings is receiving serious attention at present due to the mounting public awareness of the shortage of conventional fuels. It is clear that this trend is creating an on-rush of solar components of various designs, all claiming high efficiency and potentially significant fuel savings if used. The purpose of the research program presently underway at the National Bureau of Standards, and whose preliminary results are described in this report, is to develop evaluation and testing methods for solar collectors and thermal storage devices so that the components can be evaluated in a meaningful and consistent way.

In discussing testing procedures, certain commercial components are identified in order to provide a descriptive characterization of their features and resulting performance for a particular test. Inclusion of a given component is this report in no case implies a recommendation or endorsement by the National Bureau of Standards, and the presentation should not be constructed as a certification that any component would provide the indicated performance. Similarly, the omission of a component does not imply that its capabilities are less than those of the included components. The information presented was obtained primarily from the open literature. This report is intended to be informative and instructive and not an evaluation of any commercially available components.

Table of Contents

# Development of Proposed Standards for Testing Solar Collectors and Thermal Storage Devices

James E. Hill, Elmer R. Streed, George E. Kelly, Jon C. Geist, Tamami Kusuda

ABSTRACT

A study has been made at the National Bureau of Standards of the different techniques that are or could be used for testing solar collectors and thermal storage devices that are used in solar heating and cooling systems. This report reviews the various testing methods and outlines a recommended test procedure, including apparatus and instrumentation, for both components. The recommended procedures have been written in the format of a standard of the American Society of Heating, Refrigerating, and Air Conditioning Engineers and have been submitted to that organization for consideration.

Key words: Solar collector; solar energy; solar radiation; standard; standard test; thermal performance; thermal storage.

## 1. Introduction

The use of solar energy for space heating, cooling, and supplying domestic hot water to buildings is receiving serious attention at present due to the mounting public awareness of the shortage of conventional fuels. It is clear that this trend is creating an on-rush of solar components of various designs, all claiming high efficiency and potentially significant fuel savings if used. The purpose of the research program presently underway at the National Bureau of Standards (NBS) and whose preliminary results are described in this report, is to develop evaluation and testing methods for solar collectors and thermal storage devices so that the components can be evaluated in a meaningful and consistent way.

One manufacturer of a solar collector [1] reports that "on a fine sunny day, about 12 gallons of 140° - 160 °F hot water or, alternately, 24 gallons of hot water at approximately 120 °F can be obtained from a single 12 gallon heater unit if the water is used throughout the day". A second manufacturer [2] provides a curve of calculated "annual thermal efficiency" as a function of hot water temperature. A third manufacturer [3] gives curves of "instantaneous efficiency" as a function of solar insolation and temperature difference between water and ambient. The three different performance levels cannot be compared in a meaningful way because they were obtained or calculated under entirely different conditions. A collectors' thermal performance varies depending upon many parameters, such as, operating temperature, liquid flow rate, solar insolation, orientation, tilt, time of day, wind conditions, outdoor temperature, clearness of the local sky, etc.

It is felt that standardized testing and rating procedures in a form similar to those published for fuel-burning heating equipment and for air conditioners and heat pumps are needed. They provide an equitable basis for competition among manufacturers and an essential basis for design and selection of equipment.

In order to fulfill the identified need for standard testing and rating methods, the Thermal Engineering Section, Center for Building Technology of the National Bureau of Standards undertook a project in Fiscal Year 1974 with support from the National Science Foundation [4] to develop such procedures for solar collectors and thermal storage devices. A thorough review was made of all available literature covering methods of analysis and methods of testing these components. In addition, visits were made to a number of facilities doing testing of solar components and systems during the latter half of Fiscal Year 1974. All of the information was then synthesized and recommended test methods for the two components were written. The purpose of the present report is to present the results of this entire effort.

In conducting the project, it was realized that the performance of solar collectors and their associated storage devices depends to some extent on the system in which they are used. However, it was felt that the evaluation process for a total system was impractical due to the large number of ways that solar energy can be applied in buildings. Therefore, the scope of the present program is to develop testing procedures for evaluating solar collectors and thermal storage devices as individual components. As a result of the recently enacted Solar Heating and Cooling Demonstration Act of 1974 [5], NBS is planning to expand the results given herein to develop guidelines for evaluating total solar heating and cooling systems.

The term evaluation can be interpreted in a limited sense or a broad one. For example, it is reasonable to assume that one of the primary factors in determining whether solar heating and cooling will be adopted on a large scale will be an economic one. (At a recent meeting of the International Solar Energy Society, it was proposed that this one be the primary factor [6].) Likewise, the difficulty in procuring, installing, operating, maintaining, and the safety in using the device must also be considered. The investigators of this study feel that these factors are all important. However, rather than attempt to produce an all-encompassing "standard", it was felt most reasonable to limit the present work to the establishment of evaluation procedures based on thermal performance alone. Many of these other factors are addressed in Reference [7] for residential solar heating and cooling systems. These procedures could then be used directly or as a basis for a broader evaluation document at a later time.

---

[a] Figures in brackets indicate literature references on page 50.

Sections 2 and 3 of this report cover a review of both methods of analysis and methods of testing solar collectors and thermal storage devices, respectively, as well as presenting some of the relevant experimental data. In addition, the recommended test procedures are outlined and the full test procedures written in the format of a standard of the American Society of Heating, Refrigerating and Air Conditioning Engineers (ASHRAE) are given in Appendices A and B, respectively.

In compiling the material that was used as the basis of the present work, a thorough search was made of the available literature including the use of published literature reviews in References [8, 9, 10, 11]. In addition, the most up-to-date material on current Australian testing techniques for solar collectors was obtained through the assistance of the late Dr. Ralph G. Nevins of the John B. Pierce Foundation. Mr. Jon Geist of the Optical Radiation Section, NBS assisted in the evaluation of the state-of-the-art in solar radiation instrumentation. His viewpoint of the current status of radiometry and its role in the characterization of solar collectors is given in Appendix C.

The test procedures in Appendices A and B were originally drafted, dated August 10, 1974, and presented to a group of 40 to 50 government, university, and industrial researchers at a specially covened workshop[a]. A list of the participants at this workshop is given in Appendix D. Following the verbal and subsequent written comments of many of these participants, a second draft was prepared and dated November 1, 1974.

In late November 1974, NBS printed copies (in draft form) of a document entitled "Interim Performance Criteria for Solar Heating and Cooling Systems" [7]. This document was written for the Department of Housing and Urban Development (HUD) as part of the Solar Heating and Cooling Demonstration Act of 1974 [5]. The November 1 version of the testing documents were referenced in this larger document. NBS convened a special panel to review the HUD document. The panel in turn reviewed the testing procedures in great detail. The make-up of this panel is also given in Appendix D.

At the end of November 1974, the solar collector test procedure was presented to another workshop in New York[b] that was convened for the public by NSF. At the conclusion of the workshop, a special working group addressed the subject of solar collector testing and made recommendations concerning the NBS test procedure [12]. There was a similar workshop on thermal storage devices held in Charlottesville, Virginia[c]. As with the collector workshop, a special working group made recommendations concerning the NBS proposed test procedure [13].

As a result of the direct feedback from these various sources, third versions of both procedures were prepared. Due to the large demand for these documents, they were published separately [14, 15]. The testing procedures included in Appendices A and B herein are essentially the same as published previously [14, 15].

At the present time, the testing procedures are being considered by recently formed committees of ASHRAE as possible ASHRAE Standards. Members of the NBS team conducting the current research are active on the ASHRAE committees and will supply the latest results from this project, as they become available.

---

[a] NSF/RANN Workshop on the NBS Draft Standards for Testing Solar Collectors and Thermal Energy Storage Devices, Colorado State University, Fort Collins, Colorado, August 23, 1974.

[b] NSF/RANN Workshop on Solar Collectors for Heating and Cooling of Buildings, New York, November 20-23, 1974.

[c] NSF/RANN Workshop on Thermal Storage for Heating and Cooling of Buildings, Charlottesville, Virginia, April 16-18, 1975.

## 2. Solar Collectors

The practical use of solar energy for the heating and cooling of buildings requires the collection of radiant solar energy, conversion to thermal energy, and the transfer of the thermal energy to storage or directly to the component or space utilizing the energy. Because of the distributed nature of incident solar radiation, special collecting surfaces are required to collect and convert this energy in a cost effective manner.

The judgment used by designers and/or consumers in selecting a specific solar collector is usually based on some combination of mathematical analysis, experimental data, cost, and expected reliability/durability. In addition, experimental data is invaluable to the manufacturer for the refinement of collector design to optimize performance as well as for verifying the performance at specific operating conditions.

Testing of collector components may be performed in the laboratory to obtain basic thermophysical property data such as solar absorptance, emittance, and transmittance. Laboratory tests can also be performed on the total collector and used to determine heat loss characteristics under non-irradiating conditions or total thermal performance under irradiating conditions. Solar simulators allowing indoor irradiation tests under controlled ambient conditions are in use. Outdoor irradiation tests allow one to determine thermal performance under in-use conditions.

This section of the report presents a summary of state-of-the-art testing procedures with typical results and describes a recommended test procedure useful for the rating of solar collectors based upon thermal performance. The results of these tests can be used as a reference for procurement, consumer information or even warranty protection.

### 2.1 Typical Collector Design and Characteristics

Collectors can be generally classified as either flat-plate or focusing types. The flat-plate collector is one in which the absorber surface for solar radiation is essentially flat and where the absorber area is equal to the aperture for incident radiation. The focusing collector is one in which the absorber area is smaller than the aperture for incident radiation and consequently there is concentration of energy onto the absorber surface.

Predominant use of the flat-plate collector for space heating and domestic water heating applications is attributed to the relatively low temperatures required (< 65 °C) as well as the reliability of operation without moving parts. However, some of the current research and development is emphasizing cooling applications requiring higher heat transfer fluid temperatures (80-120 °C) and collector designs which include optical concentrating elements. The concentration ratio of collectors used for heating and cooling applications are usually below approximately four or five and the generalized analysis techniques for flat-plate collectors will usually apply to these types of collectors as well.

Another major classification of solar collectors is according to whether they use a liquid or gas as the heat transfer fluid. Water has been the principal fluid for applications in the lower latitudes of the U.S. but as installations in the colder climates become economically feasible, the potential freezing problem may encourage the use of air or other gaseous fluids.

The cross-section of a typical flat-plate liquid-heating solar collector is shown in Figure 1 [16]. The collector consists of an absorber plate with integral flow passages, two covers, thermal insulation and protective pan, and a semi-hermetically sealed edge construction with a metal-edge retaining system. Each 3 mm (1/8 in.) thick cover is made of fully tempered clear float glass. The spectral transmittance of the cover glass is shown in Figure 2 and varies from 90 percent in the 0.4 to 0.6 μm wavelength range to about 80 percent at 1.6 μm. Integration with the air mass 2 spectral distribution[a] gives

[a] Air mass is approximately equal to the secant of the zenith angle ($\theta_z$) of the sun, i.e. i.e. $\theta_z = 0°$ (overhead), air mass = 1.0; $\theta_z = 60°$, air mass = 2.0.

a total solar transmittance of 0.84. The glass emittance for the temperature range of -20° to 70 °C is reported as 0.90. The absorber plate consists of two diffusion-bonded metal sheets containing integral liquid fluid passages. Each end of the plate has a manifold section for connection to the fluid distribution system. The glass covered side of the metal plate is coated with a black paint which has a spectral reflectance of approximately 5 percent throughout the visible and infrared wavelength regions as shown in Figure 3. The equivalent transmission-absorption product as a function of angle of incidence for this type of collector with 1, 2, 3, or 4 cover glasses is shown in Figure 4 [17]. The product is relatively constant for incident angles out to approximately 40°.

The heat transfer coefficient for heat loss out the top of the collector is shown in Figure 5 as a function of average plate temperature [18]. The coefficient for 1, 2, and 3 covers is relatively linear with ambient temperature over the range of -20° to 40 °C as shown. Typical thermal response for this type of collector with 2 glass cover plates and with good thermal insulation is shown in Figure 6 [19].

## 2.2 Methods of Analysis

It has been shown and discussed by a number of investigators [20-26] that the performance of flat-plate collectors operating under steady-state conditions can be adequately described by the following relationship:

$$\frac{q_u}{A} = I\,(\tau\alpha)_e - U_L\,(\bar{t}_p - t_a) \qquad (1)$$

where

$q_u$ = rate of useful energy extraction from the solar collector, W

$A$ = cross-sectional area, $m^2$

$I$ = total solar energy incident upon the plane of the solar collector per unit time per unit area, $W/m^2$

$(\tau\alpha)_e$ = effective transmission-absorptance product for the solar collector

$U_L$ = heat transfer loss coefficient for the solar collector, $W/(m^2 \cdot °C)$

$\bar{t}_p$ = average temperature of the absorber surface of the solar collector, °C

$t_a$ = ambient air temperature, °C

A very similar equation can be used to describe the performance of concentrating collectors [18, 27, and 28]. Equation (1) becomes modified as follows [18]:

$$\frac{q_u}{A_a} = I\,(\tau\alpha)_e\,\rho\,\gamma - U_L\,\frac{A_r}{A_a}\,(\bar{t}_r - t_a) \qquad (2)$$

where

$A_a$ = area of aperture for the concentrating collector, $m^2$

$\rho$ = specular reflectance of the solar collector reflector

$\gamma$ = the fraction of specularly reflected radiation from the reflector which is intercepted by the solar collector absorbing surface

$A_r$ = absorbing or receiving area of the concentrating solar collector, $m^2$

$\bar{t}_r$ = average temperature of the absorber surface of the concentrating solar collector, °C

To assist in obtaining detailed information about the performance of various kinds of solar collectors, it has been convenient to introduce two parameters F' and $F_R$ where

$$F' = \frac{\text{[actual useful energy collected]}}{\text{[useful energy collected if the entire collector surface were at the average fluid temperature]}}$$

and

$$F_R = \frac{\text{[actual useful energy collected]}}{\text{[useful energy collected if the entire collector surface were at the temperature of the fluid entering the collector]}}$$

Introducing these factors into equation (1) results in new performance equations, repectively:

$$\frac{q_u}{A} = F' \left[ I (\tau\alpha)_e - U_L \left( \frac{t_{f,i} + t_{f,e}}{2} - t_a \right) \right] \qquad (3)$$

and

$$\frac{q_u}{A} = F_R \left[ I (\tau\alpha)_e - U_L (t_{f,i} - t_a) \right] \qquad (4)$$

where

$t_{f,e}$ = temperature of the fluid leaving the collector, °C

$t_{f,i}$ = temperature of the fluid entering the collector, °C

If the solar collector efficiency can be defined as

$$\eta = \frac{\text{[actual useful energy collected]}}{\text{[solar energy incident upon or intercepted by the collector]}}$$

or in equation form

$$\eta = \frac{q_u/A}{I} \qquad (5)$$

then the efficiency of the flat-plate collector is given by:

$$\eta = (\tau\alpha)_e - U_L \frac{(\bar{t}_p - t_a)}{I} \qquad (6)$$

or

$$\eta = F' (\tau\alpha)_e - F' U_L \left( \frac{\frac{t_{f,i} + t_{f,e}}{2} - t_a}{I} \right) \qquad (7)$$

or

$$\eta = F_R (\tau\alpha)_e - F_R U_L \frac{(t_{f,i} - t_a)}{I} \qquad (8)$$

Regardless of which form of the efficiency equation is used, equations (6, 7, 8) indicate that if the efficiency is plotted against some appropriate $\frac{\Delta t}{I}$, a straight line will result where the slope is some function of $U_L$ and the y intercept is some function of $(\tau\alpha)_e$. In reality $U_L$ is not a constant but rather a function of the operating temperature of the collector and of the ambient weather conditions as shown in Figure 5. In addition, the product $(\tau\alpha)_e$ varies with incident angle to the collector as shown in Figure 4.

Figures 7, 8, and 9 show typical test results taken from reference [29] for a flat-plate collector using water as the transfer fluid. The tests were run indoors using a solar simulator. The value of using three curves is that the slopes and y intercepts can be used together to determine the values of $F_R$, $F'$, $U_L$, and $(\tau\alpha)_e$. As discussed by Duffie and Beckman [18], solar collector performance for specific operating conditions can be predicted with reasonable accuracy once the values of $F_R$, $U_L$, and $(\tau\alpha)_e$ have been determined.

## 2.3 Methods of Testing and Experimental Data

The literature review of test methods revealed many minor variations of two basic procedures identified, herein as the instantaneous procedure and the calorimetric procedure. Each method or procedure will allow the determination of the fundamental characteristics of a collector such as heat loss coefficient, transmittance-absorptance product and short or long term efficiency. The calorimetric method is limited primarily to those collectors using a liquid as the transfer fluid because the heat capacity of a gas is relatively small and the collected energy cannot be readily stored and determined without transfer to another medium.

When using the instantaneous method, one measures the mass flow rate of the transfer fluid, the difference in fluid temperature between the inlet and outlet and the insolation all simultaneously and under steady-state conditions. The instantaneous efficiency is then determined by

$$\eta = \frac{q_u/A}{I} = \frac{\dot{m} c_{tf} (t_{f,e} - t_{f,i})}{I} \qquad (9)$$

where

$c_{tf}$ = specific heat of the transfer fluid, J/(kg · °C)

In the calorimetric method, one employs a closed system in which the time rate of change of the temperature of a constant thermal mass is measured and related to the incident solar energy by:

$$\eta = \frac{q_u/A}{I} = \frac{\int_0^\tau m c_p \, dt}{I} \qquad (10)$$

where

$m$ = the mass of the media in the calorimeter, kg

$c_p$ = the specific heat of the media in the calorimeter, J/(kg · °C)

$t$ = average temperature of the media in the calorimeter, °C

$\tau$ = time, s

Figure 10 shows conceptually the distinction between these two approaches.

There are advantages and disadvantages to each method. With the instantaneous procedure, one only has to make measurements on or around the collector. The requirement for accurate measurements is more stringent though since $\dot{m}$, $\Delta t$, and I must all be independently measured. In the calorimetric method one only has to measure I and $\frac{dt}{dt}$ of the mass in the system. If the calorimetric method is employed however, a very careful analysis of the calorimeter must be conducted in order to eliminate errors due to temperature gradients inside and to minimize or at least accurately determine the calorimeter thermal losses to the external environment. It is probably more accurate to determine the "instantaneous efficiency" with the instantaneous procedure, whereas the average efficiency over a day is probably more easily determined with a calorimeter. In that latter case, one would not have to determine the rate of temperature change $\frac{dt}{dt}$ of the mass in the calorimeter system, but rather just the temperature change ($\int_{day} dt$) and total of insolation ($\int_{day} I dt$) over the day. In addition, the calorimetric method is primarily limited to those collectors using a liquid as the heat-removal fluid because the heat capacity of a gas is relatively small and the collected energy cannot be readily stored and determined without transfer to another medium.

Some of the specific procedures used in various parts of the world during the past twenty-five years will be briefly described. The procedures will include those for all types of flat-plate or low concentration ratio collectors used for domestic water heating, space heating, or refrigeration applications.

Although solar domestic water heating systems numbering in the thousands were used in Southern California in the 1920's and 30's and in Florida in the 1940's and 1950's, the number of collector manufacturers was small and there is no record of attempts to standardize test procedures. The earliest record of quantitative data related to performance of flat-plate collectors in the United States was published by Brooks in 1936 [30]. Experimental investigation and verification of the theory related to the performance of flat-plate collectors was commenced by Hottel and Woertz [20] at M.I.T. in the 1940's and ultimately resulted in methods for predicting long-term average collector performance [22]. The application of these studies led to the development of a standard test proposed by Whillier and Richards of South Africa [31][a].

South African Procedures

The test apparatus proposed by Whillier and Richards [31], is shown in Figure 11, and employs an overhead liquid reservoir to continuously supply transfer fluid to the collector. The liquid is heated to a constant temperature and flows at a fixed rate while a blower maintains a constant air speed over the collector outer surfaces. Continuous measurements are made of the following parameters:

a) liquid flow rate,
b) total incident insolation in the collector plane,
c) entering liquid and ambient air temperatures, and
d) temperature difference between entering liquid and ambient air and entering and leaving liquid.

Tests are repeated for values of entering liquid temperature covering the collector in-service operating range. From the results of tests at approximately five operating temperatures, the numerical values of $F_R$, $(\tau\alpha)_e$, and $F_R U_L$ can be determined and the efficiency of the absorber can be computed for any practical operating condition.

[a] Austin Whillier had conducted a major part of the basic work done previously at M.I.T.

The following test conditions are suggested for uniformity:

a) Position the collector so that the direct solar radiation incidence angle is within 30° of normal to the collector,
b) Liquid flow rate of 0.02 kg/s per $m^2$ of collector area (14.7 lb/(h · $ft^2$)),
c) Constant air speed over the collector of 2.2 m/s (5 mi/h).
d) The transparent cover of the collector should be cleaned before testing.
e) The collector, if new, should be left outdoors to age in the sun approximately four weeks before testing. The purpose is to allow latent defects in joints, seals, or materials of construction to become evident. Often a deposition of resins or dust occurs on the inner glass surfaces, resulting from distillation from paints or insulation material.
f) The solar radiation measuring instrument should be carefully calibrated and mounted with its sensitive surface parallel to the plane of the collector.
g) The pressure drop across the collector should be measured and presented on a log-log plot of pressure drop versus water flow rate.

Whillier states that the full test of a collector using this procedure would require only about three hours of sunshine at any time of the year.

Subsequent studies by Whillier [32, 33] and Khan [34] have stressed the importance of materials and construction techniques on collector performance. In order to obtain more detailed information about the heat transfer mechanisms occuring, tests were performed (in addition to the outdoor test above) in which basic thermal properties of the cover glass and absorber surface were measured along with indoor tests on the collector as a whole with zero irradiation. This latter test involves pumping hot water through the collector and enables one to directly measure a loss coefficient for the collector. One possible source of error in using this procedure is that the collector surface is radiating to a sink that is at ambient temperature and may not approximate the true sink temperature for a collector radiating to a normal earth-sky environment.

The South Africans have also developed and published a procedure for testing solar water heaters where the collector and the storage tank are connected, the flow occurs by thermosyphon, and the two components are tested together as a single unit [35, 36][a]. It is possible to compare the performance of collector of different designs if one if careful to control such factors as pipe diameters, lengths of pipe, thickness of insulation, height of storage tank, and capacity of storage tank. However, strictly speaking, the efficiencies determined are representative of the solar water heating system as a whole and not just the collector. The testing procedure covers a series of tests occuring over a three-week period in which the efficiency is calculated as the ratio of the total energy content of a measured volume of water drawn off to the total energy incident on the collector surface. The procedure for the three-week testing period is summarized in Table 1. Tests I and II are related to loss and storage characteristics of the system and are not used in determining the average efficiency.

A comparison of the measured average efficiency of 12 water heating systems in which the primary variable studied was collector type is shown in Table 2. Testing was performed throughout the year to establish that the efficiency was independent of seasonal condition. The two most important factors influencing the efficiency results of this particular test program were climatic conditions and the duration of the individual tests. For example, tests on a clear day resulted in efficiencies 29 percent higher than those conducted on a cloudy day for the same collector and water temperature. The use of thermosyphon flow control and storage containers resulted in substantially large efficiency variations are averaged out.

---

[a] Reference [37] also describes a test that was used for testing a thermosyphon-type water heater.

Table 1 Three-Week Performance Testing Program for Solar Water Heaters [36]

| Day | Test | Time (hours) | Nature of test |
|---|---|---|---|
| *1st Week* | | | |
| Monday | I | 0830 | Run off all hot water collected during week-end |
| Tuesday | II | 0830 | Run off all hot water |
| Wednesday | II | 0830 | Run off all hot water |
| | III | 1530 | Run off all hot water |
| Thursday | IV | 1530 | Run off all hot water |
| Friday | IV | 1530 | Run off all hot water |
| *2nd Week* | | | |
| Monday | I | 0830 | Run off all hot water collected during week-end |
| | V (a) | 1400 | Run off 15 litres hot water |
| | | 1530 | Run off all remaining hot water |
| Tuesday | V (b) | 1400 | Run off 15 litres hot water |
| | | 1530 | Run off all remaining hot water |
| Wednesday | V (b) | 1400 | Run off 15 litres hot water |
| | | 1530 | Run off all remaining hot water |
| Thursday | VI | 0900 | Run off 5 litres hot water |
| | | 1100 | Run off 10 litres hot water |
| | | 1400 | Run off 15 litres hot water |
| | | 1530 | Run off all remaining hot water |
| Friday | VI | 0900 | Run off 5 litres hot water |
| | | 1100 | Run off 10 litres hot water |
| | | 1400 | Run off 15 litres hot water |
| | | 1530 | Run off all remaining hot water |
| *3rd Week* | | | |
| Monday | I | 0830 | Run off all hot water collected during week-end |
| | V (a) | 1400 | Run off 15 litres hot water |
| | | 1530 | Run off all remaining hot water |
| Tuesday | VII | 0830, 0930<br>1030, 1130<br>1230, 1430 | Run off 10 litres hot water |
| | | 1530 | Run off all remaining hot water |
| Wednesday | VII | 0830, 0930<br>1030, 1130<br>1230, 1430 | Run off 10 litres hot water |
| | | 1530 | Run off all remaining hot water |
| Thursday | VIII | 0830, 0930<br>1030, 1130<br>1430 | Run off all water above 40°C |
| | | 1530 | Run off all remaining hot water |
| Friday | VIII | 0830, 0930<br>1030, 1130<br>1430 | Run off all water above 40°C |
| | | 1530 | Run off all remaining hot water |

Note: (i) For experimental purposes 'hot' water was defined as water with a temperature of 5°C or more above cold water temperature.

(ii) Quantities of water run off apply to a 70 litre tank, but can be altered proportionately to suit a larger capacity tank.

Table 2 Comparison of Average Efficiencies for Different Solar Collectors[a] [36]

| Type of absorber | Average efficiency (%) |
|---|---|
| B: commercial radiator | 56,4 |
| C: two corrugated galvanized steel sheets | 50,8 |
| D: corrugated galvanized steel sheet on flat galvanized steel sheet | 50,4 |
| E: aluminium tube-in-strip | 57,1 |
| F: galvanized steel pipe framework on copper strips | 54,6 |
| G: low-cost unit, galvanized steel | 55,9 |
| G: low-cost unit, fibre-glass | 55,6 |
| G: asbestos-cement, uninsulated | 34,7 |
| G: asbestos-cement, insulated | 44,0 |
| H: copper tube-in-strip | 49,2 |
| I: two flat steel plates | 48,9 |
| J: black polyethylene piping | 53,5 |

[a] All absorbers were covered with single glazing and insulated on the back.

Israeli Procedures

The heat transfer studies on solar collectors performed by Tabor [38, 39] have resulted in relatively large scale use of flat-plate collectors in Israel. The need to establish an objective test procedure for the determination of the thermal efficiency in terms "comprehensible to scientists, engineers, salesman and customers" was recognized and a standard test code was proposed [40]. The collector properties to be reported are:

a) The total net exposed area (N.E.A.), including only the active absorbed area
b) The area required for installation
c) The weight of the installation per unit N.E.A.
d) The volumetric capacity for:
   (1) absorber
   (2) storage tanks
   (3) piping and containers
e) The maximum safe operating pressure
f) The weather resistance
g) The corrosion resistance for parts in contact with humidity or heated water
h) The quantity of insulating material used per unit N.E.A. and insulating material properties:
   (1) thermal conductivity
   (2) specific heat
   (3) heat capacity
   (4) hygroscopic properties
i) The water treatment requirements (descaling, cleaning, draining, and hygienic contamination)

Additional information to be reported includes:

j) The materials used
   (type, quantity and general dimensions)
k) The thermal efficiency reported as a function of temperature
l) The aerial efficiency: $\eta_a$ . . . . . .
m) The orientation efficiency: $\eta_{or}$ . . . .

The term "aerial efficiency" refers to the ratio of the net exposed area to the total area for regular operation and maintenance of the system such that

$$\eta_a = A_{N.E.A.}/A_{total} \tag{11}$$

The "orientation efficiency" is defined as:

$$\eta_{or} = \cos \psi_m \tag{12}$$

where

$$\psi_m = \frac{1}{\tau} \int_{day} \psi dt \tag{13}$$

and is the mean daily value of the angle between the incoming solar flux and the normal axis to the N.E.A. This value defines the relationship between the N.E.A. and the area of the projection of the N.E.A. For example, the orientation efficiency of a tracking solar collector would be 100 percent.

The actual test procedure for determining the thermal efficiency of the collector is described in reference [41] and is very similar to the procedure proposed by Whillier and Richards [31] (see Figure 11).

In connection with work on solar power units, the Israelis have also developed a quick and simple way of measuring the output and/or efficiency of a collector at a given site of interest [42]. Depending upon whether the collector operates at essentially a constant temperature, for example, when boiling a fluid to drive a turbine - or for heating water on a once-through basis, two different schemes are used.

The apparatus shown in Figure 12 is used with boiling fluids. A fluid having a boiling point approximately that of the design temperature boils in the collector, the vapor emerging is condensed and returns by gravity to the collector. On its way back, the liquid condensate is measured by a tipping-bucket flow meter of the type used in some rain gauges. A mechanical counter indicates the number of times the bucket has filled up. A drop separator is inserted in the vapor pipe to prevent liquid drops from being carried over to the condenser. The apparatus is automatic; no power supply is needed. For daily output totals, it is necessary only to read the counter in the morning and evening; if the variations of yield during the day are required, the time at which the counter clicks over is recorded on a time chart or by an observer. If thermal efficiency is required the insolation must also be measured.

The Israelis built this apparatus for use with a typical collector operating at 100 °C (using water as the transfer fluid). The bucket had a volume of 80 $cm^3$ and the apparatus gave about 40 counts per day with an uncertainity of approximately 2 1/2%.

When the fluid is only being heated and no boiling occurs, the apparatus in Figure 13 is used. Here, it is necessary to control the flow of liquid through the collector, so that, on a once-through basis, the fluid is heated from the inlet temperature to the outlet temperature. A single thermostatic control is used. A sealed bellows, containing a fluid such as acetone (the fluid is chosen to give convenient pressures at the maximum expected test temperature) is inserted in the upper header of the collector and controls the flow of heated liquid from the collector (or a commercial liquid expansion thermostatic valve can be used instead). The fluid cannot return to the system after heating and a reserve tank adequate for one day's operation must be provided. The inlet temperature should be known to a reasonable accuracy and should preferably be constant. The reserve tank should therefore be large, preferably insulated and shaded from the sun.

Recently, Tabor [43] has described a testing procedure aimed at defining the "governing equation of the collector". The "governing equation" that is the basis of the analysis is very similar to equation (3). The unique feature of the proposed procedure is that several collectors (say four) are connected in series and the temperature rise of the transfer fluid is measured across each. Since, at any instant of time, the flow rates and the solar intensity are identical for all the collectors, a number of points on the efficiency-temperature plot are obtained from which the characteristic equation of the collectors is established. Tabor also outlines a procedure for limiting the temperature rise across an individual collector as well as specifying the way to correct the curves to "standard day" conditions.

Australian Procedures

Testing for rating of solar collectors with application for domestic water heating and residential space heating is a major area of study in Australia. The method used currently by the CSIRO (Commonwealth Scientific and Industrial Research Organization) Division of Mechanical Engineering is to determine an equation of the instantaneous efficiency as a function of the radiation level and temperature difference between the mean fluid temperature and the equivalent temperature of the surroundings [44, 45].

The analytical basis used by the Australians in defining the instantaneous collection efficiency is an equation very similar to equation (7):

$$\eta = \eta_0 - \frac{F' U_L (\bar{t}_w - t_e)}{I} \qquad (14)$$

where

$\eta_0$ = local efficiency at the collector inlet when the inlet temperature $t_{f,i}$ is equal to the equivalent temperature $t_e$ (essentially equal to $F'(\tau\alpha)_e$), °C

$\bar{t}_w = \frac{t_{f,i} + t_{f,e}}{2}$ = mean fluid temperature in the collector, °C

$t_e$ = equivalent temperature of the surroundings (essentially equal to $t_a - 3$), °C

Since the loss coefficient $U_o$ (= $F' U_L$) is approximately linearly related to the temperature difference

$$U_o = a + b (\bar{t}_w - t_e) \qquad (15)$$

the efficiency of the collector can be expressed as a second order function of the temperature difference:

$$\eta = \eta_0 - a \frac{\bar{t}_w - t_e}{I} - bI \left( \frac{\bar{t}_w - t_e}{I} \right)^2 \qquad (16)$$

Currently, wind effects are not taken into account because too little is known of the nature and modelling of wind.

The efficiency is determined over a 10 minute period by flowing constant temperature fluid into the collector under test and measuring the solar radiation intensity, mass flow rate of the fluid, inlet and outlet temperatures, sky temperature and wind speed and direction over the test period. The test rig is shown schematically in Figure 14. The collector to be tested is mounted on an orientable stand which considerably extends the period available during which 'steady' radiation conditions can be achieved. In addition, angle of incidence effects are eliminated as the collector is faced directly at the sun for a given test.

The constant temperature water supply can be quickly preset to a desired level and constant flow is assured by using a constant head system. A series of data points are generated by varying $\bar{t}_w$ (and hence $\bar{t}_w - t_e$) at a constant value of I. It is apparent from equation (16) that tests conducted at different values of solar radiation will not give the same value of efficiency for a constant value of $(\bar{t}_w - t_e)/I$, though this is not of consequence at lower values of $(\bar{t}_w - t_e)/I$.

Having measured a series of values of $\eta$ at constant I, a second order fit in $(\bar{t}_w - t_e)$ can be made and the values of $\eta_0$, a and b found. The results of a typical test are shown in Figure 15.

It is apparent that with many collectors, high values of $(\bar{t}_w - t_e)/I$ at high radiation levels expected with an orientable collector will lead to boiling of the water. One method of overcoming this problem is to place an attenuating mesh completely over the collector which reduces the radiation level by about a factor of 2. It is then possible to generate another curve at a lower value of I and take into account the full range of efficiencies experiences in operation from $\eta_0$ to zero.

Because of the difficulty of generating data points with all variables constant except mean fluid temperature, another test facility has been used which combines a number of identical collectors in series similar to what has been described by Tabor [43]. It is possible to generate a greater number of data points in a given time than with the single Fig, but the times available for testing are limited because of the fixed orientation of the collector. The method, together with some initial results, is given in reference [46].

Testing of Plastic-Bag Water Heaters

Solar water heaters using plastic as the container material have been used in Japan [47, 48] and have been studied in the United States with the idea of reducing collector costs. Harris et. al. [49, 50] have applied conventional flat-plate collector theory to obtain semi-empirical correlations for the performance of plastic water heaters. The unique feature of their approach [50] to evaluating the collectors is that the thermal losses (by convection and conduction) are determined separately from the optical losses (due to absorption and reflection in the cover plates), both being determined experimentally. Basically the same test procedure is used in both cases; however, one series of tests is run with the water essentially at ambient temperature so that the losses can all be attributed to absorption and reflection in the covers. These losses are then subtracted from the total losses determined at higher operating temperatures thus resulting in a determination of the thermal losses. A large number of tests are run and statistical methods are used to correlate the performance of the collector with all the important operating variables.

Modified Instantaneous Procedures

Bartera and Davis [51] have reported the testing of a double-glazed flat-plate collector in which the results were analyzed in terms of what are called effective absorptance and effective heat loss coefficients. The effective heat loss coefficient is shown in Figure 16 and was obtained by pumping hot water through the collector at night and measuring the temperature drop and flow rate through the collector. A conventional instantaneous efficiency type test was then run during the day and the results plotted as shown in Figure 17. Lines were drawn to join the points equally distant from noon (equal angle of incidence) and all the lines were drawn with a slope equal to the effective heat loss coefficient previously determined. The intercept of these lines with the efficiency axis gives the effective absorptance for those times. Since one can calculate the corresponding angle of incidence, the curve shown in Figure 19 was drawn. All of this analysis is consistent with the assumed governing equation for the solar collector, one similar to equation (7) where $F'(\tau\alpha)_e$ corresponds to the effective absorptance and $F' U_L$, the effective heat loss coefficient. The results in Figures 17 and 19 can be considered to define the operating characteristics of the collector and should allow one to predict its performance under specified conditions.

Another modification to the use of the instantaneous test procedure it to assume that an equation such as equation (8) adequately describes the performance of the collector once the parameters $(\tau\alpha)_e$, $F_R$, and $U_L$ have been determined. The test results are then simply presented in terms of the deviation from this assumed performance. This was the approach used by Moore, et.al. [52] in a report of the performance of three different flat-plate collector panels where over 300 data points were taken. The average prediction error and standard deviation in prediction error for the 300 points was as follows:

| Panel | Glazings | Average Prediction Error Btu/(h · ft²) | Standard Deviation of Prediction Error Btu/(h · ft²) |
|---|---|---|---|
| 1 | 1 | -1.5 ± 0.6 | 10 |
| 2 | 1 | 4.3 ± 0.6 | 10 |
| 3 | 2 | 6.4 ± 0.7 | 13 |

Data points taken during obvious transient periods were not used in the analysis. In addition, the selection of data from tests performed on cloudless days near solar noon exhibited appreciable less scatter as shown in Figure 19. The diagonal line represents exact correspondence between predicted and measured performance and the horizontal distance of the points from the line is the absolute error in the output. A similar plot is shown in Figure 20 for a 236 $m^2$ (2540 $ft^2$) collector array used on one of the recent NSF-sponsored school heating projects [53].

Collector Testing at the University of Pennsylvania

A considerable amount of work was done in the period 1971-1974 at the University of Pennsylvania's National Center for Energy Management and Power related to the use of solar collectors for supplementary heating in buildings [54]. In addition to developing a sophisticated analytical model for predicting the performance of solar collectors [55], three different test facilities were designed, constructed, and successfully operated for the testing of water-heating flat-plate collectors [56]. All were operated in the conventional way for determining instantaneous efficiency (measurement of $\dot{m}$, $\Delta t$, and I).

One facility [57] consisted of twin 0.3 x 0.3 m (1 x 1 ft) collector mounts which permitted the simultaneous testing of a reference collector and a developmental collector configuration. Thus both absolute and relative performance values for various collector designs were obtained. The standard collector had a double-glazed cover plate with 9.5 mm (3/8 in.) air gap spacings and the absorber was painted with flat-black paint. The second facility [56] was a 1.2 x 2.4 m (4 x 8 ft) vertical rack enabling the testing of a full scale vertical collector facing south. As with the first facility, it was mounted on the roof of a 4-story campus building. The third facility [56] built was for testing 1.2 x 1.2 m (4 x 4 ft) modular collectors with any orientation and tilt and was a completely portable facility.

All three experimental facilities consisted essentially of the collector, a heat transfer water flow loop and the measuring instruments. In the 0.3 x 0.3 m (1 x 1 ft) and 1.2 x 2.4 m (4 x 8 ft) test facilities, the water temperature was maintained constant at the inlet to the absorber plate by means of a system combining an automatic temperature controller and electric heaters, and could arbitrarily be varied (no temperature control existed in the 1.2 x 1.2 m (4 x 4 ft) test facility). The flow was regulated by means of needle valves. The insolation was always measured by a global pyranometer which was located next to the collector and in the same plane.

The 1.2 x 2.4 m (4 x 8 ft) test facility is illustrated in Figure 21. A 0.16 $m^3$ (42 gallon) domestic hot water heater was used as a preheater for the inlet water. Finer control, to within $\pm$ 0.75 °C, was accomplished by subsequently passing the water through a 12 m length of copper tubing immersed in an oil bath. The temperature of the bath was maintained by a temperature-controlled 1 kW heater. The water then passed through a 3.2 x $10^{-5}$ $m^3/s$ (1/2 gpm) capacity pump, the collector, a liquid-to-air heat exchanger, and back to the water heater. The heat exchanger was there to extract heat from the water in order to make closed-loop operation possible. It was forced-air-cooled by a louver-throttled fan.

The 1.2 x 1.2 m (4 x 4 ft) test facility is shown schematically in Figure 22. The flow-loop was closed and designed similarly to that of the second facility described above. It contained, however, no preheaters. The liquid was circulated by a centrifugal pump. Heat was rejected from the loop by a fan-coil unit with its fan speed regulated by a variable autotransformer. An expansion tank fitted with a glass "S" vent was included in the loop to allow for thermal expansion of the liquid.

Nineteen different collectors were tested in the 0.3 x 0.3 m (1 x 1 ft) test apparatus and one each tested and reported for the other two facilities [56, 58, 59]. In addition, separate tests were conducted indoors to determine the heat loss coefficient by circulating hot water through the collector and measuring the energy loss[a].

[a] It should be noted that the heat loss coefficient for the top of the collector as measured inside was as much as a factor of 3 smaller than that indicated from the outdoor tests for several of the collectors. The heat loss coefficient under outside conditions was determined from the slope of the efficiency versus $\Delta t/I$ plot.

A collector in which the absorber was coated with flat-black paint and the cover was two panes of glass was tested on all three facilities. The results for the 0.3 x 0.3 m (1 x 1 ft) collector were adjusted so that the edge loss was comparable to that of the larger collectors. The results for all three collectors are shown in Figure 23. Scaling up the performance of a small collector module and compensating for edge losses appears feasible from this data.

The University of Pennsylvania has also just recently published what is called an "Interim Standard for Solar Collectors" [60]. It is written in the format of an industry standard and in many ways is similar to standard test procedure described herein and included in Appendix A. However, in addition to specifying the testing and rating procedure, other factors such as safety, durability, and the use of materials are addressed.

The technique used to test and rate the collector on thermal performance is the instantaneous procedure where one measures $\dot{m}$, $\Delta t$, and I. The major difference between the procedure being recommended by the University of Pennsylvania and the one included in Appendix A is that the former requires day long testing and the reporting of a daily efficiency whereas the NBS procedure requires only 15 minute integrated efficiency points as will be explained.

Day-Long Testing

The value of determining average daily efficiency of a collector has been recognized by a number of investigators and proposed as the meaningful way to report performance. Either of the two basic test techniques could be used. However, the instantaneous procedure requires the integration of the appropriate energy quantities for the day whereas the calorimetric technique is more directly applicable provided the calorimeter has the capacity of absorbing the energy collected throughout the day.

San Martin [61] calculated instantaneous efficiency from measurements of $\dot{m}$, $\Delta t$, and I taken at 12 minute intervals (instantaneous values, not integrated) for three different collectors over a six-month period. Typical results are shown for one-day in Figure 24. The inlet fluid temperature to the collectors was not controlled and varied between 60 and 70 °C (140 and 160 °F) during the day. The results were also used to compute a daily average efficiency as shown in Figure 24.

Similar results are shown for a commercially available double-glazed collector with a flat-black absorber in Figure 25 [66]. Data was taken every 30 minutes (instantaneous, not integrated) to make the plot. The data from a day-long test such as this can also be used to plot the conventional efficiency versus $\Delta t/I$ (or just $\Delta t$) curve as shown in Figure 26.

Arthur D. Little Solar Calorimeter

The calorimetric technique has been adopted for use by the Arthur D. Little Company as explained in reference [67].

The collector delivers heat to a carefully controlled water chamber in which the rate of heat addition is measured. Heat can be automatically extracted so as to maintain the collection water flow temperature to a nearly fixed value if desired. Sufficient liquid volume is used to insure quasi-steady state collector performance.

The calorimeter is shown in Figure 27 and a schematic of its operation in Figure 28 [68]. For measurements of the collector efficiency, a two channel recorder mounted in the calorimeter housing is used to display the rate of heat addition and the incident solar radiation. The measurement of instantaneous rate of energy delivery is accomplished by a real time differentiator giving the time rate of change of temperature in the liquid storage tank. Automatic control of the heat shield, heat transfer fluid pump, and heat exhaust is also indicated in Figure 28.

For long term testing, the fully automatic operation of the calorimeter can be utilized. By using the automatic removal of heat from the calorimeter chamber to maintain the collector fluid temperature at a preset value, a very accurate accounting of the long term integrated heat delivery of a collector can be made.

Collector Testing at the NASA Lewis Research Center

Perhaps the most comprehensive test program to date for evaluating solar collectors has been undertaken at the NASA Lewis Research Center in Cleveland, Ohio [29, 69-77]. The major portion of the work has been done on an indoor test facility using a solar simulator [69]; however, just recently an outdoor facility has been made operational [73]. The experimental technique being used is the conventional instantaneous approach in which $\dot{m}$, $\Delta t$, and I are independently measured.

A schematic of the indoor facility is shown in Figure 29 and description summarized in Table 3. The simulator is composed of lamps, lenses, and cooling equipment. The lamps are commercially available units consisting of an integral tungsten-halogen lamp and reflector assembly. The reflector has a dichroic coating that absorbs infrared radiation, thereby reducing the infrared content of the reflected radiation. During operation, the lamp voltage is adjusted with two autotransformers, each transformer supplying power to half the lamps. The lenses are commercially available fresnel type.

A useful method of determining how well a solar simulator's spectral distribution matches the sun is to compare how various materials respond when irradiated by the simulator and by the sun. Table 4 provides a comparison of properties, including absorptivity of a selective coating, the transmittance of ordinary window glass, the reflectance of a silicon solar cell, under radiant flux with the spectral distribution of air mass 2 and of the solar simulator. The spectral irradiance from the simulator has been shown to be essentially constant over the range of lamp voltages used during testing (90 to 120 V) [69].

The flow loop for the indoor test facility is shown in Figure 30 and consists of storage and expansion tanks, pump, heater, test collector, and the required piping. The hot fluid storage tank is a commercially available water heater for home use. The tank has two electrical immersion heaters, 500 W each, and has a capacity of 0.3 $m^3$ (80 gallons). The pump is a gear type unit driven by a 187 W (1/4 hp) electric motor through a variable speed drive. A heat exchanger using city water as a coolant is used to control the temperature of the collector coolant fluid at the collector inlet. A 50/50 by weight mixture of ethylene-glycol and water is used in the liquid loop. The specific gravity of the mixture is checked with a precision grade hydrometer. To suppress vapor formation, the entire flow loop is pressurized to approximately $1.03 \times 10^5$ $N/m^2$ (15 psig) by applying a regulated inert gas pressure to the top of the expansion tank.

The collector to be tested is mounted on a support stand that allows rotation about either the horizontal axis or the vertical axis. This permits variation of the incident angle of the radiant energy to simulate both seasonal and daily variations, if desired.

The test procedure that has been used involves mounting the collectors on the test stand and positioning them so that the radiant flux is either normal to or at different angles to the collector. Variation of the incident angle is accomplished by rotating the test stand about the vertical axis. Most of the reported tests have been run at an incident angle of zero degrees and a tilt angle of approximately 60 degrees. Although the flow rate is adjustable as indicated in Table 3, most tests have been run at a value per unit area of 0.014 $kg/(s \cdot m^2)$ (10 $lb/(h \cdot ft^2)$).

Before the simulator is turned on, the collector is given time to achieve thermal equilibrium at the inlet temperature chosen (1 h or more). After thermal equilibrium is established for a given inlet temperature, the simulator is turned on and the desired radiant flux is obtained by adjusting the lamp voltage. After steady-state conditions occur, usually in 10 to 15 minutes, data are recorded. The radiant flux is then readjusted to a second value at the same collector inlet temperature, steady-state conditions obtained, and data again recorded. The collector inlet temperature is then set to another value, and the procedure repeated.

Table 3 NASA Lewis Solar Simulator Summary [29]

Radiation source,

143 Lamps, 300 W each

GE-type ELH, tungsten-halogen Dichroic Coating

12° Total divergence angle

Test area,

1.2 x 1.2 m (4 x 4 ft)

Test condition limits,

Flux; 470 to 1100 $W/m^2$ (150 to 350 Btu /(h · $ft^2$))

Flow: up to 6 x $10^{-5}$ $m^3/s$ (1 gpm)

Inlet temp; 24 to 99°C (75° to 210°F)

Wind; 0 to 4.5 m/s at 24°C (0 to 10 mph at 75°F)

Table 4 Comparison of the NASA Lewis Solar Simulator and Air Mass Characteristics [29]

| Frequency Range of Irradiation | Air-Mass 2 Sunlight | Simulator |
|---|---|---|
| | Energy Output, % | |
| Ultraviolet | 2.7 | 0.3 |
| Visible | 44.4 | 48.3 |
| Infrared | 52.9 | 51.3 |
| Test Item | Thermophysical Performance | |
| Selective Surface Absorptivity | 0.90 | 0.90 |
| Glass Transmission | 0.85 | 0.86 |
| Al Mirror Reflectivity | 0.86 | 0.88 |
| Solar Cell Efficiency, % | 12.6 | 13.4 |

Typical data reported for this facility were previously given in Figures 7, 8, and 9 [29]. The procedure of reporting the data in other publications [70, 71] has been to show the three different plots which require the determination of average absorber plate temperature, inlet fluid temperature, and exit fluid temperature in addition to measurements of $\dot{m}$, $\Delta t$, and I. However, as noted previously, this does enable one to calculate the value of $F_R$, $F'$, $U_L$, and $(\tau\alpha)_e$, thus defining the pertinent performance factors for the collector. In one of the recent publications [29], the summary performance data for fifteen different collectors described in Table 5 was presented as shown in Figure 31.

It should be noted that a similar indoor test facility has been built at the Honeywell Corporation and results have been presented [78-80].

A simplified schematic of the outdoor test facility recently constructed at the Lewis Center is shown in Figure 32 [73]. As in the case of the indoor facility, the liquid in the flow loop is a mixture of 50 percent ethylene-glycol and 50 percent water by weight. A conventional home-hot-water heater (0.3 $m^3$ capacity) is used for storage. The electric heating elements in the storage tank are controlled by a thermostat. The storage tank heaters provide a ready means to raise the temperature of the entire liquid when desired. A centrifugal pump, driven by a 187 W (1/4 hp) electric motor, circulates the liquid. A filter provides continuous filtration of the liquid. A conventional air-liquid heat exchanger, with an on-off fan control, is used to reject energy when desired. A by-pass around the heat exchanger and the associated proportional control valves permit modulation of the liquid temperature at the outlet of the heat exchanger.

The flow through each collector is manually adjusted with a remotely operated valve. The flow rate through the collector by-pass line is controlled to maintain a constant pressure in the collector inlet manifold. Thus, when the flow rate through one collector is varied, the flow through the remaining collectors remains constant with no adjustment of the flow-control valves. The flow rate through each collector is determined with a calibrated turbine-type flowmeter. Auxiliary heaters with electric immersion elements are located at the inlet of each collector. These heaters provide a controlled variation of inlet temperature from collector to collector. The liquid discharge from the collectors is returned to the storage tank. An expansion tank accommodates volume changes of the liquid. The facility includes two identical loops (only one indicated in Figure 32) with the capability of testing ten collectors simultaneously.

Preliminary results from this facility are given in Figure 33 for a collector fabricated at the Lewis Research Center from two copper heat-transfer panels. The panels were sprayed with a nonselective black paint (solar absorptance = 0.97). Two glass covers were placed over the panels and 10 cm (4 in.) of glass fiber insulation beneath. The panels, plumbed in parallel, each measured 0.56 x 1.1 m (22 x 45 in.). The outside dimensions of the collector frame were 1.2 x 1.2 m (48 x 49 in.).

Testing of Air Collectors

The potential corrosion and freezing problems associated with liquid-heating collectors have resulted in interest in collectors which can heat a gas, usually air. Although there have been some excellent analytical treatments of air-heating collectors [81-86], there have been very few experimental studies reported on the determination of air-heater efficiency.

Gupta and Garg [87] investigated the performance of four air-heaters utilizing an apparatus similar to the one described by Whillier and Richards [31]. Efficiencies were calculated from outdoor tests where instantaneous measurements were made of $\dot{m}$, $\Delta t$, and I. Typical results are shown in Figure 34 and 35 for two of the four collectors. The measured efficiency values agreed well with analytical predictions made previously by Close [81]. The scatter in the data evident in Figures 34 and 35, apart from experimental error, was attributed to variations in heat loss coefficient, the factors $F'$ and $F_R$ which in turn resulted from variations in ambient wind speed and sky temperature.

Table 5 Flat-Plate Water-Heating Solar Collector Types Tested-Efficiency Curves Given in Figure 31 [29]

| | Collector Description | Absorber Panel Material |
|---|---|---|
| 1. | Double Glass Cover, Black Painted Absorbing Surface | Copper |
| 2. | Single Glass Cover, CuO Selective Surface on the Absorber | Copper |
| 3. | Single Glass Cover, Aluminum Honeycomb, CuO Selective Surface on the Absorber | Copper |
| 4. | Double Glass Cover, CuO Selective Surface on the Absorber | Copper |
| 5. | Single Glass Cover, Black Nickel Selective Surface on the Absorber | Aluminum |
| 6. | Double Glass Cover, Black Nickel Selective Surface on the Absorber | Aluminum |
| 7. | Double Glass Cover, Black Nickel Selective Surface on the Absorber | Aluminum |
| 8. | Single Tedlar Cover, Black Nickel Selective Surface on the Absorber | Aluminum |
| 9. | Double Tedlar Cover, Black Nickel Selective Surface on the Absorber | Aluminum |
| 10. | Single Glass Cover, Black Painted Absorbing Surface | Aluminum |
| 11. | Single Glass Cover, Honeycomb, Black Painted Absorbing Surface | Aluminum |
| 12. | Double Glass Cover, Honeycomb, Black Painted Absorbing Surface | Aluminum |
| 13. | Double Glass Cover, Black Painted Absorbing Surface | Aluminum |
| 14. | Double Glass Cover, Black Painted Absorbing Surface | Aluminum |
| 15. | Double Glass Cover, Black Painted Absorbing Surface | Steel |

The performance of an overlapped-glass plate air-heater was reported by Selcuk [88] using the experimental apparatus shown in Figure 36. In addition to the instrumentation shown, thermocouples were required in the air outlet stream because of transverse variations. A comparison of measured and calculated efficiencies as well as air outlet temperatures are shown in Figure 37 as a function of air velocity. Analysis at low velocities and accompanying higher absorber temperatures showed that significant natural convection currents occurred which resulted in larger discrepancies between measured and predicted temperatures and efficiencies at these conditions.

Satcunanathan and Deonarine conducted experimental tests on an air heater which employed two passes of air through the collector [89]. The air passed between the glass panes of the two cover collector before passing over or through the metal absorber. Consequently, part of the energy normally lost through the two cover plates was recovered. Air flow rate was measured with a flow nozzle, temperatures with thermocouples, and insolation with a conventional pyranometer. Calculated efficiencies are shown in Figure 38 indicating a clear improvement through the use of the two-pass mode of operation.

Löf, Shaw, and Conk have recently reported efficiency data for a double-glazed air collector with 14 separate air passages having a cross-section of 1.43 x 59.6 cm and a length of 3.65 m each [90]. The collector area normal to the sun was 31.2 $m^2$ and the air flow rate was 0.431 $m^3$ (min · $m^2$). The results of the test are shown in Figure 39 and compared with theoretical predictions for the same air flow rate and also for an air flow rate 75% larger.

## 2.4 Recommended Test Procedure

Based on a review of the state-of-the-art in testing solar collectors as outlined in the previous section, the test procedure in Appendix A is being recommended. The series of tests that comprise the testing procedure is conducted outside under real sun conditions[a] and the results of the tests are displayed in graphical and tabular form.

The test procedure has been written in a format consistent with other standards of the American Society of Heating, Refrigerating and Air Conditioning Engineers. The outline of the Appendix is as follows:

| Section | |
|---|---|
| 1 | Purpose |
| 2 | Scope |
| 3 | Definitions |
| 4 | Classifications |
| 5 | Requirements |
| 6 | Instrumentation |
| 7 | Apparatus and Method of Testing |
| 8 | Test Procedure and Calculations |
| 9 | Data to be Recorded and Test Report |
| 10 | Nomenclature |
| 11 | References |

with the major portion of the document being in Sections 5 through 9.

The test procedure is limited to collectors that can be isolated so that they have effectively one inlet and one outlet. The energy of the fluid entering and leaving the collector can be determined by making appropriate measurements. These quantities are then compared to the energy incident upon the collector (also determined by measurement) in order to calculate the collector efficiency. The fluid can be either a liquid or a gas but not a combination of the two.

---

[a] The testing procedure itself is equally applicable for testing indoors using a solar simulator; however, the present version of the document does not list the requirements for such a facility.

As part of Appendix A, separate apparatuses are specified for when a liquid (Figure A1) or a gas (Figure A2) is to be the transfer fluid. The detailed requirements of the apparatus are given along with specifications for instrumentation to be used in measuring incident solar radiation, temperature, temperature difference, liquid flow rate, air flow rate, pressure, pressure drop, time, and weight. For the specification of instrumentation, emphasis was placed on utilizing existing standards and other manuals of acceptable practice as given in references [5-16] of Appendix A.

The series of tests consist of determining the average efficiency for 15 minute periods (integrating the energy quantities) over a range of temperature differences between the average fluid temperature and the ambient air. The efficiency is then calculated by:

$$\eta = \frac{\int_0^\tau \dot{m}\, c_{tf} (t_{f,i} - t_{f,e})\, d\tau}{\int_0^\tau I\, d\tau} \qquad (17)$$

The flow rate is required to be steady and vary by less than $\pm$ 1.0% for the duration of each test. In addition, the transfer fluid shall have a known specific heat which varies by less than 0.5% over the temperature range of the fluid during a particular 15 minute test period. Consequently, the efficiency can be determined by:

$$\eta = \frac{\dot{m}\, c_{tf} \int_0^\tau (t_{f,i} - t_{f,e})\, d\tau}{\int_0^\tau I\, d\tau} \qquad (18)$$

The test apparatuses specified in Appendix A have been designed so that the temperature of the fluid entering the collector can be controlled to selected values. This feature is used to obtain the data over the temperature range desired. At least sixteen "data points" are required for a complete test series and they must be taken symmetrically with respect to solar noon (to prevent biased results due to possible transient effects).

During each test period, the incident solar radiation must be "quasi-steady" as indicated in Figure A13 (in contrast to days in which cloud cover can cause a time distribution such as shown in Figure A14). Other requirements that must be satisfied for each "data point" are that the 15 minute average insolation be greater than 630 $W/m^2$ (200 $Btu/(h \cdot ft^2)$) and the incident angle between the sun and the outward drawn normal from the collector be less than 45°. In addition, the range of ambient temperatures for the entire test series must be less than 30 °C (54 °F).

The measurements made and the calculated efficiency for each "data point" are reported in tabular form as well as in graphical form as shown in Figures 8, 35, and 39. The ordinate is the efficiency and the abscissa is the measured temperature difference divided by the insolation. It is recommended that the units be standard SI or that the abscissa be made dimensionless by dividing the temperature difference by either 100 °C or 212 °F and the insolation by the solar constant. It is expected that a "straight-line" representation will suffice for most conventional flat-plate collectors such as the one in Figure 1. Representation of the performance of a concentrating collector or high-performance flat-plate collector on such a plot will probably require the use of a "higher order fit" due to the larger variation in $U_L$ and the product $(\tau\alpha)_e$.

In developing the test procedure and writing the specific requirements, there were two main areas of concern. These were insuring that the measurements made would be sufficiently accurate and that the specification of test conditions would be such that the plot of collector efficiency would indeed be meaningful and allow comparison of different collectors.

## Accuracy of Measurements

The uncertainty associated with the reported efficiency can be expressed as a function of the uncertainty associated with the measurement of the independent parameters as follows [91]:

$$\frac{\sigma_\eta}{\eta} = \sqrt{\frac{\sigma_{\dot{m}}^2}{\dot{m}^2} + \frac{\sigma_{c_{t,f}}^2}{c_{t,f}} + \frac{\sigma_{\Delta t}^2}{\Delta t^2} + \frac{\sigma_I^2}{I^2}} \qquad (19)$$

Consequently, the accuracy to which the efficiency can be determined is limited by the accuracy to which the independent variables $\dot{m}$, $c_{t,f}$, $\Delta t$, and I can be measured or determined.

In reviewing the state-of-the-art in making the measurements, it became obvious that the critical measurement was that of insolation. As stated in Appendix C, an accuracy of no better than ± 5% is the state-of-the-art. This is confirmed by Latimer [92] in a recent treatise, on making solar radiation measurements using commercially available pyranometers.

Latimer [92] lists a number of requirements for pyranometers that he feels are necessary in order to make sufficiently accurate measurements. These include:

(1) change of response due to variation in ambient temperature.
(2) variation in spectral response.
(3) nonlinearity of response.
(4) time response.
(5) variation of response with attitude (tilt up or down from the horizontal).
(6) variation of response with angle of incidence.

Specific requirements listed under each of the categories above have been adopted and are given in Section 6.1 of Appendix A.

Reference [92] describes the characteristics of five of the more popularly used pyranometers[a]:

(1) Kipp and Zonen pyranometer
(2) Eppley black and white pyranometer
(3) Eppley (180° pyrheliometer) pyranometer
(4) Eppley precision spectral radiometer (model 2) (now known as model PSP)
(5) Eppley precision spectral radiometer (model 15) (no longer available)

Manufacturers' specifications as well as test results from the Eppley Laboratory and the National Atmospheric Radiation Centre (NARC) in Toronto are given. Figure 40 shows the Eppley (180° pyrheliometer) pyranometer in use at NBS and Figure 41 shows a pyranometer in use at CSIRO that is similar in construction and appearance to both the Kipp and Zonen and Eppley model PSP.

Perhaps the two most critical requirements made with regard to the pyranometers relate to the variation of response with angle of incidence and with attitude. Figure 42 shows results of tests made on the five pyranometers discussed by Latimer. The tests were conducted to determine the deviation of the pyranometers response from a true cosine response as the incident angle is varied. An optical bench, a stable lamp source with collimated beam and an instrument turntable graduated in degrees were used in the tests. The Kipp and Zonen, Eppley 180°, and Eppley model 15 pyranometers were tested at NARC and the Eppley black and white and model 2 at the Eppley Laboratory in Newport, R.I. According to specification 6.1.1.6 in Appendix A, "---the deviation from a true cosine response shall be less than ± 1% for the incident angles encountered during the test(s)". Since the incident angles are limited to ± 45° in the present test procedure, Figure 42 indicates that four of the five pyranometers tested would meet this requirement.

[a] Identification of commercial products does not imply recommendation or endorsement by the National Bureau of Standards.

According to specification 6.I.1.5 in Appendix A, "the instruments' calibration factor (including corrections) shall change less than ± 0.5 percent compared with the calibrated orientation when placed in the orientation used during the test(s)". The concern here is that the calibration factor for the instrument could be different in the horizontal position (normally used for calibration) than in a tilted position (normal position for collector testing). Two choices are available. One could have the instrument calibrated against an absolute normal incidence pyrheliometer (see Appendix C) in the tilted position to be used during the collector testing. The other choice would be to use a pyranometer whose calibration factor is known to be independent (within ± 0.5%) of tilt angle up to the angle used during the collector testing.

Latimer [92] states, based on inversion tests in the laboratory, that the Kipp and Zonen and Eppley model 2 showed less than ± 0.5% change in their factors. However, the Eppley (180° pyrheliometer) pyranometer showed a 3 to 4 percent decrease in response in the inverted position and the newer black and white model showed a 2 percent decrease.

A more comprehensive analysis of this effect has been recently reported by Norris [93]. He constructed the apparatus shown in Figure 43 to test the output of selected pyranometers as a function of inclination angle from the horizontal. The apparatus was designed so that the light source was maintained in a fixed position. The light beam was reflected by a first surface mirror inclined at 45 degrees so that the light was turned about 90 degrees. The pyranometer was attached to the end of a beam which could be rotated about the horizontal axis which contained the mirror and lamp. Thus the pyranometer could be swung through 360 degrees without changing the position of the lamp. An indexing head was placed on the pivot so that reproducible positions of inclination could be obtained. A sliding balance weight was attached to the rotating arm to balance the various types of pyranometers tested.

Norris tested four different instruments three of which had been previously tested by Latimer:

(1) Kipp and Zonen pyranometer
(2) Eppley 180° pyranometer
(3) Eppley model 2 pyranometer
(4) Trickett-Norris (T-N) pyranometer

The Trickett-Norris pyranometer was designed at CSIRO and is shown in Figure 41.

Measurements were made at set angles of 0°, 20°, 40°, 60°, 90°, and 180° from the horizontal. No tests were made with the pyranometers inclined at angles between 90° and 180°, since it is very unlikely that they would be used at this inclination. The pyranometers were maintained in each position for approximately five minutes. In this time the output, as measured by a digital voltmeter, had reached a steady state. Several traverses were made with the pyranometer exposed to an air speed of approximately 5 m/s. This was found to have no effect if the air used was at ambient temperature (20 °C) or at 35 °C.

Results of all tests are summarized in Table 6 and shown in Figure 44. The response or output of each pyranometer has been normalized with respect to its output in the horizontal position. As can be seen, the variation with attitude is significant. In fact, for the use of the instruments in the vertical or inverted position, correction factors based on these test results should probably be applied.

Norris explains in great detail [93] the apparent reasons why the variation with attitude differs for the different instruments. The explanation is based on the difference in construction and the associated free convection patterns that are set up inside the glass envelopes covering the thermopile sensors.

Taking all of the various factors into account, Latimer [92] presents what is felt to be the estimated instrument error for the various pyranometers he analyzed when they have been

Table 6 Response of Inclined Pyranometers Normalized with Respect to the Response in the Horizontal Position [93]

| Angle | Trickett-Norris | Kipp and Zonen // light | Kipp and Zonen ⊥ light | Eppley 180° | Precision Eppley (Model 2) |
|---|---|---|---|---|---|
| 0 | 1.00 | 1.00 | 1.00 | 1.00 | 1.00 |
| 20 | 1.00 | 1.01 | 1.00 | 0.98 | 1.00 |
| 40 | 1.00 | 1.02 | 1.01 | 0.97 | 1.01 |
| 60 | 0.99 | 1.02 | 1.00 | 0.97 | 1.02 |
| 80 | 1.04 | 1.08 | 1.06 | 1.01 | 1.08 |
| 90 | 1.05 | 1.10 | 1.10 | 1.04 | 1.11 |
| 180 | 1.01 | 0.98 | 0.98 | 0.95 | 1.01 |
| No. of Runs | 8 | 4 | 4 | 10 | 4 |

calibrated directly against a primary or a working standard pyrheliometer using the sun as a source and the pyranometers are properly installed and cared for. His results are as follows:

| | |
|---|---|
| Kipp and Zonen | 4.1% (3.6%) |
| Eppley black and white | 3.6% |
| Eppley 180° | 5.0% (3.6%) |
| Eppley Model 2 | 2.3% |
| Eppley Model 15 | 2.3% |

The figures in parentheses can be attained when the readings are corrected for ambient temperature. The Kipp and Zonen and Eppley 180° pyranometers do not have a built-in temperature compensation circuit.

Figure 45 is a plot of the uncertainty in the collector efficiency as a function of the uncertainty in determining the insolation, I, using equation (19). In making the plot, very optimistic assumptions have been made concerning the accuracy to which $\dot{m}$, $c_{t_f}$, and $\Delta t$ can be determined. Even so, if the Eppley model 2 (or comparable) pyranometer were used and $\dot{m}$ and $\Delta t$ could be determined to within $\pm$ 0.2 °F and $\pm$ 0.5% respectively, the collector efficiency determined using the present techniques and instrumentation is probably accurate to no better than $\pm$ 5%.

Effect of Test Conditions on Collector Efficiency Plot

For a given collector design, the test variables that affect the thermal performance of the collector are:

(1) mass flow rate, $\dot{m}$
(2) operating temperature, $(t_{f,i} + t_{f,e})/2$
(3) ambient temperature, $t_a$
(4) wind speed
(5) insolation, I
(6) sky temperature
(7) dirt on the cover plate(s)

In the recommended test procedure, the mass flow rate is specified at a constant value for the test, the wind speed is required to be measured and reported, no specification is made concerning the sky conditions in this first version, and the collector cover(s) are required to be cleaned prior to testing. Limits are placed on the range of insolation and ambient temperature during the test(s).

In order to obtain a basic understanding of how variations in test conditions affect the reported performance of solar collectors, a simplified mathematical analysis was made of the heat transfer processes that occur in and around a conventional flat-plate collector. The basic equation assumed to describe the instantaneous energy balance on the collector is similar to equation (1) of Section 2.2:

$$q_u/A = I\,\tau\alpha - U_L\,(t_p - t_a) \qquad (20)$$

For the analysis here, it was assumed that the collector was well insulated around its perimeter as well as over its shaded side and that the collector loss coefficient could be adequately represented by the calculated loss coefficient through the collector cover plate. The following equation was used for this calculation:

$$\frac{1}{U_L} = \frac{1}{h} + \sum_{i=1}^{N}\left[\left(\frac{\delta_g}{k_g}\right)_i + \frac{0.176}{(h_c + h_r)}\right] \qquad (21)$$

where

$h$ = outside surface heat transfer coefficient of the outermost cover plate, $W/(m^2 \cdot °C)$

$N$ = total number of cover plates in the collector

$(\delta_g)_i$ = thickness of the ith cover plate, m

$(k_g)_i$ = thermal conductivity of the ith cover plate, $W/(m \cdot °C)$

$(h_c)_i$ = convection heat transfer coefficient for the air space inside the ith cover plate (designated here as the ith cavity), $Btu/(h \cdot ft^2 \cdot °F)$

$(h_r)_i$ = radiation heat transfer coefficient across the ith cavity $Btu/(h \cdot ft^2 \cdot °F)$

Since $h_c$ and $h_r$ are both strongly affected by the temperature level as well as by the temperature difference across the cavity space, $U_t$ has not been considered a constant in the present analysis. According to references [94, 95], the value of $h_c$ may be calculated by:

$$h_c = \frac{a}{d} \left((\Delta t)_i \, d^3\right)^n \left[1 - b\left(\frac{t_i + t_{i-1}}{2} - 50\right)\right] \qquad (22)$$

where

$a$ = 0.213 for tilt angles > 45°

$d$ = thickness of the ith cavity, in.

$\Delta t_i = (t_i - t_{i-1})$, °F

$t_i$ = surface temperature of the ith cover plate surface facing the cavity, °F

$t_{i-1}$ = surface temperature of the (i-1)th cover plate surface or absorbing surface facing the cavity, °F

$n$ = 0.27 for tilt angles > 45°

$b$ = 0.001 for $h_c \, d > 0.3$

= 0.0017 for $h_c \, d > 0.3$

The radiation heat transfer coefficient was obtained by:

$$h_r = 0.00686 \left(\frac{T_m}{100}\right)^3 E \qquad (23)$$

where

$$T_m = \frac{T_i + T_{i-1}}{2}$$

$$\frac{1}{E} = \frac{1}{\varepsilon_1} + \frac{1}{\varepsilon_{i-1}} - 1$$

and

$$T_i = t_i + 460$$

$$T_{i-1} = t_{i-1} + 460$$

$\varepsilon_1$ = emissivity of the surface of the ith cover plate facing the cavity

$\varepsilon_{i-1}$ = emissivity of the surface of the (i-1)th cover plate or absorbing surface facing the cavity

Assuming that the efficiency of the collector can be written as:

$$\eta = \frac{q_u/A}{I} = \tau\alpha - U_L \frac{t_p - t_a}{I} \qquad (24)$$

a routine was written to solve equations (20)-(24) simultaneously for specified values of $t_a$, $t_p$, I, and h.

In performing the calculations for typical flat-plate solar collectors, the following values of the appropriate parameters were used:

$\tau = 0.87$

$\alpha = 0.90$

$\varepsilon_{glass} = 0.876$

$\delta_g = 3.175$ mm

$k_g = 1.02$ W/(m$^2$ · °C)

d = 0.375 in.

$\varepsilon_{absorbing\ surface} = 0.90$ for a flat-black surface

$\varepsilon_{absorbing\ surface} = 0.1$ for a selective surface

$h_c = 0$ for an evacuated collector

The exterior surface heat transfer coefficient was determined from information in reference [96] (Figure 1, page 348). Its dependence on wind speed is shown in Figure 46.[a]

Results of the calculations are shown in Figures 47-56. Figure 47 is a plot of the predicted performance of a flat-plate collector of different designs ranging from one with a single cover plate and a flat-black surface to one having a double cover plate with a selective surface on the absorber. All calculations were for conditions of I = 790 W/m$^2$ (250 Btu/h · ft$^2$)) and $t_a$ = 15 °C (59 °F).

Figures 48-52 are for a collector with a single cover plate and a flat-black absorber and are presented to demonstrate the effect of variations in I, $t_a$, $t_p$, and wind velocity on the type of plot being recommended for collector efficiency. Figures 48 and 49 show that for this type of collector, the scatter in the efficiency plot should not be large as long as I and $t_a$ do not vary more than being recommended in Section 5 of Appendix A. Figure 50 shows that significant scatter would result if the data points were taken over the wide range of collector operating temperatures shown. Figure 51 demonstrates that a large

[a] The reader should be cautioned that these values were determined from tests made on 0.3 m (12 in.) square samples of glass at a mean temperature of 7 °C (20 °F).

amount of scatter would also result from large variations in wind velocity. Although some thought was given to specifying that the wind velocity across the collector should be controlled in some manner, the present version of the testing procedure only requires that the wind velocity be measured and reported. Figure 52 demonstrates the degree of scatter that might occur as a result of simultaneous extreme values of I, $t_a$, and wind speed.

Figures 53-56 have been included to show the scatter likely to occur when a high performance flat-plate collector is used in comparison to the more conventional single-cover flat-black collector. As can be seen, for the same variation in I, more scatter is likely to occur with the high performance collector. On the other hand, since the heat loss will be reduced, there should be less scatter due to changes in ambient temperature and wind speed.

Additional Considerations

Although the current test procedure requires that the relative portion of the insolation that is direct and diffuse be measured and reported, there are no allowable limits set for the tests. After further study of the effect this factor could have on the reported efficiency, modification to the test requirements might be made.

The variability of the incident solar radiation in terms of spectral distribution and the ratio of direct to diffuse radiation are illustrated in Figures 57 and 58 [97], respectively. The comparison of measured solar spectral distribution for conditions approximating air mass 1.7 with the calculated distribution for air mass 0, 1, 2, and 3 is shown in Figure 57. The poor correlation at short wavelengths is attributed to atmospheric scattering. Unfortunately, measured spectral variations as a function of azimuth angle, attitude, and atmospheric conditions are not available. The spectral changes in Figure 57 were calculated as a function of air mass using a standard atmospheric model. These variations combined with the spectral properties of selected optical materials shown in Figures 59 [56] and 60 [98] (used to enhance the absorption and/or minimize the emission of thermal energy by the collector) could require modification of the test procedure to include more detailed exposure tests.

An indication of the influence of scattered solar radiation on the performance of a flat-plate collector with two Tedlar[a] covers and a selective black coating on the absorber is shown in Figures 61 and 62 [99]. At normal incidence (Figure 61), 50% diffuse radiation causes a reduction in the efficiency of the collector by about 3% under maximum irradiance conditions and about 6% for minimum irradiance. At an incident angle of 40° (Figure 62), the 50% diffuse radiation condition causes a decrease in efficiency by about 4% at maximum irradiance and 10% at minimum irradiance. These calculations were made assuming idealized conditions of a cosine distribution for the diffuse radiation and a black Lambertian distribution for the absorbing surface.

The results of using the test procedure being proposed for a specific collector should allow a designer to make a realistic assessment of the output of that collector for his particular application. The broad question of how one takes an efficiency curve such as Figure 8 and predicts the performance for other than test conditions will be discussed in the next section. It should be noted here though that additions will likely be made to the test procedure itself to enable the determination of information in addition to collector efficiency as well as efficiency at other than near normal incidence conditions.

Smith and Weiss [100] have suggested that in addition to determining the overall thermal efficiency, determination of the collector design factors $F_R$, $F'(\tau\alpha)_e$, and $U_L$ is desirable. Two collectors under specified conditions may exhibit the same overall efficiency, however, their efficiencies may be achieved in different ways. One collector might have a minimum loss coefficient, $U_L$, and the other might have a minimum collector heat removal factor, $F_R$. Consequently, the two collectors could very well perform differently in specific locations or types of service (i.e., high wind or high operating temperatures).

The modifications suggested by Smith and Weiss are to initially evaluate the effective transmittance-absorptance product and the heat removal factor, which are nearly constant for

[a] Identification of commercial products does not imply recommendation or endorsement by the National Bureau of Standards.

a given collector design. The effective transmittance-absorptance product is experimentally determined from three pyranometer measurements. $F_R$ is subsequently determined by operating the collector with no heat loss, that is, with $(t_{c,R} - t_a)$ equal to zero. Finally, it is possible to determine $U_L$ as a function of wind speed and operating temperatures by operating the collector with zero insolation (i.e., at night). There is thus developed from these tests, a value of $F'(\tau\alpha)_e$ and $F_R$ along with plotted values of $U_L$ as a function of wind speed and operating temperatures.

The determination of collector efficiency at other than near normal incidence conditions could be done in one of two ways. The collector tests could be conducted at several ranges of incident angles and an efficiency curve determined for each range. A second method would be to revert to a day-long test where the variation with incident angle would automatically be accounted for. Of course for simple flat-plate collector geometries, where the absorber is coated with black paint, the performance at off-normal-incidence can already be predicted as will be pointed out in the next section.

In order to demonstrate the importance of angular response and its possible effect on collector efficiency, the directional properties of typical high performance collectors will be cited.

One method of reducing the thermal losses from a collector is the addition of selective absorber coatings as has already been noted. In addition to having spectral selectivity, the properties of the coatings vary with the incident angle as shown in Figures 63 and 64 [98].

The use of a honeycomb structure between the cover plates of flat-plate collectors as shown in Figure 65 has been and is being given serious attention for reducing convective and radiative heat losses [101-111]. The relative transmission of Mylar[a], aluminum, and paper honeycomb material as a function of incident angle is shown in Figure 66 [104]. The significant reduction in transmission of the paper and aluminum materials at angles larger than 15° will certainly effect the day-long performance of a non-oriented collector. Figure 67 [17] shows how the $(\tau\alpha)_e$ product for a flat-plate collector with a black-painted absorber is affected by the addition of the honeycomb material (compared to Figure 4 without it).

Figure 68 shows the results of tests conducted at the NASA Lewis Research Center's indoor test facility where a two-cover-glass collector with a black-painted absorber and Mylar[a] honeycomb was tested at normal incidence and at 41° off-normal-incidence [29]. For this test, the collector stand was rotated about its vertical axis which meant that the tilt angle for the collector was the same in both cases and hence the heat loss should have been the same for both tests. This did result as indicated by the fact that the slope of both "curves" in Figure 68 are the same. There was a nine percent reduction in $(\tau\alpha)_e$ at 41° compared to the normal incidence condition.

Modifications of the hexagonal honeycomb configuration to a rectangular configuration has been extensively analyzed and tested for air and liquid heating collectors by Buchberg et. al. [102]. The experimental results were obtained with 0.3 $m^2$ (1 $ft^2$) instrumented test modules utilizing multiple rectangular cells with specularly reflecting walls coated with a solar transparent dielectric film. For the tests where air was used as the transfer fluid, the cells were located on a blackened fiberglass porous bed absorber. For the liquid heating tests, a black flat-plate absorber was used. The thermal efficiency for three honeycomb configurations is shown in Figure 69. The correlation between a mean curve and data taken at different flow rates had a maximum variation from $\pm$ 5 to $\pm$ 8 percent but exhibited a linear relationship with the rates of temperature difference to solar insolation.

Determining angular response characteristics is equally important for cylindrical collectors. Vincze [112] developed a non-evacuated cylindrical collector shown in Figure 70 that is now commercially available in this country [1]. Speyer built and tested collectors in which the technology for making fluorescent tubes was adapted for building evacuated elements which housed a liquid-heating absorber [113]. Collectors very similar to the ones designed

[a]Identification of commercial products does not imply recommendation or endorsement by the National Bureau of Standards.

by Speyer are being investigated by at least two U.S. manufacturers [114, 115] and by the Philips Company in Aachen [116].

Simon of the NASA Lewis Research Center has recently reported the performance of a first prototype of an evacuated tubular collector obtained from the Owens-Illinois Corporation [75]. It was an all-glass, nonfocusing, nontracking collector. It consisted of twelve 1.05 m (41 1/2 in.) long tubes (length exposed to sunlight) spaced 5 cm (2 in.) apart with a diffuse reflector placed 5 cm (2 in.) in back of the tubes. A flow distribution header for the glass tubes was at the bottom of the collector. The total area available for solar energy collection (essentially the area of back reflector) was 1.33 $m^2$ (14.35 $ft^2$). Each tube of the collector consisted of an inner tube of 4.1 cm diameter placed within an outer tube of 5.1 cm diameter. The inner tube through which the liquid flowed was coated with a selective coating with an absorptance of about 0.8 and an emittance of about 0.09. The annular region between the inner and outer tube was evacuated to a vacuum sufficient to prevent convection and conduction thermal losses. The transmittance of the cover tube relative to the absorber tube cross section was 0.91.[a]

The collector was tested using the Lewis indoor solar simulator. Tests were run at incident angles of 0°, 33°, and 52° and the results are shown in Figure 71. For comparison purposes, the experimental curve for a selective coated, nonevacuated two-glass flat-plate collector is also shown in Figure 71 [29, 76]. The more horizontal slope of the data for the evacuated collector indicates lower heat losses for this collector compared to the non-evacuated two-glass collector. The other point of interest is that in contrast to flat-plate collectors, the efficiency increases with incident angle. This is due to the direct radiation being received by the tubes being independent of incident angle. These efficiency curves emphasize the need for angular response of collectors to be accounted for in the evaluation.

In analyzing the two collectors of Figure 71, a day-long performance comparison would probably be more meaningful. To demonstrate this, Simon used day-long insolation data for a June day in Blue Hill, Massachusetts and calculated day-long performance for an inlet temperature of 116 °C (240 °F) and the tubular collector had a day-long efficiency of 35% compared to only 31% for the flat-plate collector.

In addition to possible modifications to account for the factors discussed above, it is envisioned that the test procedure will also be modified to include a standard procedure for testing collectors operating in the thermosyphon mode, and a specification of an acceptable artificial sun or solar simulator such as the ones used at the NASA Lewis Research Center and the Honeywell Corporation. Other additions will probably include an acceptable alternate method for a comparative test using a "standard collector design" as a reference as well as an experimental procedure for determining the heat capacity of the collector.

The motivation for a comparative test is to simplify the current procedure. One would simply test the collector side by side with a reference collector whose thermal characteristics are well defined. Then by comparing the "output" of the two collectors, one should be able to determine the thermal characteristics of the collector in question.

Even though the relative importance of the transient characteristics of conventional collectors is being debated [117, 118], there is little question about the fact that some standard way of evaluating it would be desirable as part of the proposed test method. In a recent unpublished note [119], Bruno et. al. proposed a technique of obtaining the "response time" of the whole collector assembly. He defines "response time" to be the 10% to 90% rise time found from the results of an indoor laboratory test. Initially the inlet, outlet, and ambient temperatures are identical. Then with a sufficiently high flow rate (such that $(t_{f,i} - t_{f,e}) < 10$ °C as $\tau \to \infty$) the inlet temperature is increased and a plot is made of $(t_{f,i} - t_{f,e}) - (t_{f,i} - t_{f,e})_{\tau \to \infty}$ for $\tau > 0$ and the 10% to 90% rise time noted.

Throughout this report, little or no emphasis has been placed on discussing the applicability of the current test procedure to concentrating collectors. It has already been noted that the governing equations for these collectors are very similar to ones for the conventional

[a] This transmittance takes into account the variation of transmittance with respect to direct radiation about the curved surface of the outer tube.

flat-plate collectors and this similarity has been used in the development of the procedure. One could argue that it is unfair to base efficiency for concentrating collectors on the total insolation (as has been done in Appendix A) since the direct component is all that is normally utilized. However, the test procedure has been written with the particular application of building heating and cooling in mind and comparison to the conventional flat-plate collector is felt to be justifiable. As more information is obtained concerning the use of promising concentrators [120-123] in and around buildings, the test procedure could be modified accordingly.

Kreith [124] has recently suggested some modifications that could be made to make the procedure more applicable for concentrating collectors. The modifications include:

a) Measure the direct component as well as the total incident radiation in the plane of the collector and include two curves like Figure 8, one where the insolation in the horizontal axis variable is the total radiation and one where it is just the direct component.
b) Measure the quality as well as the temperature and pressure of the working fluid so as to allow for a change of phase of the working fluid as it passes through the collector.
c) Measure separately the reflectance of the reflector surface and the absorptance and emittance of the selective surface on the absorber if used.

Using Test Results for Design Purposes

How does one use an efficiency curve such as in Figure 8 to predict the performance of the collector for conditions other than those of the test? This can be done with different degrees of sophistication as will be explained. It is assumed that the output of a given collector is desired over a specified period of time ranging from weeks to a year. There is interest in developing tabular design data using the efficiency plots, actual weather data, and currently available computer programs; however, that has not been done as far as the authors of this report know.

In a recent study on a large commercial office building, Kusuda et. al. [125] used an efficiency plot from reference [58] to predict the hour-by-hour output of a south-facing double-glazed flat-plate collector for an entire year (8760 hours). A semi-empirical routine was written which used input data from an hour-by-hour weather tape and an equation for the efficiency of the collector as a function of $\frac{t_{f,i} + t_{f,e}}{2}$, $t_a$, and I which was derived from the slope and y intercept of the efficiency curve. The $\frac{t_{f,i} + t_{f,e}}{2}$ value was assumed constant depending upon the operational mode of the building's mechanical system and $t_a$ was read directly from the weather tape. The available solar energy impinging on the collector surface was estimated by first calculating the clear or cloudless day solar radiation using a theoretical model [96, 126] and then modifying it by the cloud cover data taken from the weather tape. The cloud cover modification was carried out using the Boeing solar transmissivity data [127].

Although no correction was made for incident angle variation, one refinement was incorporated to adjust the efficiency values for variations in wind speed. Since the outer surface temperature of the upper cover plate was known and reported and the hour-by-hour values of wind speed could be read from the weather type, an hourly calculation was made of the coefficient h for the outer cover (see Figure 46).

Figure 73 was taken from reference [125] and shows the cumulative collected energy for the collector tilted up at an angle of 60° during January and February, 1962. If the average collector energy were estimated on the basis on this 55 day period, the solar heating and cooling system would be sized assuming a daily collection of $4 \times 10^6$ J/m$^2$ (360 Btu/ft$^2$) if the fluid temperature were maintained at 38 °C (100 °F). This figure indicates, however, that if a 60 °C (140 °F) fluid temperature were maintained, the collector could be sized only on the basis of $2.7 \times 10^6$ J/m$^2$ (240 Btu/ft$^2$).

A very similar approach was taken by Proctor of CSIRO [128]. Using the basic equation assumed to describe the collectors tested at CSIRO, and using experimentally determined values of the collector performance factors, the output of a 0.79 $m^2$ single-glazed selectively-surfaced flat-plate collector was predicted on an hour-by-hour basis for an eight-year period. The daily totals were computed and the average daily total for each month of each year determined. The eight-year average daily output for each month was then determined. The average daily output for the eight-year period is shown in Figure 74 as a function of the mean water temperature in the collector.

Simon and Buyco [129] have recently presented a procedure for predicting flat-plate collector performance from the solar simulator test data. The procedure is equally applicable for predicting the performance of flat-plate collectors under specified conditions which are different from those of test conditions. The procedure can be considered to provide a framework for modifying test data. Three correction factors are defined as follows:

$$K_{F_R} = \frac{F_R}{(F_R)_s} \tag{25}$$

$$K_{U_L} = \frac{U_L}{(U_L)_s} \tag{26}$$

$$K_{\alpha\tau} = \frac{\alpha\tau}{(\alpha\tau)_s} \tag{27}$$

where the subscript s refers to the values determined from the solar simulator test results and the variable without the subscript s refer to the values under the new conditions. One then determines the value of the correction factor and in turn the new value of $F_R$, $U_L$, and $\alpha\tau$ which can be used in the performance equation (4).

Simon outlines the procedure for determining the correction factor $K_{F_R}$ when the flow rate, heat loss factor $U_L$, and transfer fluid are different from what was used in the original test(s); $K_{U_L}$ when the ambient temperature, sky conditions, wind speed, tilt angle, and collector operating temperature are different; and $K_{\alpha\tau}$ when the incident angle is different. In addition, a procedure is given for predicting the performance of the collector when the ratio of direct to diffuse solar radiation is different than what was present during the original tests.

## 3. Thermal Storage Devices

Thermal storage devices which are used as components in building solar heating and cooling systems are usually classified as either sensible-heat or latent-heat devices. Sensible-heat devices are those in which the heat absorbed by or removed from the unit results in an increase or decrease in the temperature of the storage medium and there is no change of phase of any portion of the storage medium. Typical components employ pressurized water, unpressurized water, rock, brick, or concrete as the storage medium.

Latent-heat devices are those where a change of phase of the storage medium occurs. In this type, most of the heat added to or removed from the unit goes into changing the enthalpy of the storage medium during a change of phase process. Storage media commonly used in this type of device are inorganic salt hydrates and organic materials.

The choice of the type of thermal storage unit to use is frequently related to the type of collector being used in the heating and cooling system. For example, if a water-heating collector is being used, the storage device is usually a sensible-heat type in the form of one or more water tanks. On the other hand, if an air-heating collector is used, the choice will probably be between a latent-heat type, or a sensible-heat type in the form of a pebble-bed heat exchanger.

The performance of a thermal energy storage device is governed by [18]: (a) its thermal capacity; (b) the temperature range over which it operates, (c) the means of addition or removal of heat and the temperature differences associated therewith; (d) the temperature stratification in the storage unit; (e) the power requirements for addition or removal of heat; (f) the containers or other structural elements associated with the storage system; (g) the thermal losses from the device, and (h) its cost.

As with the solar collector, emphasis has been placed on developing a testing procedure that will allow different components to be evaluated on the basis of thermal performance alone. It is assumed that the results of such tests can and will be coupled with other factors related to cost, structural integrity, etc., prior to the selection of a particular device.

As with solar collectors, thermal storage devices have been treated here as "black boxes" which are characterized by the relationship between their input and output. This is basically the same way they are considered by designers who are selecting the equipment. In addition, attention has only been given to those devices which do not alter the phase or composition of the transfer fluid as it passes through the unit.

There is one significant difference between the solar collector and the thermal storage unit which has influenced the development of the test procedure. The performance of the solar collector is largely determined by its characteristics under steady or "quasi-steady" operating conditions. Consequently, the test outlined in the previous section is conducted under "quasi-steady" conditions. In contrast, the performance of a thermal storage unit is determined largely by its characteristics under transient operating conditions. One storage device compared against a second one whose thermal capacity is identical might be far superior due to the rate at which it can store or give-up energy during typical transient operating conditions.

### 3.1 Methods of Analysis and Testing

The development of analytical models which would aid in predicting the performance of thermal energy storage units has been handicapped by the extreme complexity of the phenomena involved. For example, water tanks involve three-dimensional mixing and systems employing inorganic salt hydrates involve complicated heat transfer, nucleation, crystal growth, and incongruent melting. In addition, the total amount of analytical and experimental work done on thermal storage devices as single components is small in comparison to the attention that has been given to solar collectors.

The most extensive work on water storage tanks has been done in Japan [130, 131, 132] where this type of device has been investigated both theoretically and experimentally. Some recent analytical work has been done in this country on the behavior of water tanks by Phillips and Pate [133, 134] and the behavior of heat-exchanger-type thermal storage units in general (including water tanks) by Yang and Lee [135]. These theories which have been developed are one-dimensional and linear. Thus while they are useful for predicting approximate behavior, they cannot be relied on in lieu of experimental testing.

Phillips and Pate analyzed a simple system consisting of a water tank connected to a water/air heat exchanger. Air is passed through the heat exchanger to deliver as well as withdraw heat from the storage tank. In one case [133] the water moves from the tank to the heat exchanger by natural convection and in the second [134], by forced convection. In both papers, results are presented in terms of dimensionless parameters to allow one to determine the transient response of the storage tank to a specified input at the heat exchanger. Some experimental data is presented which shows very good agreement with the predicted analytical results.

The analytical and experimental work of the Japanese [130, 131, 132] and the recent paper by Yang and Lee [135] will be reviewed in great detail later in this section since the approaches are closely tied with the one used in the testing procedure in Appendix B.

One of the original studies done on pebble-bed energy storage devices was by Löf and Hawley [136] in which relationships were developed for the heat transfer coefficient as a function of fluid flow rate and pebble dimension. More recent analytical work has been presented by Handley and Heggs [137]. A summary of the trade offs between heat transfer and pressure drop that must be made for this type of energy storage device is given by Close [138]. The basic governing equations which can be solved to give the transient response of a pebble-bed energy storage unit are presented by Duffie and Beckman [18].

The most significant experimental data obtained to date for this type of energy storage unit has been for the two cylindrical storage units being used in the house of George Löf in Denver, Colorado. 10,640 kg (23, 500 lb) of rock of a nominal size of 3 cm (1 to 1.5 in.) and having a specific heat of 750 J/(kg · °C)(0.18 Btu/(lb · °F)) are stored in two cylindrical tubes of 0.9 m (3 ft) in diameter and 5.5 m (18 ft) high. Experimental data showing the transient response of these units are given in [139, 140, 18].

The use of latent-heat devices for energy storage has had wide acceptance for some applications such as in the space program where a complete materials handbook has been prepared [141]. However, the use of such materials for energy storage in solar heating and cooling systems has had only limited acceptance because of a variety of operational problems.

Dr. Maria Telkes now of the University of Delaware has pioneered much of the work for this application. In the late 1940's, she was responsible for the construction of a house in Dover, Massachusetts in which energy was stored in the heat of fusion of sodium sulfate decahydrate [142]. Her timely reviews of the status of this form of energy storage were published in 1955 [143], 1964 [144], and most recently in 1974 [145, 146].

The most comprehensive work done to date on this form of energy storage in solar heating and cooling systems has been done over the last four years at the University of Pennsylvania [54, 147-159]. Part of the work has dealt with using latent-heat type materials as integral parts of electric air-conditioning units that are deliberately undersized and run continuously using the thermal storage material to reduce the peak electrical demand. In addition to conducting analysis for typical residential and commercial applications [148, 149, 150 158], two units were built and tested in the laboratory [153, 154]. The other major part of the University of Pennsylvania work has dealt directly with determining the characteristics of typical latent-heat type materials [151, 152, 155, 159] and making a comparison of the cost-effectiveness of using this type of an energy storage unit in a typical solar heating system [156, 157]. Although some experimental work was conducted to determine the properties of the materials and how the thermal capacity of selected ones changed with time, no testing was done on a fully-designed storage unit typical of what might be installed in a working system.

The solar heating and cooling system installed in an experimental house at the University of Delaware [160] uses two thermal storage units in which air is blown through the storage unit. Either unit delivers or removes energy from latent-heat material encapsulated in cylindrical tubes. No operating data has yet been published on the performance of this unit.

Other theoretical studies are available that will enable one to predict the transient behavior of very specific configurations of phase-change materials subjected to specific boundary conditions. Typical examples include a sandwiched plate where the space between the plates are filled with a combination of metal fins and phase-change material [161], and a composite cylinder in which the latent-heat material fills one of the layers [162]. Such examples are usually only beneficial in predicting the performance of a unit of the particular configuration and boundary conditions covered.

Two of the analytical and/or experimental studies mentioned previously will now be described in some detail due to their general applicability in providing a framework for the evaluation of thermal storage units.

## 3.2 Alternatives for a Testing Procedure

The method which has been most commonly employed in testing of water storage tanks in Japan [130, 131, 132] is to cause the transfer fluid entering the storage device to undergo a step change in temperature and to measure the temperature response of the transfer fluid leaving the storage unit. By integrating the difference in temperature between the inlet and outlet over the testing period and multiplying the result by the transfer fluids' mass flow rate and specific heat, one can determine the amount of heat added or removed during this time period.[a] If the time period chosen for the test were some characteristic time depending upon the size of the storage device chosen, the heat storage capability of different devices could be compared. This will be illustrated by citing typical results taken from reference [135].

Yang and Lee [135] performed an analysis to determine the nature of the transient heat transfer between a heat storage unit and a circulating or transfer fluid due to variations in the inlet temperature of the transfer fluid. The configurations chosen for analysis are shown in Figures B7, B8, and B9 of Appendix B. Figure B7 shows a specific-heat type storage device in which a liquid storage medium is heated or cooled by a fluid passing through thin tubes inside the container. Figure B8 shows a pebble-bed type unit in which the transfer fluid comes in direct contact with the storage medium. Figure B9 shows as in Figure B7, a heat-exchanger type storage device except in this case, the transfer fluid is circulated around tubes which encapsulate a latent-heat type material such as a salt hydrate.

The basic one-dimensional transient equations governing the temperature distribution of both the transfer fluid and storage medium are presented and solved using the Laplace transformation technique. Yang and Lee point out that the boundary conditions most appropriate to simulate a real storage device would be some arbitary variation of inlet fluid temperature with time. However, since it is impractical to calculate the system response for energy possible inlet variation and since the storage system is described by linear equations, its dynamic characteristics may be conveniently investigated by using a step input or a sinusoidal input. Solutions are given in [135] for both the step input and the sinusoidal input for the configurations of Figure B7 and B8 but only for the step input for the latent-heat type device.

Typical results are shown in Figures B10 and B11 of Appendix B for the water tank in which water is also circulated through the heat exchanger as the transfer fluid and where the input is a step function. Figure B10 shows the temperature distribution of the transfer fluid as a function of position down the tube and time. Figure B11 shows the same thing for the storage medium or water in the tank. These results were for the case of negligible resistance to heat transfer at the interface between the tubes and the storage medium.

---

[a] This is strictly true only if the losses from the outside of the storage unit are negligible. Otherwise, the losses must be accounted for in the energy balance.

One should note that it has been possible to present the results in dimensionless form where the temperature difference between the fluid and the initial value is divided by the difference between the inlet value and the initial value (step function) to get t*. The space dimension is divided by the total path length through the storage device to get x* and time has been made dimensionless by dividing it by the time required for a fluid particle to travel through the system of length $\ell$, $\ell/u$ where u is the flow velocity. The process of non-dimensionalizing the results has been possible due to the fact that the system behavior is described by linear equations. In reality, the response of storage devices will only approximate a linear behavior. Consequently, the testing procedure being proposed by NBS has been written in such a way as to determine the response of the system to different degrees of step input and for both heat storage and heat removal processes even though the results of the linear theory would indicate that this is unnecessary.

To demonstrate how different storage devices can be compared based on their response to a step function input, the results of reference [135] have been used to plot the curves in Figure B12. The curves are plots of dimensionless temperature difference between the inlet and outlet of a storage tank configured as in Figure B7. Both curves are for the same flow rate of water (transfer fluid) through the storage device. The only difference between the two is that on one hand there is a finite resistance to heat transfer on the outside of pipes ($h_o = 56.7\ W/(m^2 \cdot {}^\circ K)$) typical of natural convection in the tank and on the other, there is negligible resistance ($h_o = \infty$). The area under the curve represents the amount of energy transferred in to or away from the storage unit.[a] As can be seen, the device with the smallest resistance to heat transfer is clearly the more effective one for absorbing or releasing the energy.

Up until this point, emphasis has been placed on discussing the comparison of storage devices based on their response to a step increase in inlet fluid temperature. Other possibilities exist.

A second method that could be employed would be to subject the transfer fluid entering the storage unit to a constant influx of heat, Q. This would result in raising the temperature of the entering transfer fluid (assuming the specific heat of the transfer fluid is constant) by a fixed number of degrees about the outlet temperature. By measuring the time dependent outlet temperature one could obtain information that would be useful in designing collector-storage systems. While this method simulates more closely the real interaction between a collector and a storage device, it has the disadvantage that one cannot measure the energy storage and removal capability of the unit. This is due to the fact that if one measured the heat absorbed by the storage unit over a period of time, it would just be equal to Q times the test period or the amount of energy added to the system. Thus the only way of comparing different storage devices would be to compare plots of outlet temperature versus time for different values of Q chosen so as to take into account the different sizes of the storage units being compared. The storage device with the lowest average outlet temperature would probably be considered best because this would tend to maximize the efficiency of a collector.

A third method would be to use a time varying Q and to measure the outlet temperature as a function of time during the testing period. This would allow one to simulate the output of a collector over one or more days and to determine the response of the storage device. If the time dependence of Q resulted in an oscillating inlet temperature, one would also be able to look at the degree of stratification attained in the storage unit. This method has the same disadvantage as the second in that it would be very difficult to compare the performance of different storage devices. In addition, one has the problem of deciding on what is the typical cycle for Q; not an easy task when one considers that the output of the collector depends not only on the weather but on the particular storage unit employed. The major advantage of this method would be that by inserting an array of thermocouples in the storage medium, the experimenter could measure the temperature stratification in the unit.

---

[a] In this case, it is only a conceptual representation since the product $mc_{t,f}$ has not been included in the ordinate and the $\Delta t$ is dimensionless.

Stratification, which in water tanks results from different temperature water seeking its own density level, is a desirable characteristic for operation in a solar heating and cooling system when the inlet fluid temperature varies up and down with time. If large stratification results when the inlet temperature is either constant or a monotonic (increasing or decreasing) function of time, it is probably a result of short circuiting flow (i.e. dead space in a water tank). This short circuiting of the flow could result in higher fluid temperatures to the collector and thus decreased efficiency, which could easily off-set the advantages of stratification.

### 3.3 Relationship Between the Three Alternative Approaches

The method chosen for the preliminary test procedure outlined herein is based upon the first alternative in which the storage device is subjected to a step change in inlet temperature and the response of the outlet temperature is measured. Some of the advantages of this approach over the other two have been cited above. In addition, the results of this approach are related to and theoretically could be used for predicting the results under the conditions of the other two approaches. Some of the theory of thermal storage in water tanks outlined in references [130, 131, 132] will be summarized to show this relationship.

The basic assumptions in the analysis are:

a) the response of the thermal storage system is a linear function of the change in the inlet temperature, and
b) the mixing process in the tank can be described by a one-dimensional diffusion equation.

Assumption a) leads to the following equation which relates the change in the outlet temperature to the change in the inlet temperature:

$$\theta_{out}(t) = \int_{o}^{t} \omega(t-\tau)\, \theta_{in}(\tau)\, d\tau \qquad (28)$$

where

$$\theta_{in} = \frac{T_{in}(t) - T_o}{\Delta t}$$

$$\theta_{out} = \frac{T_{out}(t) - T_o}{\Delta t}$$

$t$ = time

$T_{in}(t)$ = inlet temperature at time $t$

$T_{out}(t)$ = outlet temperature at time $t$

$T_o$ = initial temperature

$\Delta t$ = step change made in inlet temperature at $t=o$

and $\omega(t)$ is referred to as a superposition function. Solving the one-dimensional diffusion equation

$$\frac{\partial \theta}{\partial \phi} = -\frac{\partial}{\partial x}\left(-E \frac{\partial \theta}{\partial x}\right) + \frac{\partial}{\partial x}(u\theta) \qquad (29)$$

with the appropriate boundary conditions at the inlet and outlet, one obtains for the superposition function,

$$\omega(\phi) = \sum_{n}^{\infty} \frac{2(-1)^{n+1}\mu_n^2 \exp(M)}{(M^2 + 2M + \mu_n^2)} \exp\left\{-\left(\frac{M^2 + \mu^2}{2M}\right)\phi\right\} \quad (30)$$

where

$\phi = t/t_F$

$t_F = \ell/u$

$\ell$ = characteristic dimension of the tank

$u$ = average flow velocity in the tank

$\mu_n$ = $n^{th}$ solution of the equation $\cot\mu = \frac{1}{2}\left(\frac{\mu}{M} - \frac{M}{\mu}\right)$

$M = \frac{u\ell}{2E}$ = mixing parameter

$E$ = diffusion coefficient

The indicial response of the outlet temperature, $\beta(\phi)$, to a unit step rise in inlet temperature is from equations (28) and (30),

$$\beta(\phi) = \int_0^{\phi} \omega(\phi-\tau)\, d\tau = \int_0^{\phi} \omega(\tau)\, d\tau =$$

$$1 - \sum_{n=1}^{\infty} \frac{4(-1)^n M \mu_n^2 \exp(M)}{(M^2 + 2M + \mu_n^2)(M^2 + \mu_n^2)} \exp\left\{-\left(\frac{M^2 + \mu_n^2}{2M}\right)\right\}\phi \quad (31)$$

If equation (31) is used to plot $1-\beta(\phi)$ as a function of $\phi$, one obtains the results shown in Figure 75. The curve obtained when $M = \infty$ ($E=0$) corresponds to the case of perfect piston flow (slug flow) in which there is no mixing in the tank. There is no response in the outlet temperature until the fill time is reached ($\phi = 1$), after which the outlet temperature becomes the same as the inlet temperature. When $M = 0$ ($E=\infty$) there is instantaneous mixing of the inlet water with the rest of the water in the tank and this is referred to as the perfect mixing case. Other values of M between 0 and $\infty$ result in outlet temperature response curves which lie between the piston flow curve and the perfect mixing curve. As in the analysis presented by Yang and Lee [135], the independent time variable here is a dimensionless quantity where time has been divided by the characteristic time $\ell/u$.

Looking only at the leading terms in equation (31), one finds that

$$\beta(\phi) \approx 1 - \exp\left[-a(\phi-\phi_o)\right] E(\phi-\phi_o) \quad (32)$$

where

$$a = \frac{M^2 + \mu_1^2}{2M}$$

$$\phi_o = \left(\frac{2M}{M^2 + \mu_1^2}\right) \ln \left\{ \frac{4M\mu_1^2 \exp(M)}{(M^2 + 2M + \mu_1^2)(M^2 + \mu_1^2)} \right\}$$

$$E(\phi) = \begin{matrix} 0 & \phi < o \\ 1 & \phi \geq o \end{matrix}$$

Taking the natural log of both sides of (32) results in the equation

$$\ln [1-\beta(\phi)] = a\,(\phi-\phi_o)\,E(\phi-\phi_o) \qquad (33)$$

Thus if the experimental results for $1-\beta(\phi)$ are plotted on semi-logarithmic paper, it becomes a simple matter to determine the values of a and $\phi_o$.

The results in equations (31) and (32) may be generalized to take into account the effect of short circuit flow and dead space in the water tank by introducing the parameters

$P = V'/V$ = effective volumetric ratio

$F = \dot{m}'/\dot{m}$ = effective flow rate ratio

and replacing $\beta(\mu)$ by

$$q\,\beta\left(\frac{F}{P}\,\phi\right)$$

where $(V-V')$ is the dead space in the tank

and $(\dot{m}-\dot{m}')$ is the flow rate which is short circuited

Once the indicial response $\beta(\phi)$ has been found by the use of equations (31) and (32) or (33), it is a simple matter to determine the response to an arbitrary inlet temperature $\theta_{in}(\phi)$. Since $\beta(0) = 0$, equation (31) gives

$$\frac{\partial\beta(\phi)}{\partial\phi} = \omega(\phi) \qquad (34)$$

and thus

$$\theta_{out}(\phi) = \int_o^\phi \beta'(\phi-\tau)\;\theta_{in}(\tau)\,d\tau \qquad (35)$$

follow from equation (28).

Methods two and three discussed previously as alternatives for the testing procedure are related in this theory to the indicial response method. This can be seen by examining the problem illustrated in Figure 76 in which the storage unit is subjected to a variable influx of heat $\dot{Q}(\phi)$. Since the inlet temperature is just

$$\theta_{out}(\phi) + \Delta(\phi)$$

and where

$$\Delta(\phi) = \frac{\dot{Q}(\phi)}{\dot{m}\,c_{p,f}}$$

is the temperature rise in the transfer fluid as a result of adding heat at the rate $\dot{Q}(\phi)$ and $c_{tf}$ is the specific heat of water, one finds that $\theta_{out}(\phi)$ is related to the superposition function by

$$\theta_{out}(\phi) = \int_0^{\phi} \omega(\phi-\tau)\,[\theta_{out}(\tau) + \Delta(\tau)]\,d\tau \qquad (36)$$

The Laplace transform of equation (36) gives

$$\theta_{out}(s) = \frac{\omega(s)}{1-\omega(s)}\,\Delta(s) \qquad (37)$$

where $\theta_{out}(s)$, $\omega(s)$ and $\Delta(s)$ are the Laplace tranforms of $\theta_{out}(\phi)$, $\omega(\phi)$, and $\Delta(\tau)$, respectively. The indicial response, $A(\phi)$, to a step change in $\Delta$ is then related to the Laplace transform of the superposition function by

$$A(s) = \frac{\omega(s)}{1-\omega(s)}\,\frac{1}{s} \qquad (38)$$

where $A(s)$ is the Laplace transform of $A(\phi)$. Figure 77 shows how $A(\phi)$ varies with $\phi$ for different values of the parameter M. The response of the outlet temperature to an arbitrary heat flux $\dot{Q}(t)$ can then be predicted using the equation

$$\dot{Q}_{out}(\phi) = \int_0^{\phi} A'(\phi-\tau)\,\frac{\dot{Q}(\tau)}{\dot{m}\,c_{tf}}\,d\tau \qquad (39)$$

Thus by finding the indicial response $\beta(\phi)$ to a step change in the inlet temperature, one may determine the superposition funetion $\omega(\phi)$. If this is done experimentally, one could force fit the data to a plot similar to Figure 75 which would allow a water storage tank to be described by a single mixing parameter M. A low value of M for a storage tank would indicate that the tank was close to having piston flow and thus had a better storage capability than a tank having a larger value of M. Once the superposition function $\omega(\phi)$ was determined, theoretically one could predict the response of the outlet temperature to an arbitrary inlet temperature $\theta_{in}(\phi)$ or to an arbitrary heat influx $\dot{Q}(\phi)$.

The problem with this procedure is that the theory outlined above is one-dimensional and linear. Storage devices and particularly water tanks are three-dimensional and are probably not completely linear. For example, it is not unreasonable to expect that a given device would respond differently to a step rise in inlet temperature than to a step decrease in inlet temperature. In addition for water tanks, when there is short circuit flow or dead space present, one would have to be able to measure the parameters R and F in order to obtain a unique value of M. Clearly this is an impossibility.

## 3.4 Recommended Test Procedure

The testing procedure that is being proposed for thermal storage devices is given in Appendix B. As with the collector test procedure, it has been written in a format consistent with other standards of the American Society of Heating, Refrigerating, and Air Conditioning Engineers.

The test procedure is limited to thermal storage devices that can be isolated so that they have effectively one inlet and one outlet. The energy of the fluid entering and leaving the thermal storage unit can be determined by making appropriate measurements. These quantities are then compared in order to calculate the amount of energy stored or retrieved during a particular test. The fluid can be either a liquid or a gas but not a combination of the two.

The stipulation of testing a thermal storage device which has effectively only one inlet and one outlet is not overly restrictive, particularly for a pebble-bed storage unit, since they usually operate in this manner. When fed with hot air from the collector, it is blown through the device in one direction; when heat is to be extracted, the air from the building distribution system is usually blown through it in the opposite direction.

However, the situation is different for other types of units such as water tanks with embedded heat exchangers. The transfer fluid from the collector is fed into and out of the unit using one set of inlet and outlet portals when storing energy. Another set is used for extracting the storage fluid and hence withdrawing energy for use in the building heating and cooling system. It is understood that in testing this latter type of device, the appropriate single inlet and single outlet should be used in the respective tests of energy storage and energy retrieval. When there is doubt about the ultimate use of the device or it has been specifically designed to be used in several different ways, all combinations of a single inlet and single outlet should be tested.

The procedure as written in Appendix B specifies the apparatus to be used when a liquid (Figure B5) or air (Figure B1) is the transfer fluid. The detailed requirements of the apparatus are given along with specification for instrumentation to be used in measuring temperature, temperature difference, liquid flow rate, air flow rate, pressure, pressure drop, time, and mass. For the specification of instrumentation, emphasis was placed on utilizing existing standards and other manuals of acceptable practice as given in references [1-10] of Appendix B. The nature of the apparatuses and test procedure makes the tests most feasible for storage units having thermal capacities on the order of $10^9$ J ($10^6$ Btu) or less.

The series of tests that are to be conducted are as follows:

1. One test to determine a heat loss factor for the storage units,
2. A series of four tests to determine the response characteristics of the device to a step increase in the entering fluid temperature (energy addition), and
3. A series of four tests to determine the response characteristics of the device to a step decrease in the entering fluid temperature (energy withdrawal).

The heat loss test consists of passing the transfer fluid through the storage unit with an inlet fluid temperature of 25 °C (45 °F) above the ambient air temperature and after steady-state conditions have been reached, measuring the average temperature difference between the inlet and outlet fluid temperature over a one hour period. The rate of heat loss is then determined by

$$L = \frac{\dot{m} c_{tf} \overline{(t_{in} - t_{out})}}{25\ ^\circ C} \qquad (40)$$

in W/°C

To test the transient response of the storage unit, the method of measuring the response of outlet temperature to a step change in inlet temperature, was chosen as a basis for the test. This method was selected because:

(a) it permits the determination of effective storage capacity and thus allows an easy comparison of different types of storage units,
(b) it appears to be the most fundamental approach since linear theory shows that the outlet temperature response to a constant or variable heat flux Q can be predicted if one knows how the outlet temperature changes with a step change in inlet temperature, and,
(c) it is felt that the relative performance of storage devices using this method will be the same if either of the other procedures were used.

Prior to discussing the test procedure for determining the transient response of the unit, the concept of a characteristic time, here called the fill time $\tau_F$, will be introduced. Recall that in the analysis of Yang and Lee [135], it was possible to present the response characteristics of the thermal storage unit in terms of a dimensionless time where real time is divided by some characteristic time $\ell/u$, the effective path length of the transfer fluid divided by the effective transfer fluid velocity. This allows a convenient way of comparing storage units of the same basic design but of different sizes. However, if one is going to compare two storage units of entirely different designs, then comparing the response of the two over the same period $\ell/u$ might be unfair. Consequently, a different time scale is introduced herein that will allow storage units of entirely different designs to be compared on an equitable basis.

If a storage unit has a specified thermal capacity or storage capacity SC, and a transfer fluid of specific heat $c_{t,f}$ is flowing through the device at a constant flow rate $\dot{m}$ and has an inlet temperature $\Delta t$ above the initial temperature of the storage device, then the fill time is defined by

$$\tau_F = \frac{SC}{\dot{m}\, c_{t,f}}\,\Delta t \qquad (41)$$

In the testing procedure, all storage units are tested for the same fill time and then the thermal responses compared. In other words, if two different sensible-heat devices had the same storage capacity and were being tested over the same $\Delta t$ but one used water (water tank) and the other air (pebble-bed type) as the transfer fluid, and the flow rates were such that the fluid dwell times (determined by $\ell/u$) were identical, it would be unfair to compare the response of the two units over the same real time period. One would be able to charge the water tank with considerably more energy over the same time period (approximately by the ratio of $((\dot{m}\, c_{t,f})_{water})/(\dot{m}\, c_{t,f})_{air}$). The recommendation here would be to test the two units for the same fill time as defined by equation (41). Consequently, the flow rates would be adjusted so that $((\dot{m}\, c_{t,f})_{water})/(\dot{m}\, c_{t,f})_{air}) = 1$. In other words, the flow rates for the different units are adjusted so that the amount of energy entering the device (or leaving for an energy removal test) per unit thermal storage capacity is identical for the two devices.[a]

The fill time $\tau_F$ and the flow rate of the transfer fluid $\dot{m}$ are related in an inverse manner according to equation (41). One possibility for specifying the test conditions of the transient tests would be to specify the $\Delta t$ to be used, allow the experimenter to select an $\dot{m}$, and then, depending upon the properties of the transfer fluid ($c_{t,f}$) and storage capacity of the unit, conduct the tests for some fraction or integral of the fill time. However; the experimenter who was concerned about the optimum performance of his unit would no doubt select a flow rate where the relationship between the energy transfer rate and pressure drop (or power required to push the fluid through the device) was an optimum. In actual installation, the flow rate through and $\Delta t$ across the storage device is controlled by the flow rate through and $\Delta t$ across the collector and/or building heating and cooling system. The flow rate is usually proportional to the collector size and in turn the storage capacity is usually proportional to the collector size. Consequently, the ratio of SC/$\dot{m}$ is constant within certain limits. As a result, in the test procedure, two different fill times are specified that are felt to be typical of installed systems, the $\Delta t$'s are specified according to whether a liquid or air is the transfer fluid[b], and the flow rate to be used is calculated according to equation (41).

---

[a] One should recognize that for an ideal water tank where there is entirely piston-type flow, the above definition of fill time is identical with the fluid dwell time.

[b] Air heating collectors impose a much higher $\Delta t$ on the storage device than do liquid heating collectors.

According to Section 8 of Appendix B, the heat loss test described previously is to be conducted first. Following this, a series of eight tests are to be conducted in which first the heat storage capacity (four tests) and then the heat removal capacity (four tests) are to be determined. At the beginning, the thermal storage unit and transfer fluid flowing through the device at a specified $\dot{m}$ are allowed to come into equilibrium at some initial temperature. The temperature of the transfer fluid is then increased by an amount $\Delta t$ (specified below) and held constant. The amount of energy stored in the device over a certain fill time (specified below) is then determined by knowing the heat loss factor and $\dot{m}$ and by making measurements of the entering and leaving transfer fluid temperatures with respect to time. After the exit fluid temperature reaches an equilibrium value, the entering fluid temperature is suddenly decreased by the same $\Delta t$ and the amount of energy removed from the device over the same fill time is then determined in exactly the same way.

This process is repeated three more times until all of the following combinations of the variables $\tau_F$ and $\Delta t$ are tested:

$\tau_F$ = 2 h, 4 h and $\Delta t$ = 16 °C (28.8 °F), 8 °C (14.4 °F) for storage devices using a liquid transfer fluid, and

$\tau_F$ = 2 h, 4 h and $\Delta t$ = 50 °C (90 °F), 28 °C (50.4 °F) for storage devices using air as the transfer fluid.

When a phase-change type thermal storage system is being tested that has been designed to be "charged" or "discharged" over a specific time period, this time period shall be used as the fill time for testing in lieu of the above specified values.

Because of the concern that the storage capacity of latent-heat type devices degrade with number of cycles of operation [152], there is a requirement in the test procedure that this type of device shall have been cycled through its change of phase at least 30 times prior to being tested. Personnel of the University of Pennsylvania have stated that this may not be sufficient. They have recommended [163] that:

> "Latent heat storage devices ought to be tested, then cycled for 50 cycles, tested, cycled for 50 cycles, and tested again. The difference in storage capacities between any two tests should be less than 10%. The difference between the storage capacities after the 50th and 100th cycles should be less than one-half the difference between the storage capacities after the 1st and 50th cycles, if both differences are of the same algebraic sign. If the former difference is larger than one-half of the latter difference, the device ought to be cycled for 50 additional cycles and retested. This procedure shall be repeated as often as required."

Certainly close examination will be made of this factor in the planned carry-on program at the National Bureau of Standards.

In addition to determining the so-called effective capacities for heat storage and heat removal[a] for the various combinations of $\tau_F$ $\Delta t$ above, the recommended testing procedure requires that these effective capacities be divided by the energy that could be stored in a water tank of equal volume and in which perfect piston-flow occurs with zero heat loss. These so-called performance coefficients are required to be reported in tabular form (see Section 9 of Appendix B along with a plot showing the time variation in outlet temperature of the transfer fluid for each set of $\tau_F$ and $\Delta t$.

[a] So labelled effective in Appendix B since it is only that part of the capacity that is utilized during the time period $\tau_F$

## 4. Summary

The National Bureau of Standards has undertaken the development of testing procedures for evaluating solar collectors and thermal storage devices as individual components. This report covers the first phase of the work which has encompassed a thorough review of previous studies involving the testing of these components. Relevant experimental results have been cited. Based on the review, two test procedures have been written and are included one each for solar collector and thermal storage devices, respectively.

### Solar Collectors

The literature review of test methods revealed many minor variations of two basic procedures identified as the instantaneous procedure and the calorimetric procedure. Each method or procedure allows the determination of the thermal efficiency of a collector. When using the instantaneous method, one measures the mass flow rate of the transfer fluid, the difference in fluid temperature between the inlet and outlet and the insolation all simultaneously and under steady-state conditions. The instantaneous efficiency is then determined by

$$\eta = \frac{q_u/A}{I} = \frac{\dot{m}\, c_{tf}(t_{f,e} - t_{f,i})}{I} \qquad (42)$$

where

$q_u$ = rate of useful energy extraction from the solar collector, W

$A$ = cross-sectional area, $m^2$

$I$ = total solar energy incident upon the plane of the solar collector per unit time per unit area, $W/m^2$

$\dot{m}$ = mass flow rate of the transfer fluid through the collector per unit cross-sectional area of the collector, $kg/(s \cdot m^2$

$c_{tf}$ = specific heat of the transfer fluid, $J/(kg \cdot {}^oC)$

$t_{f,e}$ = temperature of the transfer fluid leaving the collector, $^oC$

$t_{f,i}$ = temperature of the transfer fluid entering the collector, $^oC$

In the calorimetric method, one employs a closed system in which the rate of change in temperature of a constant thermal mass is measured and related to the incident solar energy by:

$$\eta' = \frac{q_u/A}{I} = \frac{\int_0^\tau m\, c_p\, dt}{I} \qquad (43)$$

where

$m$ = the mass of the media in the calorimeter, kg

$c_p$ = the specific heat of the media in the calorimeter, $J/(kg \cdot {}^oC)$

$t$ = average temperature of the media in the calorimeter, $^oC$

$\tau$ = time, s

The report reviews the testing procedure proposed by Whillier and Richards of South Africa [31], Robinson and Stotter of Israel [40], a method used by CSIRO in Australia [44, 45], and the test procedures used in the United States by Bartera and Davis of the Jet Propulsion Laboratory [51], Moore et.al. of the Los Alamos Scientific Laboratory [52], the University of Pennsylvania [56], and at the NASA Lewis Research Center [29, 69-77]. All of the above cited studies involving the testing of water-heating collectors using the instantaneous method. All the tests are or were conducted outside under real sun conditions except for the tests at the NASA Lewis Research Center which involved the use of an indoor simulator. Only one study was cited where the calorimetric approach has been proposed and used for testing water-heating collectors [67]. Very little testing has been done on air-heating collectors. Four different studies were cited [87, 88, 89, 90] all involving the use of the instantaneous method.

Based on the literature review, the test procedure in Appendix A was written.[a] The series of tests that comprise the testing procedure is conducted outside under real sun conditions and the results of the tests are displayed in graphical and tabular form.

The test procedure is limited to collectors that can be isolated so that they have effectively one inlet and one outlet. The energy of the fluid entering and leaving the collector can be determined by making appropriate measurements. These quantities are than compared to the energy incident upon the collector (also determined by measurement) in order to calculate the collector efficiency. The fluid can be either a liquid or a gas but not a combination of the two.

As part of the test procedure, the apparatus to be used is specified both for when a liquid or air is to be the transfer fluid. The detailed requirements of the apparatus are given along with specifications for instrumentation to be used in measuring incident solar radiation, temperature, temperature difference, liquid flow rate, air flow rate, pressure, pressure drop, time, and weight. For the specification of instrumentation, emphasis was placed on utilizing existing standards and other manuals of acceptable practice.

The series of tests consist of determining the average efficiency for 15 minute periods (integrating the energy quantities) over a range of temperature differences between the average temperature and ambient air. The efficiency is then calculated by:

$$\eta = \frac{\int_0^\tau \dot{m}\, c_{tf}\, (t_{f,i} - t_{f,e})\, d\tau}{\int_0^\tau I\, d\tau} \qquad (44)$$

The flow rate is required to be steady and vary by less than $\pm$ 1.0% for the duration of each test. In addition, the transfer fluid shall have a known specific heat which varies by less than 0.5% over the temperature range of the fluid during a particular 15 minute test period. Consequently, the efficiency can be determined by:

$$\eta = \frac{\dot{m}\, c_{tf} \int_0^\tau (t_{f,i} - t_{f,e})\, d\tau}{\int_0^\tau I\, d\tau} \qquad (45)$$

The test apparatuses specified have been designed so that the temperature of the fluid entering the collector can be controlled to selected values. This feature is used to obtain the data over the temperature range desired. At least sixteen "data points" are required for a complete test series and they must be taken symmetrical with respect to solar noon (to prevent biased results due to possible transient effects).

---

[a] The testing procedure itself is equally applicable for testing indoors using a solar simulator, however, the present version of the document does not list the requirements for such a facility.

During each test period, the incident solar radiation must be "quasi-steady". Other requirements that must be satisfied for each "data point" are that the 15 minute average insolation be greater than 630 $W/m^2$ (200 $Btu/(h \cdot ft^2)$), and the incident angle between the sun and the outward drawn normal from the collector be less than 45°. In addition, the range of ambient temperatures for the entire test series must be less than 30 °C (54 °F).

The measurements made and the calculated efficiency for each "data point" are reported in tabular form as well as on a two-dimensional plot. The ordinate is the efficiency and the abscissa is the measured temperature difference divided by the insolation. It is recommended that the units be standard SI or that the abscissa be made dimensionless by dividing the temperature difference by either 100 °C or 212 °F and the insolation by the solar constant. It is expected that a "straight-line" representation will suffice for most conventional flat-plate collectors. Representation of the performance of a concentrating collector or high-performance flat-plate collector on such a plot will probably require the use of a "higher order fit".

Thermal Storage Devices

The development of analytical models which would aid in predicting the performance of thermal energy storage units has been handicapped by the extreme complexity of the phenomena involved. For example, water tanks involve three-dimensional mixing. The systems employing inorganic salt hydrates involve complicated heat transfer, nucleation, crystal growth, and incongruent melting. In addition, the total amount of analytical and experimental work done on thermal storage devices as single components is small in comparison to the attention that has been given to solar collectors.

The most extensive work on water storage tanks has been done in Japan [130, 131, 132] where this type of device has been investigated both theoretically and experimentally. Some recent analytical work has been done in this country on the behavior of water tanks by Phillips and Pate [133, 134] and the behavior of heat exchanger-type thermal storage units in general (including water tanks) by Yang and Lee [135]. The above cited papers have been reviewed and discussed in the report.

The method which has been most commonly employed in testing of water storage tanks in Japan [130, 131, 132] is to cause the transfer fluid entering the storage device to undergo a step change in temperature and to measure the temperature response of the transfer fluid leaving the storage unit. By integrating the difference in temperature between the inlet and outlet over the testing period and multiplying the result by the transfer fluids' mass flow rate and specific heat, one can determine the amount of heat added or removed during this time period. If the time period chosen for the test is some characteristic time depending upon the size of the storage device chosen, the heat storage capability of different devices can be compared. This procedure has been adopted and is an integral part of the proposed test procedure for thermal storage devices given in Appendix B.

The test procedure is limited to thermal storage devices that can be isolated so that they have effectively one inlet and one outlet. The energy of the fluid entering and leaving the thermal storage unit can be determined by making appropriate measurements. These quantities are then compared in order to calculate the amount of energy stored or retrieved during a particular test. The fluid can be either a liquid or a gas but not a combination of the two.

The procedure as written in Appendix B specifies the apparatus to be used when a liquid or air is to be the transfer fluid. The detailed requirements of the apparatus are given along with specifications for instrumentation to be used in measuring temperature, temperature difference, liquid flow rate, air flow rate, pressure, pressure drop, time, and mass. For the specification of instrumentation, emphasis was placed on utilizing existing standards and other manuals of acceptable practice. The nature of the apparatuses and test procedure makes the tests most feasible for storage units having thermal capacities on the order of $10^9$ J ($10^6$ Btu) or less.

The series of tests that are to be conducted are as follows:

1. One test to determine a heat loss factor for the storage unit,
2. A series of four tests to determine the response characteristics of the device to a step increase in the entering fluid temperature (energy addition), and
3. A series of four tests to determine the response characteristics of the device to a step decrease in the entering fluid temperature (energy withdrawal).

The heat loss test consists of passing the transfer fluid through the storage unit with an inlet fluid temperature of 25 °C (45 °F) above the ambient air temperature and after steady-state conditions have been reached, measuring the average temperature difference between the inlet and outlet fluid temperature over a one hour period. The rate of heat loss is then determined by

$$L = \frac{\dot{m} c_{tf} (t_{in} - t_{out})}{25\ ^{\circ}C} \qquad (46)$$

in w/°C.

Following the heat loss test, a series of eight tests are to be conducted in which first the heat storage capacity (four tests) and then the heat removal capacity (four tests) are to be determined. At the beginning, the thermal storage unit and transfer fluid flowing through the device at a specified average mass flow rate are allowed to come into equilibrium at some initial temperature. The temperature of the transfer fluid is then increased by an amount $\Delta t$ (specified below) and held constant. The amount of energy stored in the device over a certain test time (specified below) is then determined by knowing the heat loss factor and $\dot{m}$ and by making measurements of the entering and leaving transfer fluid temperatures with respect to time. After the exit fluid temperature reaches an equilibrium value, the entering fluid temperature is suddenly decreased by the same $\Delta t$ and the amount of energy removed from the device over the same test time is then determined in exactly the same way.

This process is repeated three more times until all of the following combinations of the test time ($\tau$) and $\Delta t$ are tested:

$\tau$ = 2 h, ½ h, and $\Delta t$ = 16 °C (28.8 °F), 8 °C (14.4 °F) for storage devices using a liquid transfer fluid, and

$\tau$ = 2 h, ½ h, and $\Delta t$ = 50 °C (90 °F), 28 °C (50.4 °F) for storage devices using air as the transfer fluid.

When a phase-change type thermal storage system is being tested that has been designed to be "charged" or "discharged" over a specific time period, this time period is used as the test time for testing in lieu of the above specified values.

## 5. References


1. "The SAV Solar Heater", Fred Rice Productions, Inc., 6313 Peach Avenue, Van Nuys, California 91401, 1974.

2. "Sunworks, Inc. Introduces a Flat-Plate Solar Heat Collector", Sunworks, Inc., 669 Boston Post Road, Guilford, Connecticut 06437, August, 1974.

3. "Revere Solar Energy Collector", Revere Publication No. ABP #128, Revere Copper and Brass Incorporated, 605 Third Avenue, New York, New York 10016, 1974.

4. Hill, J.E., Kusuda, T., and G.E. Kelly, "Development of Methods of Evaluation and Test Procedures for Solar Collectors and Storage Devices", a proposal to the National Science Foundation, July 18, 1973.

5. "Solar Heating and Cooling Demonstration Act of 1974", Public Law 93-409, 1974.

6. Shurcliff, W.A., "Criticism of the Concept: 'Efficiency of a Collector' of a Solar Heated House", presented at the United States Section Meeting of the International Solar Energy Society, Fort Collins, Colorado, August 21-23, 1974.

7. "Interim Performance Criteria for Solar Heating and Combined Heating/Cooling Systems and Dwellings", prepared for HUD by NBS, available from the U.S. Government Printing Office, Washington, D.C. 20402, Stock No. 0324-01043, January 1, 1975.

8. de Winter, F., "Solar Energy and the Flat-Plate Collector - An Annotated Bibliography", Santa Clara, California, February, 1975 (to be published by ASHRAE).

9. "Appendix M - A State-of-the-Art Review of Solar Heating and Cooling Systems and Subsystems", Solar Heating and Cooling of Buildings-Phase 0, Report No. NSF-RA-N-74-023C, Westinghouse Electric Corporation, May, 1974.

10. "Solar Energy", prepared for the Air Force Office of Scientific Research, Advanced Research Projects Agency by Information, Incorporated, Report No. AD-788 846, available from NTIS, Springfield, Virginia 22151, March 1, 1974.

11. "Solar Energy - a Bibliography", U.S. Atomic Energy Commission, Office of Information Services, Technical Information Center, Report No. TID-3351, available from NTIS, Springfield, Virginia 22151, December, 1974.

12. Yellott, J.I., "Report of the Working Group on Testing and Standards", Proceedings of the Workshop on Solar Collectors for Heating and Cooling of Buildings, New York, November 20-23, 1974, Report No. NSF-RA-N-75-019, University of Maryland, May, 1975.

13. Lorsch, H.G., "Report of the Working Group on Testing and Standards", Proceedings of the Workshop on Thermal Storage for Heating and Cooling of Buildings, Charlottesville, Virginia, April 16-18, 1975, published by the University of Virginia, 1975.

14. Hill, J.E., and T. Kusuda, "Method of Testing for Rating Solar Collectors Based on Thermal Performance", NBS Report NBSIR 74-635, December, 1974.

15. Kelly, G.E., and J.E. Hill, "Method of Testing for Rating Thermal Storage Devices Based on Thermal Performance", NBS Report NBSIR 74-634, May, 1975.

16. "Solar Heating and Cooling Experiment for a School in Atlanta - Design Report", Report No. NSF-RA-N-74-122, Westinghouse Electric Corporation, December, 1974.

17. "Solar Thermal Electric Power Systems - First Quarter Progress Report", Report No. NSF/RANN/SE/GI-37815/PR/74/1, Colorado State University, April, 1974.

18. Duffie, J.A., and W.A. Beckman, Solar Energy Thermal Processes, John Wiley and Sons, 1974.

19. Schmidt, R., "Honeywell Flat-Plate Collector Code", Proceedings of the Solar Heating and Cooling for Buildings Workshop, Washington, D.C., March 21-23, 1973, Part I: Technical Sessions, Report No. NSF/RANN/SE/GI-32488/73, University of Maryland, July, 1973.

20. Hottel, H.C., and B.B. Woertz, "The Performance of Flat-Plate Solar Heat Collectors", ASME Transactions, Vol. 64, p. 91, 1942.

21. Whillier, A., Solar Energy Collection and its Utilization for House Heating, ScD. Thesis, MIT, 1953.

22. Hottel, H.C., and A. Whillier, "Evaluation of Flat-Plate Collector Performance", Transactions of the Conference on the Use of Solar Energy, Vol. 2, Part I, p. 74, University of Arizona Press, 1958.

23. Bliss, R.W., "The Derivation of Several 'Plate-Efficiency Factors' Useful in the Design of Flat-Plate Solar Heat Collectors", Solar Energy, Vol. 3, No. 4, p. 55, 1959.

24. Liu, B.Y.H., and R.C. Jordan, "A Rational Procedure for Predicting the Long-Term Average Performance of Flat-Plate Solar Energy Collectors", Solar Energy, Vol. 7, No. 2, 1963.

25. Whillier, A., "Design Factors Influencing Collector Performance", Low Temperature Engineering Application of Solar Energy, American Society of Heating, Refrigerating and Air-Conditioning Engineers, Inc., 345 East 47th Street, New York, N.Y. 10017, 1967.

26. Klein, S.A., "Calculation of Flat-Plate Collector Loss Coefficients", Solar Energy, Vol. 17, pp. 79-80, 1975.

27. Nevins, R.G., and P.E. McNall, "A High-Flux Low-Temperature Solar Collector", ASHRAE Transactions, Vol. 64, pp. 69-82, 1958.

28. Löf, G.O.G., Fester, D.A., and J.A. Duffie, "Energy Balance on a Parabolic Cylinder Solar Reflector", ASME Transactions, Vol. 84A, p. 24, 1962.

29. Simon, F.F., "Collector Test Procedure and Experiments with a Solar Simulator", NASA TM X-71658, Proceedings of the Workshop on Solar Collectors for Heating and Cooling of Buildings, New York, November 20-23, 1974, Report No. NSF-RA-N-75-019, University of Maryland, May, 1975.

30. Brooks, F.A., "Solar Energy and its Use for Heating Water in California", University of California Agricultural Experiment Station, Bulletin No. 602, November, 1936.

31. Whillier, A., and S.J. Richards, "A Standard Test for Solar Water Heaters", Proceedings of the Conference on New Sources of Energy, paper S/97, Rome, August 21-31, 1961.

32. Whillier, A., "Thermal Resistance of the Tube-Plate Bond in Solar Heat Collectors", Solar Energy, Vol. 8, No. 3, pp. 95-98, 1964.

33. Whillier, A., and G. Saluja, "Effect of Materials and Construction Details on the Thermal Performance of Solar Water Heaters", Solar Energy, Vol. 9, No. 1, 1965.

34. Khan, E.U., "Evaluation of Bond Conductance in Various Tube-in-Strip Types of Solar Collector", Solar Energy, Vol. 11, No. 2, 1967.

35. Chinnery, D.N.W., "Some Results of Performance Tests on Solar Water Heaters", CSIR Reference No. RD 97, reprinted from the Proceedings of the Building Research Symposium, Windhoek, South West Africa, May, 1963.

36. Chinnery, D.N.W., "Solar Water Heating in South Africa", CSIR Research Report 248, UDC 649.1551,521.1 (680), Pretoria, South Africa, 1967.

37. Yellott, J.I., and R. Sobótka, "An Investigation of Solar Water Heater Performance", ASHRAE Transactions, Vol. 70, pp. 425-433, 1964.

38. Tabor, H., "Solar Energy Collector Design", Bulletin of the Research Council of Israel, Vol. 5C, pp. 5-27, 1955.

39. Tabor, H., "Radiation, Convection, and Conduction Coefficients in Solar Collectors", Bulletin of the Research Council of Israel, Vol. 6C, pp. 155-176, 1958.

40. Robinson, N., and A. Stotter, "A Proposed Standard Test Code for the Determination of the Efficiency of Solar Water Heaters of the Flat Collector Type", Solar Energy, Vol. 3, No. 2, pp. 30-33, 1959.

41. Israel Standard, "Solar Water Heaters: Test Methods", The Standards Institution of Israel, Tel Aviv, U.D.C. 602.93, S.I. 609, May, 1966.

42. Doron, B., "Testing of Solar Collectors", Solar Energy, Vol. 9, No. 2, pp. 103-104, 1965.

43. Tabor, H., "Testing of Solar Collectors", presented at the 1975 International Solar Energy Congress, "Solar Use Now - A Resource for People", Los Angeles, California, July 28 - August 1, 1975.

44. Cooper, P.I., "A Method of Testing Flat-Plate Solar Water Heaters to Determine Performance Characteristics", presented at the Australian and New Zealand Section Meeting of the International Solar Energy Society, Melbourne, July 2, 1975.

45. Cooper, P.I., Symons, J.G., and P. Pott, "Thermal Performance Characteristics for Analysis Design and Rating of Flat-Plate Solar Collectors", presented at the 1975 Solar Energy Congress, "Solar Use Now - A Resource for People", Los Angeles, California, July 28 - August 1, 1975.

46. Dunkle, R.V., and P.I. Cooper, "A Proposed Method for the Evaluation of Performance Parameters of Flat-Plate Solar Collectors", presented at the 1975 Solar Energy Congress, "Solar Use Now - A Resource for People", Los Angeles, California, July 28 - August 1, 1975.

47. Tanishita, I., "Present Situation of Commercial Solar Water Heaters in Japan", presented at the International Solar Energy Society Meeting, Melbourne, 1970.

48. Kusuda, T., "Solar Water Heating in Japan", Proceedings of the Solar Heating and Cooling for Buildings Workshop, Washington, D.C., March 21-23, 1973, Part I: Technical Sessions, Report No. NSF/RANN/SE/GI-32488/73, University of Maryland, July, 1973.

49. Harris, W.B., Davidson, R.R., and D.N. Wood, "Design and Operating Characteristics of an Experimental Solar Water Heater", Solar Energy, Vol. 9, No. 4, 1965.

50. Gopffarth, W.H., Lavidson, R.R., Harris, W.B., and M.J. Baird, "Performance Correlation of Horizontal Plastic Solar Water Heaters", Solar Energy, Vol. 12, pp. 183-196, 1968.

51. Rastera, R.E., and E.S. Davis, "Performance of a Flat-Plate Solar Collector", Jet Propulsion Laboratory Report 1200-179, prepared for the Southern California Gas Company, July 1, 1974.

52. Moore, S.W., Balcomb, J.E., and J.C. Hedstrom, "Design and Testing of a Structurally Integrated Steel Solar Collector Unit Based on Expanded Flat Metal Plates", presented at the United States Section Meeting of the International Solar Energy Society, Fort Collins, Colorado, August 19-23, 1974.

53. "Solar Energy School Heating Augmentation Experiment - Design, Construction, and Initial Operation", Report No. NSF-RA-N-74-019, Intertechnology Corporation, December, 1974.

54. Lorsch, H.G., "Conservation and Better Utilization of Electric Power by Means of Thermal Energy Storage and Solar Heating - Final Summary Report", Report No. NSF/RANN/SE/GI27976/PR73/5, University of Pennsylvania, July, 1973.

55. Ostad-Hosseini, A., "Performance of a Vertical Flat-Plate Solar Collector", Report No. NSF/RANN/SE/GI27976/TR72/15, University of Pennsylvania, December, 1972.

56. Lior, N., and A.P. Saunders, "Solar Collector Performance Studies", Report No. NSF/RANN/SE/GI27976/TR31/1, University of Pennsylvania, August, 1974.

57. Saunders, A.P., "Test Facility for Experimental Solar Collectors", Report No. NSF/RANN/SE/GI27976/TR72/12, University of Pennsylvania, 1972.

58. Lorsch, H.G., "Performance of Flat-Plate Solar Collectors", Proceedings of the Solar Heating and Cooling for Buildings Workshop, Washington, D.C., March 21-23, 1973, Part I: Technical Sessions, Report No. NSF/RANN/SE/GI-32488/73, University of Maryland, July, 1973.

59. Lior, N., and H.G. Lorsch, "A Comparative Experimental Study of Flat-Plate Solar Collectors", presented at the United States Section Meeting of the International Solar Energy Society, Fort Collins, Colorado, August 19-23, 1974.

60. Lior, N., "Interim Standard for Solar Collectors", Report No. NSF/RANN/SE/GI297290/PR74/2, University of Pennsylvania, July, 1974.

61. San Martin, R.L., and G.J. Fjeld, "Experimental Performance of Three Solar Collectors", presented at the United States Section Meeting of the International Solar Energy Society, Fort Collins, Colorado, August 19-23, 1974.

62. San Martin, R.L., "Performance of the Thermal Trap Solar Collector", ASME paper 74-WA/Sol-5, presented at the ASME Winter Annual Meeting, New York, November 17-22, 1974.

63. Thomason, H.E., "Solar Space Heating and Air Conditioning in the Thomason Home", Solar Energy, Vol. 4, No. 4, pp. 11-19, 1960.

64. Thomason, H.E., "Experiences with Solar Houses", Solar Energy, Vol. 10, No. 1, pp. 17-22, 1966.

65. Thomason, H.E., and H.J.L. Thomason, Jr., "Solar Houses/Heating and Cooling Progress Report", Solar Energy, Vol. 15, No. 1, pp. 27-40, 1973.

66. "PPG Prototype Baseline Solar Collector", Publication No. G-483 5M84, PPG Industries, Inc., 1 Gateway Center, Pittsburgh, Pennsylvania 15222, 1974.

67. Lee, W.D., "Solar Collector Testing by Calorimetry", Proceedings of the NSF/RANN Workshop on Solar Collectors for Heating and Cooling of Buildings, New York, November 20-23, 1974, Report No. NSF-RA-N-75-019, University of Maryland, 1975.

68. "Measured Efficiency - Test Results on the Sunsource/Miromit Model 100 Solar Collector", Technical Note 74-1201, Sunsource, 9606 Santa Monica Blvd., Beverly Hills, California 90210, 1974.

69. Yass, K., and H.B. Curtis, "Low-Cost Air Mass 2 Solar Simulator", NASA TM X-3059, presented at the United States Section Meeting of the International Solar Energy Society, Cleveland, Ohio, October 3-4, 1973.

70. Simon, F.F., and P. Harlamert, "Flat-Plate Collector Performance Evaluation, the Case for a Solar Simulator Approach", NASA TM X-71427, presented at the United States Section Meeting of the International Solar Energy Society, Cleveland, Ohio, October 3-4, 1973.

71. Vernon, R.W., and F.F. Simon, "Flat-Plate Collector Performance Determined Experimentally with a Solar Simulator", NASA TM X-71602, presented at the United States Section Meeting of the International Solar Energy Society, Fort Collins, Colorado, August 19-23, 1974.

72. Simon, F.F., "Status of the NASA-Lewis Flat-Plate Collector Tests with a Solar Simulator", NASA TM X-71658, Proceedings of the Workshop on Solar Collectors for Heating and Cooling of Buildings, New York, November 21-23, 1974, Report No. NSF-RA-N-75-019, University of Maryland, May, 1975.

73. Vernon, R.W., "Solar Collector Performance Evaluated Outdoors at NASA-Lewis Research Center", NASA TM X-71689, Proceedings of the Workshop on Solar Collectors for Heating and Cooling of Buildings, New York, November 20-23, 1974, Report No. NSF-RA-N-75-019, University of Maryland, May, 1975.

74. Simon, F.F., "An Evaluation Under a Simulated Sun of Two Black-Nickel Coated Flat-Plate Solar Collectors, NASA TM X-3226, 1975.

75. Simon, F.F., "Solar Collector Performance Evaluation with the NASA-Lewis Solar Simulator - Results for an All-Glass-Evacuated - Tubular Selectively-Coated Collector with a Diffuse Reflector", NASA TM X-71695, 1975.

76. Vernon, R.W., "Initial Comparison of Solar Collector Performance Data Obtained Out-of-Doors and with a Solar Simulator", NASA TM X-71626, presented at the 1975 International Solar Energy Congress, "Solar Use Now - A Resource for People", Los Angeles, California, July 28 - August 1, 1975.

77. Simon, F.F., "Flat-Plate Solar Collector Performance Evaluation with a Solar Simulator as a Basis for Collector Selection and Performance Prediction", NASA TM X-71973, presented at the 1975 International Solar Energy Congress, "Solar Use Now - A Resource for People", Los Angeles, California, July 28 - August 1, 1975.

78. Ramsey, J., "Experimental Evaluation of Flat-Plate Collector Configurations", Proceedings of the Workshop on Solar Collectors for Heating and Cooling of Buildings, New York, November 20-23, 1974, Report No. NSF-RA-N-75-019, University of Maryland, May, 1975.

79. Ramsey, J.W., Borzoni, J.T., and T.H. Holland, "Development of Flat-Plate Collectors for the Heating and Cooling of Buildings", NASA CR-134804, June, 1975.

80. Ramsey, J.W., and J.R. Borzoni, "Effects of Selective Coatings on Flat-Plate Solar Collector Performance", presented at the 1975 International Solar Energy Congress, "Solar Use Now - A Resource for People", Los Angeles, California, July 28 - August 1, 1975.

81. Close, D.J., "Solar Air Heaters for Low and Moderate Temperature Applications", Solar Energy, Vol. 7, No. 3, pp. 117-124, 1963.

82. Whillier, A., "Performance of Black-Painted Solar Air Heaters of Conventional Design", Solar Energy, Vol. 8, No. 1, pp. 31-37, 1964.

83. Chiou, J.P., El-Wakil, M.M., and J.A. Duffie, "A Slit-and-Expanded Aluminum Foil Matrix Solar Collector", Solar Energy, Vol. 9, No. 2, pp. 73-80, 1965.

84. Rankine, A.D., and W.W.S. Charters, "Combined Convective and Radiative Heat Losses from Flat-Plate Solar Air Heaters", Solar Energy, Vol. 12, pp. 517-523, 1969.

85. Suri, R.K., and J.S. Saini, "Performance Prediction of Single and Double Exposure Solar Air Heaters", Solar Energy, Vol. 12, pp. 525-530, 1969.

86. Charters, W.W.S., and R.W.G. Macdonald, "Heat Transfer Effects in Solar Air Heaters", paper E37, presented at the Congress - The Sun in the Service of Mankind, UNESCO House, Paris, July 2-6, 1973.

87. Gupta, C.L., and H.P. Garg, "Performance Studies on Solar Air Heaters", Solar Energy, Vol. 11, No. 1, pp. 25-31, 1967.

88. Sulcuk, K., "Thermal and Economic Analysis of the Overlapped-Glass Plate Solar Air Heater", Solar Energy, Vol. 13, pp. 165-191, 1971.

89. Satcunanathan, S., and S. Deonarine, "A Two-Pass Solar Air Heater", Solar Energy, Vol. 15, pp. 41-49, 1973.

90. Löf, G.O.G., Shaw, L.E., and R.L. Oonk, "Comparison of Performance of Solar Collectors of the Air Heating and Water Heating Types", presented at the 1975 International Congress, "Solar Use Now - A Resource for People", Los Angeles, California, July 28 - August 1, 1975.

91. Kline, S.J., and F.A. McClintock, "Describing Uncertainties in Single-Sample Experiments", Mechanical Engineering, p. 3, January, 1953.

92. Latimer, J.R., "Radiation Measurement", Technical Manual Series No. 2, Canadian National Committee for the International Hydrological Decade, Building No. 8, Carling Avenue, Ottawa, Canada, 1971.

93. Norris, D.J., "Calibration of Pyranometers in Inclined and Inverted Positions", paper E48, presented at the International Congress - The Sun in the Service of Mankind, UNESCO House, Paris, July 2-6, 1973.

94. "The Thermal Insulating Value of Airspaces", Housing Research Paper 32, Housing and Home Finance Agency, Division of Housing Research, Washington, D.C., April, 1954.

95. Robinson, H.E., Cosgrove, L.A., and F.J. Powell, "Thermal Resistance of Airspaces and Fibrous Insulations Bounded by Reflective Surfaces", Building Materials and Structures Report 151, National Bureau of Standards, November 14, 1957.

96. ASHRAE Handbook of Fundamentals, American Society of Heating, Refrigerating and Air-Conditioning Engineers, Inc., 345 East 47th Street, New York, N.Y. 10017, 1972.

97. Millard, J.P., and J.C. Aversen, "Effects of Skylight Polarization, Cloudiness, and View Angle on the Detection of Oil on Water", Paper No. 71-7025, presented at the AIAA Conference on Sensing of Environmental Pollutants, Palo Alto, California, November, 1971.

98. Streed, E.R., "Some Design Considerations for Flat-Plate Collectors", Proceedings of the Solar Heating and Cooling for Buildings Workshop, Washington, D.C., March 21-23, 1973, Part I: Technical Sessions, Report No. NSF/RANN/SE/GI-32488/73, University of Maryland, July, 1973.

99. O'Neill, M.J., McDanal, A.J., and W.H. Sims, "The Development of a Residential Heating and Cooling System Using NASA-Derived Technology", LMSC-HREC D306275, Lockheed Missiles & Space Company, Huntsville, Alabama, November, 1972.

100. Smith, C.C., and T. Weiss, "Design Application of the Hottel-Whillier-Bliss Equation", presented at the 1975 International Congress, "Solar Use Now - A Resource for People", Los Angeles, California, July 28 - August 1, 1975.

101. Hollands, K.G.T., "Honeycomb Devices in Flat-Plate Solar Collectors", Solar Energy, Vol. 9, No. 3, pp. 159-164, 1965.

102. Buchberg, H., Lalude, O.A., and D.K. Edwards, "Performance Characteristics of Rectangular Honeycomb Solar-Thermal Converters", Solar Energy, Vol. 13, pp. 193-221, 1971.

103. Charters, W.W.S., and L.F. Peterson, "Free Convection Suppression Using Honeycomb Cellular Material", Solar Energy, Vol. 13, No. 4, pp. 353-361, 1972.

104. Cunnington, G.R., and E.R. Streed, "Experimental Performance of a Honeycomb Covered Flat-Plate Solar Collector", presented at the United States Section Meeting of the International Solar Energy Society, Cleveland, Ohio, October 3-4, 1973.

105. Charters, W.W.S., "Heat Flux Measurements for Free Convection within Inclined Cellular Structures", Paper E36, presented at the International Congress - The Sun in the Service of Mankind, UNESCO House, Paris, July 2-6, 1973.

106. Chun, K.R., and W.E. Crandall, "Effect of a Mylar Honeycomb Layer on Solar Collector Performance", Paper 74-WA/HT-11, presented at the ASME Winter Annual Meeting, New York, November 17-22, 1974.

107. Marshall, K.N., Wedel, R.K., Haslim, A., and G.A. Bell, "Thermal Radiation Characteristics of Transparent Plastic Honeycombs for Solar Collector Applications", presented at the 1975 International Congress, "Solar Use Now - A Resource for People", Los Angeles, California, July 28 - August 1, 1975.

108. Baldwin, C.M., Dunn, B.S., Hilliard, W.G., MacKenzie, J.D., Buchberg, H., and D.K. Edwards, "Transparent Performance of Glass Honeycombs in Flat Plate Collectors", presented at the 1975 International Congress, "Solar Use Now - A Resource for People", Los Angeles, California, July 28 - August 1, 1975.

109. Koutsoheras, W., and W.W.S. Charters, "Natural Convection Phenomena in Inclined Cells", presented at the 1975 International Congress, "Solar Use Now - A Resource for People", Los Angeles, California, July 28 - August 1, 1975.

110. Edwards, D.K., Arnold, J.N., and I. Catton, "End-Clearance Effects on Rectangular-Honeycomb Solar Collectors", presented at the 1975 International Congress, "Solar Use Now - A Resource for People", Los Angeles, California, July 28 - August 1, 1975.

111. Hollands, K.G.T., and T.E. Unny, "Convection Suppression in Inclined Honeycombs", presented at the 1975 International Congress, "Solar Use Now - A Resource for People", Los Angeles, California, July 28 - August 1, 1975.

112. Vincze, S., "A High Speed Cylindrical Solar Water Heater", Solar Energy, Vol. 13, No. 3, p. 339, 1971.

113. Speyer, E., "Solar Energy Collection with Evacuated Tubes", ASME Journal of Engineering for Power, pp. 270-276, 1965.

114. Beekley, D.C., and G.R. Mather, "Analysis and Experimental Tests of High Performance Tubular Solar Collectors", presented at the 1975 International Congress, "Solar Use Now - A Resource for People", Los Angeles, California, July 28 - August 1, 1975.

115. Ortabasi, U., and N. Buehl, "Analysis and Performance of an Evacuated Tubular Collector", presented at the 1975 International Congress, "Solar Use Now - A Resource for People", Los Angeles, California, July 28 - August 1, 1975.

116. Bruno, R., Herman, W., Honster, H., Kersten, R., and F. Mahdjuri, "High Efficiency Solar Collectors", presented at the 1975 International Congress, "Solar Use Now - A Resource for People", Los Angeles, California, July 28 - August 1, 1975.

117. Klein, S.A., Duffie, J.A., and W.A. Beckman, "Transient Considerations of Flat-Plate Collectors", Paper No. 73-WA/Sol-1, presented at the ASME Winter Annual Meeting, Detroit, Michigan, November 11-15, 1973.

118. Shurcliff, W.A., "Thermal Capacity of a Flat-Plate Collector for a Solar Heated House: Does it Make much Difference Whether the Capacity is Large or Small?", available from the Author, 19 Appleton St., Cambridge, Mass. 02138, November 27, 1973.

119. Bruno, R., Hermann, W., Horster, H., Kersten, R., and F. Mahdjuri, "On Collector Testing Methods", unpublished note, Philips Forschungslaboratorium, 5100 Aachen, Postfach 1980, Federal Republic of Germany, February, 1975.

120. "Pyramidal Optics Solar Energy Collection System", Bulletin SS-2, Wormser Scientific Corporation, Stamford, Conn., 1974.

121. Boyd, D.A., Gajewski, R., and R. Swift, "A Cylindrical Blackbody Solar Collector", presented at the United States Section Meeting of the International Solar Energy Society, Fort Collins, Colorado, August 19-23, 1974.

122. Winston, R., "Solar Concentrators of a Novel Design", Solar Energy, Vol. 16, No. 2, pp. 89-95, 1974.

123. Northrup, L.L., and M.J. O'Neill, "A Practical Concentrating Solar Energy Collector", presented at the 1975 International Congress, "Solar Use Now - A Resource for People", Los Angeles, California, July 28 - August 1, 1975.

124. Kreith F., "Evaluation of Focusing Solar Energy Collectors", ASTM Standardization News, pp. 30-38, August, 1975.

125. Kusuda, T., "NBSLD, Computer Program for Heating and Cooling Loads in Buildings", NBS Report NBSIR 74-574, November, 1974. Available from the National Technical Information Services, Springfield, VA 22161.

126. Kusuda, T., Liu, S.T., Bean, J.W., and J.P. Barnett, "Solar Energy Analysis for the GSA/Manchester Building", NBS Report (in review), 1975.

127. "Procedure for Determining Heating and Cooling Loads for Computerized Energy Calculations", ASHRAE Task Group on Energy Requirements for Heating and Cooling, American Society of Heating, Refrigerating, and Air-Conditioning Engineers, 345 East 47th Street, New York, N.Y. 10017, February, 1975.

128. Proctor, D., "Methods of Predicting the Heat Production of Solar Collectors for System Design", presented at the 1975 International Congress, "Solar Use Now - A Resource for People", Los Angeles, California, July 28 - August 1, 1975.

129. Simon, F.F., and E.H. Buyco, "Outdoor Flat-Plate Collector Performance Prediction from Solar Simulator Test Data", NASA TM X-71707, presented at the 10th AIAA Thermal Physics Conference, Denver, Colorado, May 27-29, 1975.

130. Nakajime, Y., "Studies on the Weighting Functions of Thermal Storage Water Tanks, Part I", Transactions of the Japanese Architectural Society, Vol. 199, pp. 37-47, September, 1972 (Japanese).

131. Nakajime, Y., "Studies on the Weighting Functions of Thermal Storage Water Tanks, Part II", Transactions of the Japanese Architectural Society, Vol. 200, pp. 75-83, October, 1972 (Japanese).

132. Nakajime, Y., "Design and Performance of Thermal Storage Water Tanks", presented at the 1975 International Congress, "Solar Use Now - A Resource for People", Los Angeles, California, July 28 - August 1, 1975.

133. Phillips, W.F., and R.A. Pate, "A Hot Liquid Energy Storage System Utilizing Natural Circulation", ASME paper 74-WA/HT-16, presented at the ASME Winter Annual Meeting, New York, 1974.

134. Pate, R.A., and W.F. Phillips, "Design Charts for Hot Liquid Energy Storage Systems Utilizing Forced Circulation", presented at the AIAA 10th Thermophysics Conference, Denver, Colorado, May 27-29, 1975.

135. Yang, W.J., and C.P. Lee, "Dynamic Response of Solar Heat Storage Systems", ASME paper 74-WA/HT-22, presented at the ASME Winter Annual Meeting, New York, 1974.

136. Löf, G.O.G., and R.W. Hawley, "Unsteady State Heat Transfer Between Air and Loose Solids", Industrial Engineering Chemistry, Vol. 40, p. 1061, 1948.

137. Handley, D., and P.S. Heggs, "The Effect of Thermal Conductivity of the Packing Material on the Transient Heat Transfer in a Fixed Bed", International Journal of Heat and Mass Transfer, Vol. 12, p. 549, 1969.

138. Close, D.J., "Rock Pile Thermal Storage for Comfort Air Conditioning", Mechanical and Chemical Engineering Transactions, Australian Institute of Engineers, MC-1, p. 11, 1965.

139. Gillette, R.B., "Analysis of the Performance of a Solar Heated House", M.S. Thesis in Mechanical Engineering, University of Wisconsin, 1959.

140. Löf, G.O.G., El-Wakil, M.M., and J.P. Chiou, "Design and Performance of a Domestic Heating System Employing Solar Heated Air - The Colorado House", Proceedings of the UN Conference on New Sources of Energy, Vol. 5, p. 185, 1964.

141. Hale, D.V., Hoover, M.J., and M.J. O'Neill, "Phase Change Materials Handbook", NASA CR-CR-61363, September, 1971.

142. Telkes, M., and E. Raymond, "Storing Solar Heat in Chemicals - A Report on the Dover House", Heating and Ventilating, Vol. 80, 1949.

143. Telkes, M., "Solar-Heat Storage", Solar Energy Research, University of Wisconsin Press, Madison, 1955.

144. Telkes, M., "Solar-Heat Storage", ASME paper 64-WA/Sol-9, presented at the ASME Winter Annual Meeting, New York, 1964.

145. Telkes, M., "Solar Energy Storage", ASHRAE Journal, pp. 38-44, September, 1974.

146. Telkes, M., "Storage of Solar Heating/Cooling", ASHRAE Transactions, Vol. 80, Part II, 1974.

147. Altman, M., "Conservation and Better Utilization of Electric Power by Means of Thermal Energy Storage and Solar Heating", Phase I Report, NTIS No. PB210359, University of Pennsylvania, October, 1971.

148. Dudley, J.C., "Thermal Energy Storage Unit for Air Conditioning Systems Using Phase Change Material", Report No. NSF/RANN/SE/GI27976/TR72/8, University of Pennsylvania, August, 1972.

149. Freedman, S.I., and J.C. Dudley, "Off-Peak Air Conditioning Using Thermal Energy Storage", Report No. NSF/RANN/SE/GI27976/TR72/9, University of Pennsylvania, August, 1972.

150. Freedman, S.I., and J.C. Dudley, "Off-Peak Air Conditioning Using Thermal Energy Storage", Proceedings of the 7th Annual Intersociety Energy Conversion Engineering Conference, San Diego, California, September, 1972.

151. Belton, G., and F. Ajami, "Thermochemistry of Salt Hydrates", Report No. NSF/RANN/SE/GI27976/TR73/4, University of Pennsylvania, May, 1973.

152. Kauffman, K.W., and Y.C. Pan, "Thermal Energy Storage in Sodium Sulfate Decahydrate Mixtures", Report No. NSF/RANN/SE/GI27976/TR72/11, University of Pennsylvania, December, 1972.

153. Lorsch, H.G., and J.C. Dudley, "Air Loop Off-Peak Air Conditioning System - Design and Operation", Report No. NSF/RANN/SE/GI27976/TR73/2, University of Pennsylvania, June, 1972.

154. Dudley, J.C., "Recondenser Off-Peak Air Conditioning System - Design and Operation", Report No. NSF/RANN/SE/GI27976/TR73/3, University of Pennsylvania, May, 1973.

155. Kauffman, K.W., and Y.C. Pan, "Congruently Melting Materials for Thermal Energy Storage in Air Conditioning", Report No. NSF/RANN/SE/GI27976/TR73/5, University of Pennsylvania, June, 1973.

156. Lorsch, H.G., "Latent Heat and Sensible Heat Storage for Solar Heating", Report No. NSF/RANN/SE/GI27976/TR72/20, University of Pennsylania, December, 1972.

157. Lorsch, H.G., "Thermal Energy Storage Devices Suitable for Solar Heating", Proceedings of the 9th Intersociety Energy Conversion Engineering Conference, San Francisco, California, August, 1974.

158. Dudley, J.C., and S.I. Freedman, "Economics of Operating Energy - Storage Air Conditioning Systems with Reduced Peak Power Demand", ASHRAE Transactions, Vol. 81, Part I, 1975.

159. Kauffman, K.W., and I. Gruntfest, "Congruently Melting Materials for Thermal Energy Storage", Report No. NCSMP-20, University of Pennsylvania, November, 1973.

160. Boer, K., "A Combined Solar Thermal Electrical House System", paper No. EH108, presented at the International Congress - The Sun in the Service of Mankind, UNESCO House, Paris, July 2-6, 1973.

161. Griggs, E.I., Pitts, D.R., and W.R. Humphries, "Transient Analysis of a Thermal Storage Unit Involving a Phase Change Material", ASME paper 74-WA/HT-21, presented at the ASME Winter Annual Meeting, New York, 1974.

162. Sreenivasan, K., and M. Altman, "Transient Temperature Response of Cylindrical Composite Energy Storage Devices", Energy Conversion, Vol. 9, pp. 99-105, 1969.

163. Personal Communication with H.G. Lorsch, University of Pennsylvania, December, 1974.

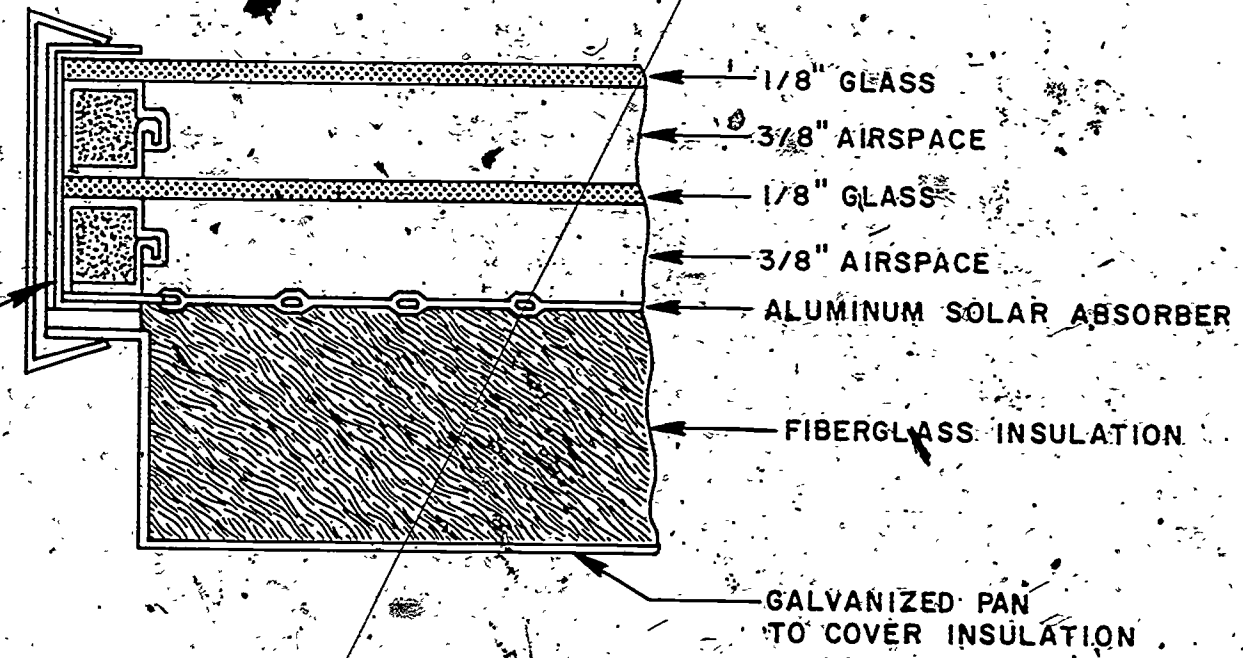


Figure 1 Schematic of Flat-Plate Liquid-Heating Solar Collector [66]

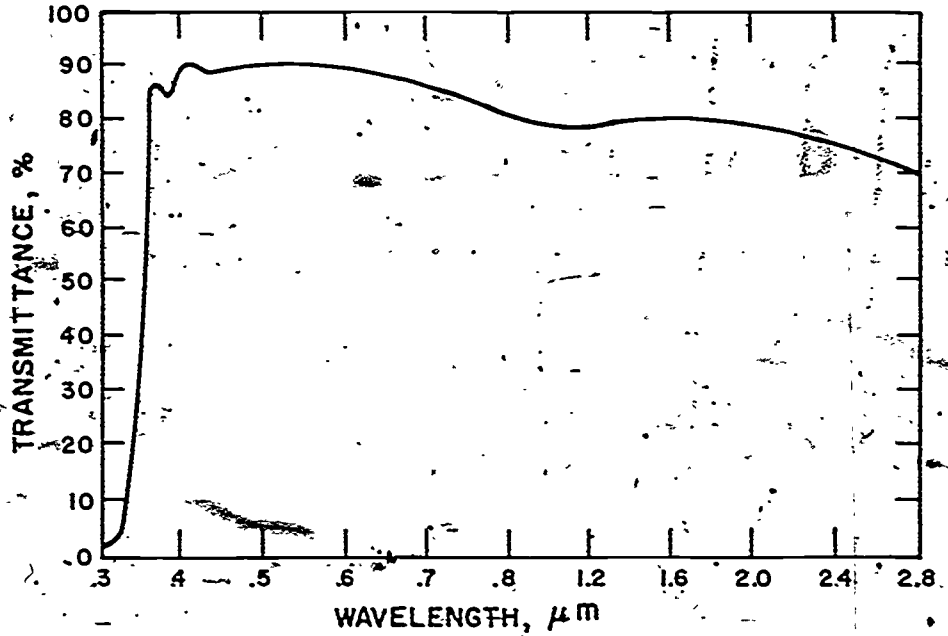


Figure 2 Spectral Transmittance of 3 mm (1/8 inch) Tempered Glass [66]

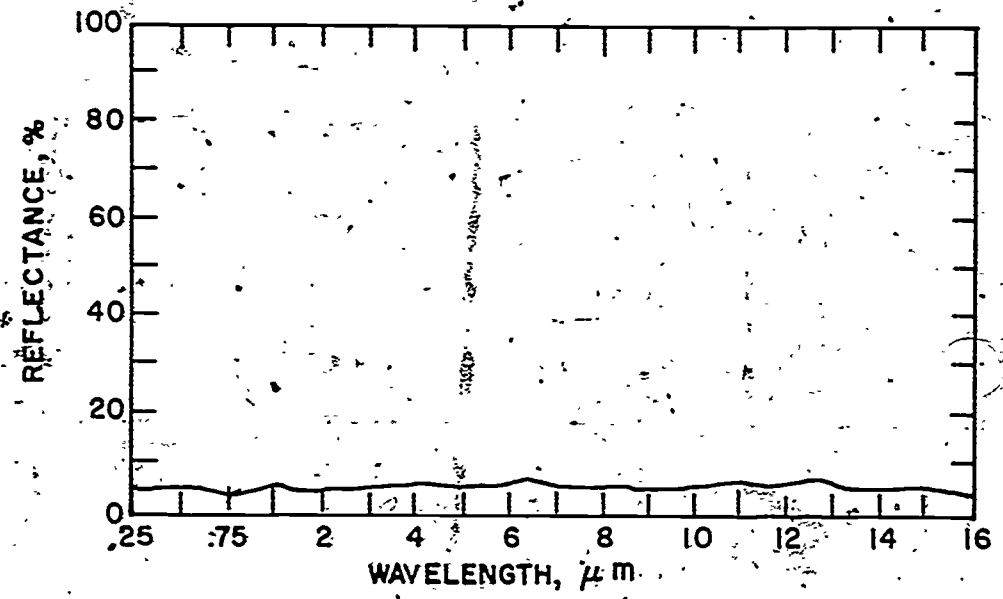


Figure 3 Spectral Reflectance of Flat-Black Paint [66]

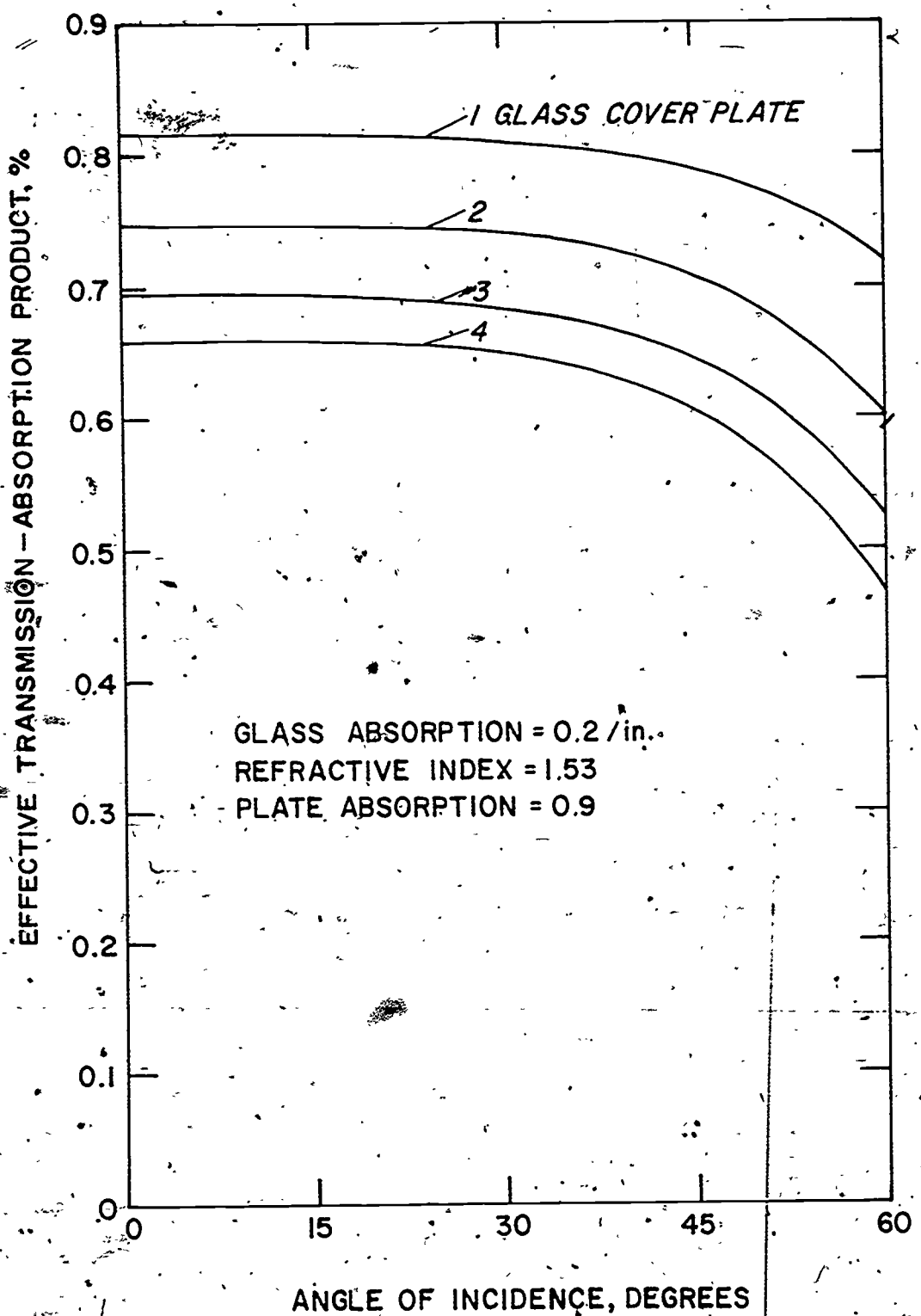


Figure 4 Transmittance-Absorptance Product for Multiple-Cover Flat-Black Coating Combinations on a Flat-Plate Solar Collector [17]

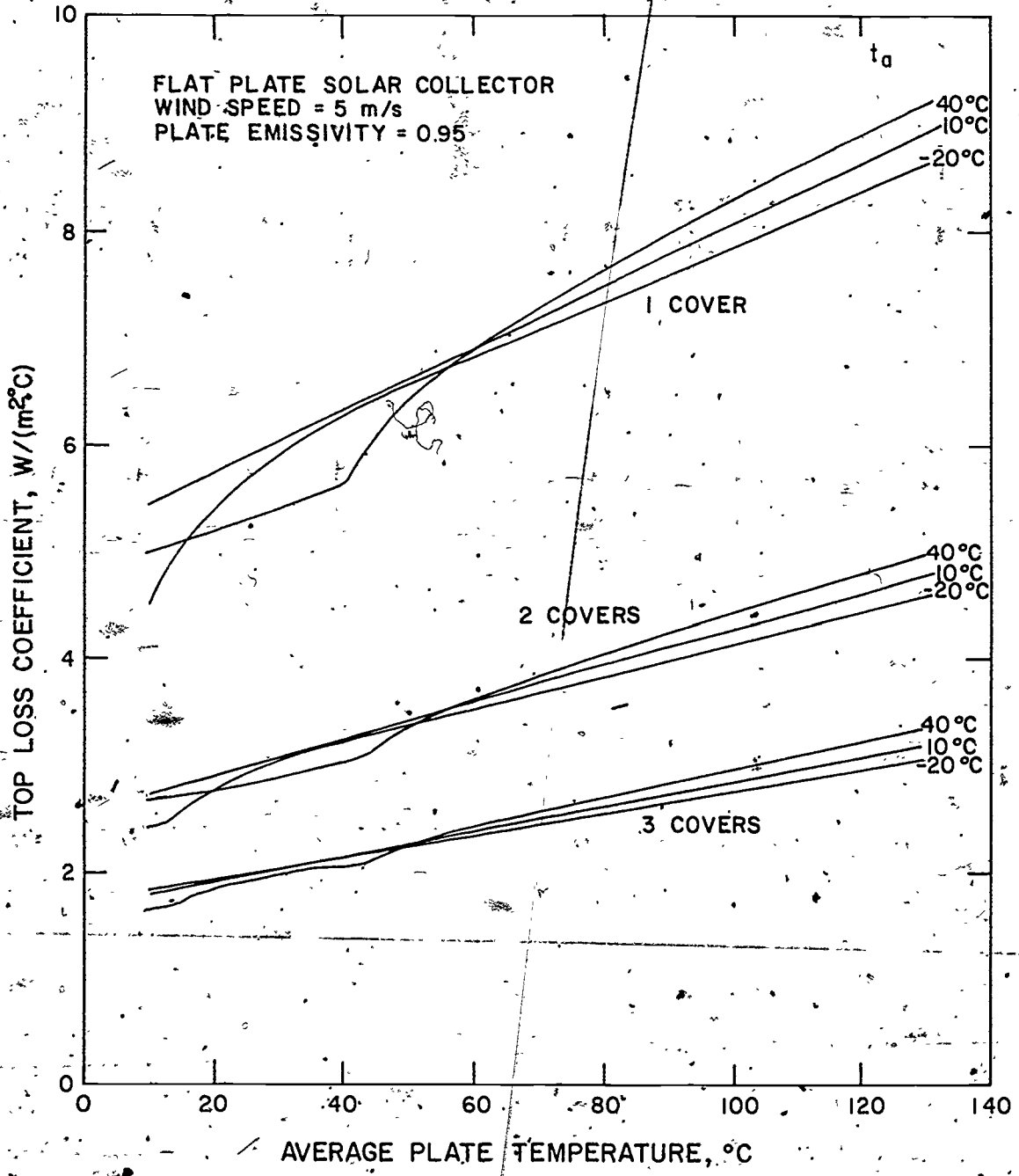


Figure 5. Top Loss Coefficient for Multiple-Cover Flat-Plate Solar Collectors as a Function of Ambient and Plate Temperature [18]

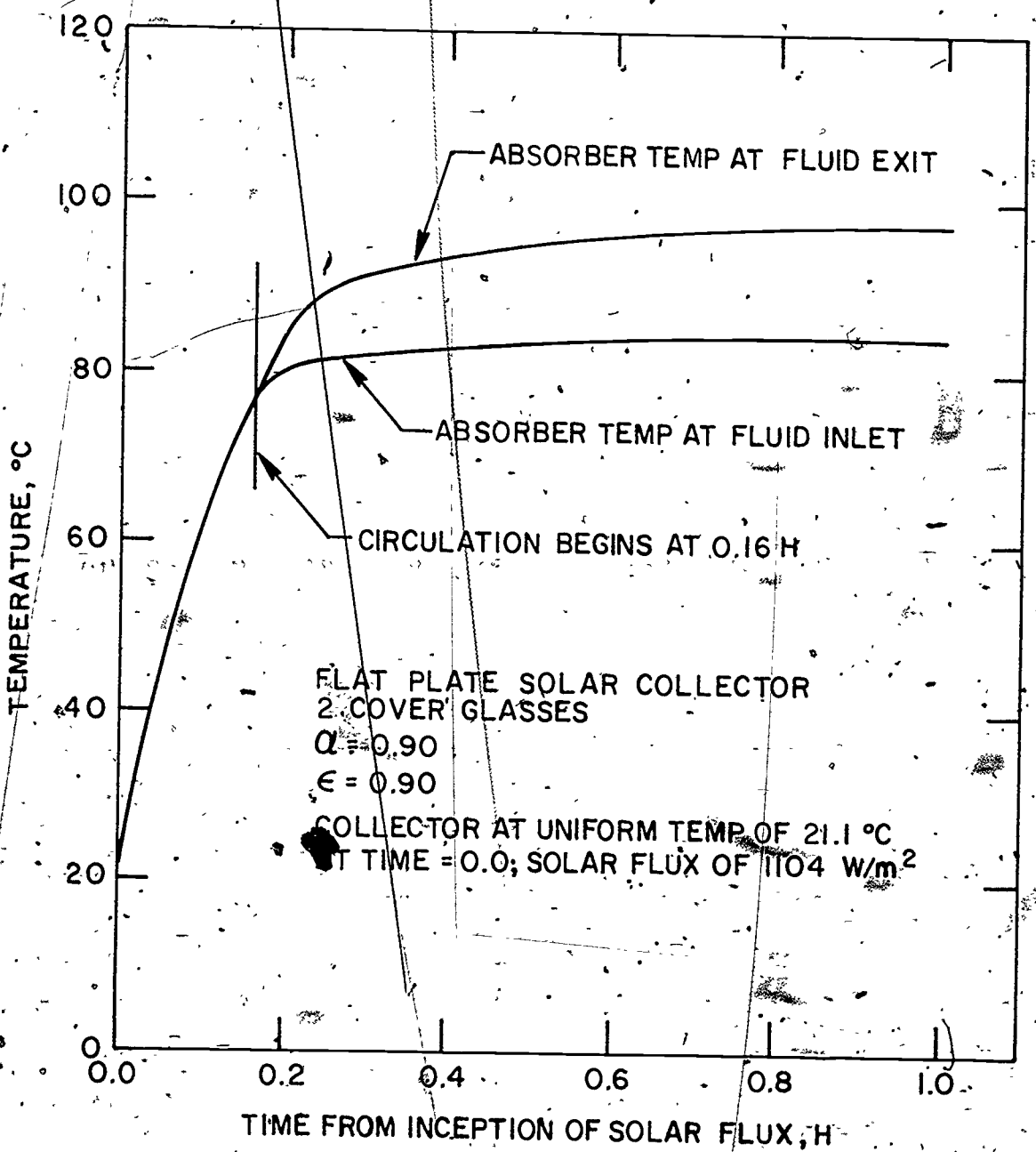


Figure 6 Thermal Response Characteristics of a Liquid-Heating Flat-Plate Solar Collector [19]

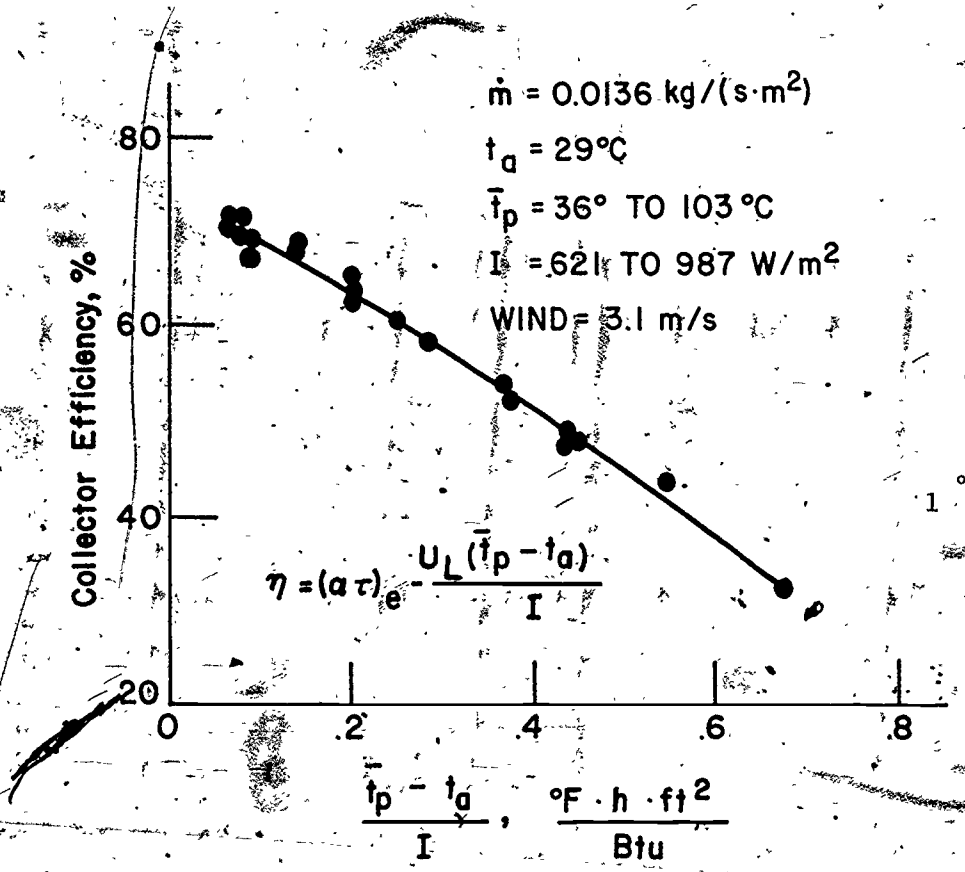


$$1 \frac{°F \cdot h \cdot ft^2}{Btu} = 0.176 \frac{°C \cdot m^2}{W}$$

Figure 7 Efficiency Curve for a Double-Glazed Flat-Plate Liquid-Heating Solar Collector with a Selective Coating on the Absorber [29]

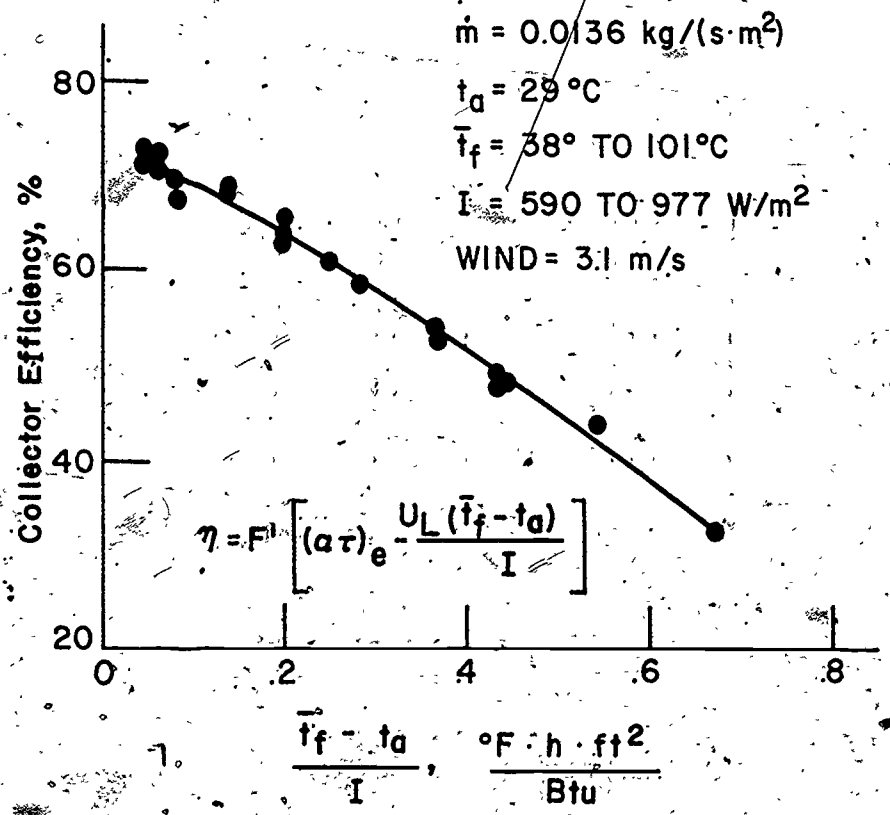


$$1 \frac{°F \cdot h \cdot ft^2}{Btu} = 0.176 \frac{°C \cdot m^2}{W}$$

Figure 8 Efficiency Curve for a Double-Glazed Flat-Plate Liquid-Heating Solar Collector with a Selective Coating on the Absorber [29]

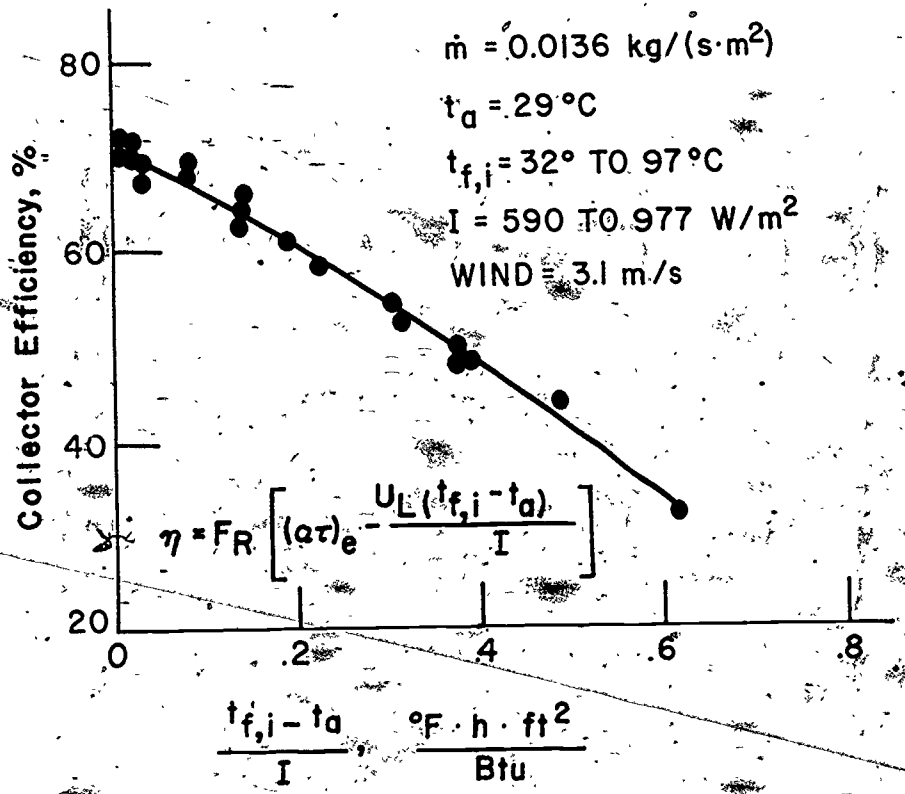


$$1\ \frac{°F \cdot h \cdot ft^2}{Btu} = 0.176\ \frac{°C \cdot m^2}{W}$$

Figure 9 Efficiency Curve for a Double-Glazed Flat-Plate Liquid-Heating Solar Collector with a Selective Coating on the Absorber [29]

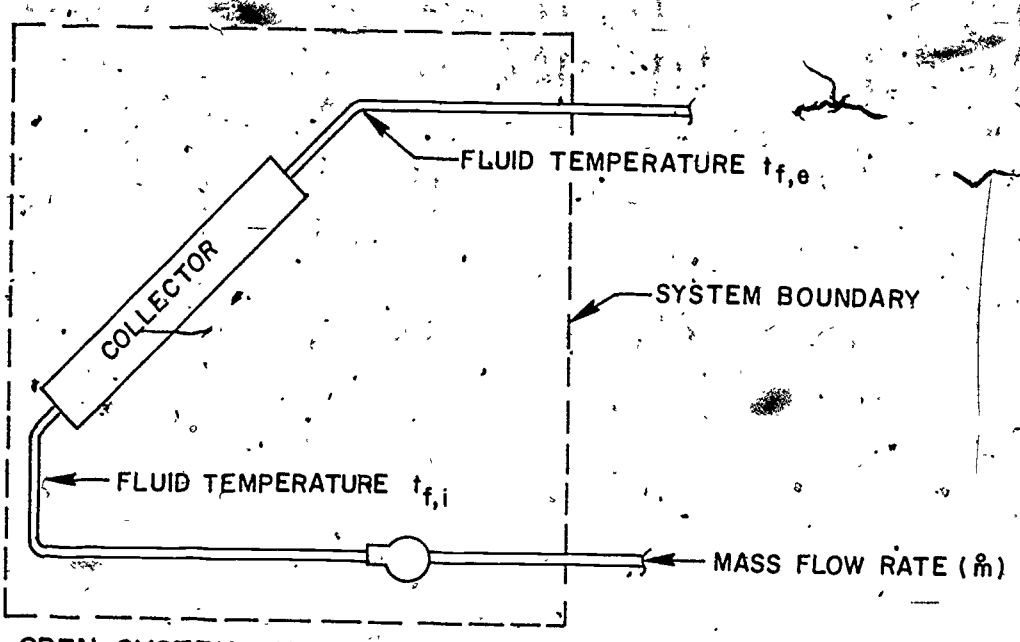


OPEN SYSTEM - INSTANTANEOUS PROCEDURE

Governing Equation : $\dot{Q} = \dot{m} c_{tf} (t_{f,e} - t_{f,i})$

Where $\dot{Q}$ = Heat Delivered by Collector,

$c_{t,f}$ = Fluid Heat Capacity ,

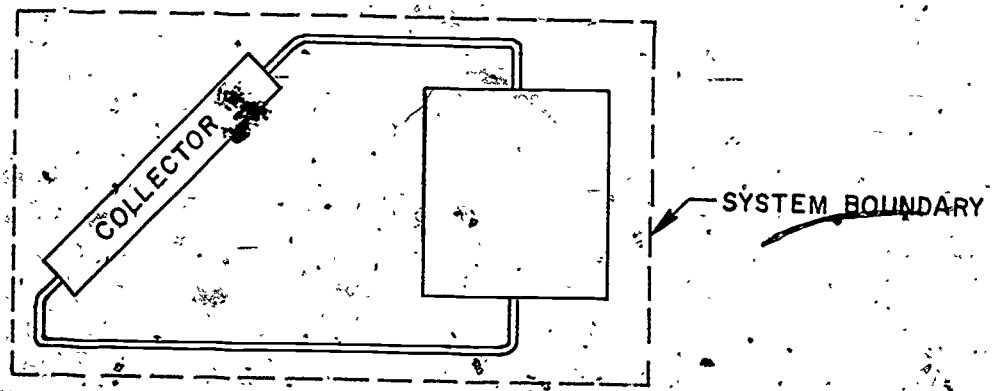


CLOSED SYSTEM – CALORIMETRIC PROCEDURE

Governing Equation: $\dot{Q} = mc_p \frac{dt}{dT}$

Where m = Total System Mass,

$\frac{dt}{dT}$ = Time Rate of Change of Temperature

Figure 10. Schematic Representation of the Two Basic Methods of Determining Solar Collector Thermal Efficiency [65]

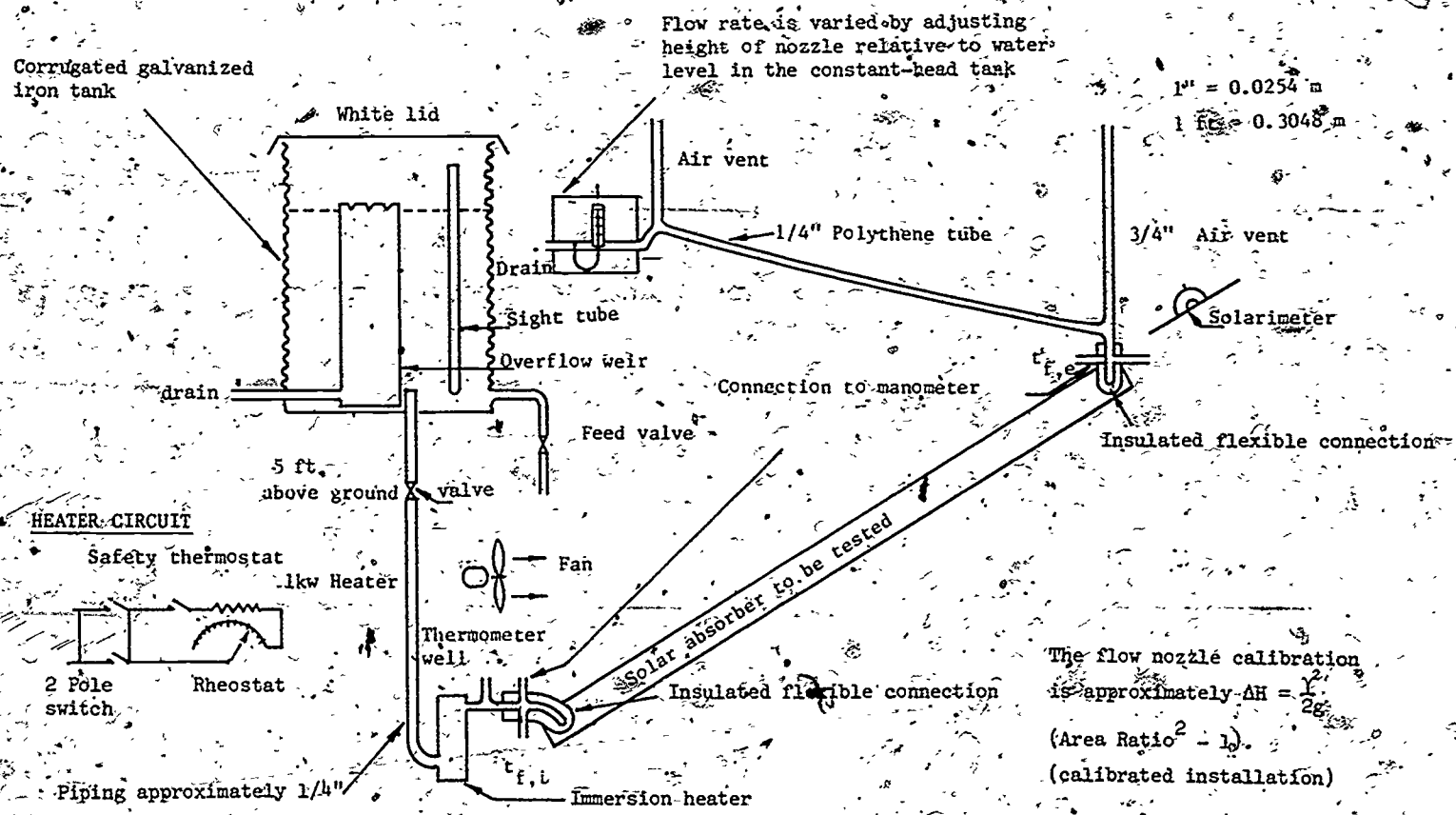


The flow nozzle calibration is approximately $\Delta H = \frac{V^2}{2g}$ (Area Ratio$^2$ - 1). (calibrated installation)

Figure 11 Apparatus Proposed by Whillier and Richards [31] for Determining the Thermal Efficiency of Solar Collectors

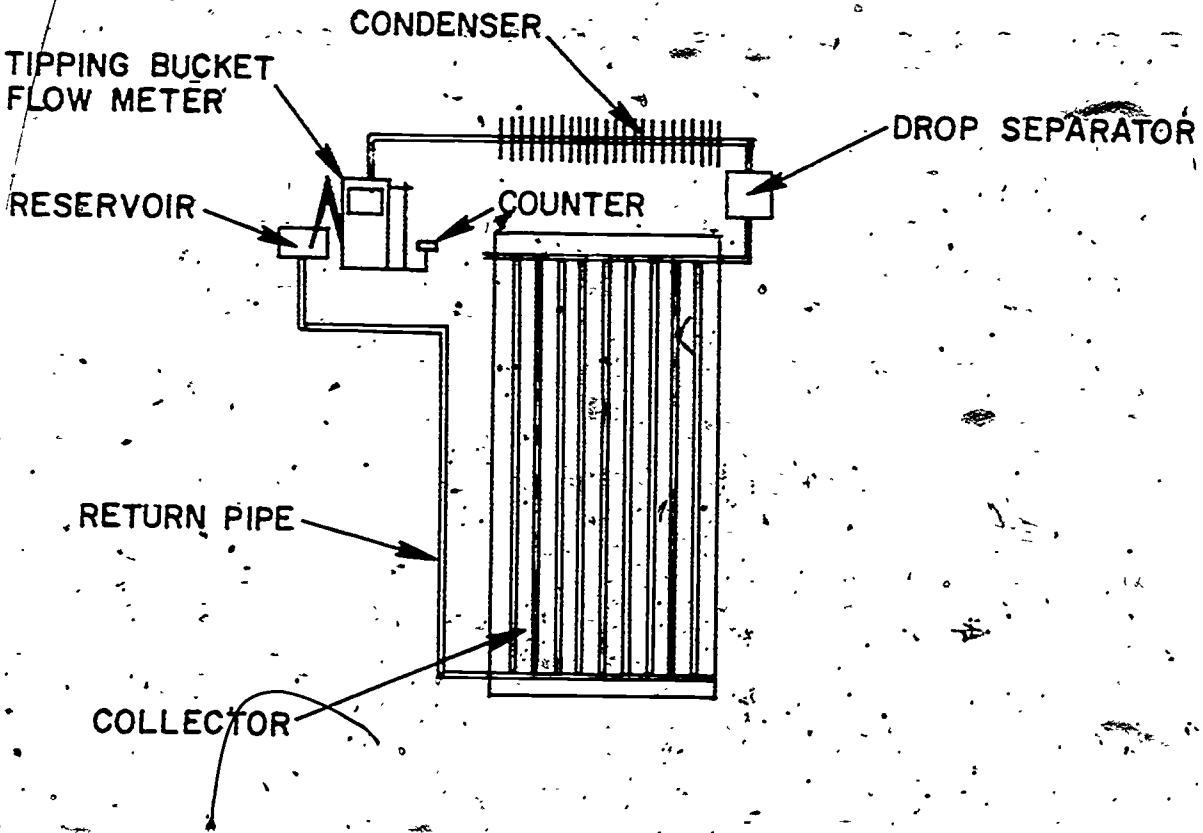


Figure 12 Apparatus Used by Doron [42] for Determining the Thermal Efficiency of Solar Collectors in which the Transfer Fluid "Boils"

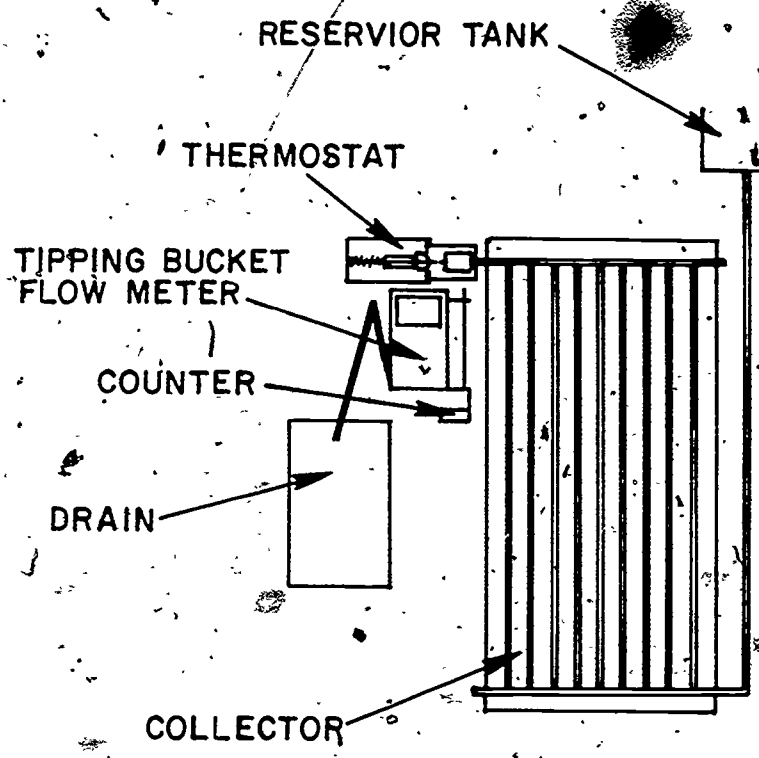


Figure 13 Apparatus Used by Doron [42] for Determining the Thermal Efficiency of Solar Collectors

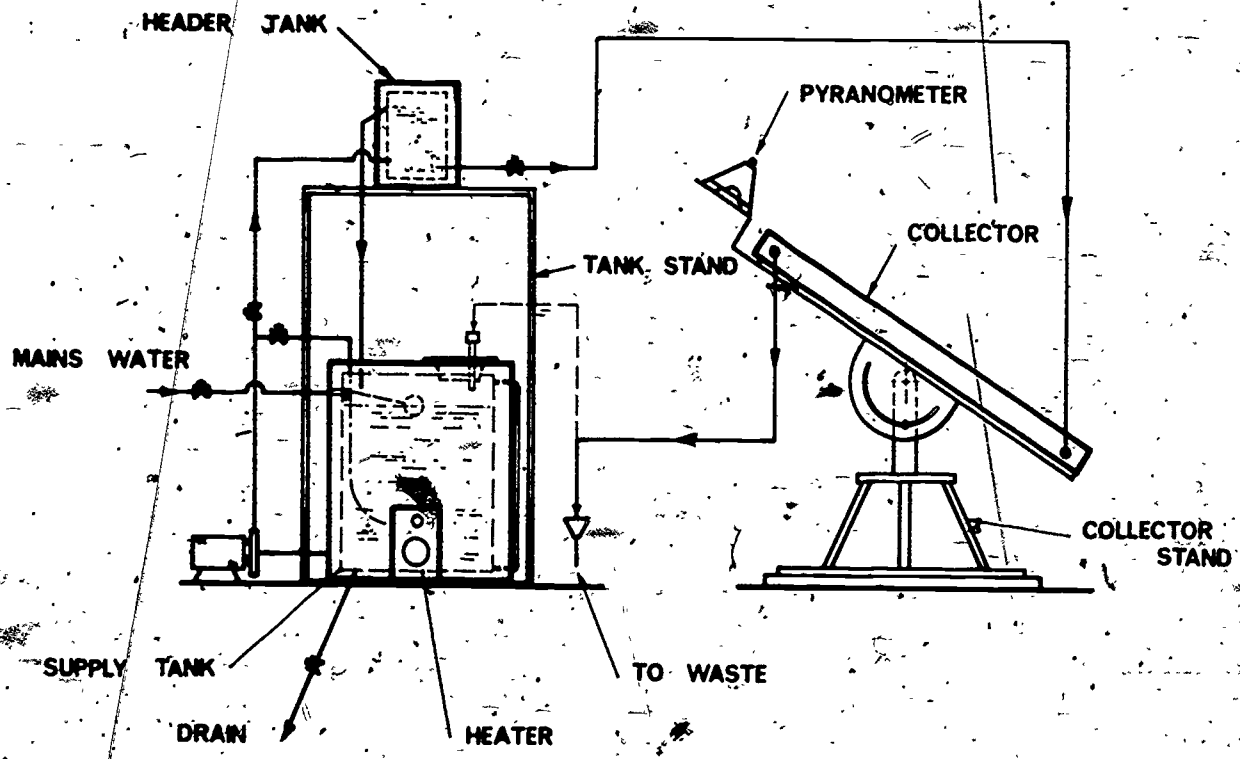


Figure 14 Schematic of the Experimental Test Rig Used at CSIRO for Determining Solar Collector Efficiency [44, 45]

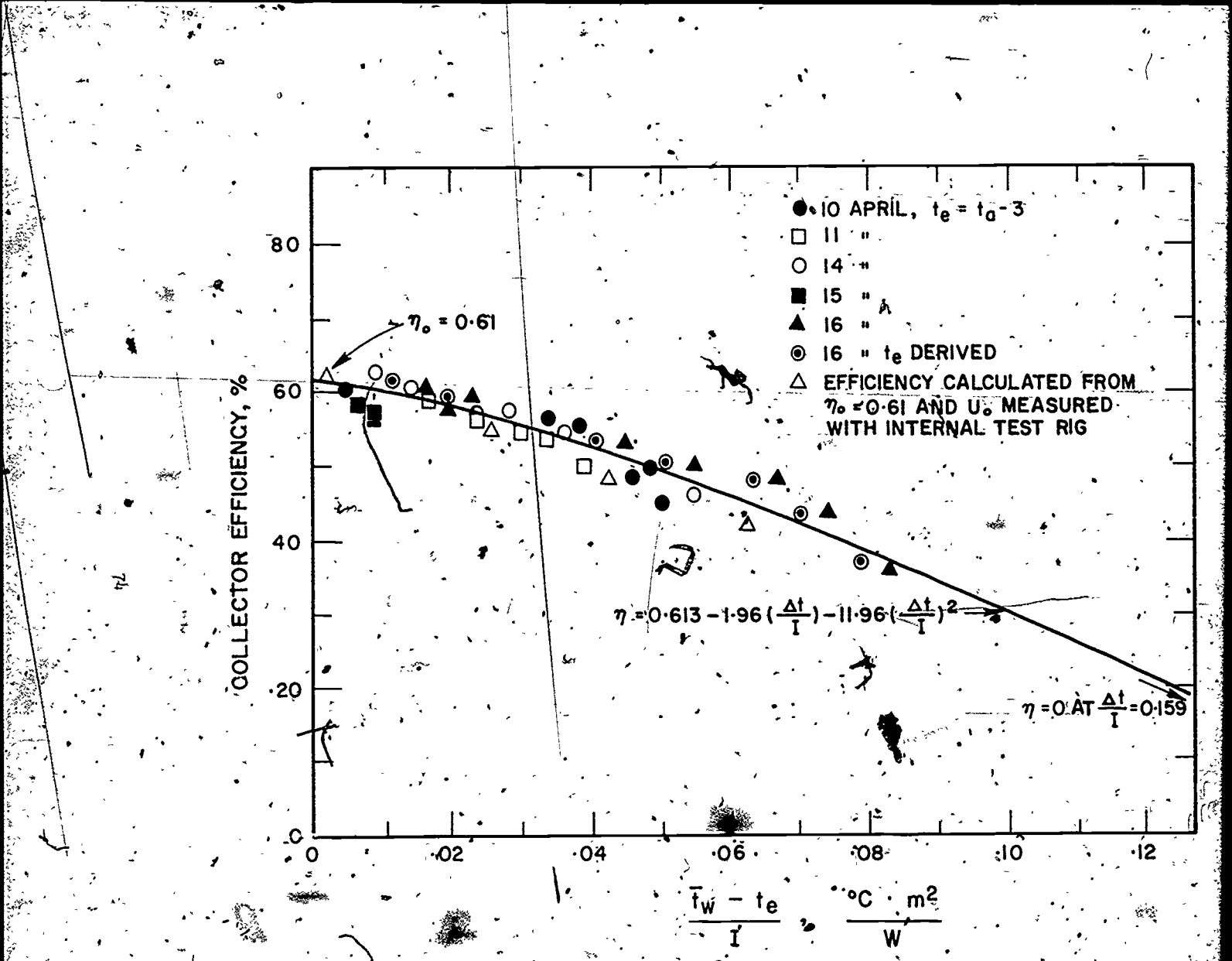


Figure 15 Solar Collector Efficiency for a Double-Glazed Selectively Coated Copper Absorber Collector [44, 45]

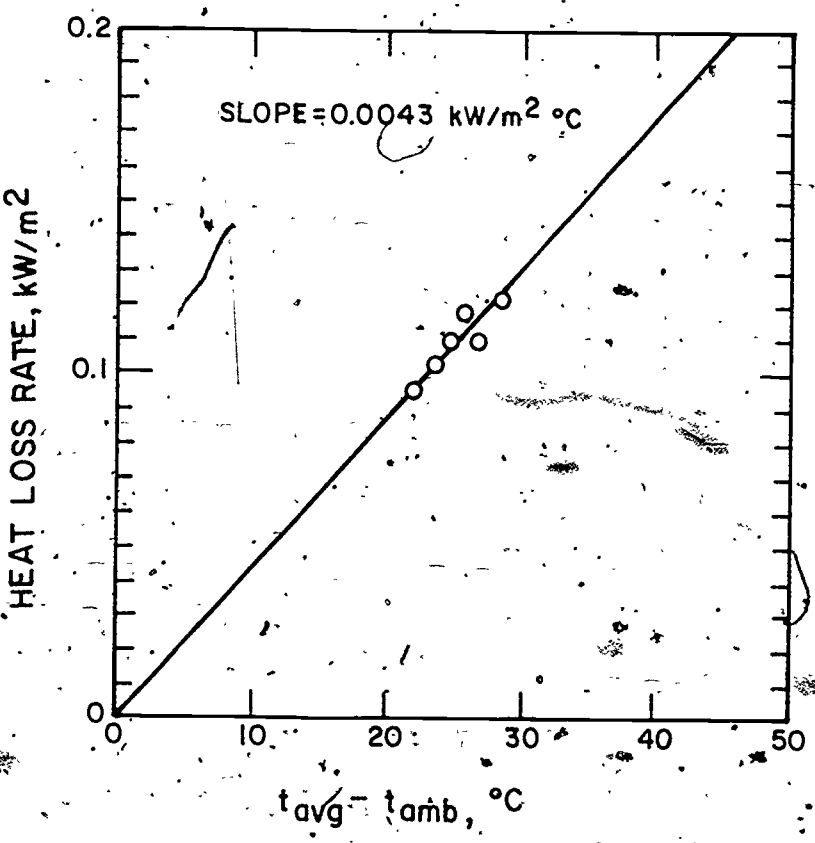


Figure 16 Heat Loss Rate as a Function of Temperature Difference for a Double-Glazed Liquid-Heating Flat-Plate Solar Collector [51]

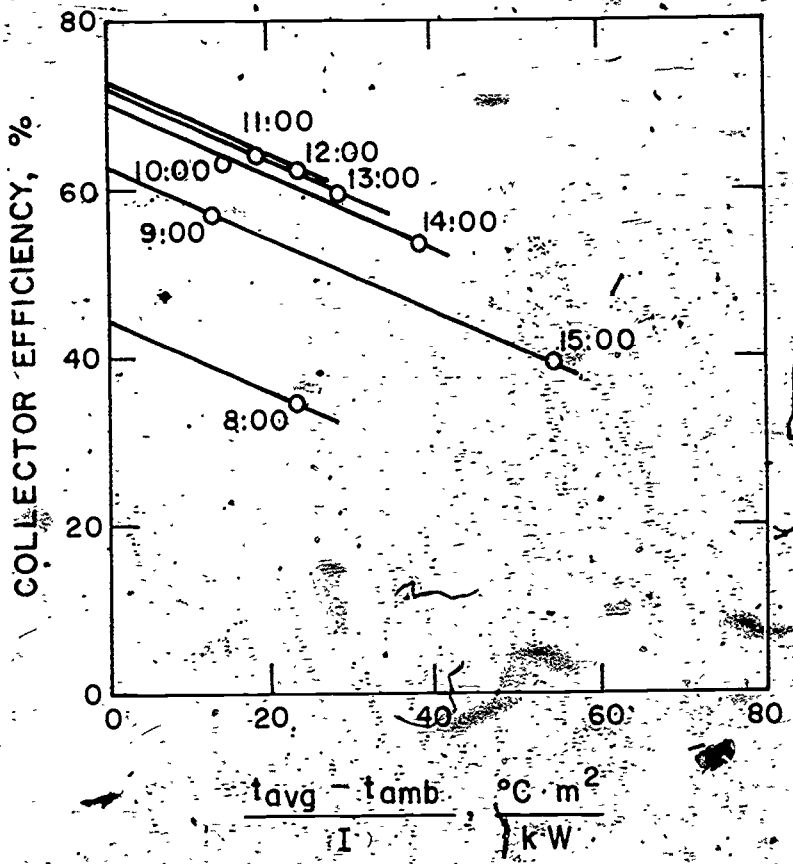


Figure 17. Efficiency Curve for a Double-Glazed Liquid-Heating Flat-Plate Solar Collector [31]

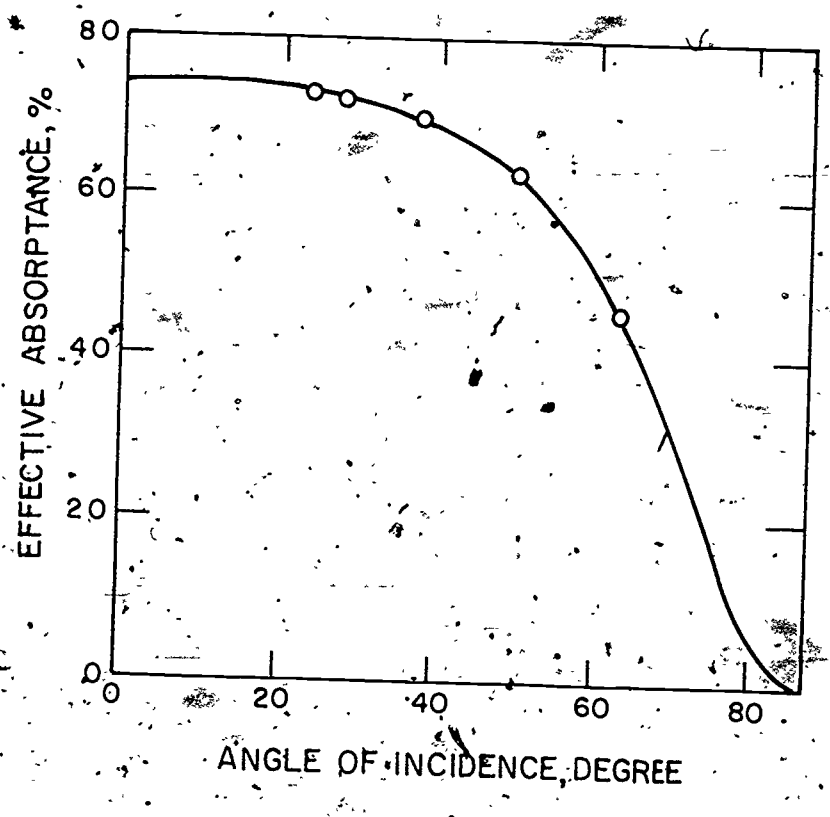


Figure 18 Effective Absorptance of a Double-Glazed Liquid-Heating Flat-Plate Collector as a Function of Incidence Angle [51]

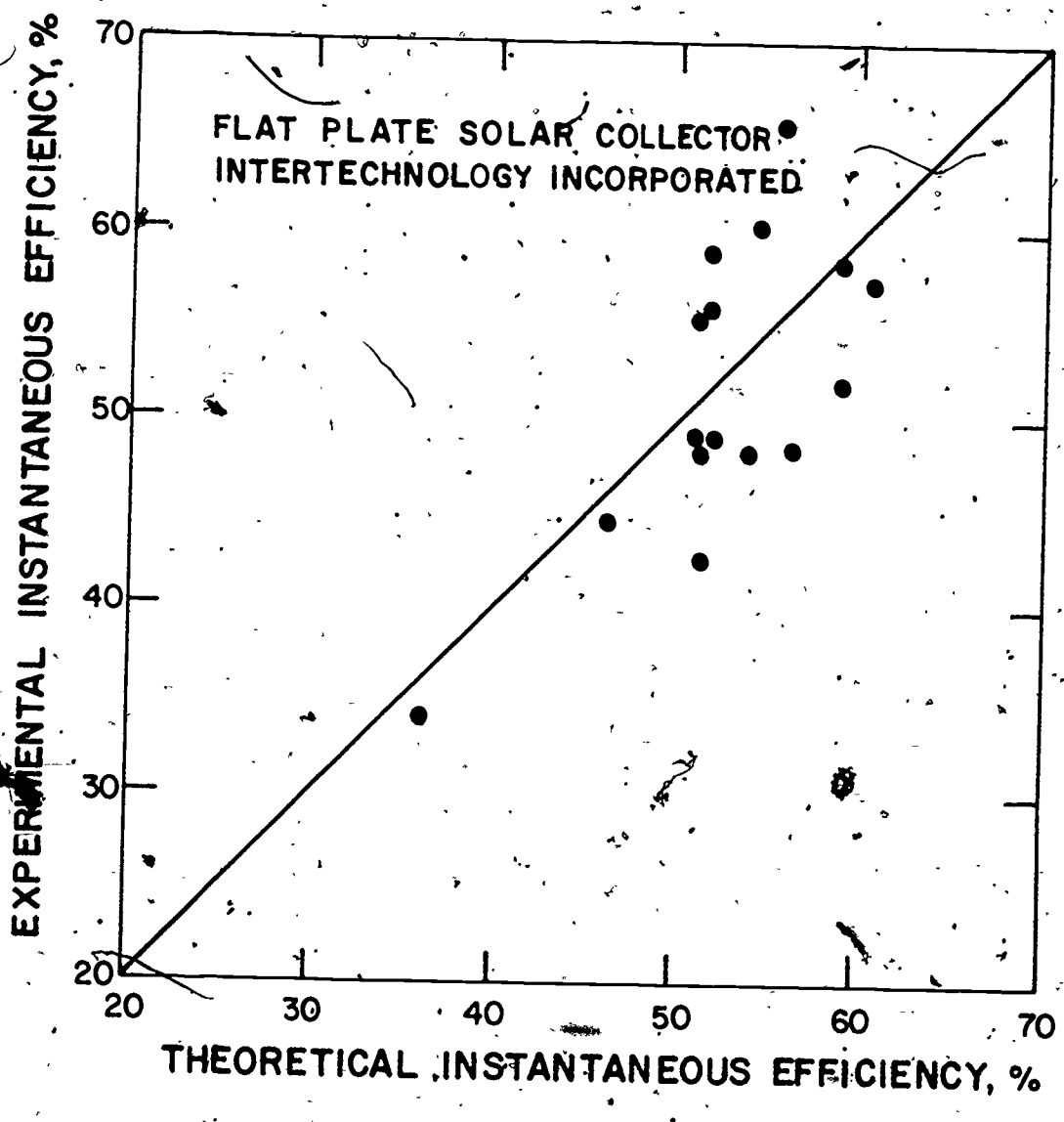


Figure 20 Measured Versus Predicted Thermal Efficiency for a Large Solar Collector Array Installed as part of a Solar Heating Experiment in Warrenton, Virginia [53]

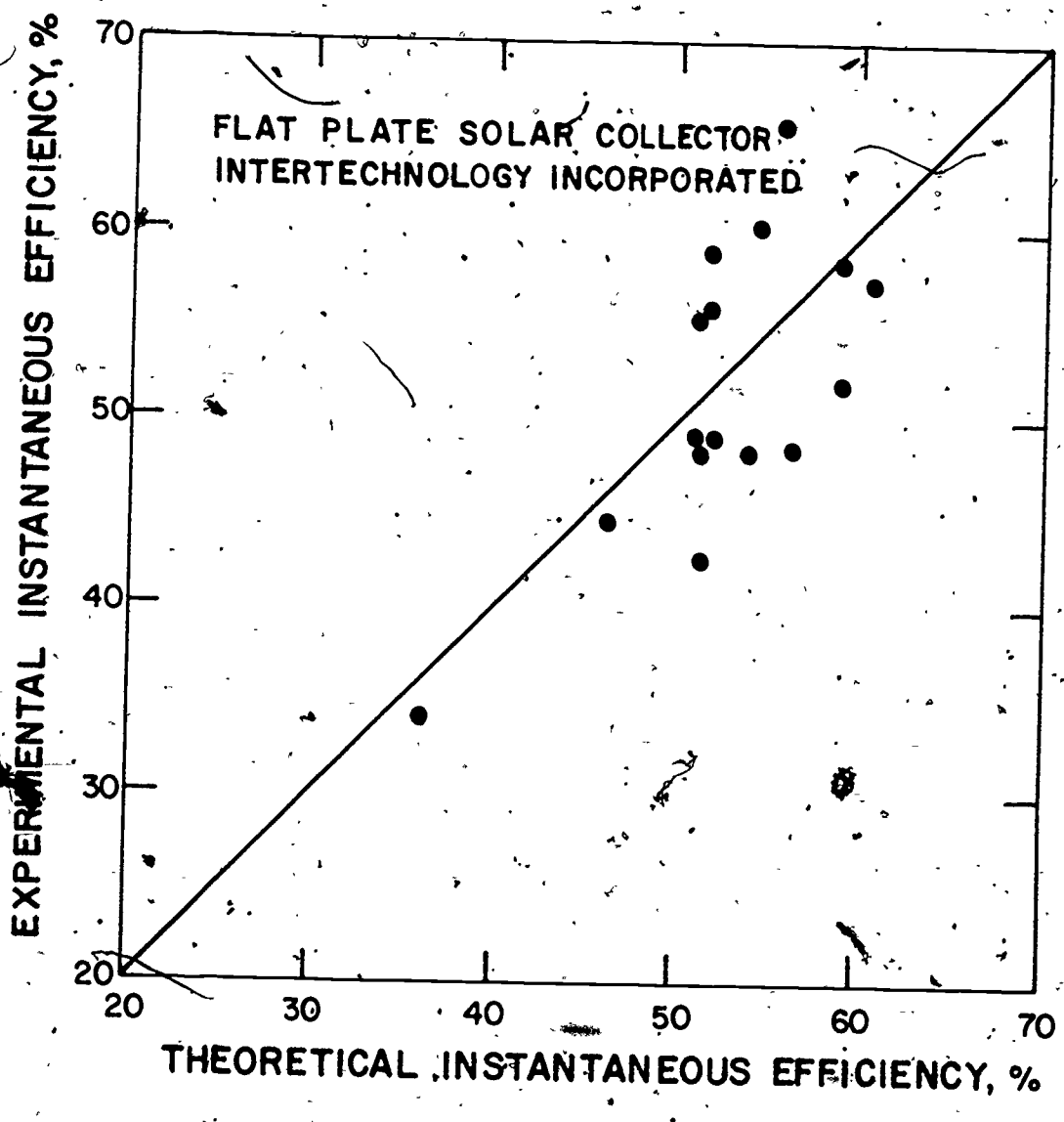


Figure 20 Measured Versus Predicted Thermal Efficiency for a Large Solar Collector Array Installed as part of a Solar Heating Experiment in Warrenton, Virginia [53]

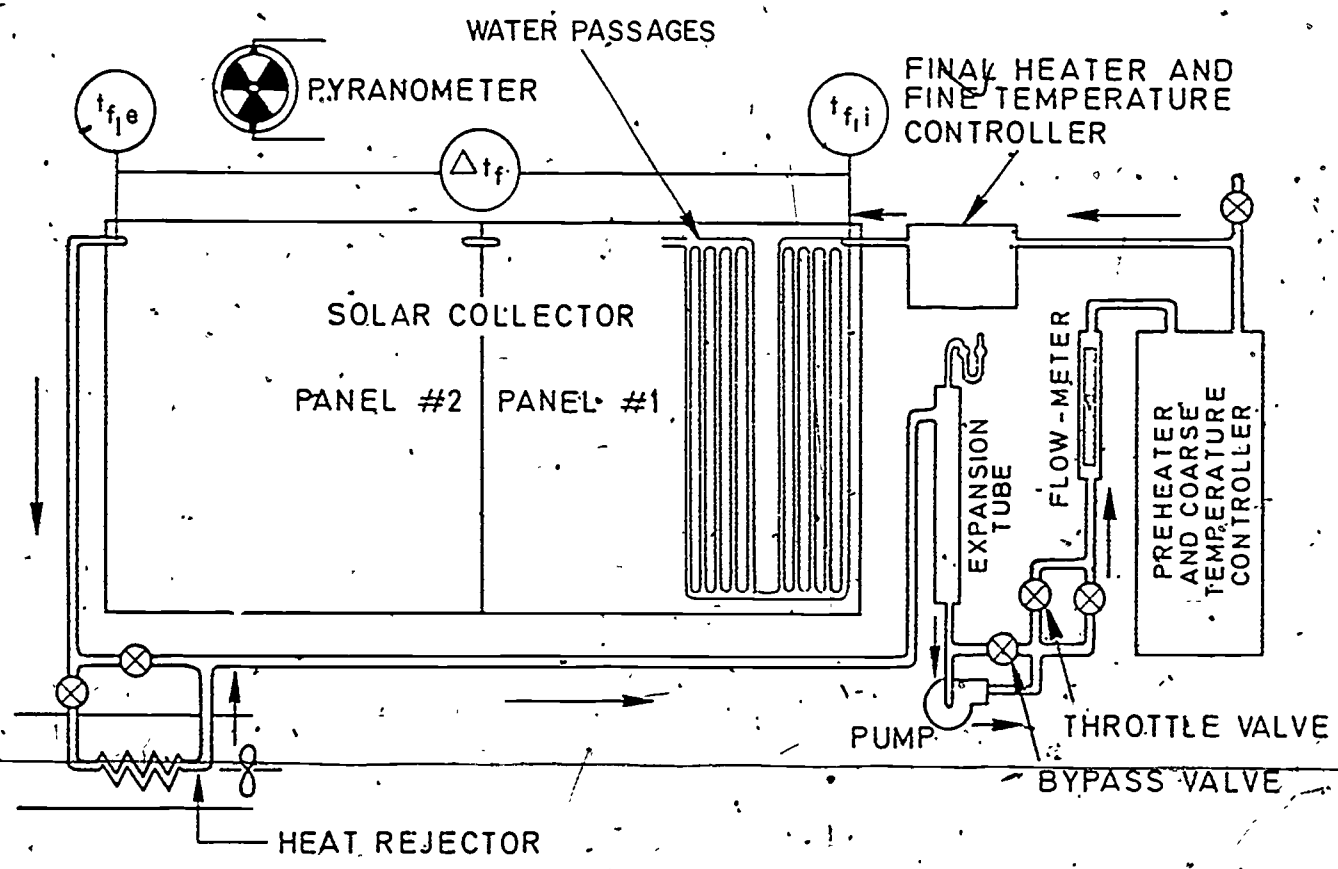


Figure 21 Schematic of the University of Pennsylvania's 1.2 x 2.4 m (4 x 8 ft) Solar Collector Test Facility

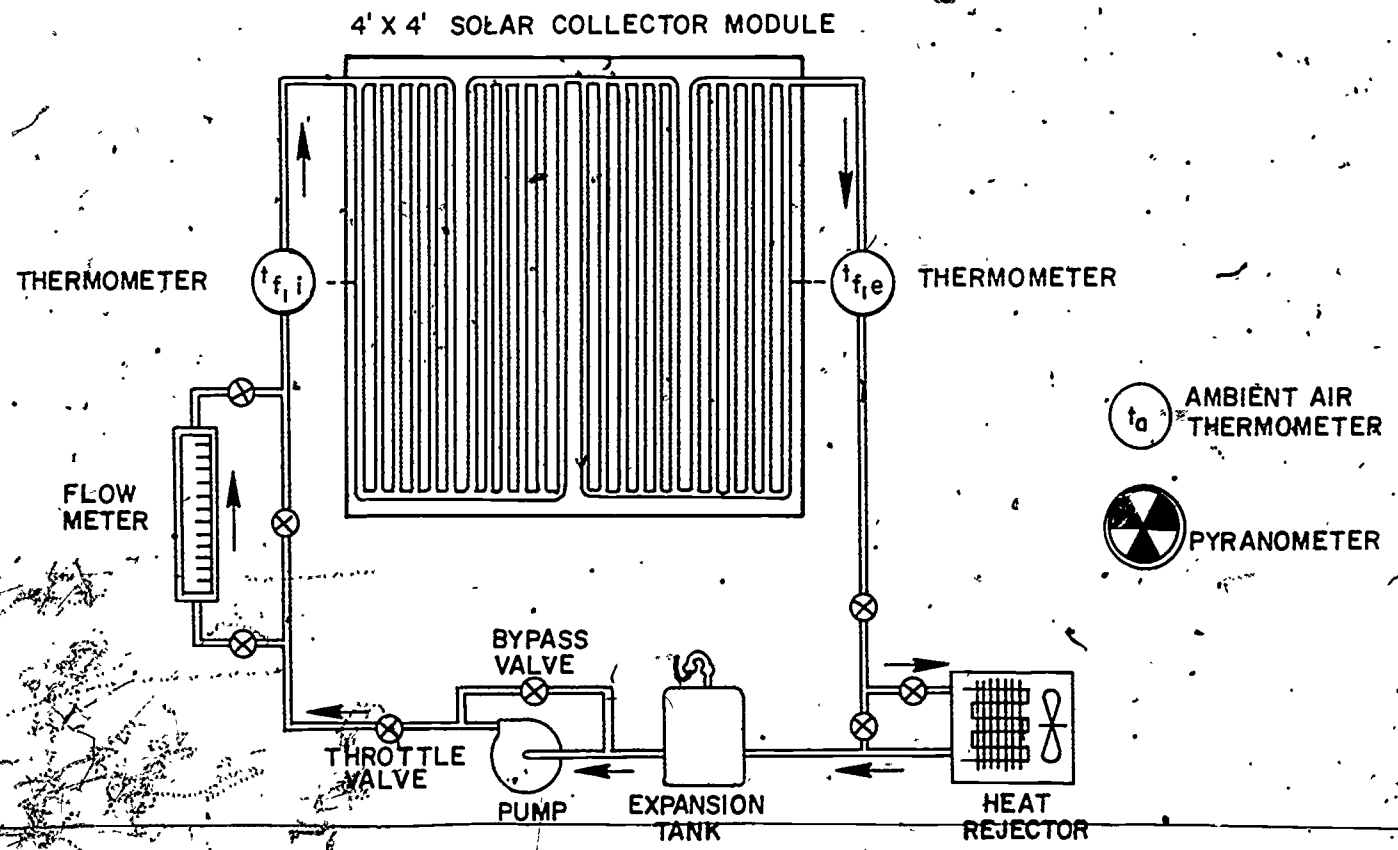


Figure 22 Schematic of the University of Pennsylvania's 1.2 x 1.2 m (4 x 4 ft) Solar Collector Test Facility

1 ft = 0.3048 m

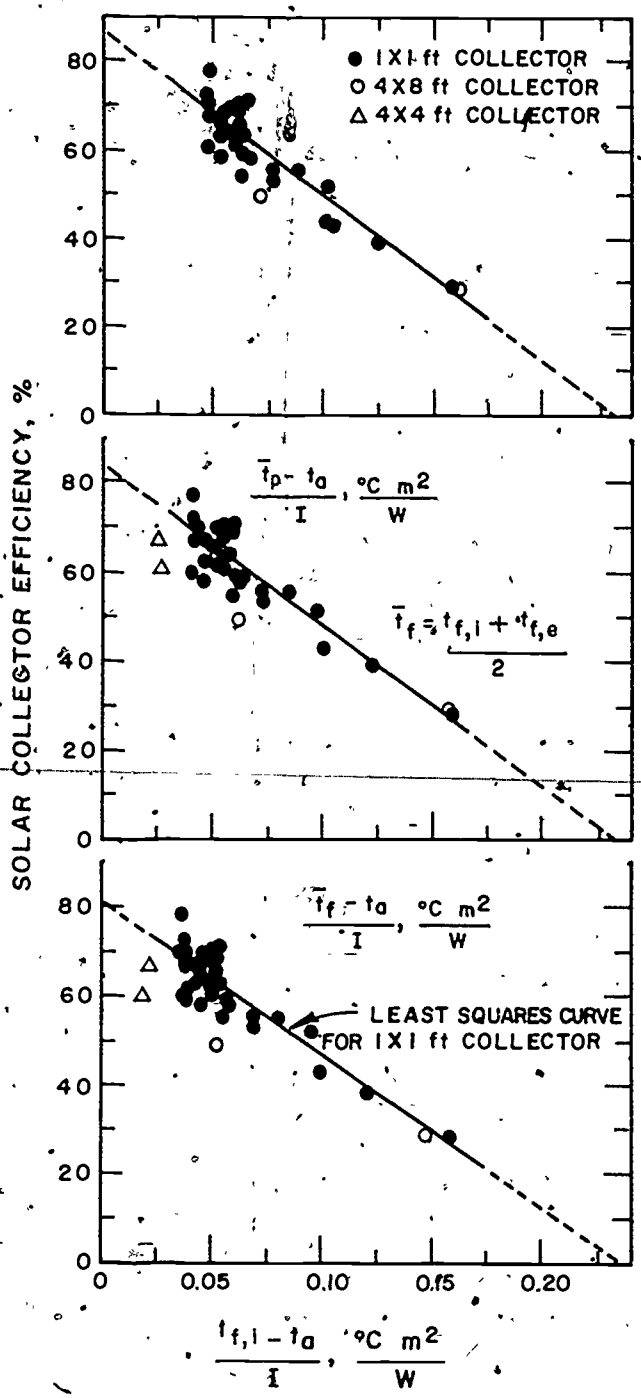


Figure 23 Efficiency Curve for a Double-Glazed Liquid-Heating Solar Collector of Three Different Sizes [56]

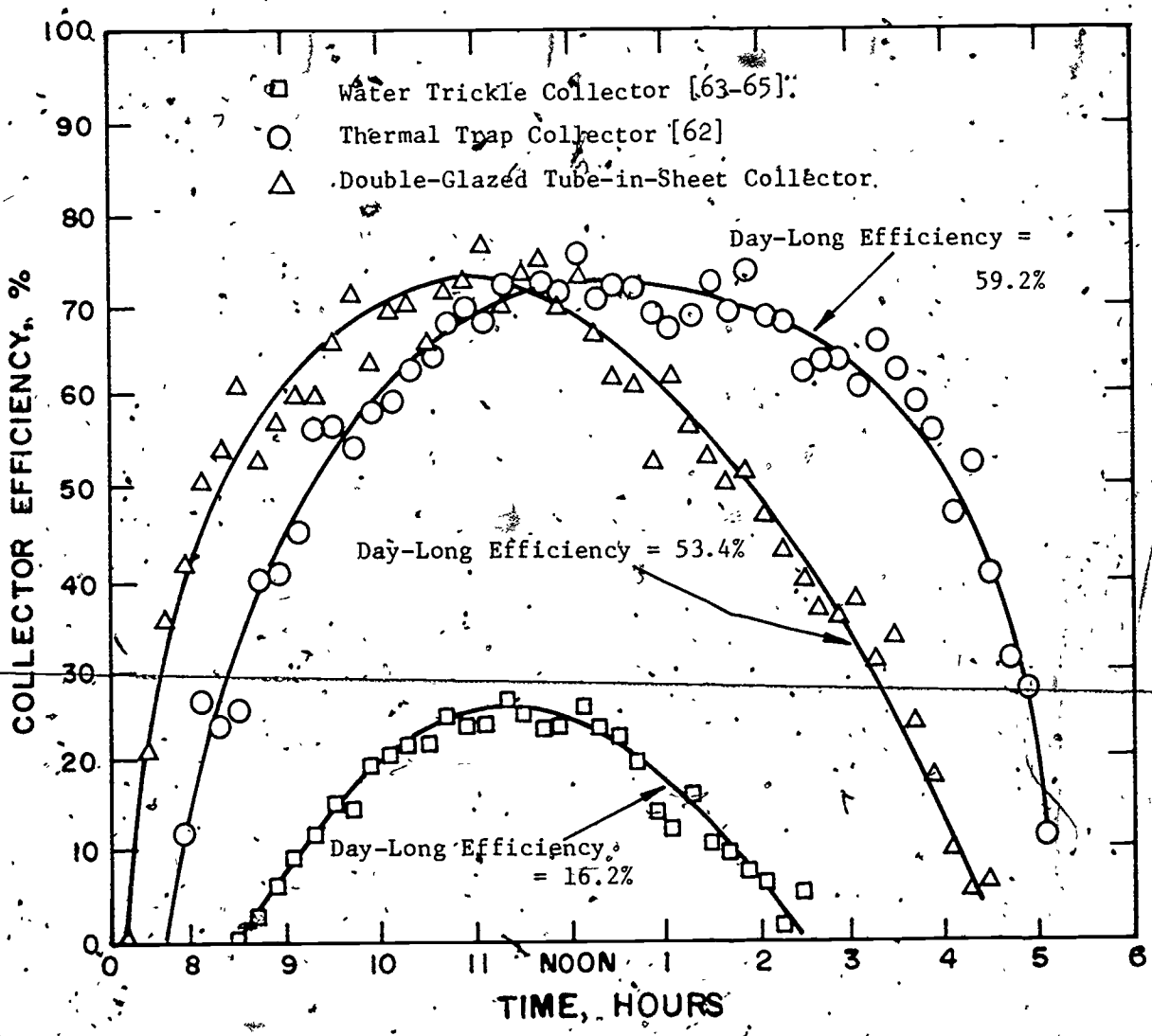


Figure 24 Thermal Efficiency of three different Liquid-Heating Solar Collectors as a Function of Time of Day [61]

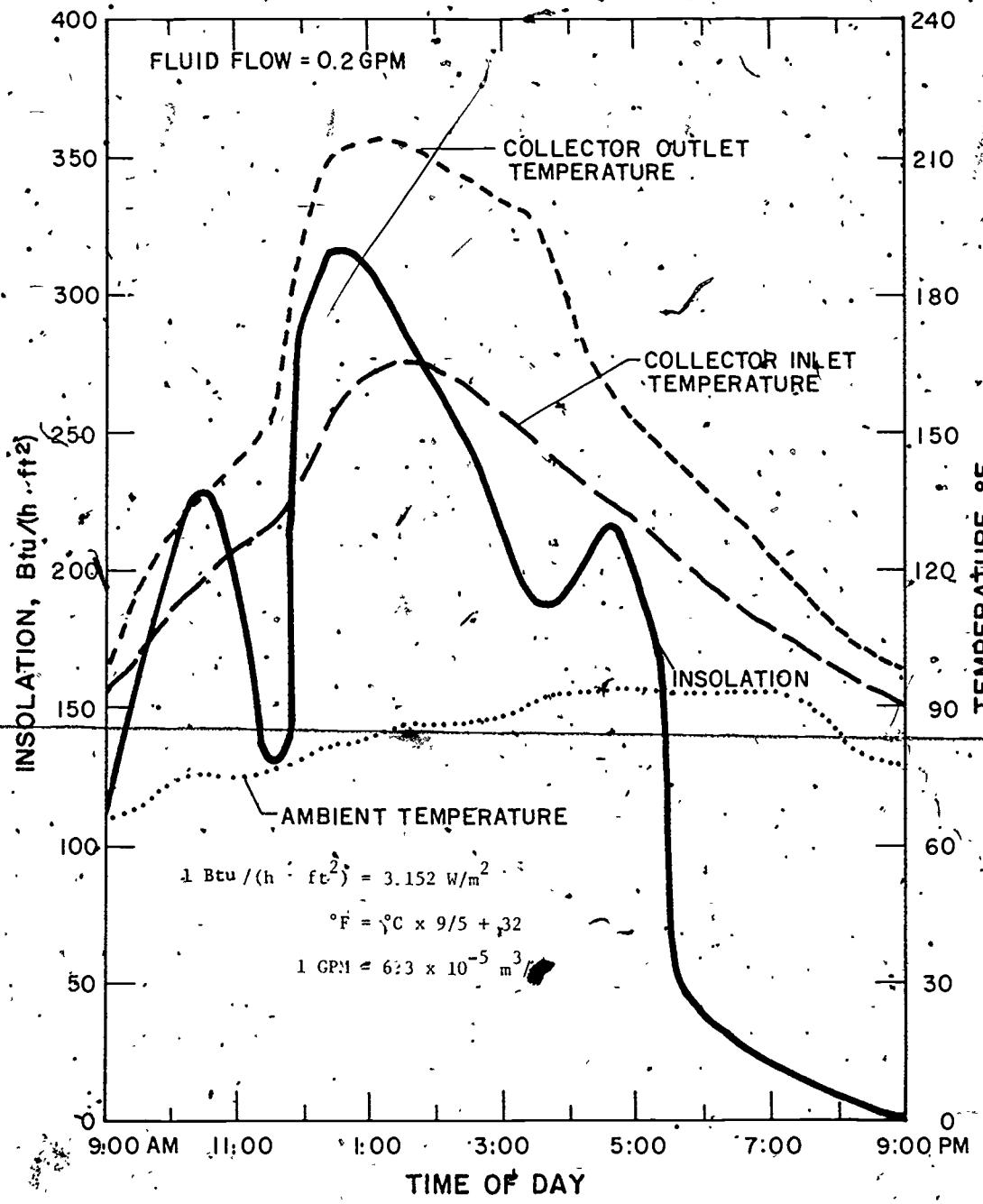


Figure 25 Thermal Efficiency of the Double - Glazed Liquid - Heating Solar Collector of Figure 1 as a Function of Time of Day [66]

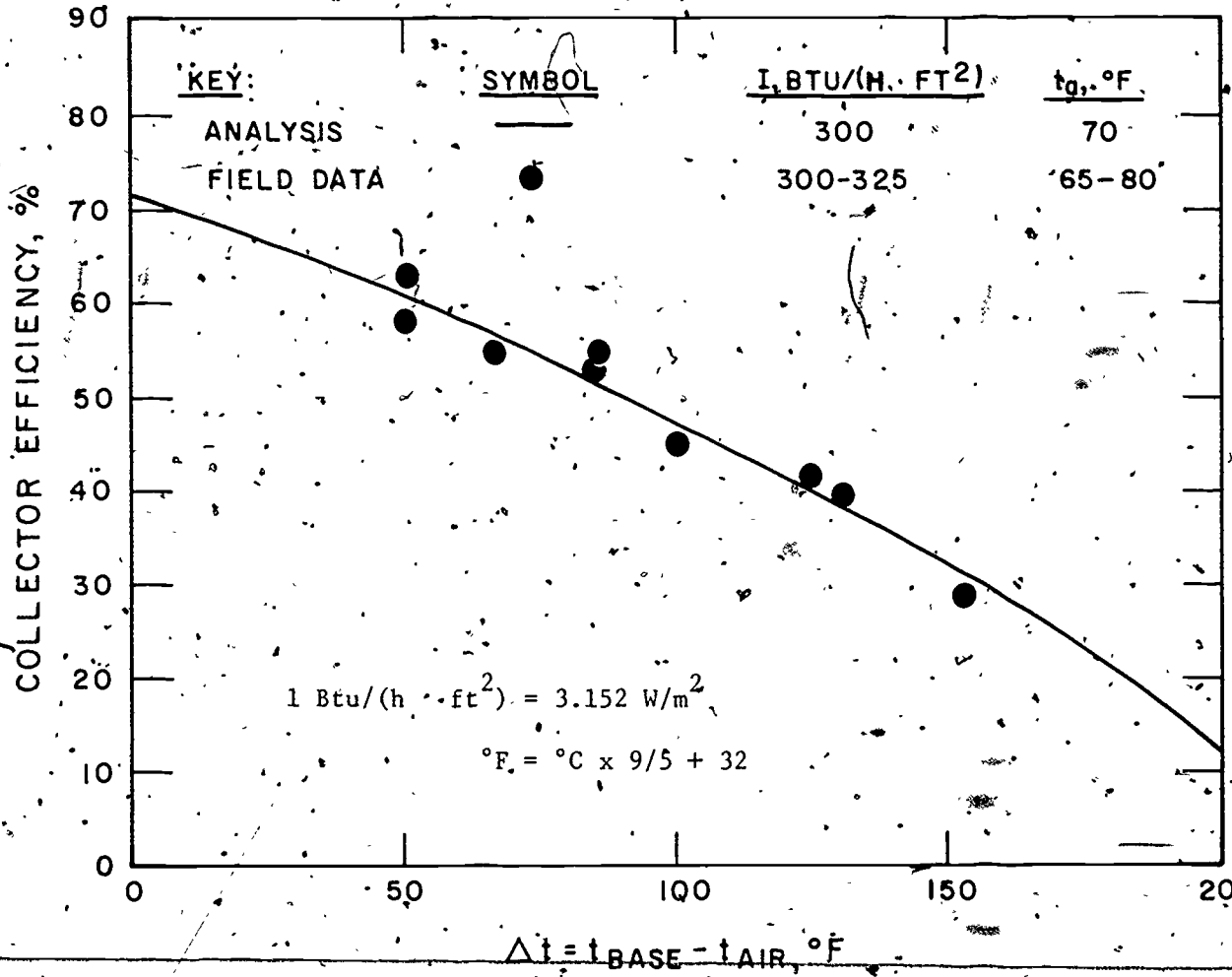


Figure 26 Efficiency Curve for the Double - Glazed Liquid-Heating Solar Collector of Figure 1 [66]

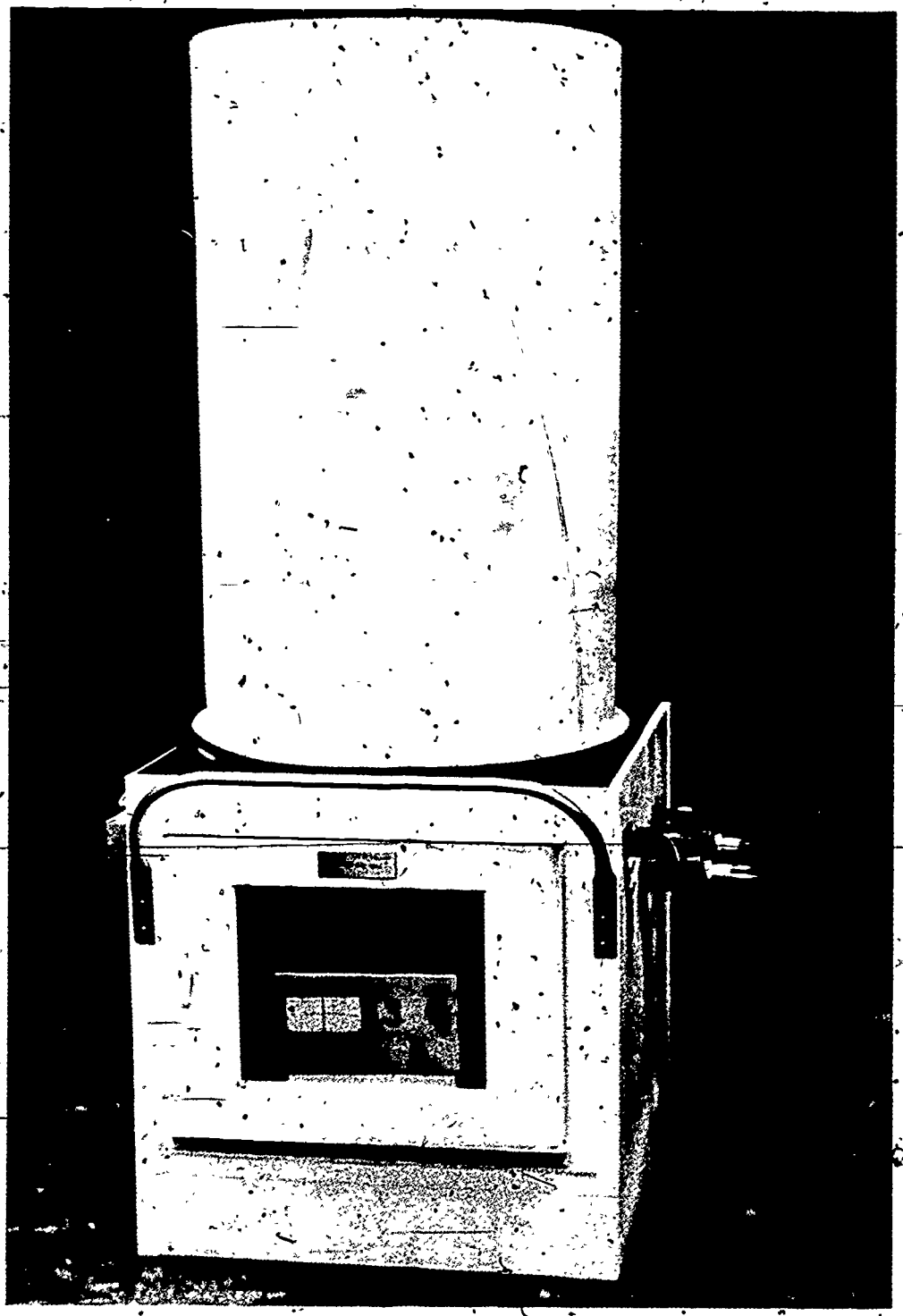

Figure 27 Arthur D. Little Calorimeter used for Determining the Thermal Efficiency of Solar Collectors [67]

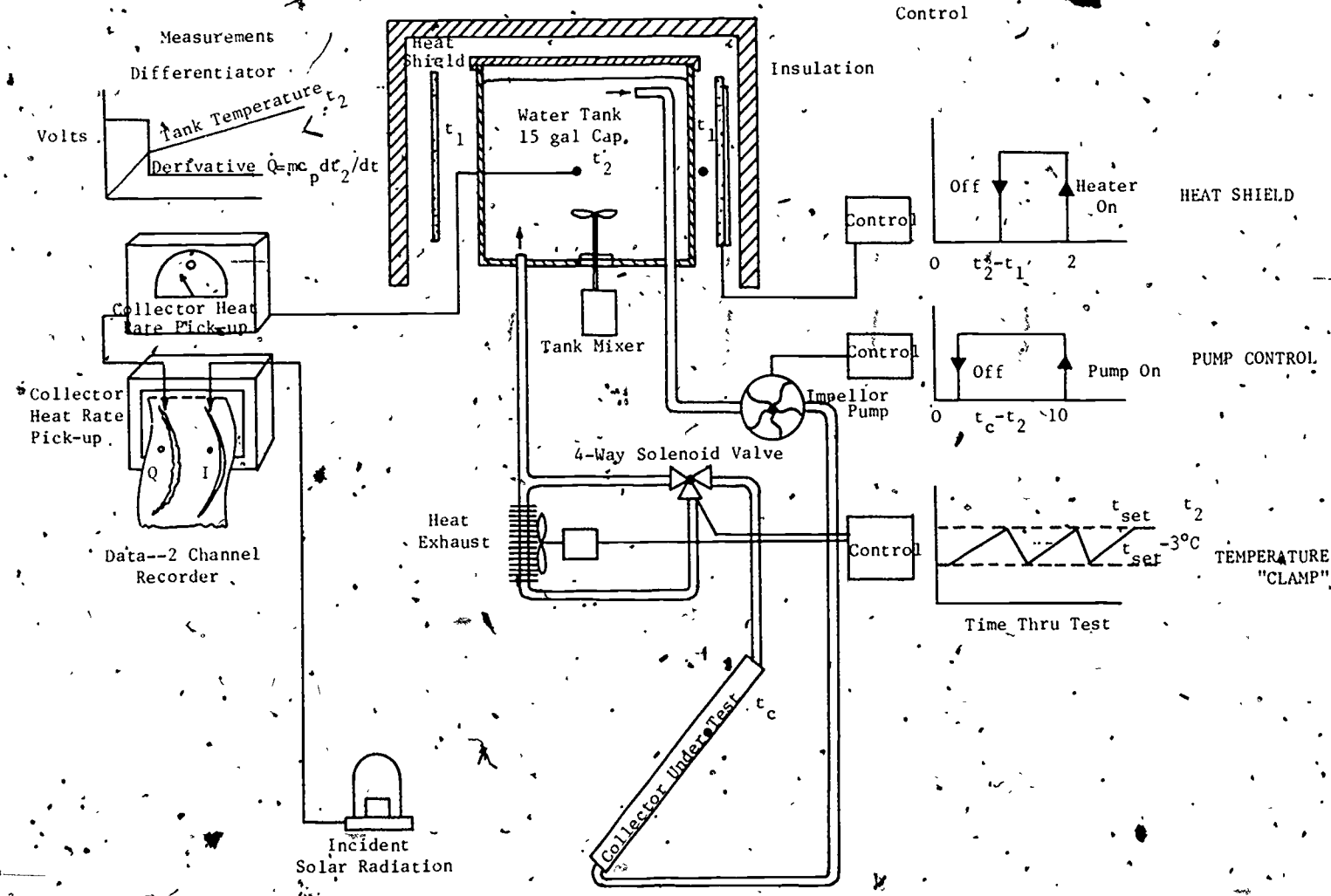


Figure 28. Schematic of the Arthur D. Little Calorimeter used for Determining the Thermal Efficiency of Solar Collectors [68]

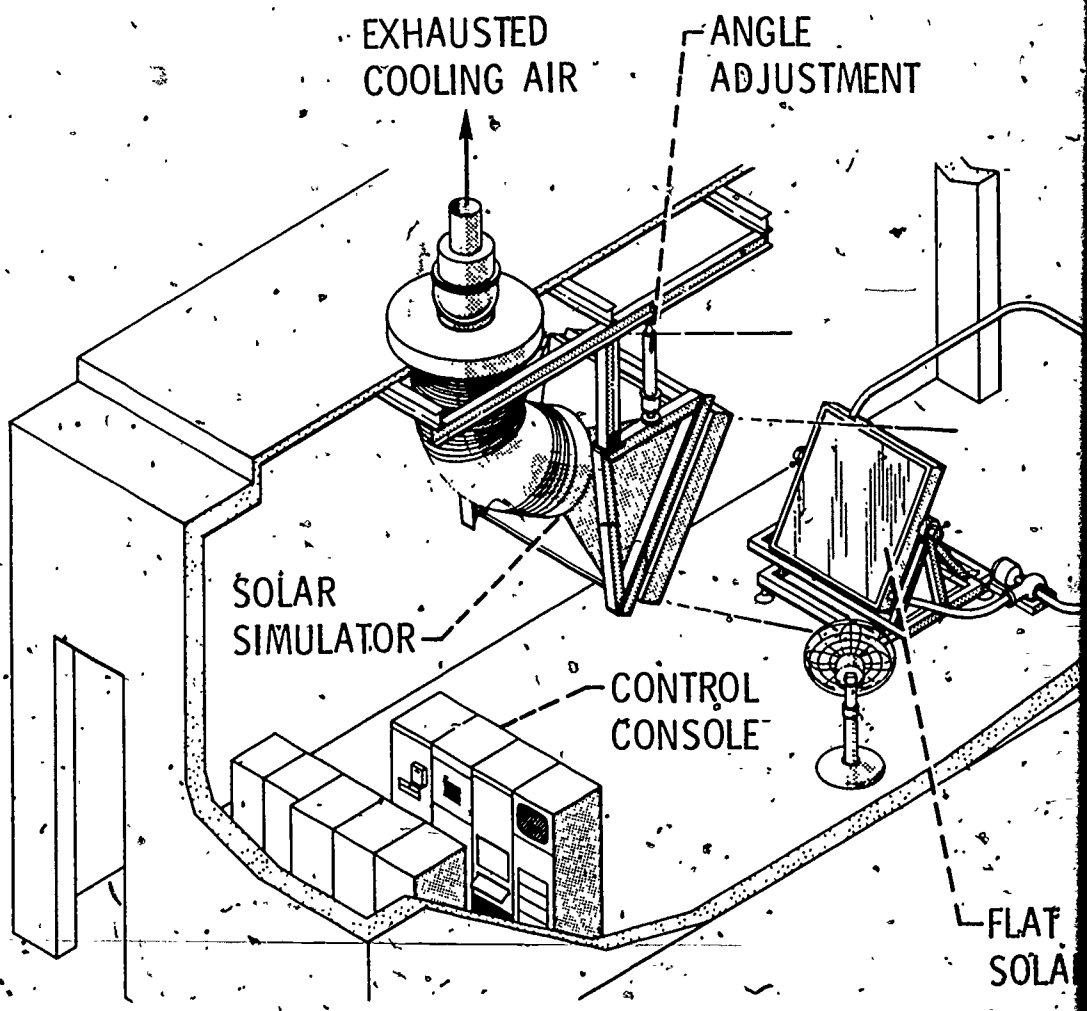


Figure 29 Schematic of the Indoor Solar Collector Test Facility at the NASA Lewis Research Center [

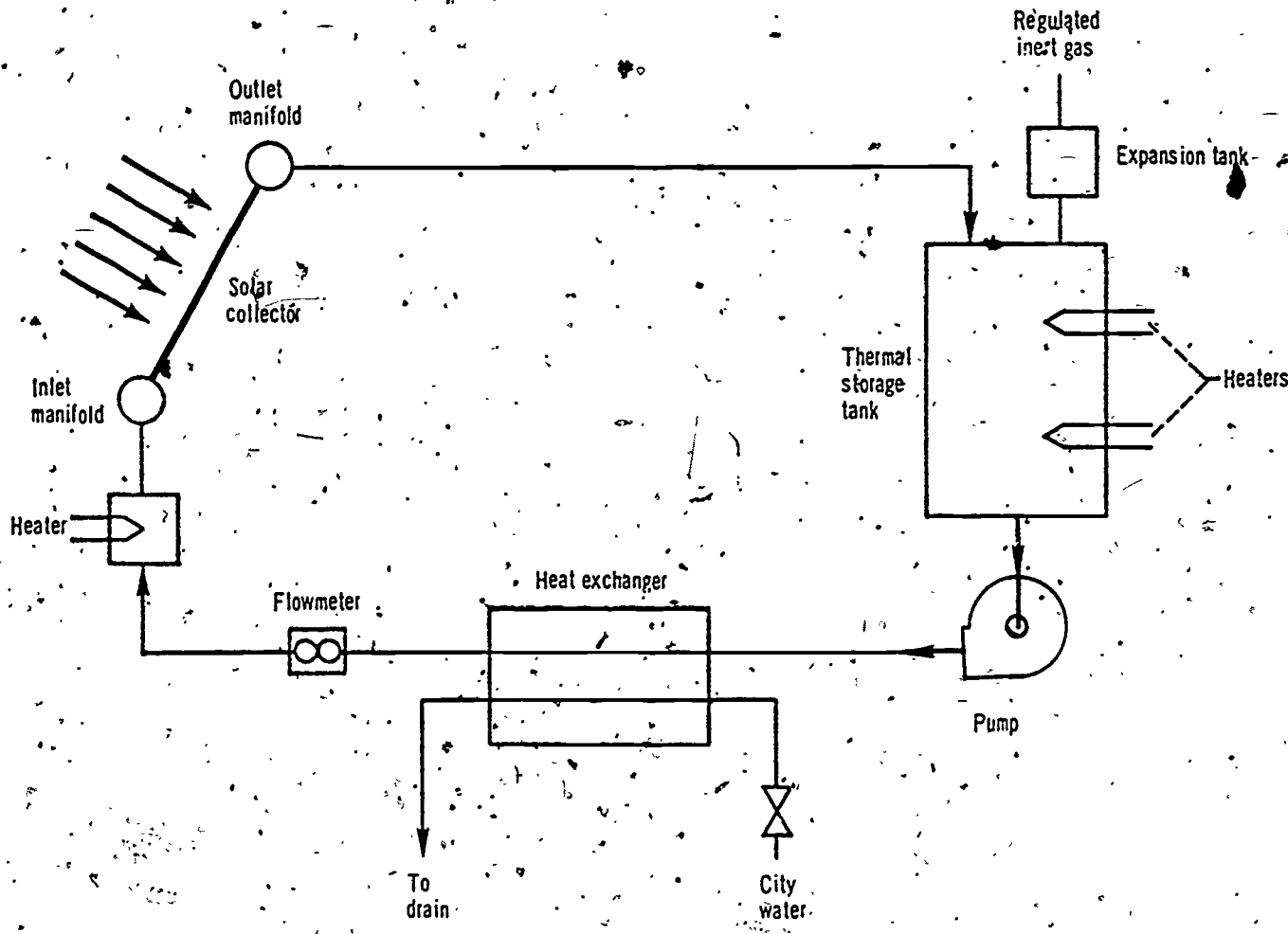


Figure 30 Schematic of the Liquid Flow Loop used in the Indoor Solar Collector Test Facility at the NASA Lewis Research Center [29]

1. Bk-Cu Absorber, 2 Glass
2. CuO-Cu Absorber, 1 Glass
3. CuO-Cu Absorber, Honeycomb, 1 Glass
4. CuO-Cu Absorber, 2 Glass
5. Bk Ni - Al Absorber, 1 Glass
6. Bk Ni - Al Absorber, 2 Glass
7. Bk Ni - Al Absrober, 2 Glass
8. Bk Ni - Al Absorber, 1 Tedlar
9. Bk Ni - Al Absorber, 2 Tedlar
10. Bk - Al Absorber, 1 Glass
11. Bk - Al Absrober, Honeycomb, 1 Glass
12. Bk - Al Absorber, Honeycomb, 2 Glass
13. Bk - Al Absorber, 2 Glass
14. Bk - Al Absorber, 2 Glass
15. Bk - Steel Absorber, 2 Glass

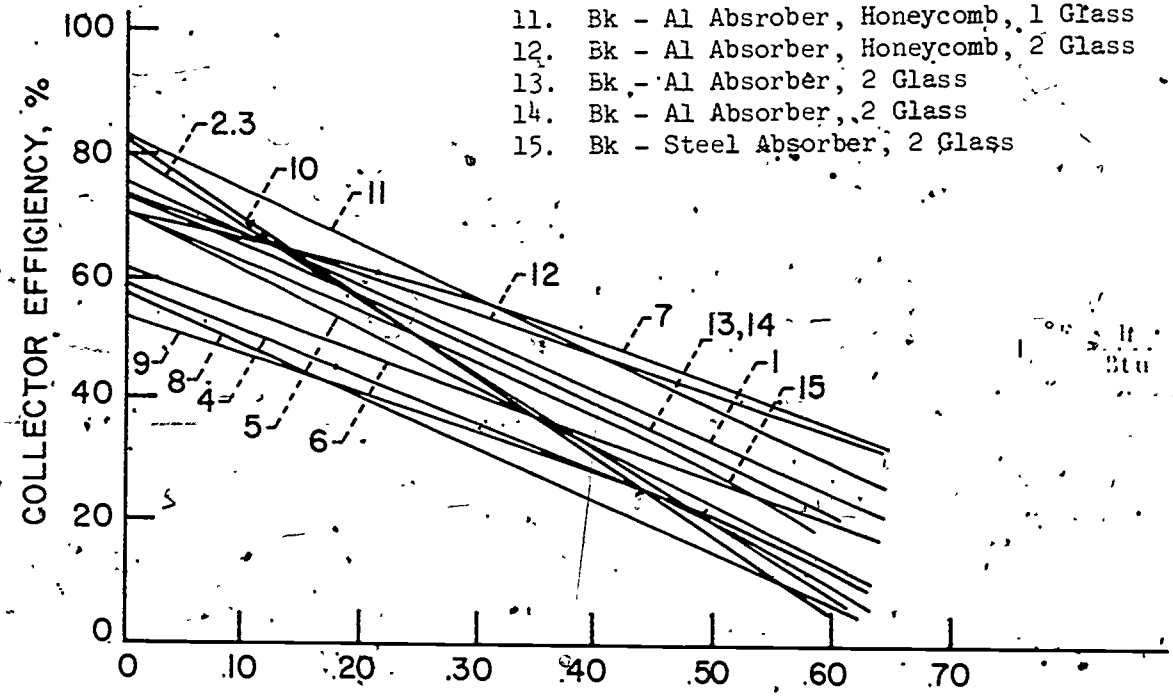


$$\frac{t_{f,i} - t_a}{I}, \quad \frac{°F \cdot h \cdot ft^2}{Btu}$$

$$1 \frac{°F \cdot h \cdot ft^2}{Btu} = 0.175 \frac{°C \cdot m^2}{W}$$

Figure 31 Efficiency Curve for Fifteen Liquid-Heating Solar Collectors Determined using the Indoor Test Facility at the NASA Lewis Research Center [29]

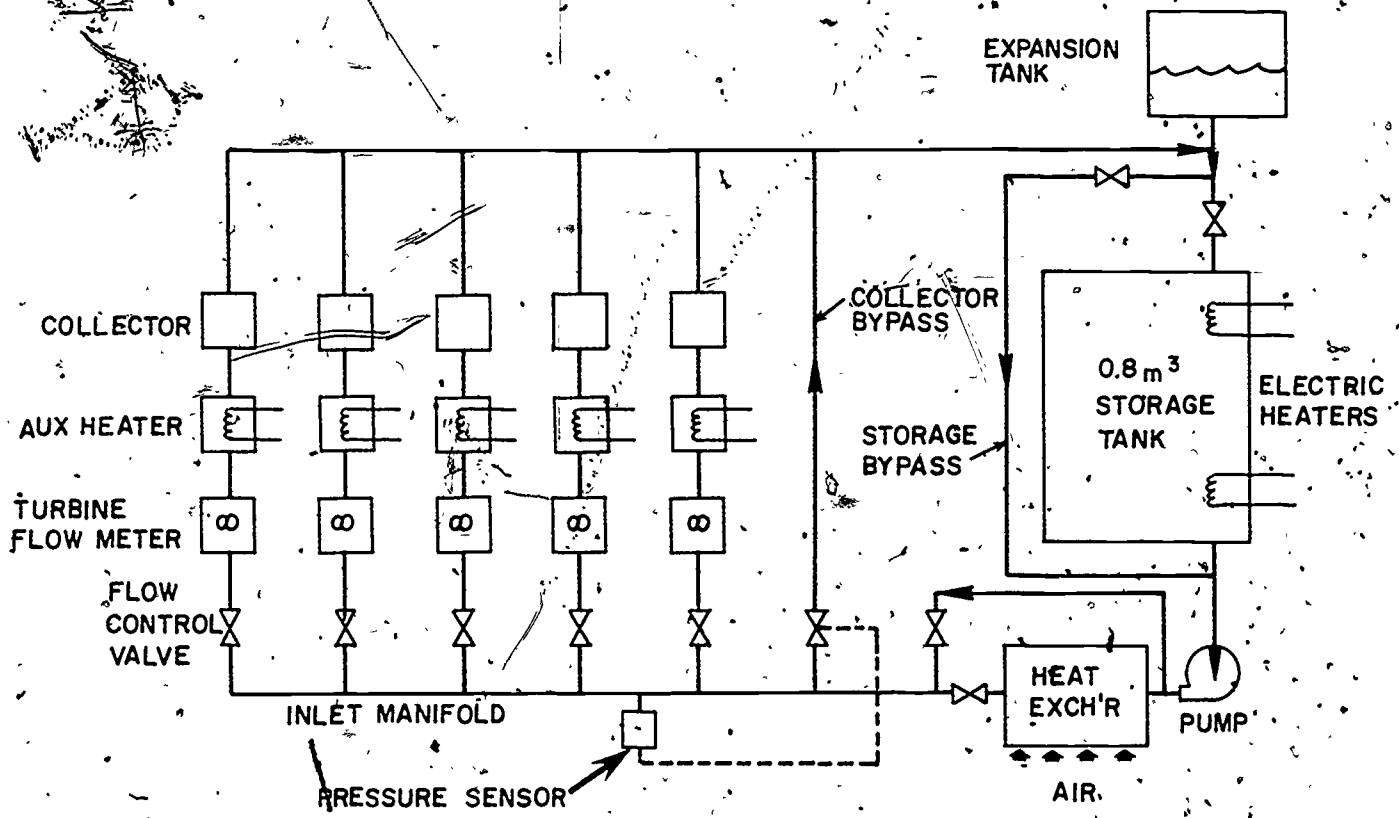


Figure 32 Schematic of the Liquid Flow loop used in the Outdoor Solar Collector Test Facility at the NASA Lewis Research Center [73]

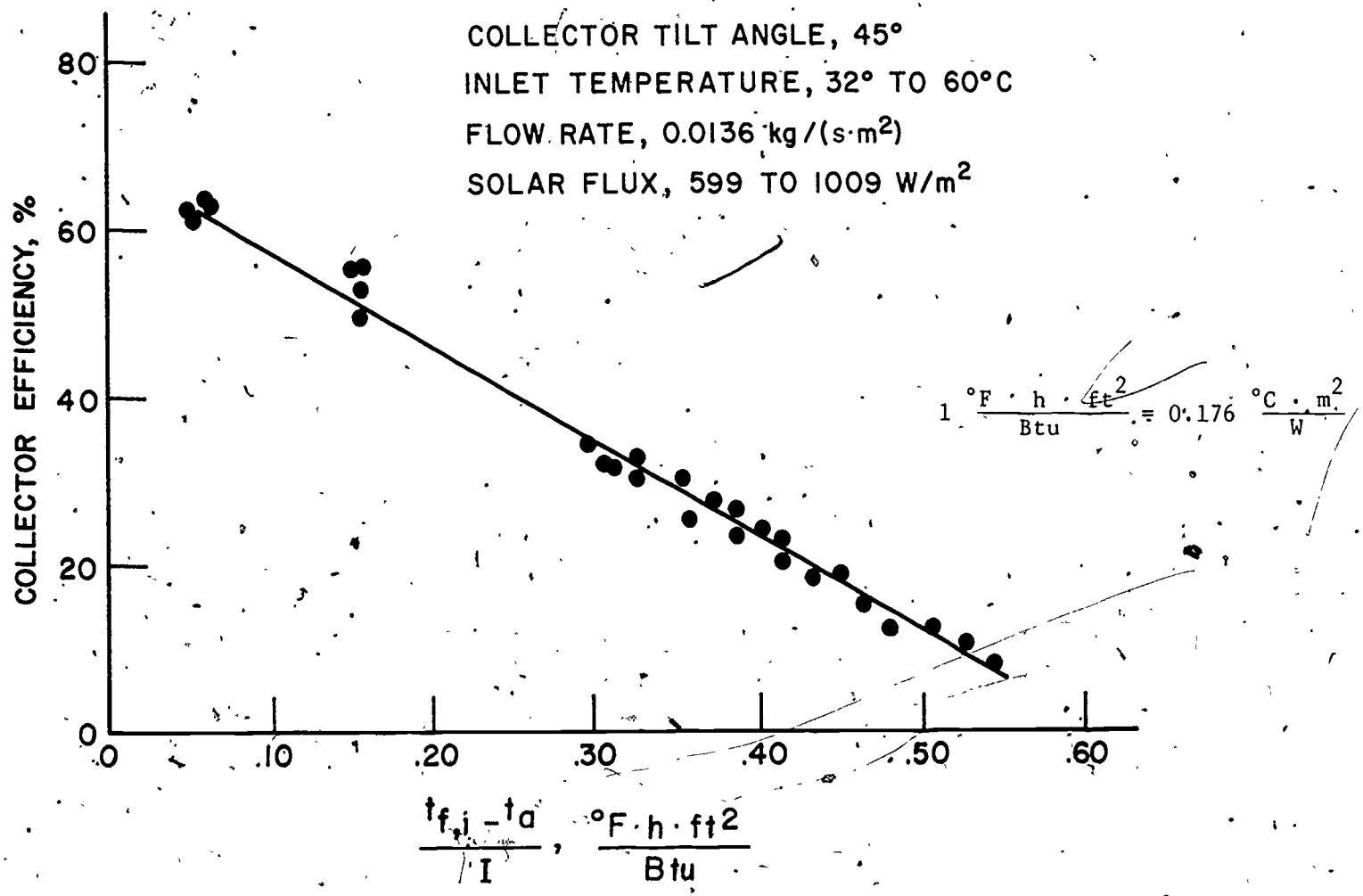


Figure 33 Efficiency Curve for a Double-Glazed Flat-Plate Liquid-Heating Solar Collector [73]

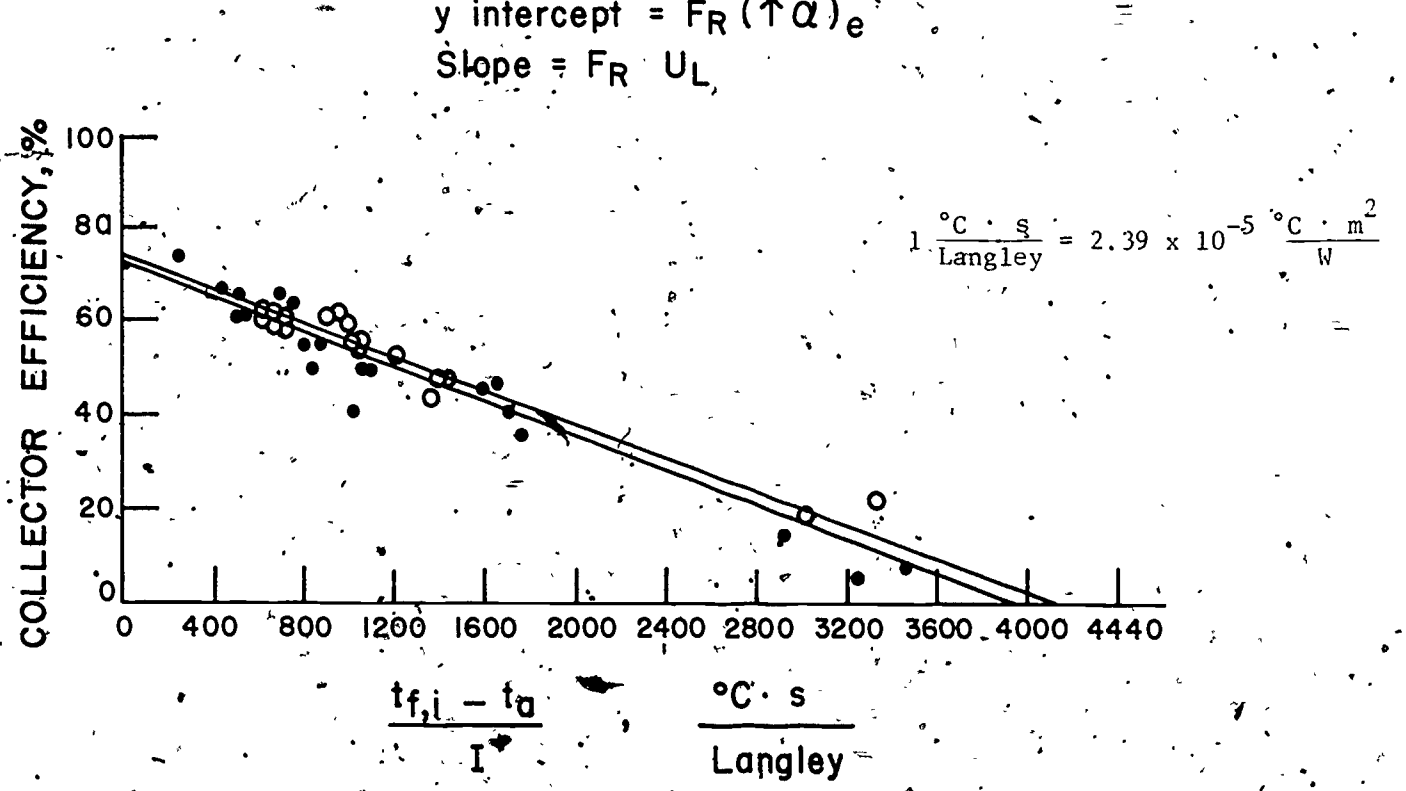


Figure 34 Efficiency Curves for Two Single-Glazed Air-Heating Solar Collectors [87]

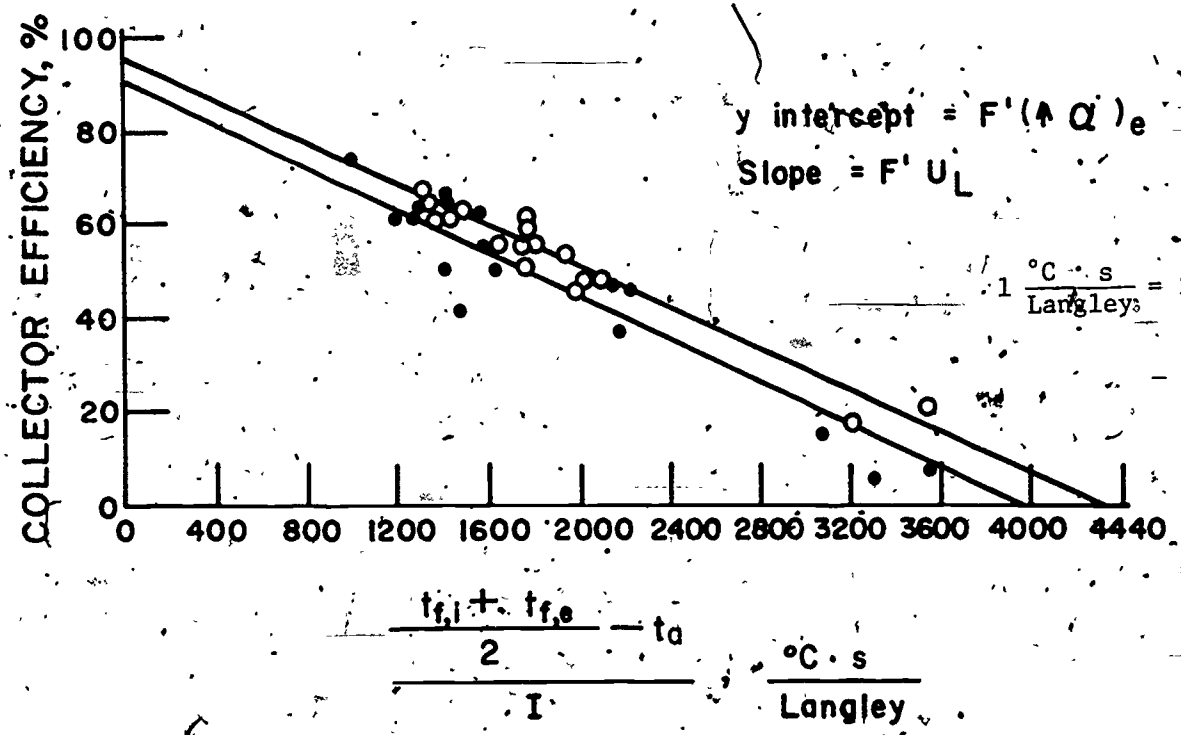


Figure 35 Efficiency Curves for Two Single-Glazed Air-Heating Solar Collectors [87]

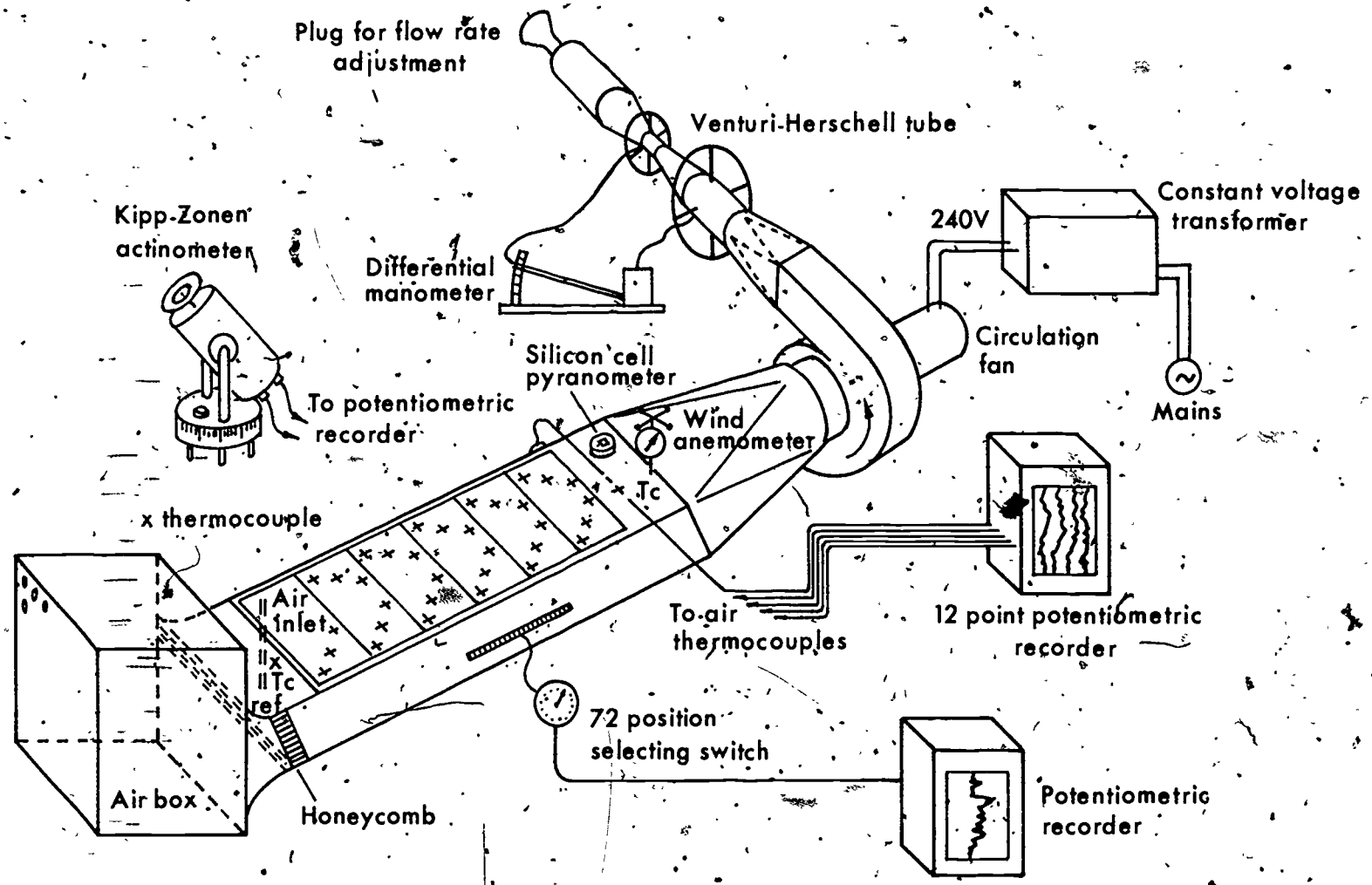


Figure 36 Schematic of the Test Apparatus Used by Selcuk for Determining the Thermal Efficiency of an Air-Heating Solar Collector [88]

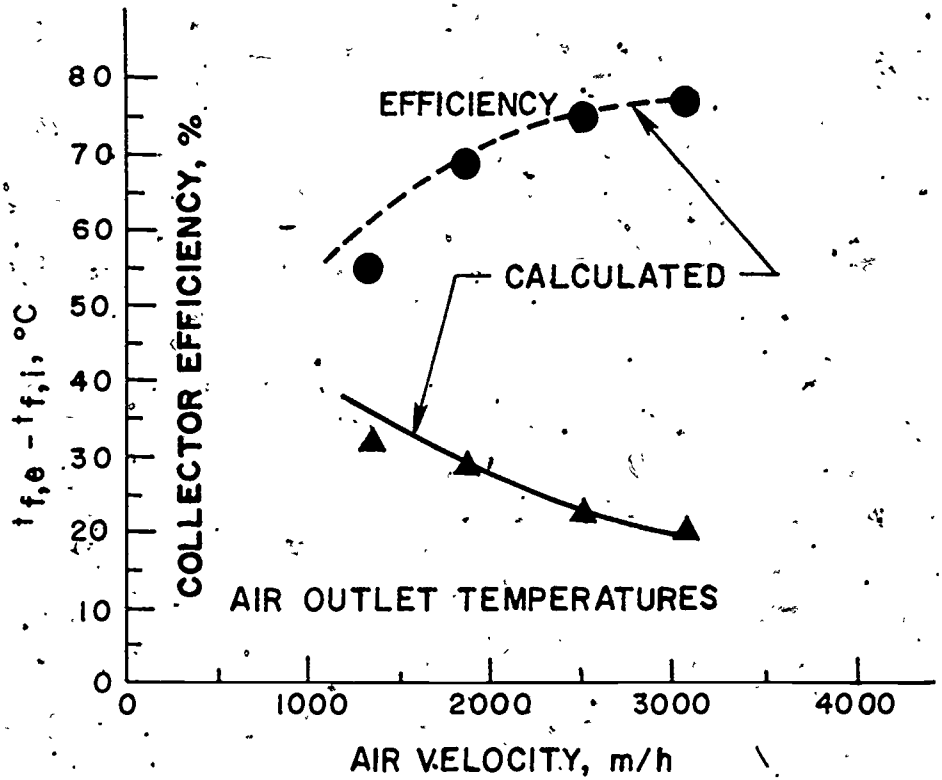


Figure 37 Comparison of Measured and Calculated Thermal Efficiency Air Outlet Temperature as a Function of Air Velocity for Overlapped-Glass-Plate Solar Air-Heater [88]

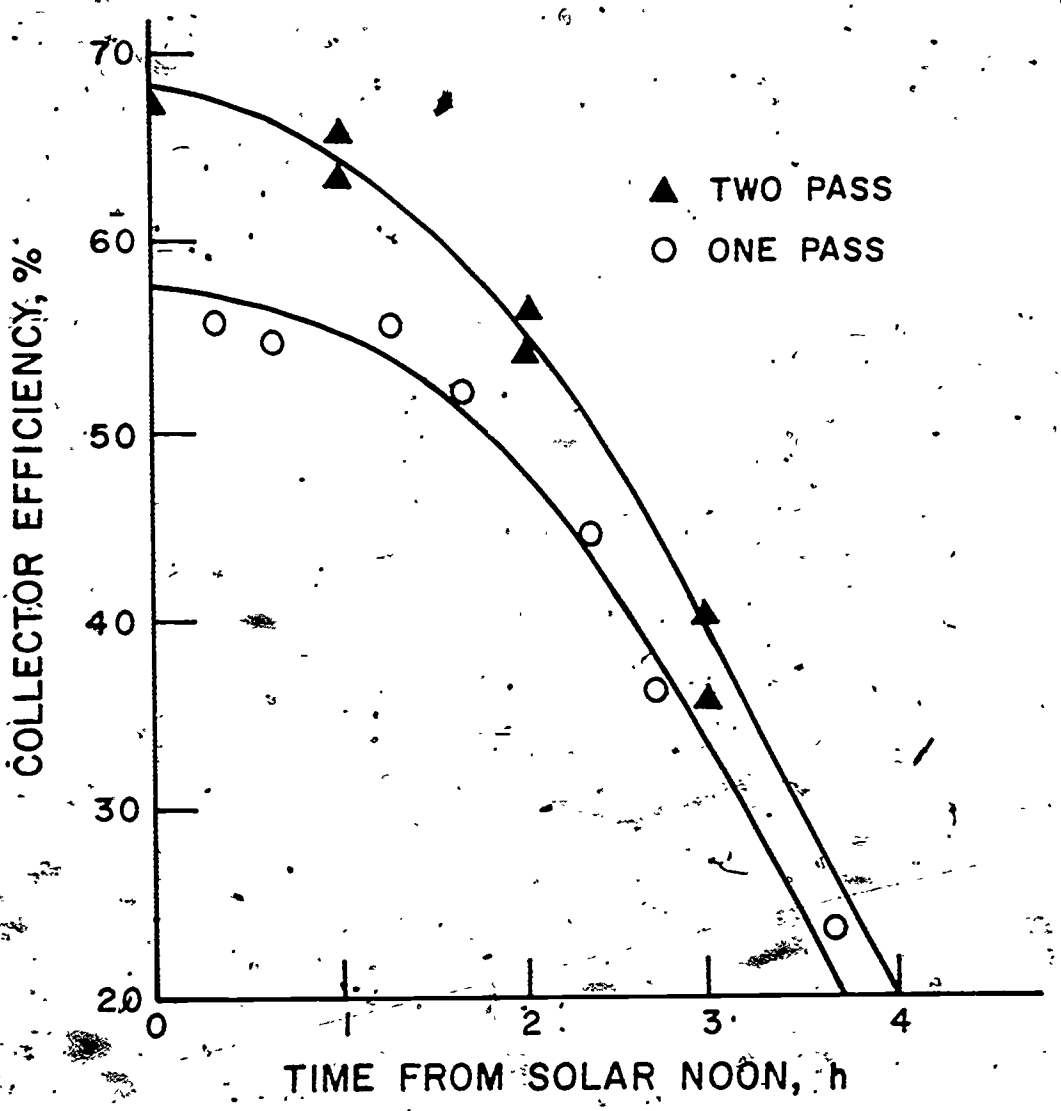


Figure 38 Thermal Efficiency as a Function of Time of Day for a One- and Two- Pass Solar Air Heater [89]

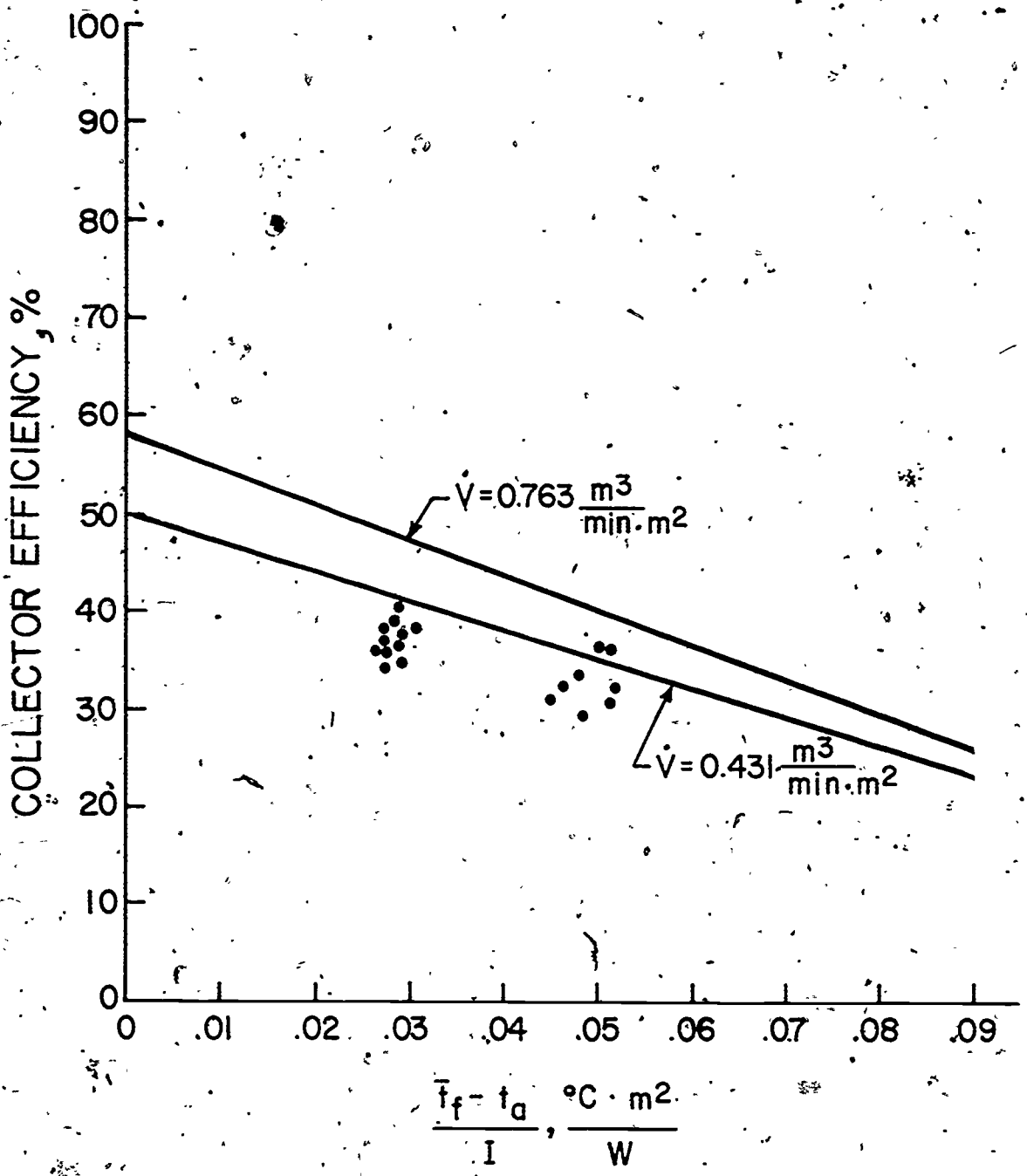


Figure 39 Comparison of Predicted and Measured Air Collector Efficiencies [90]

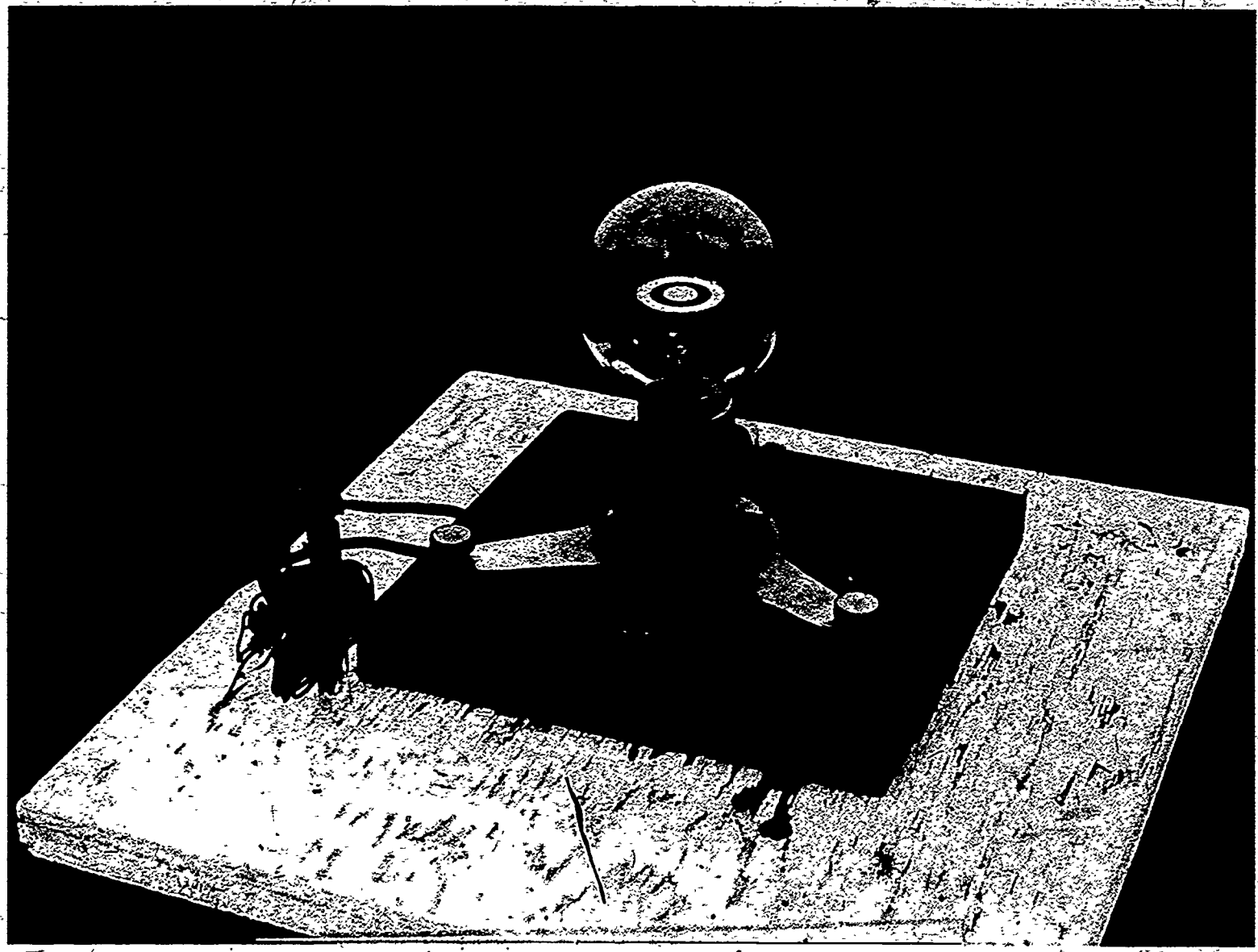

Figure 40 Eppley (180° Pyrheliometer) Pyranometer in use at the National Bureau of Standards

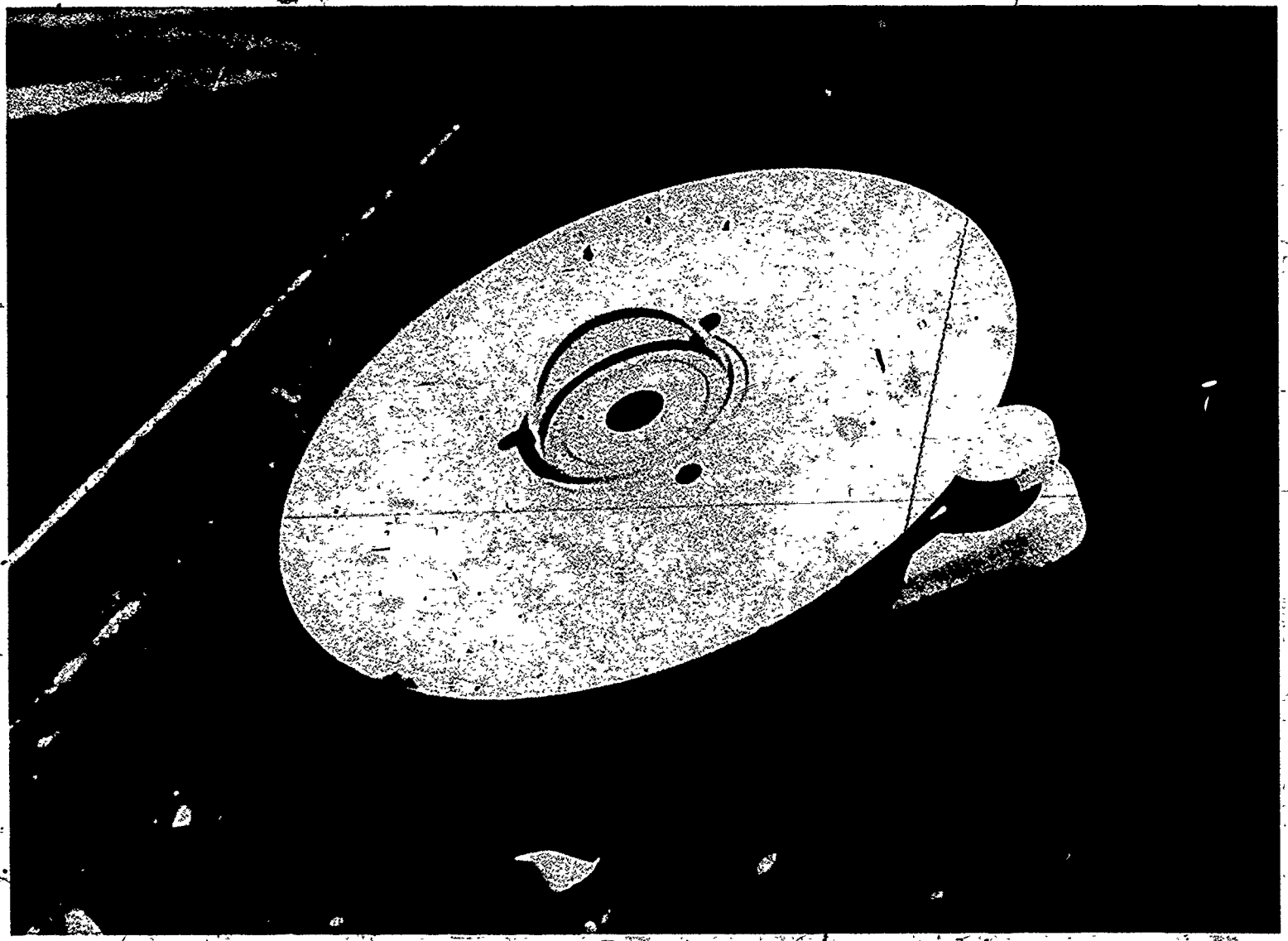

Figure 41 Trickett and Norris Pyranometer in Use at CSIRO

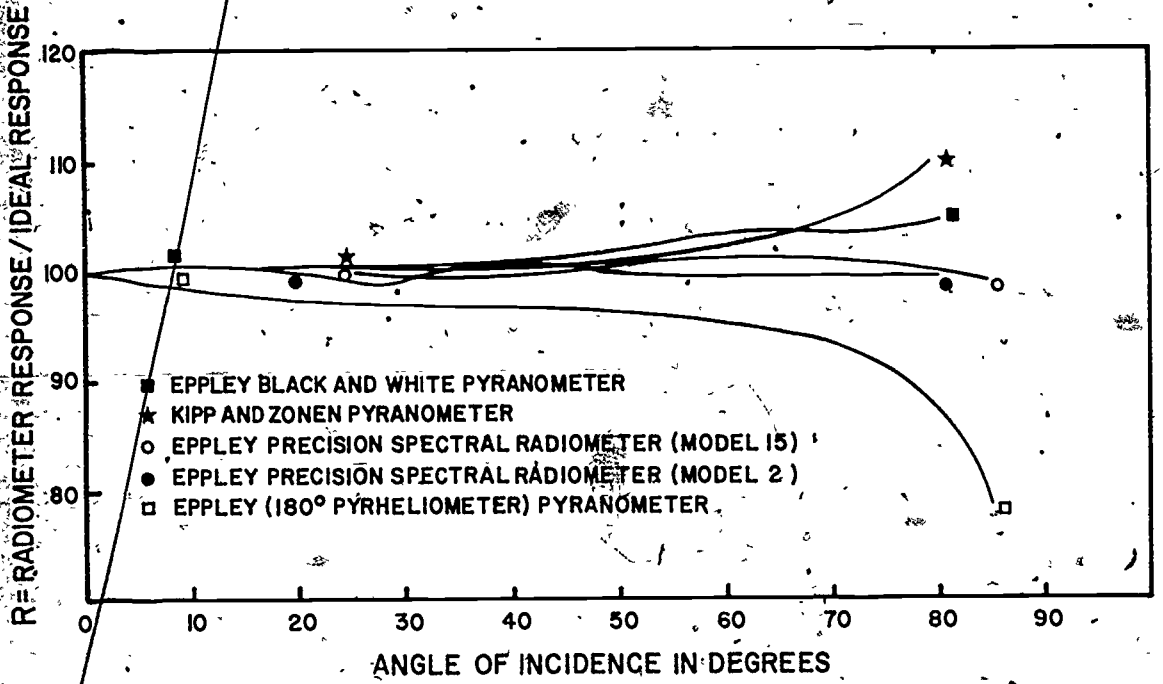


Figure 42. Deviation of Response from a True Cosine Response of Selected Pyranometers as a Function of Incident Angle [92]

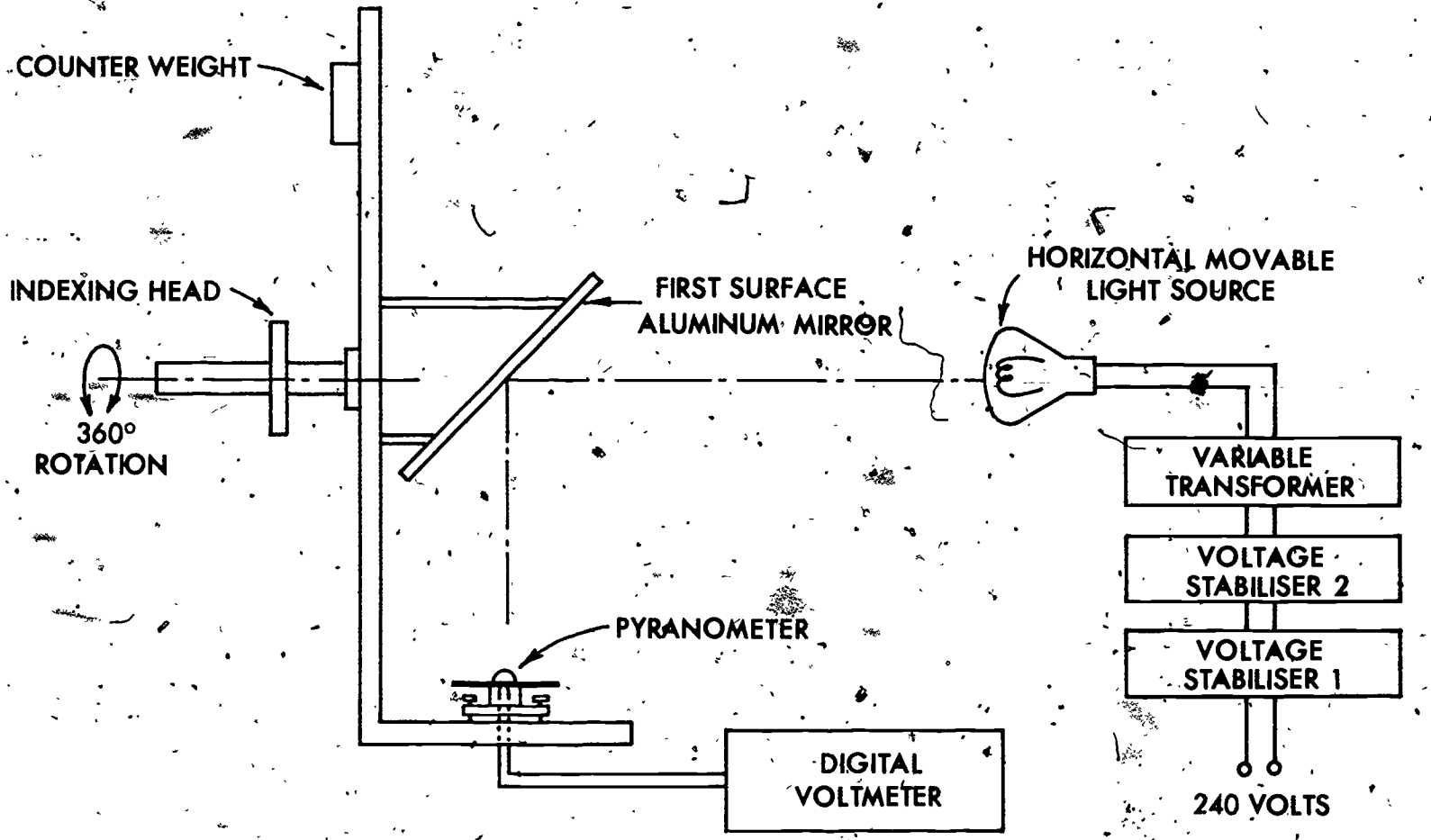


Figure 43 Schematic of the Test Apparatus Used by Norris in Determining the Change in Pyranometer Response with Attitude [93]

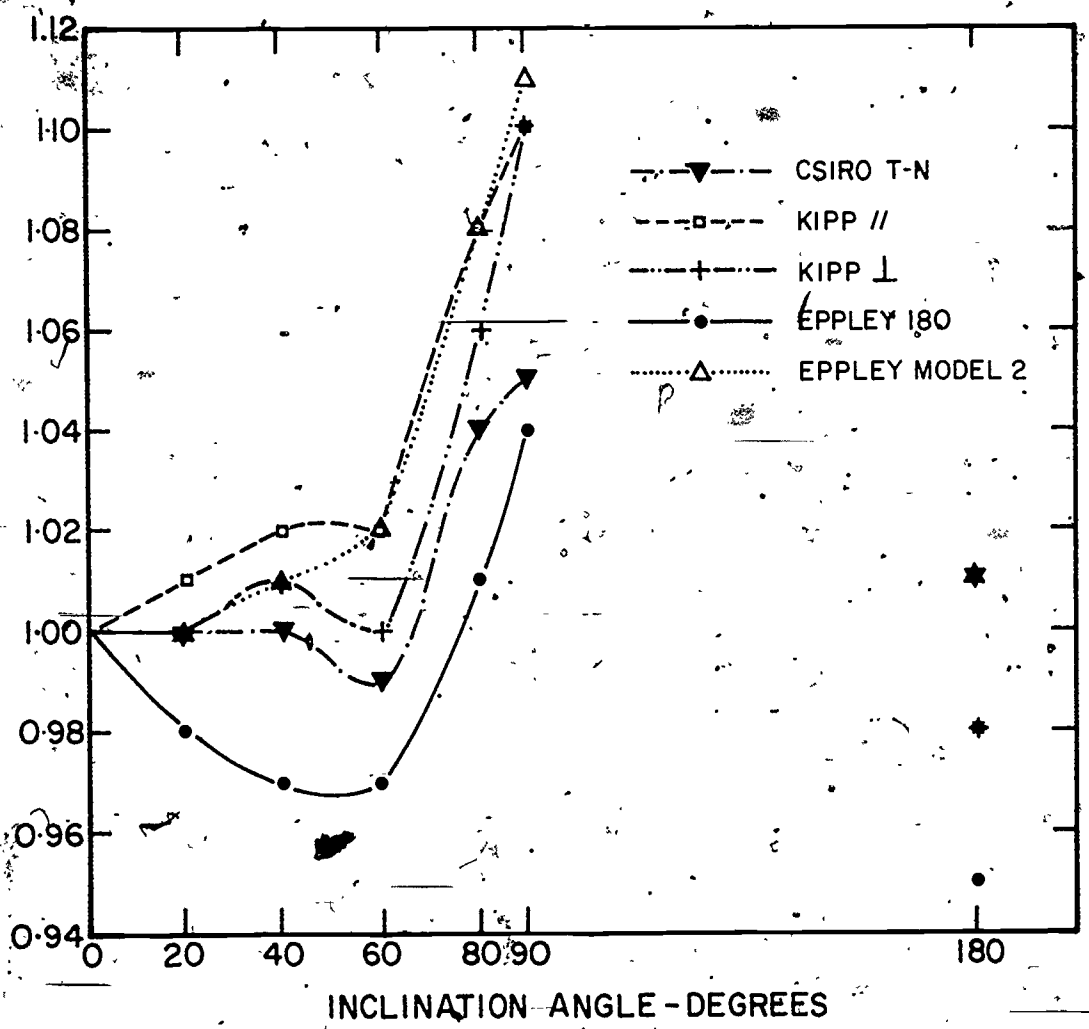


Figure 44 Variation in Response with Attitude for Selected Pyranometers as Determined by Norris [93]

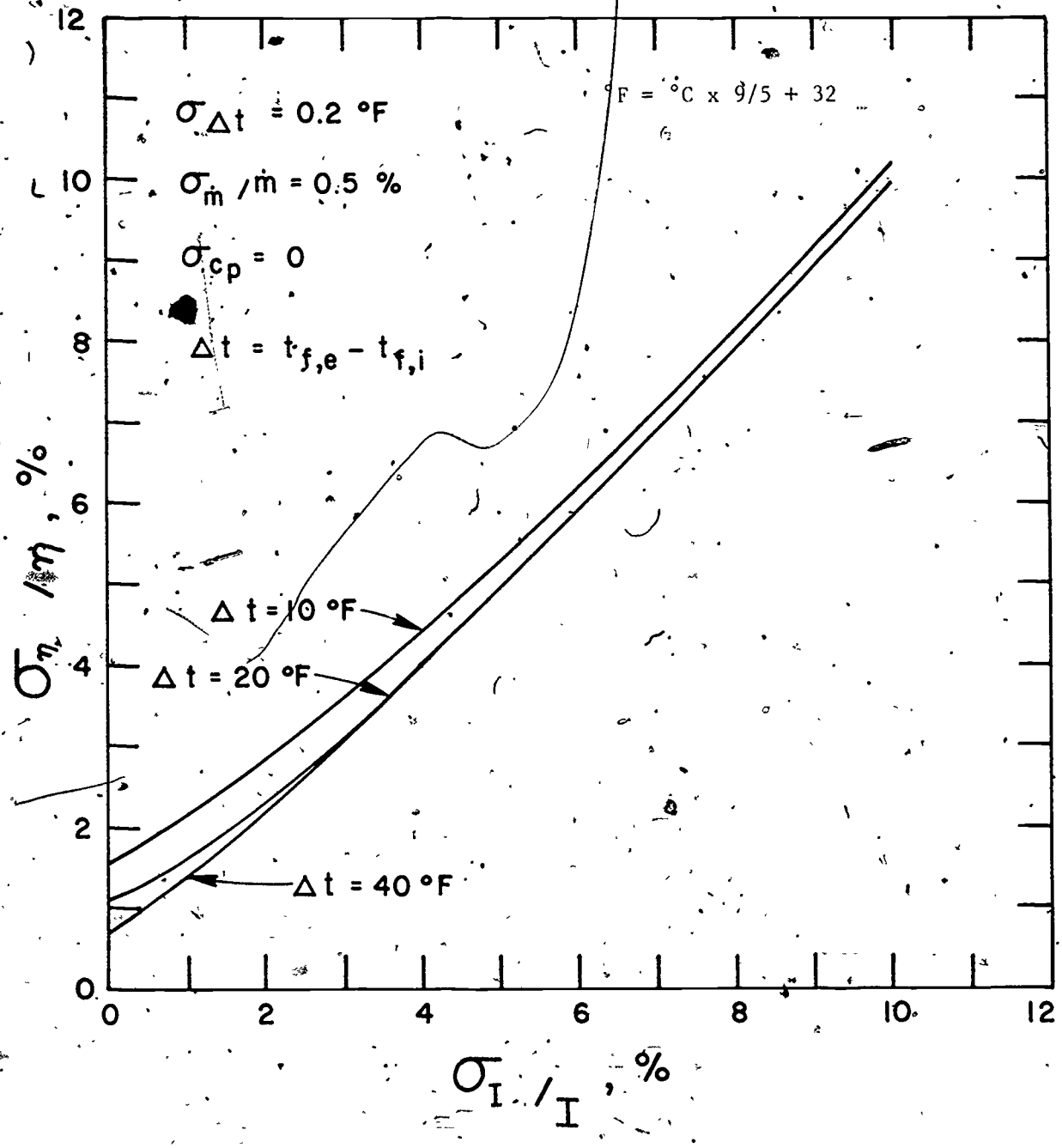


Figure 45 Uncertainty in Solar Collector Thermal Efficiency as a Function of the Uncertainty in Insolation

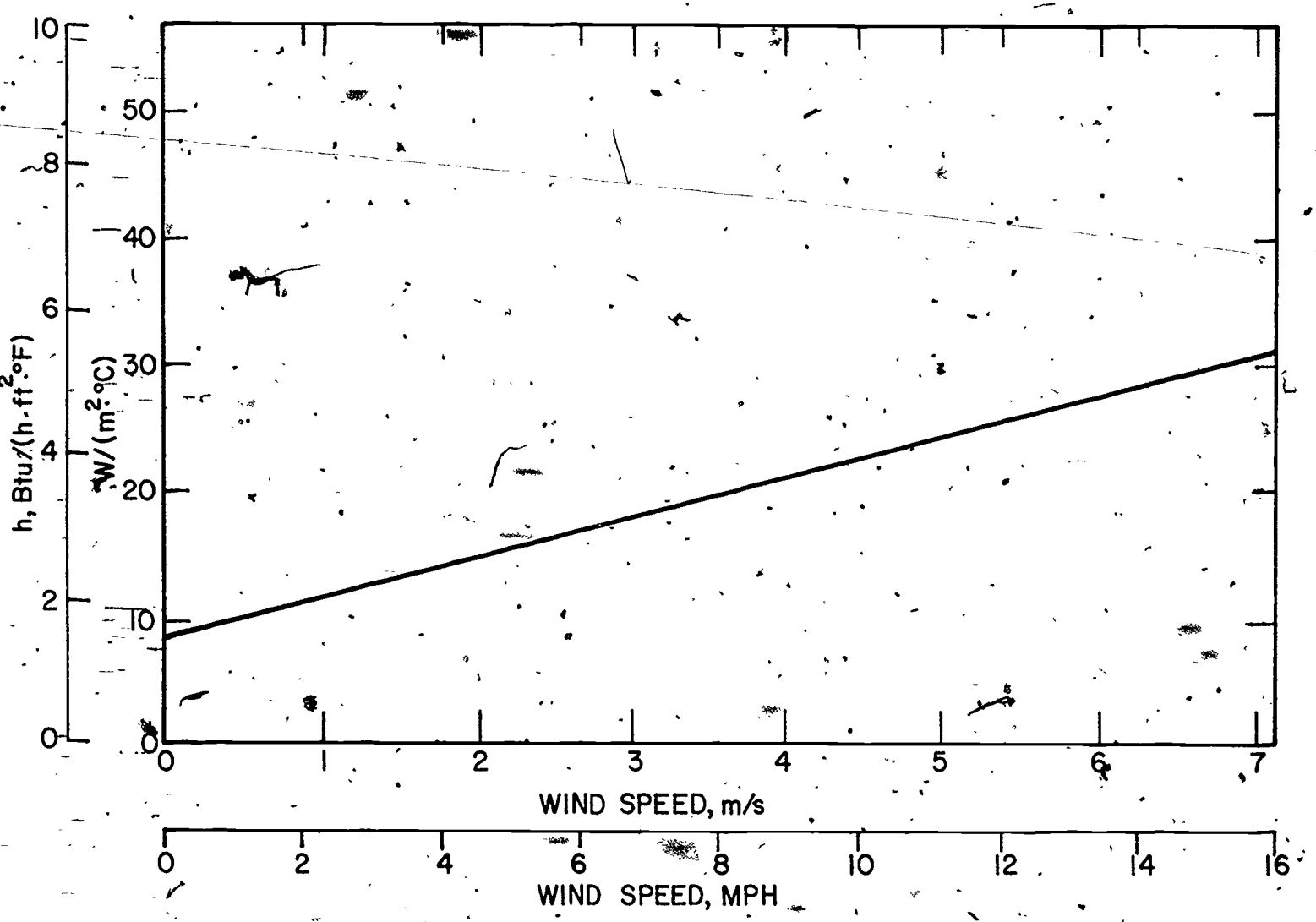


Figure 46 The Outside Surface Heat Transfer Coefficient of a Solar Collector Versus the Wind Speed

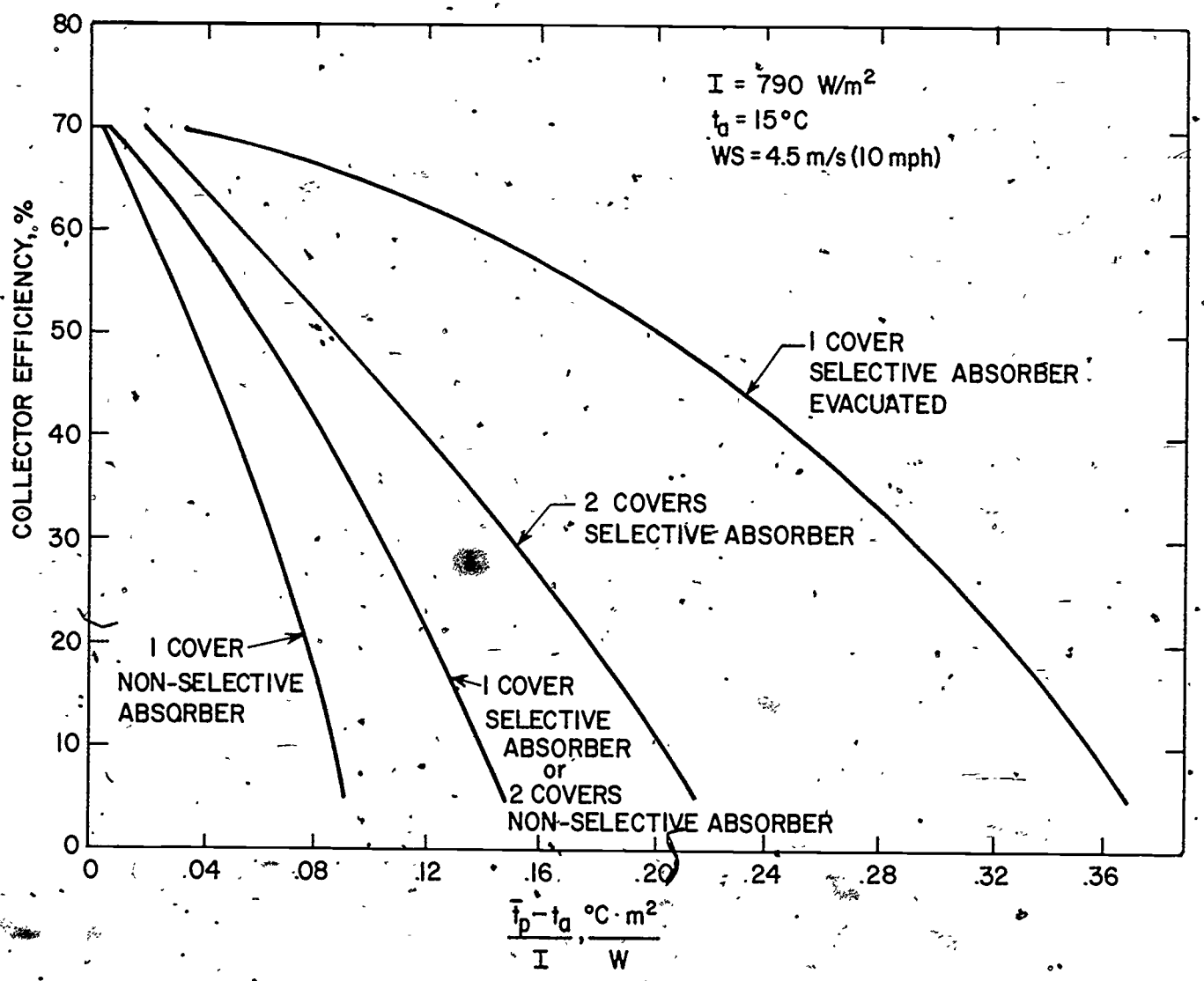


Figure 47 Efficiency Curves for Flat-Plate Solar Collectors of Various Designs

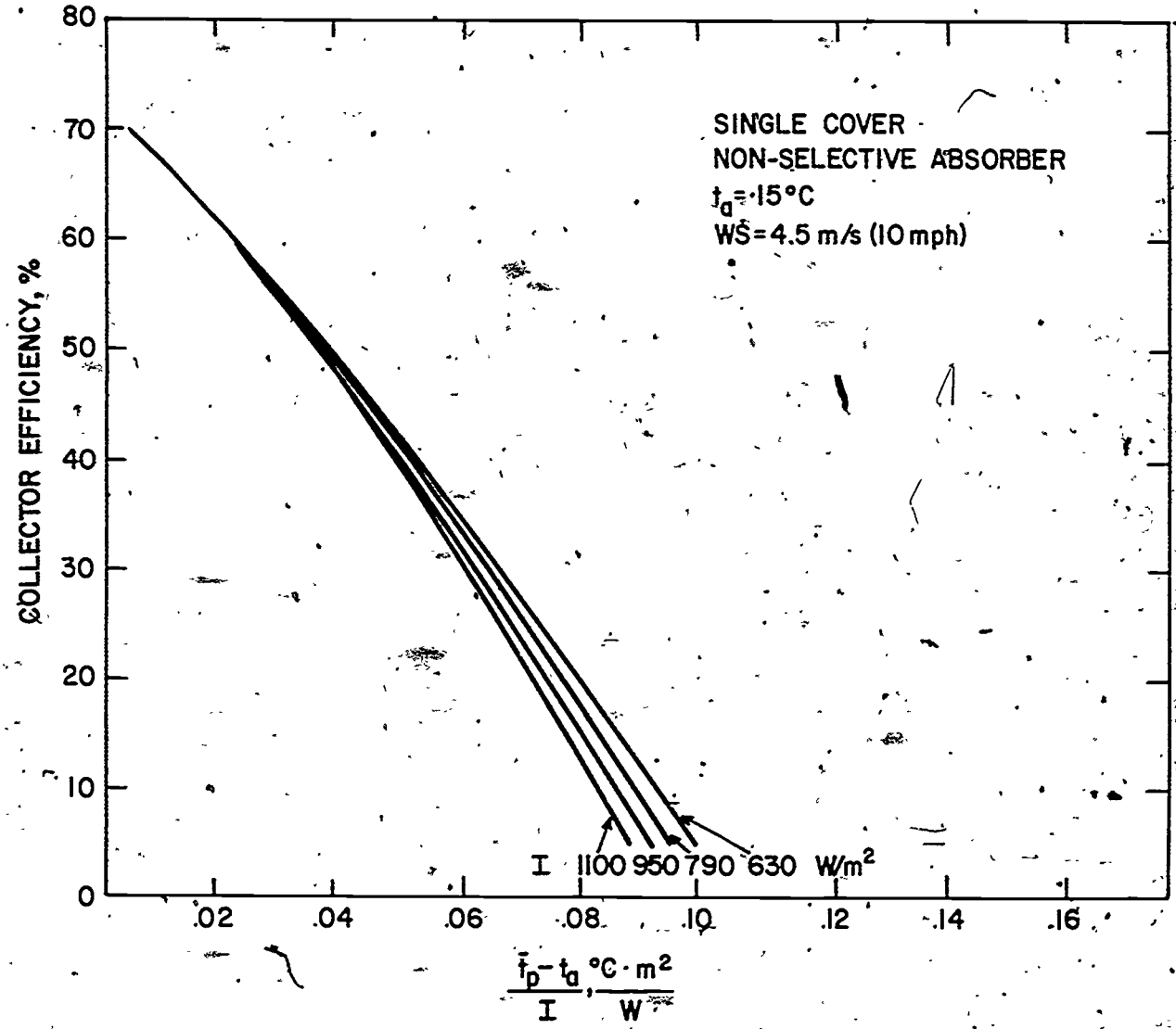


Figure 48 The Effect of Variations in Insolation on the Efficiency Curve for Single-Glazed Flat-Plate Solar Collectors

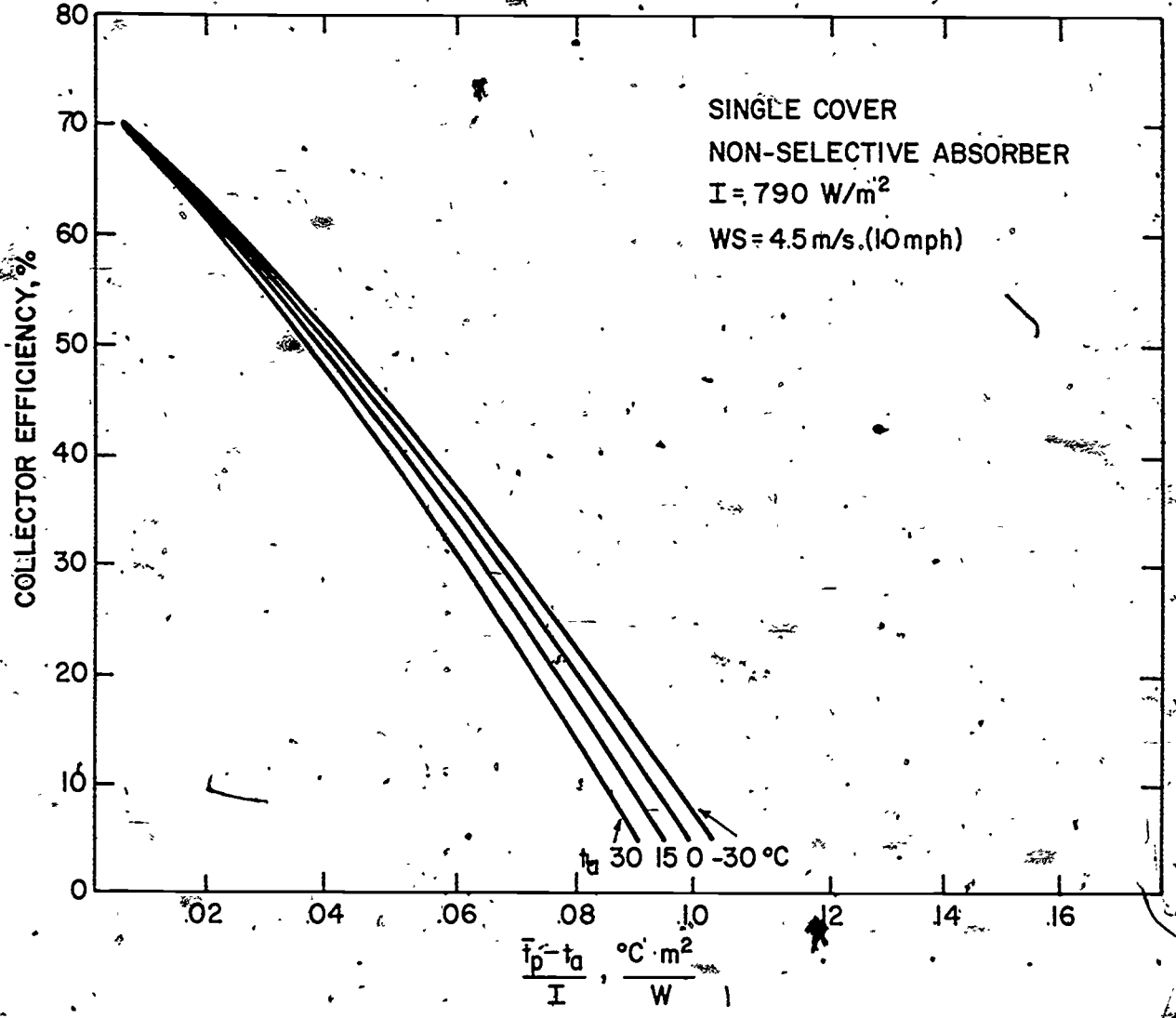


Figure 49 The Effect of Variations in Ambient Temperature on the Efficiency Curve for Single-Glazed Flat-Plate Solar Collectors

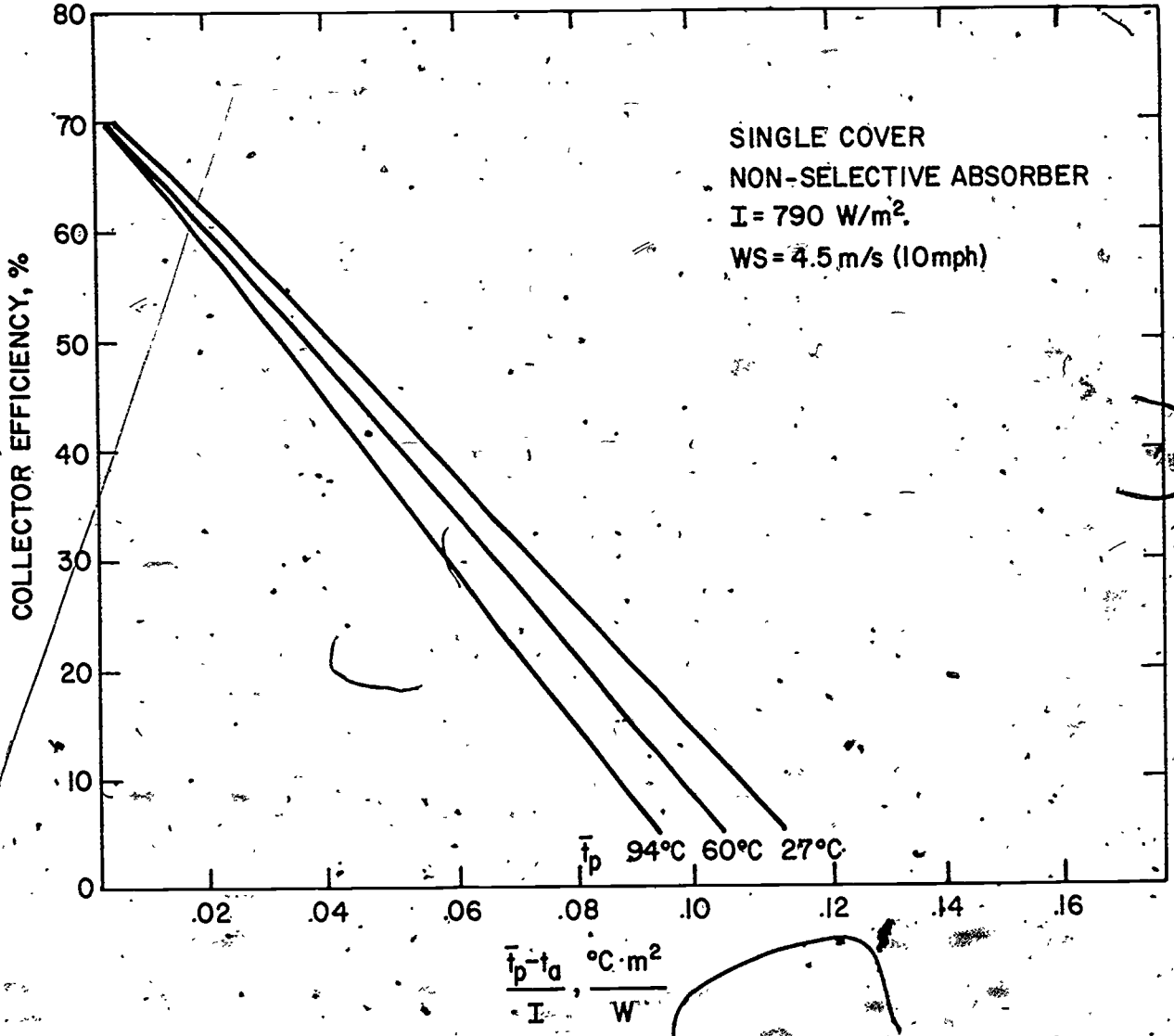


Figure 50 The Effect of Variations in Operating Temperature on the Efficiency Curve for Single-Glazed Flat-Plate Solar Collectors

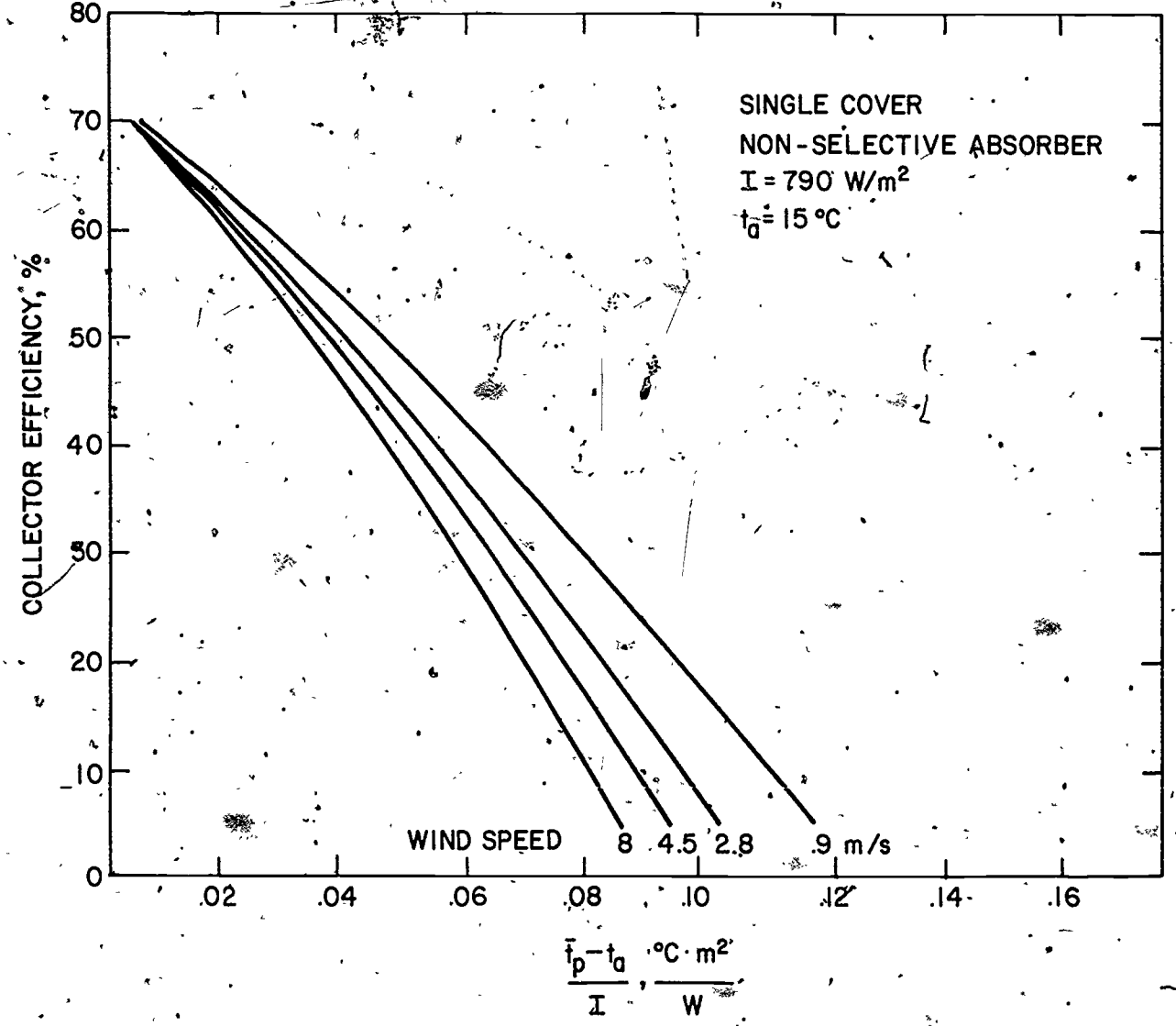


Figure 51 The Effect of Variations in Wind Speed on the Efficiency Curve for Single-Glazed Flat-Plate Solar Collectors

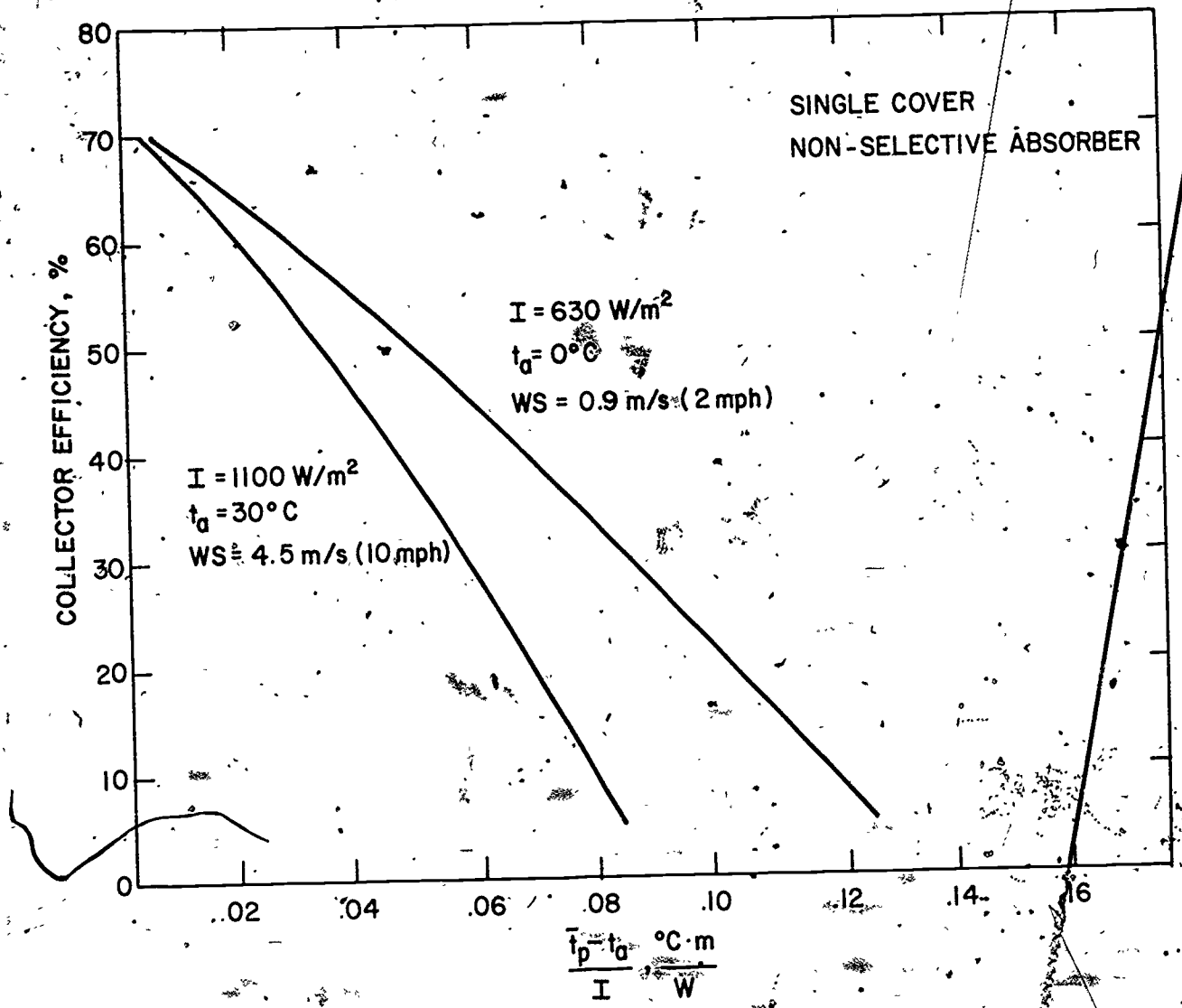


Figure 52 The Effect of Simultaneous Variations in Insolation, Ambient Temperature, and Wind Speed on the Efficiency Curve for Single-Glazed Flat-Plate Solar Collectors

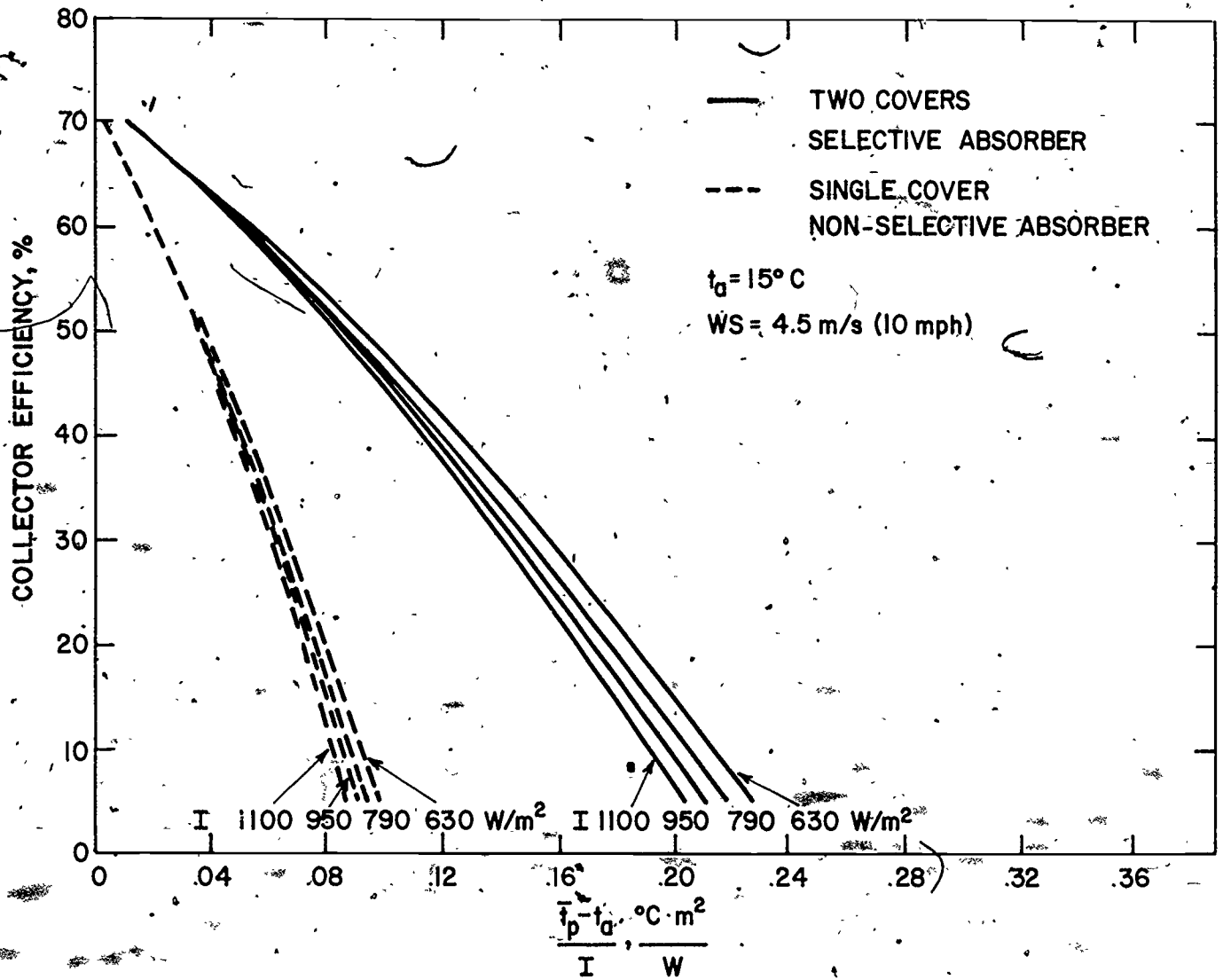


Figure 53 The Effect of Variations in Insolation on the Efficiency Curve for Single- and Double-Glazed Flat-Plate Solar Collectors

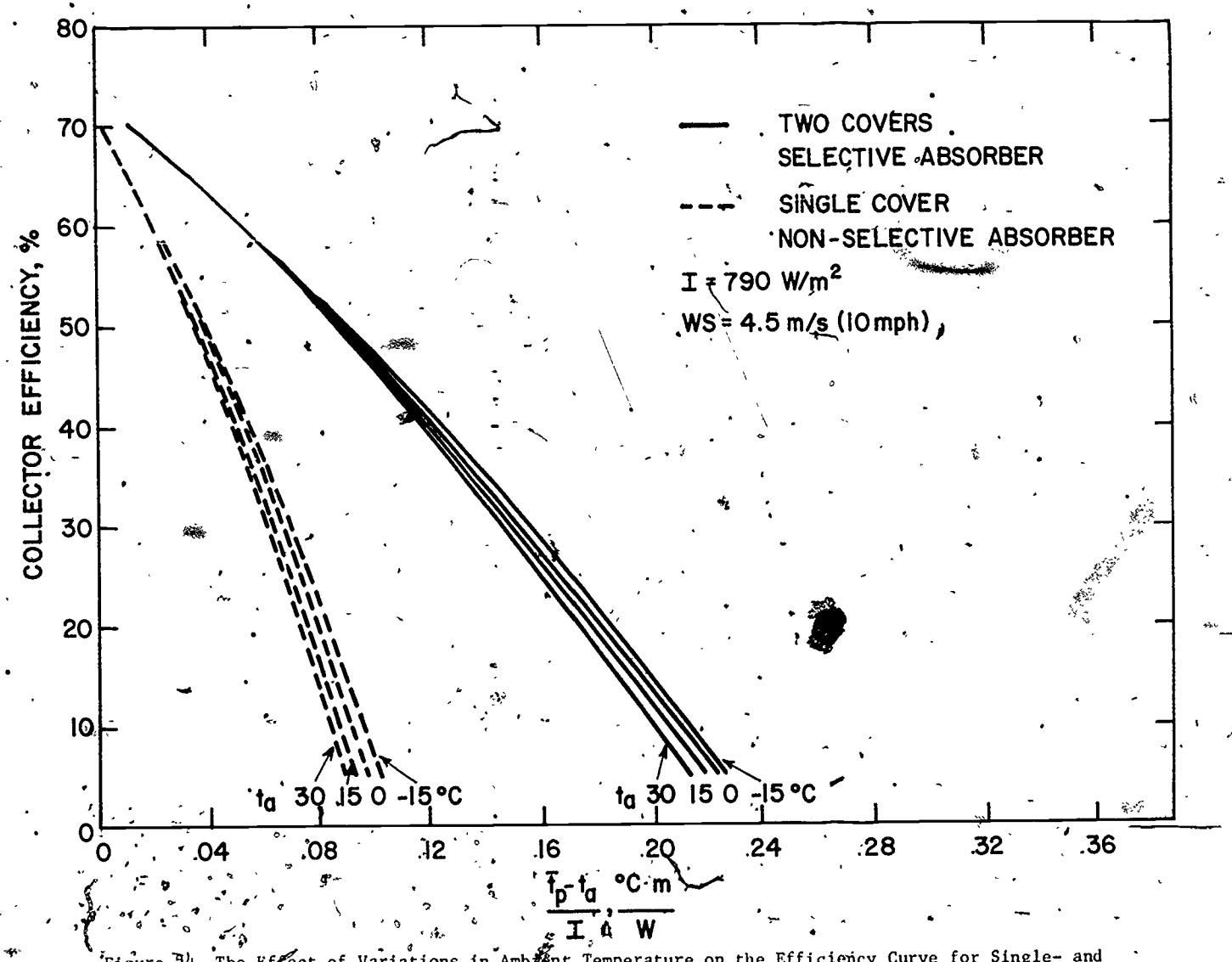


Figure 74 The Effect of Variations in Ambient Temperature on the Efficiency Curve for Single- and Double-Glazed Flat-Plate Solar Collectors

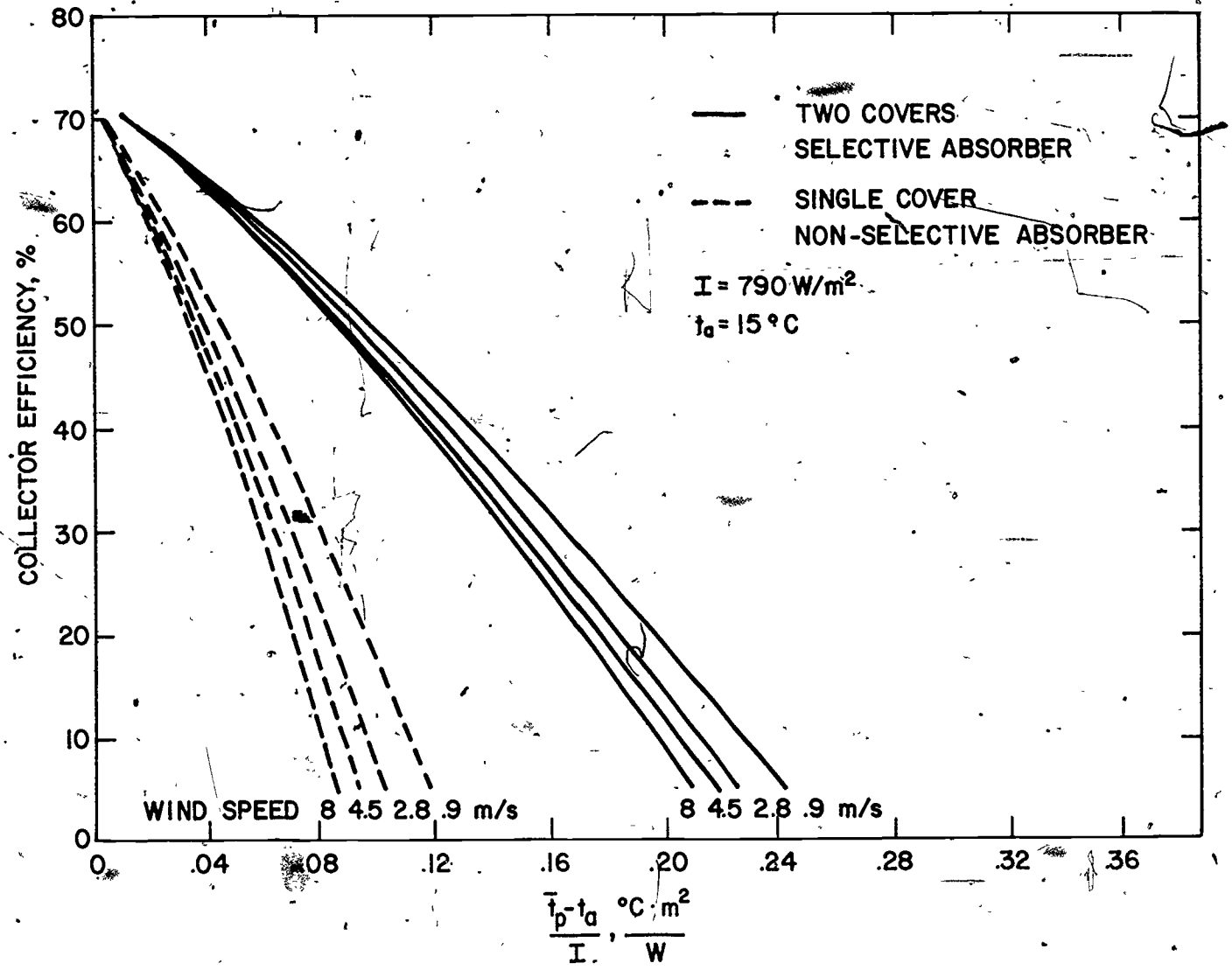


Figure 55 The Effect of Variations in Wind Speed on the Efficiency Curve for Single- and Double-Glazed Flat-Plate Solar Collectors

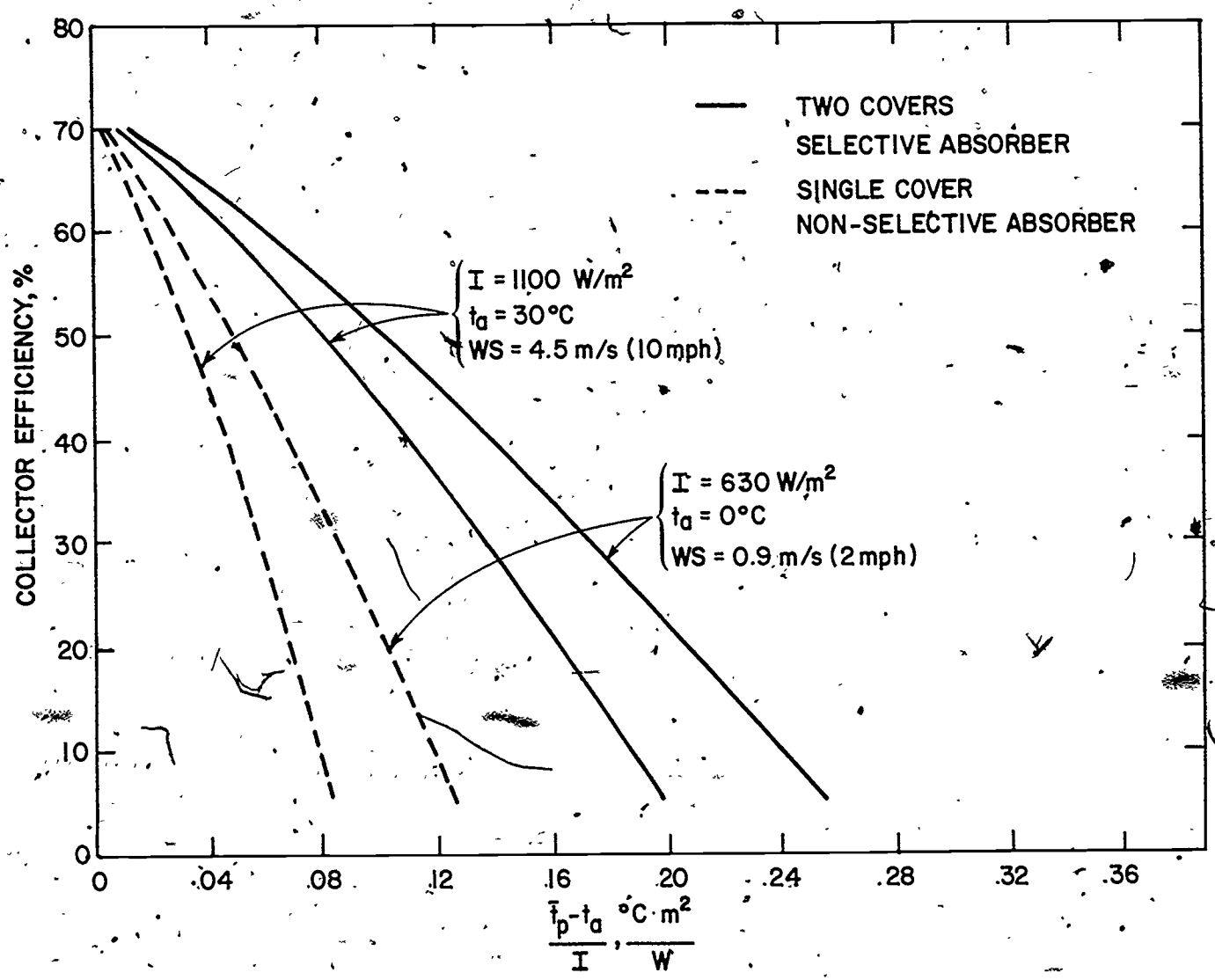


Figure 56 The Effect of Simultaneous Variations in Insolation, Ambient Temperature, and Wind Speed on the Efficiency Curve for Single- and Double-Glazed Flat-Plate Solar Collectors

# COMPARISON OF MEASURED AIR MASS ≈ 1.7, WITH MODEL AIR-MASS SPECTRAL DISTRIBUTIONS

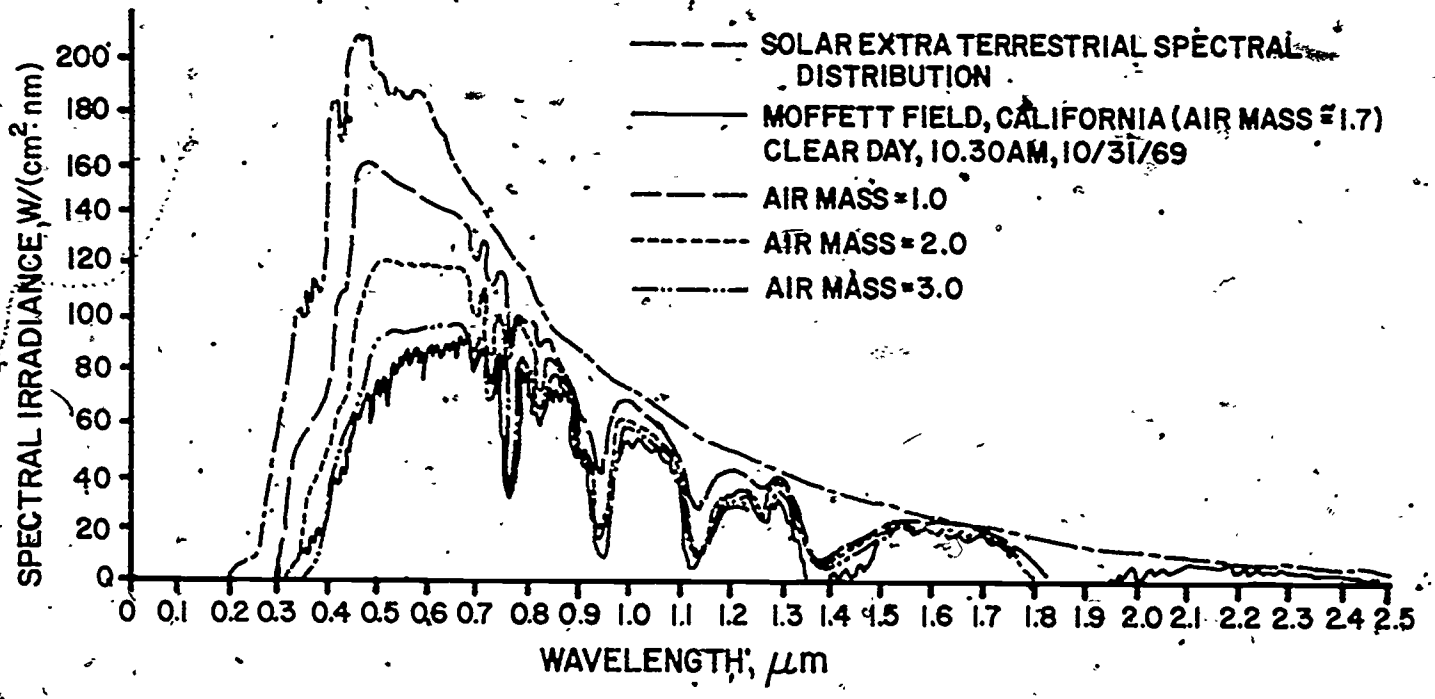


Figure 57 Comparison of Measured (Air Mass ≈ 1.7) and Calculated Spectral Distributions of Incident Solar Radiation [98]

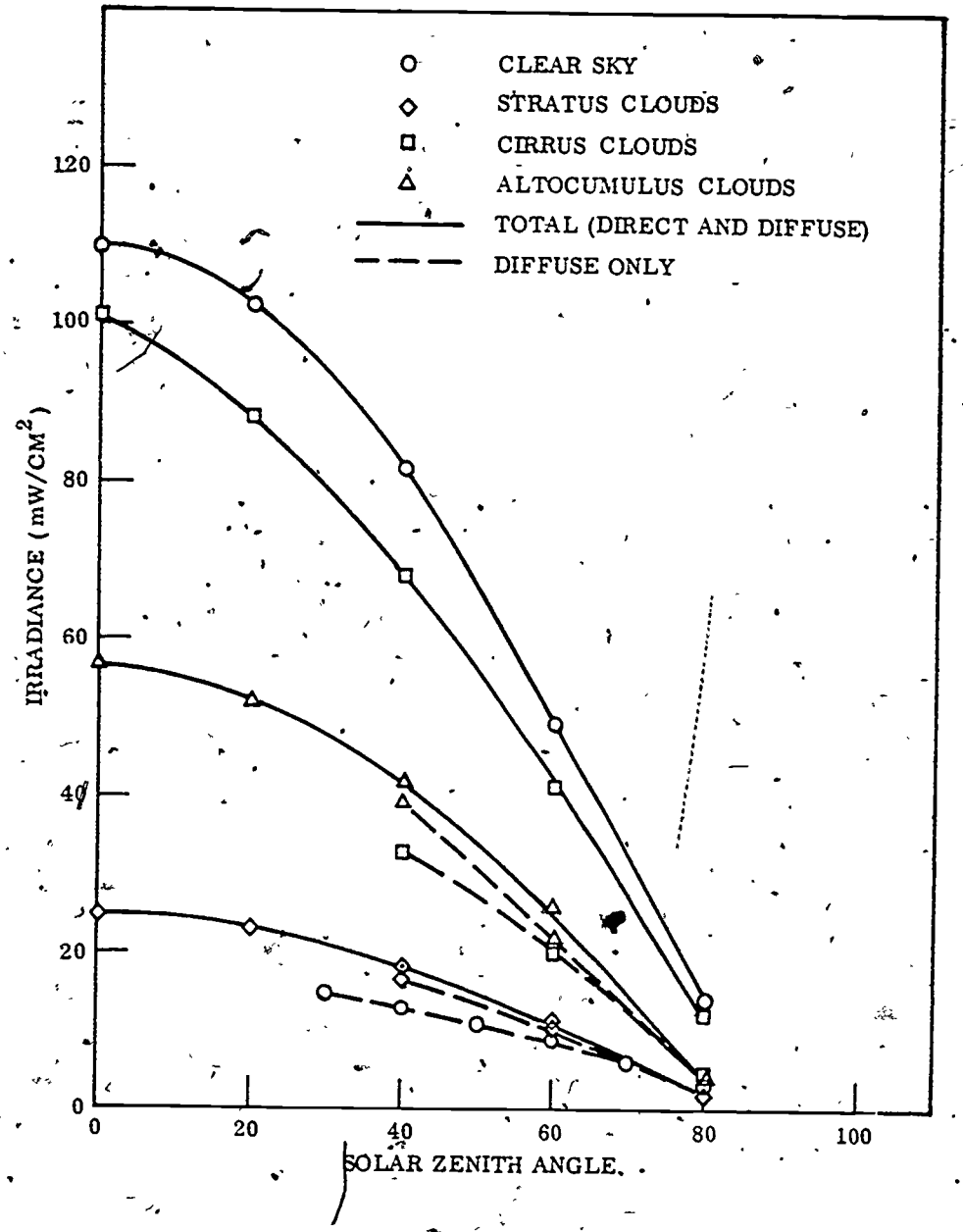


Figure 58 Ground Solar Irradiance for Various Cloud Conditions [97]

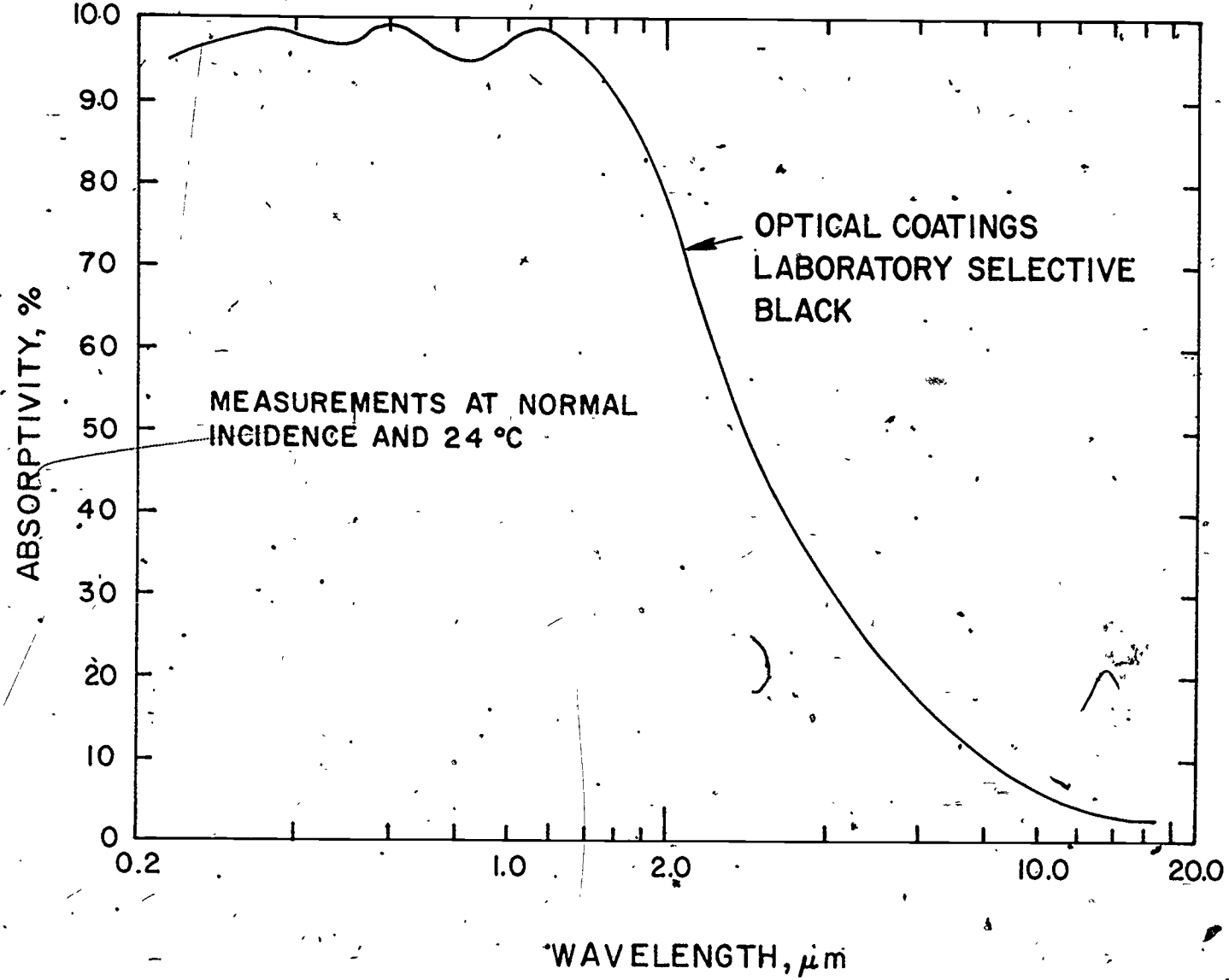


Figure 59 Absorptivity as a Function of Wavelength for a Selective Coating [56]

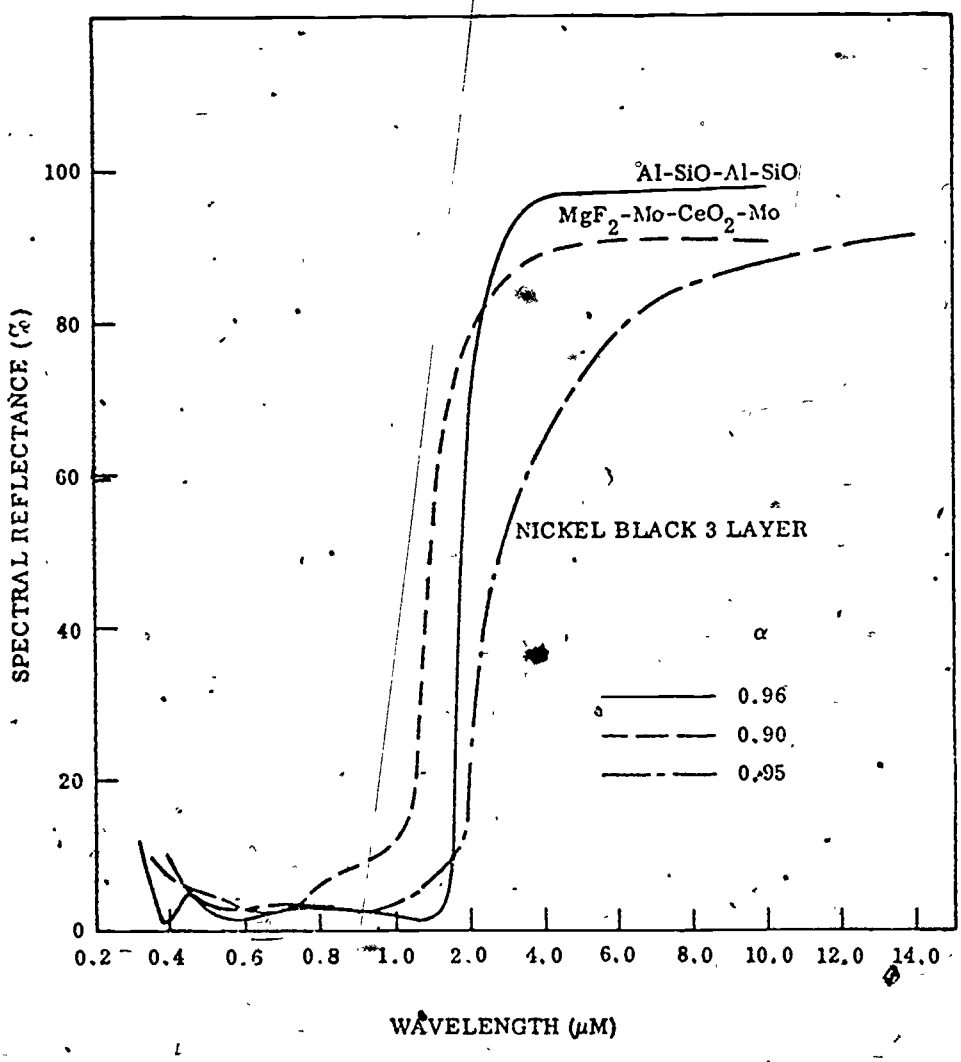


Figure 60 Reflectance of Spectrally Selective Coatings [98]

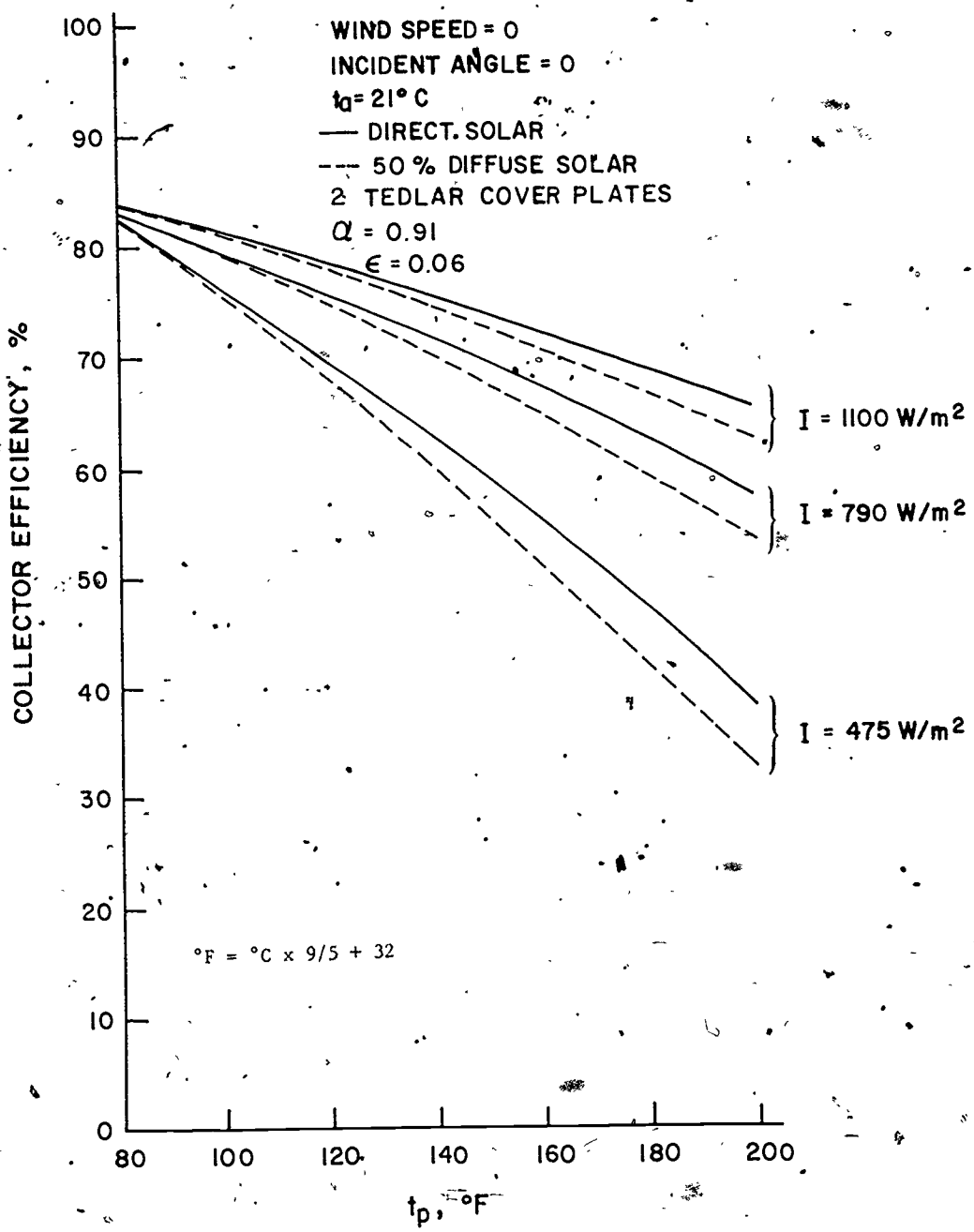


Figure 61 Comparison of Calculated Solar Collector Efficiency for Direct and 50% Diffuse Solar Radiation and with the Sun Normal to the Collector

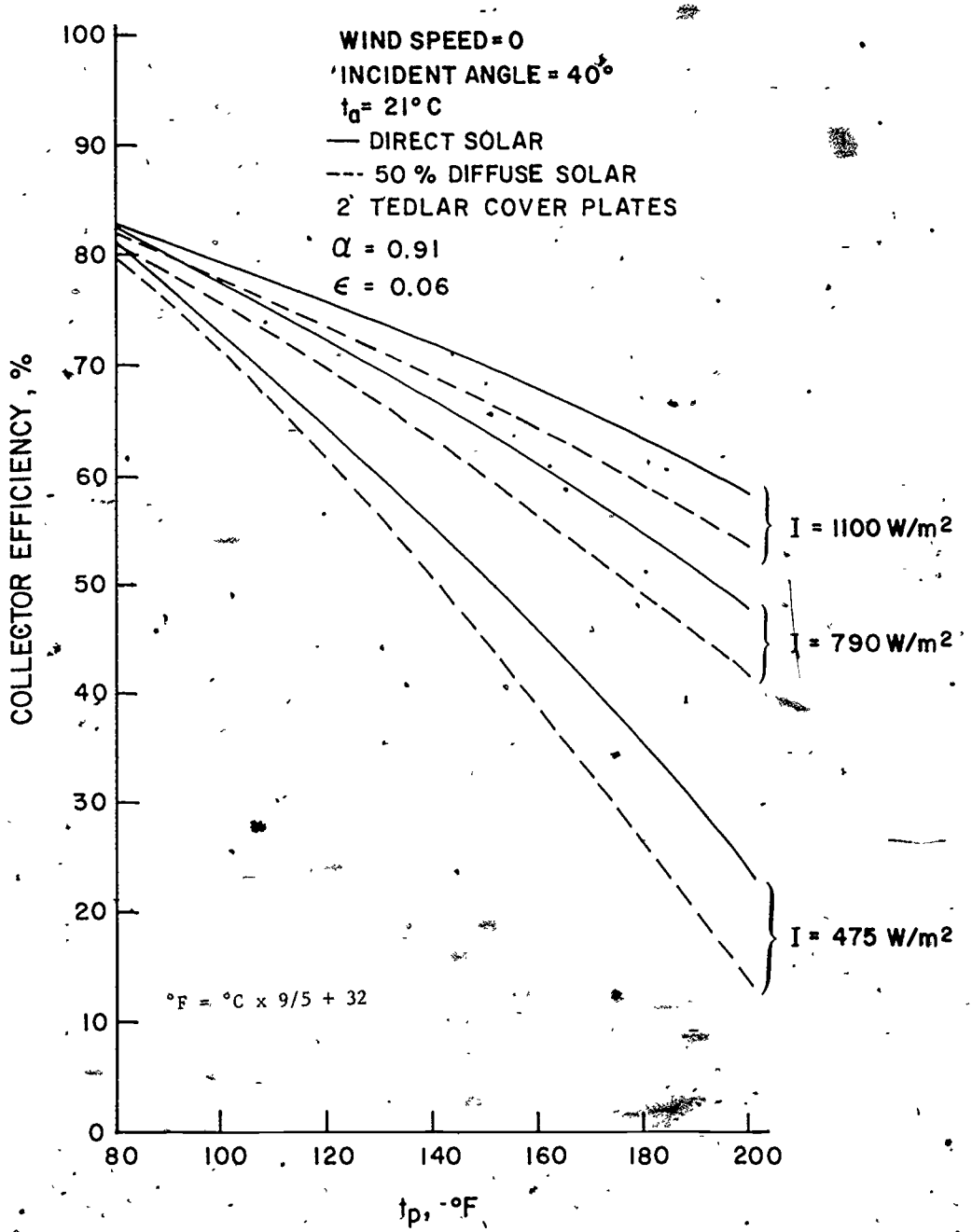


Figure 62 Comparison of Calculated Solar Collector Efficiency for Direct and 50% Diffuse Solar Radiation with the Sun 40° Off the Collector Normal

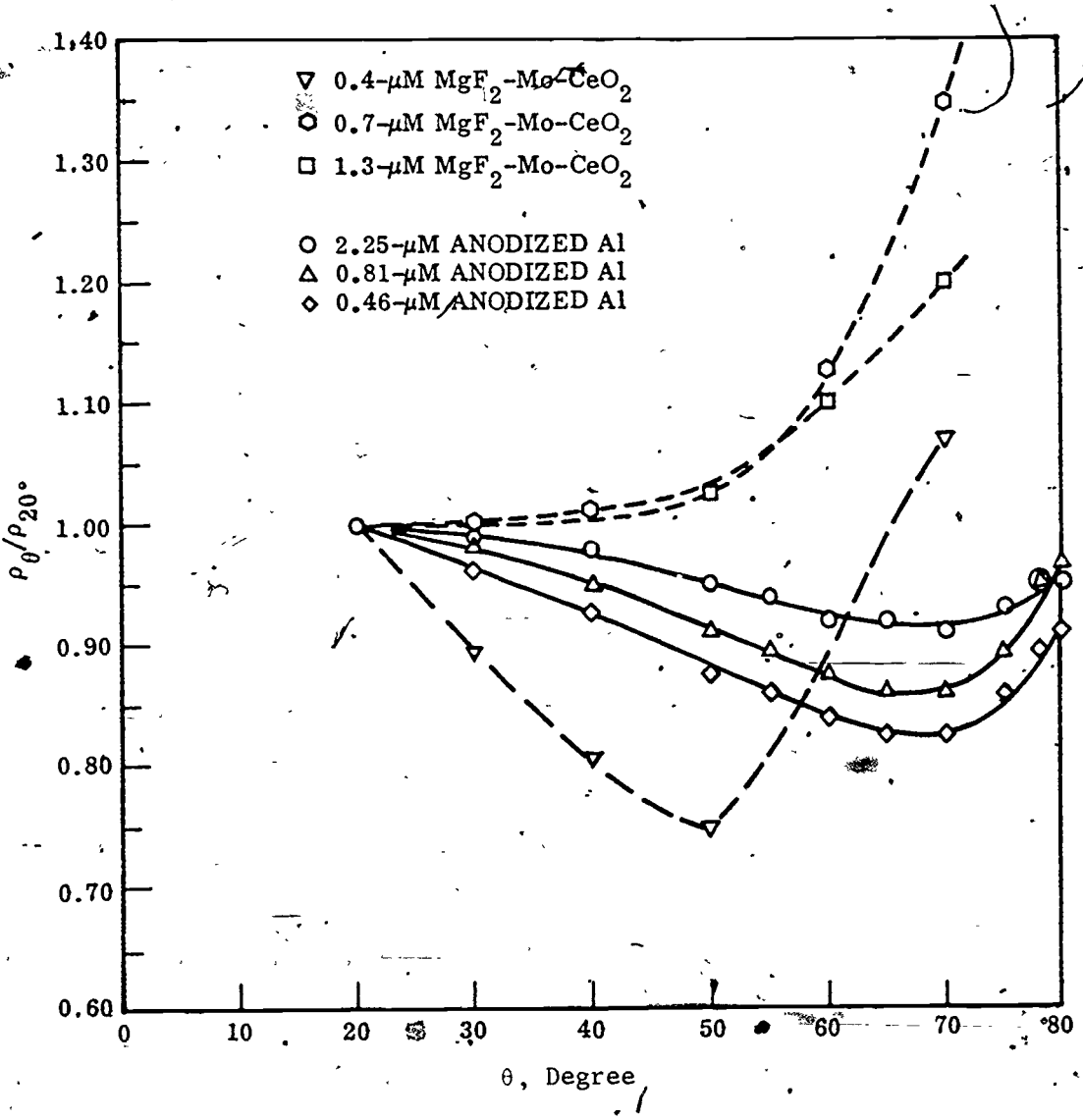


Figure 63 Normalized Directional Reflectance of Two Types of Solar Absorber Coatings [98]

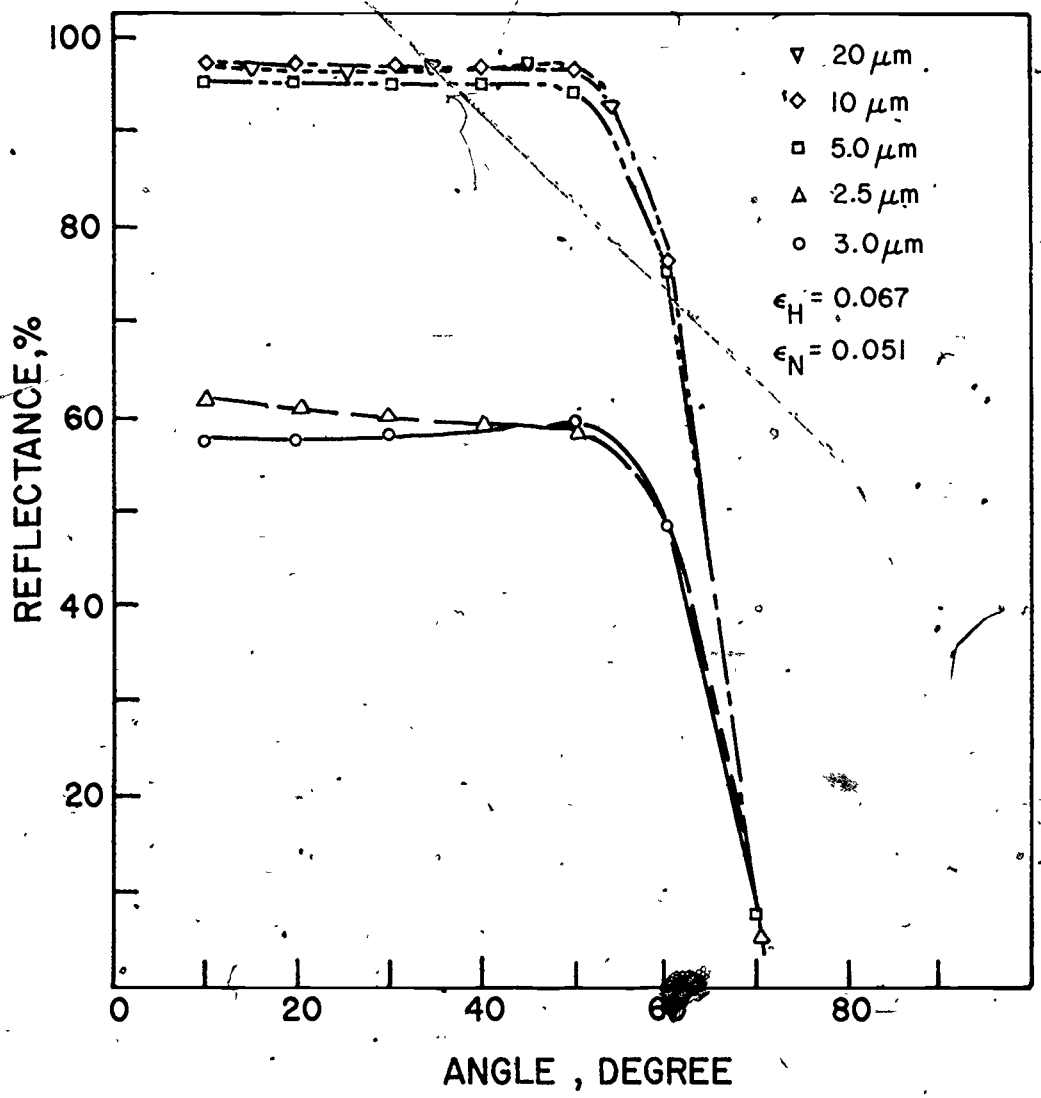


Figure 64 Infrared Reflectance of Cobalt Oxide Versus Incident Angle [98]

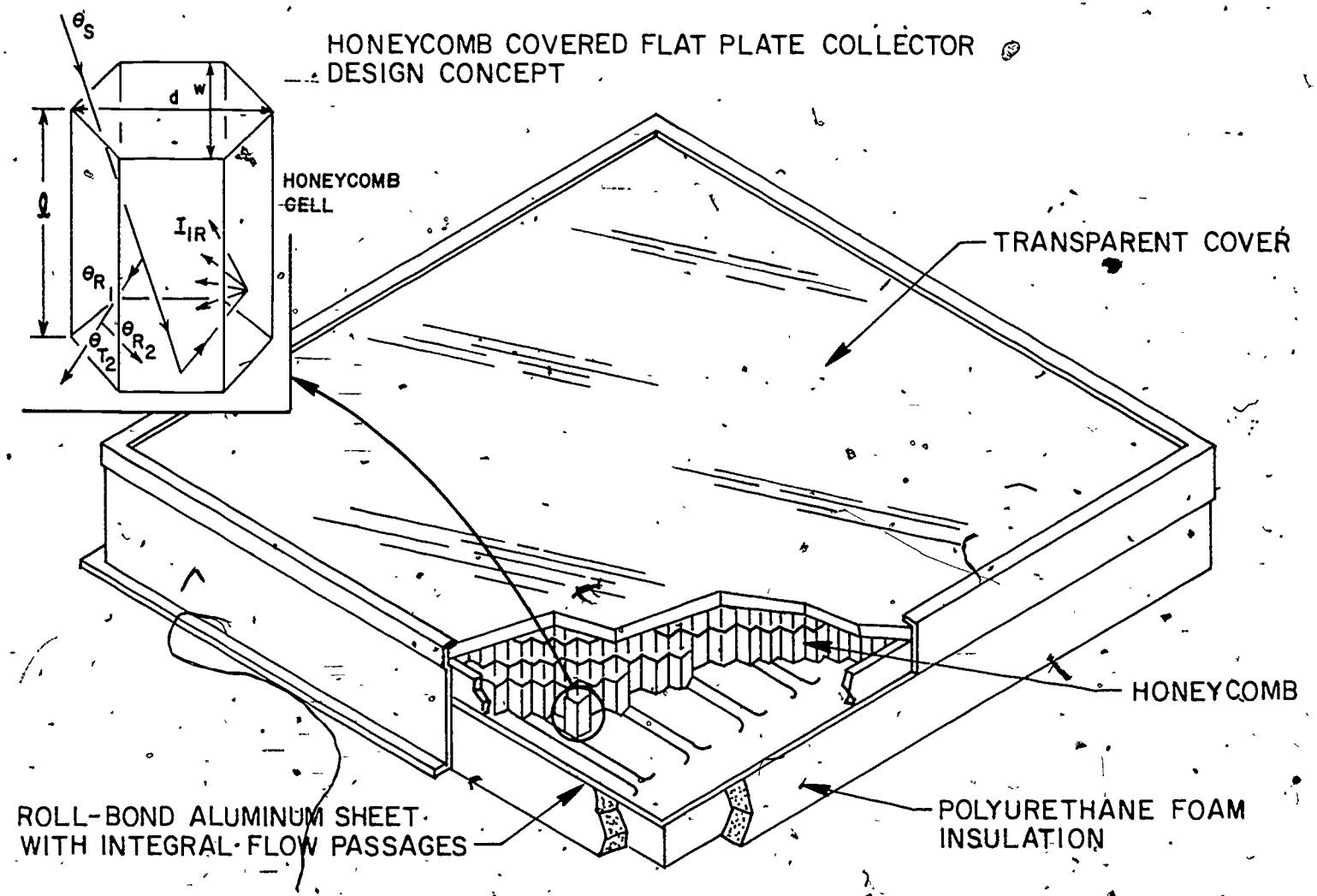


Figure 65 Schematic of a Flat-Plate Liquid-Heating Solar Collector Incorporating Honeycomb Convection Suppressors

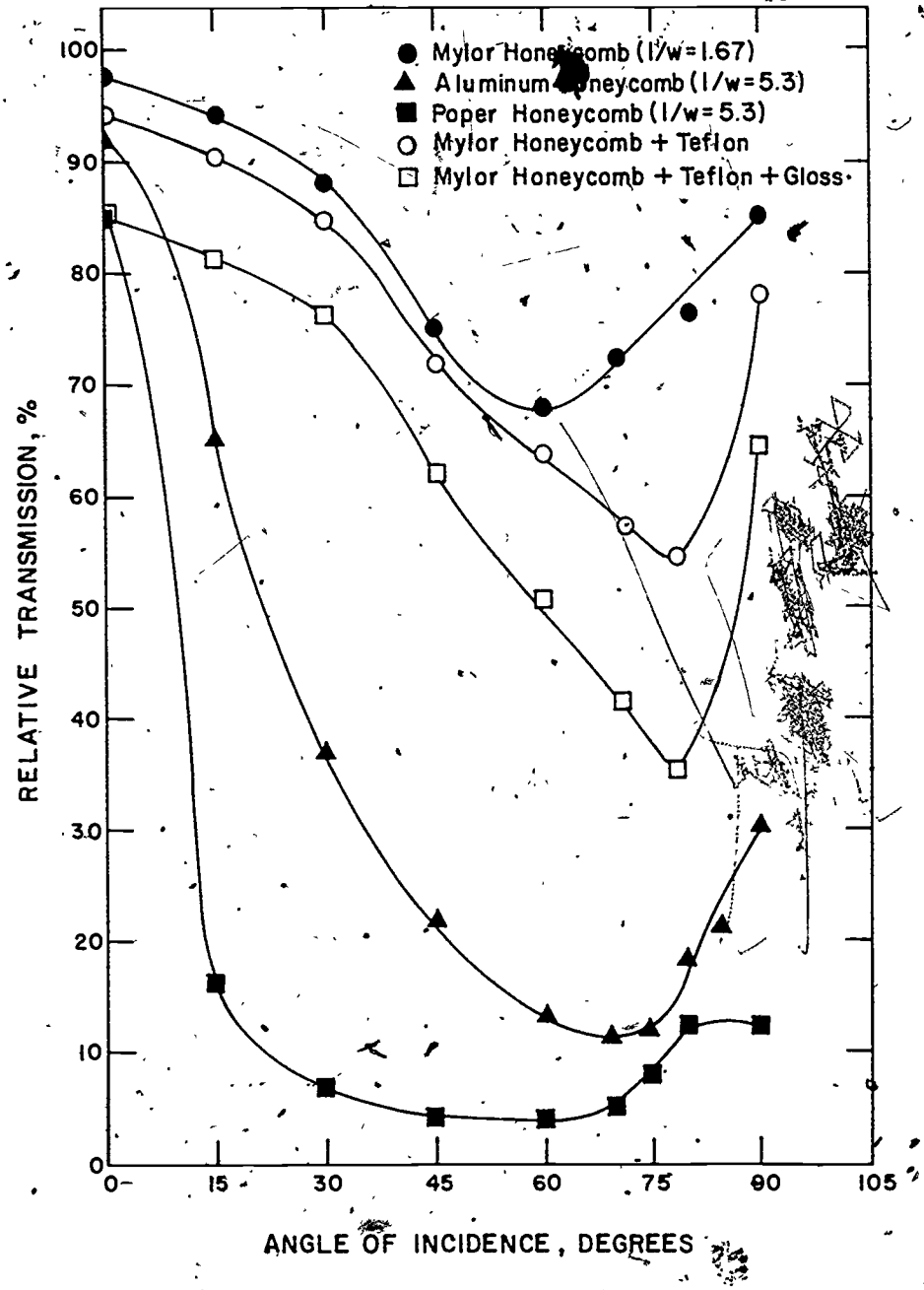


Figure 66 Relative Transmission of Selected Honeycomb Materials as a Function of Incident Angle[104]

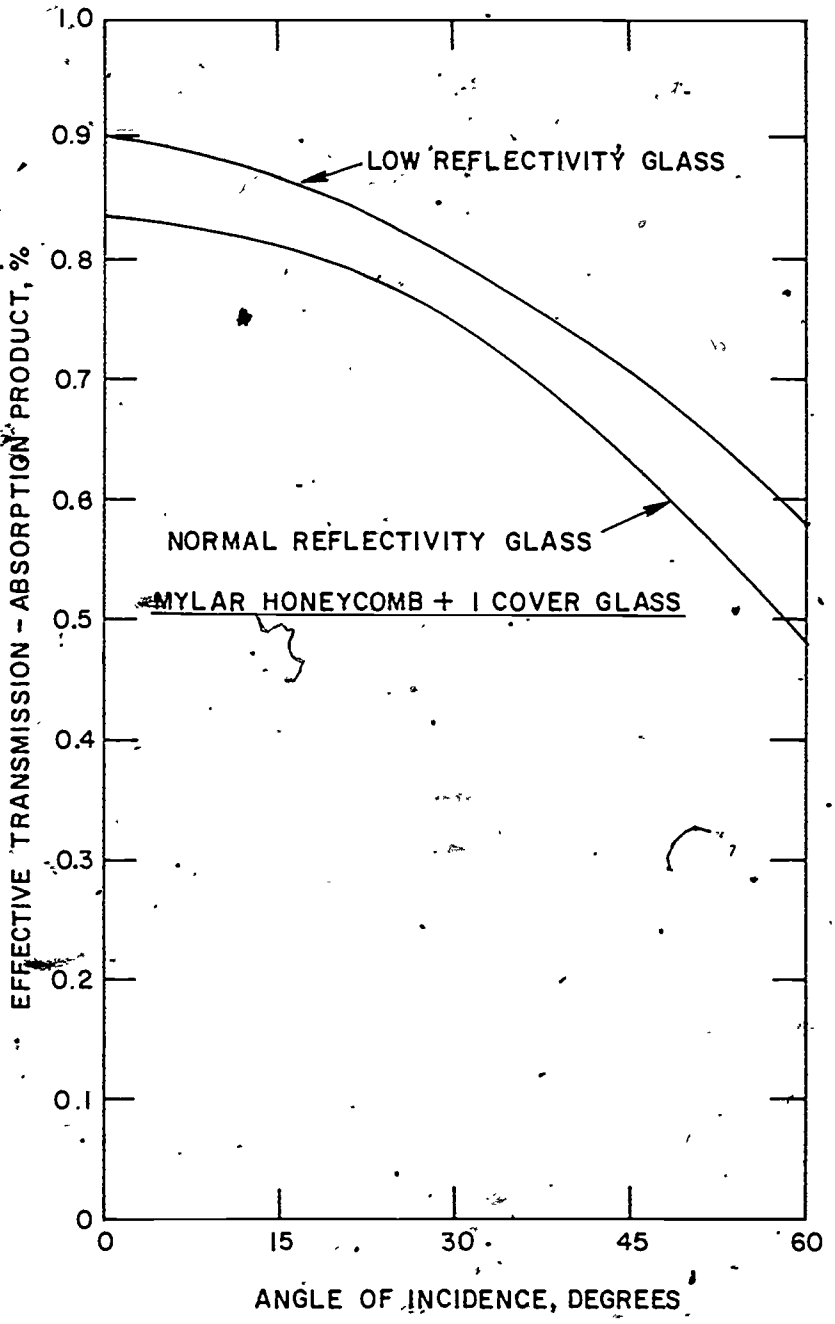


Figure 67 Transmission - Absorptance Product for a Single-Glazed Flat-Plate Solar Collector Incorporating a Honeycomb Convection Suppressor [17]

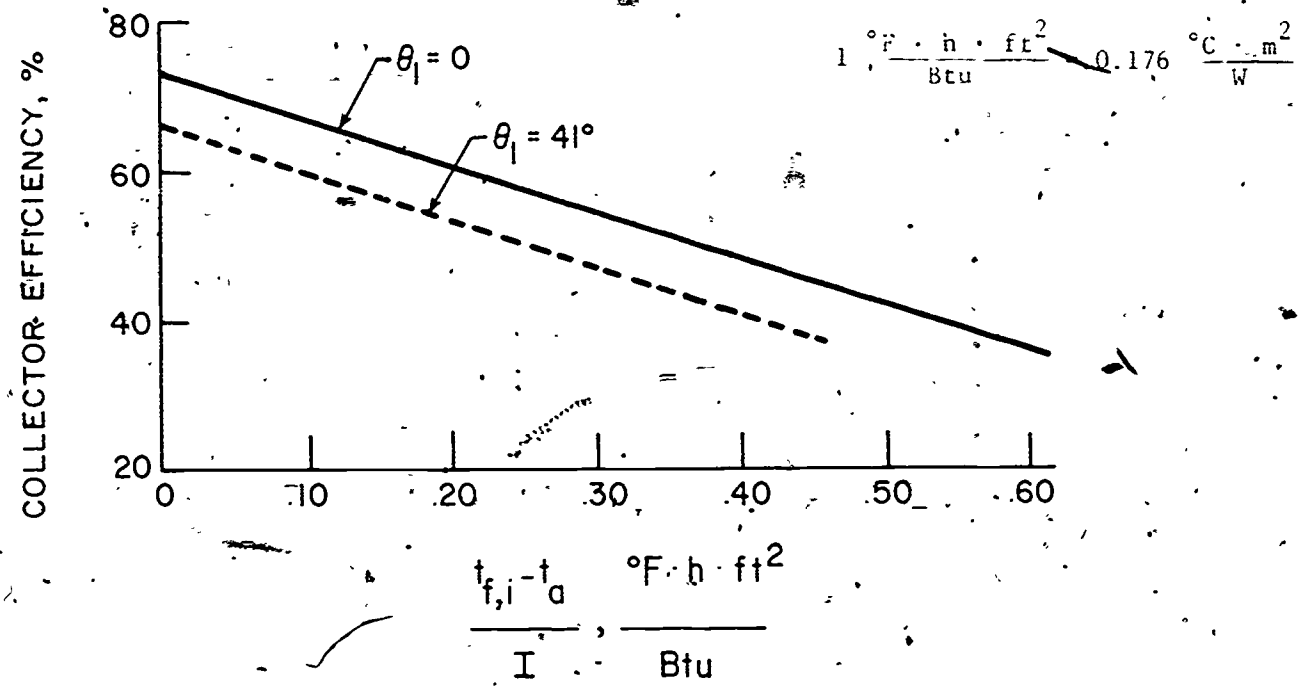


Figure 68 Efficiency Curve for a Double-Glazed, Flat-Plate Liquid-Heating Solar Collector Incorporating a Honeycomb Convection Suppressor [29]

$$1 \frac{°F \cdot h \cdot ft^2}{Btu} = 0.176 \frac{°C \cdot m^2}{W}$$

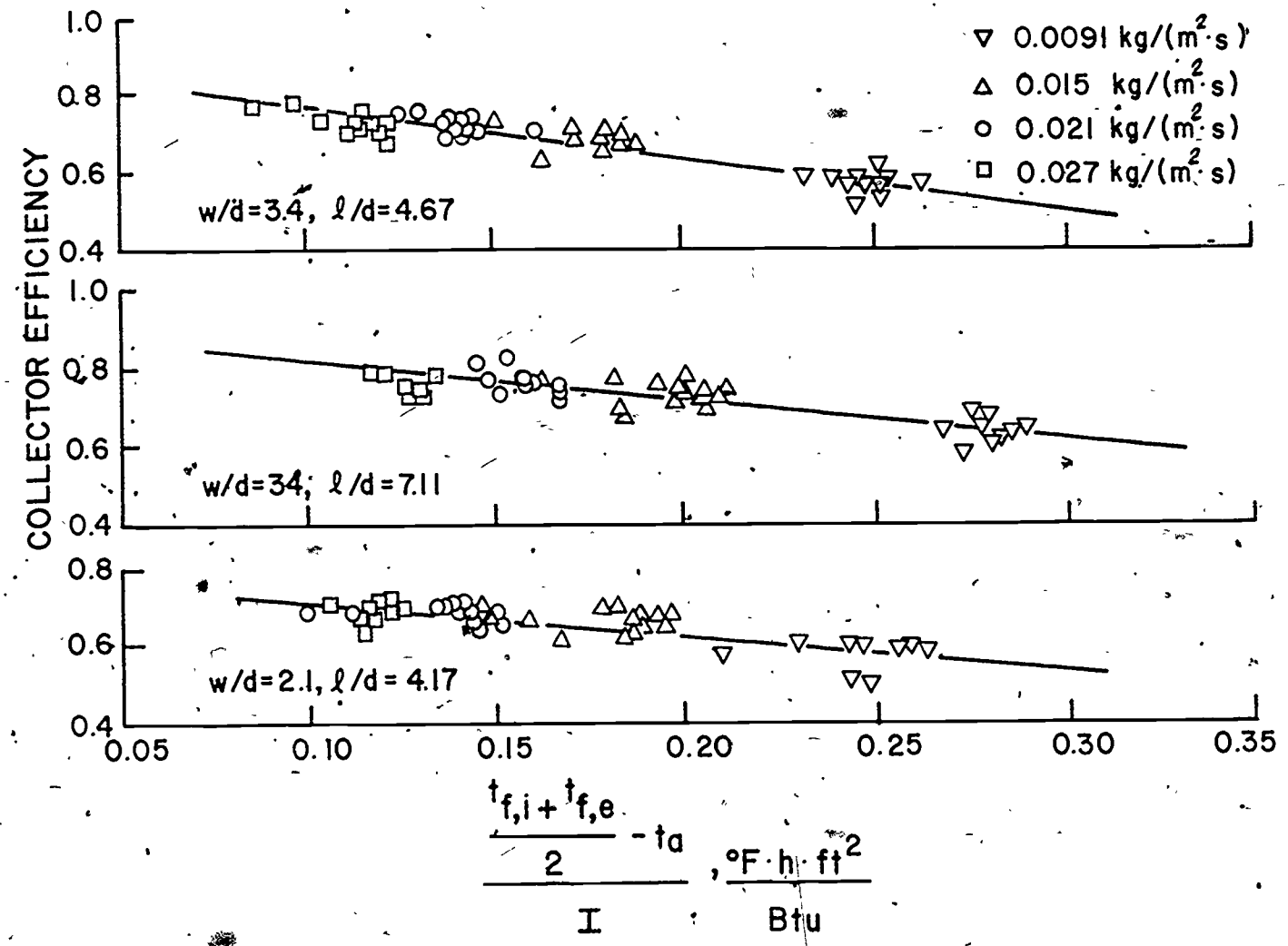


Figure 69 Efficiency Curves for Three Flat-Plate Solar Collectors Incorporating Rectangular Honeycomb Convection Suppressors [102]

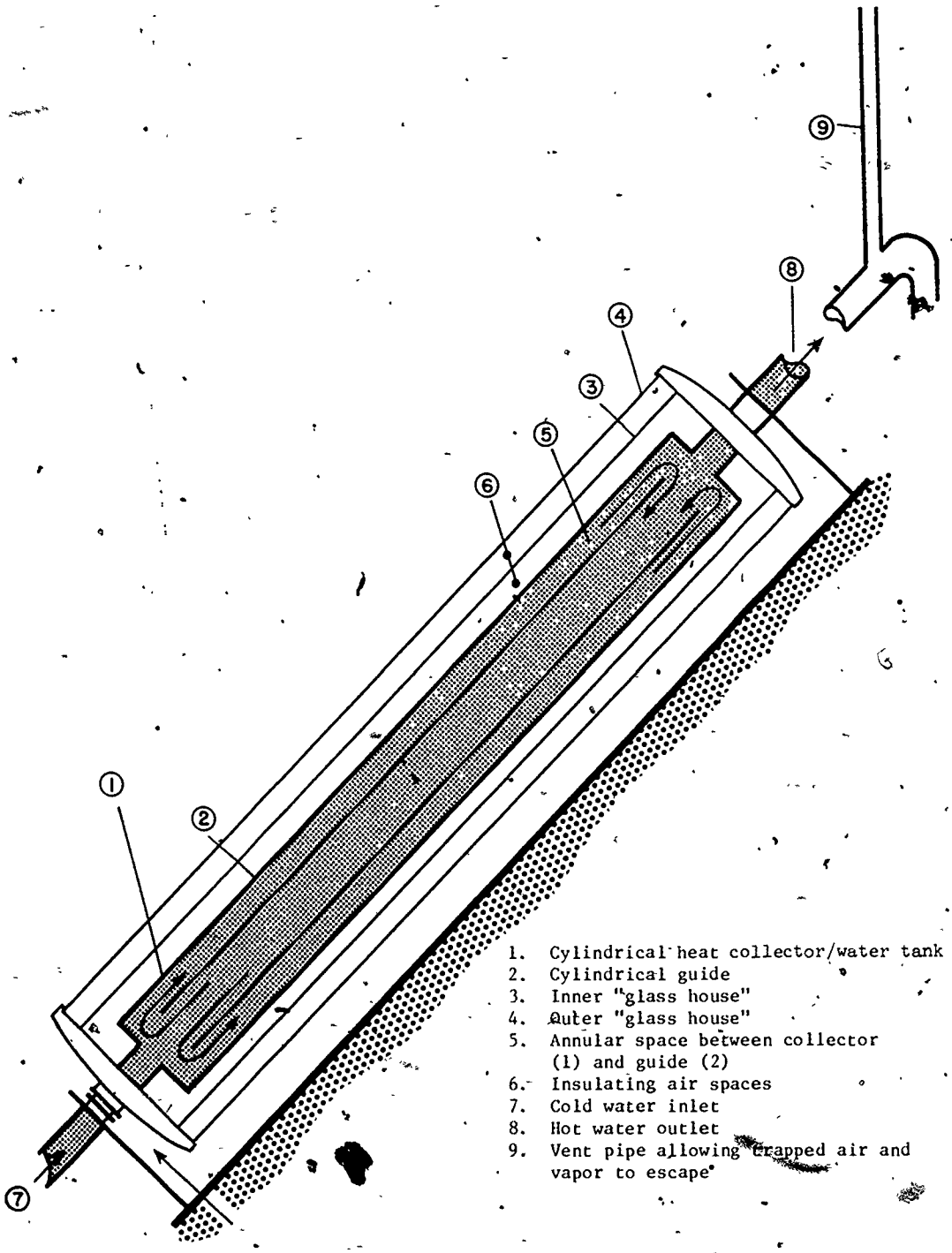


Figure 70 Schematic of a Non-Evacuated Cylindrical Liquid-Heating Solar Collector [1]

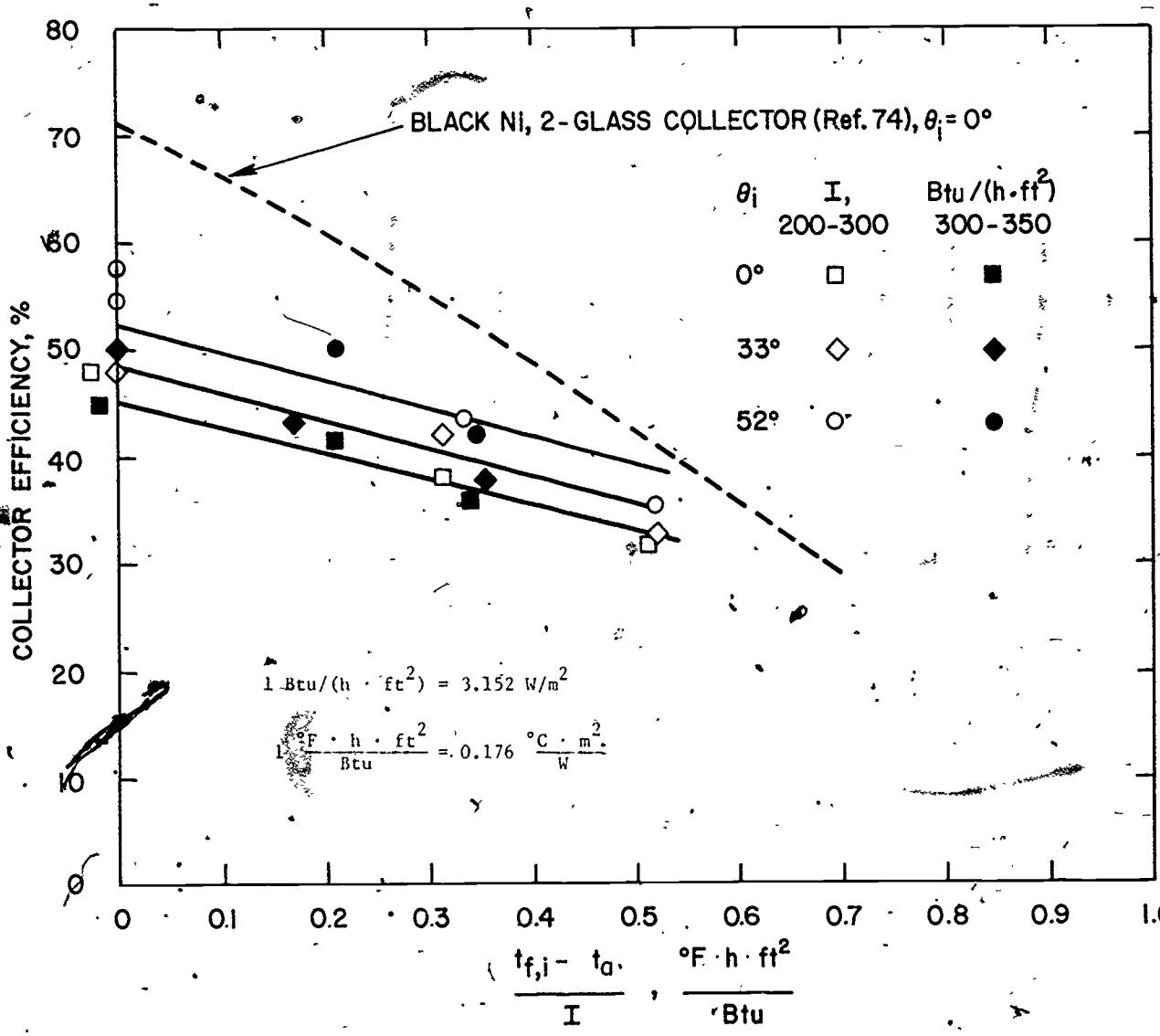


Figure 71 Efficiency Curves for an Evacuated Cylindrical Liquid-Heating Solar Collector with a Selectively Coated Absorber Determined Using the Indoor Test Facility at the NASA Lewis Research Center [75]

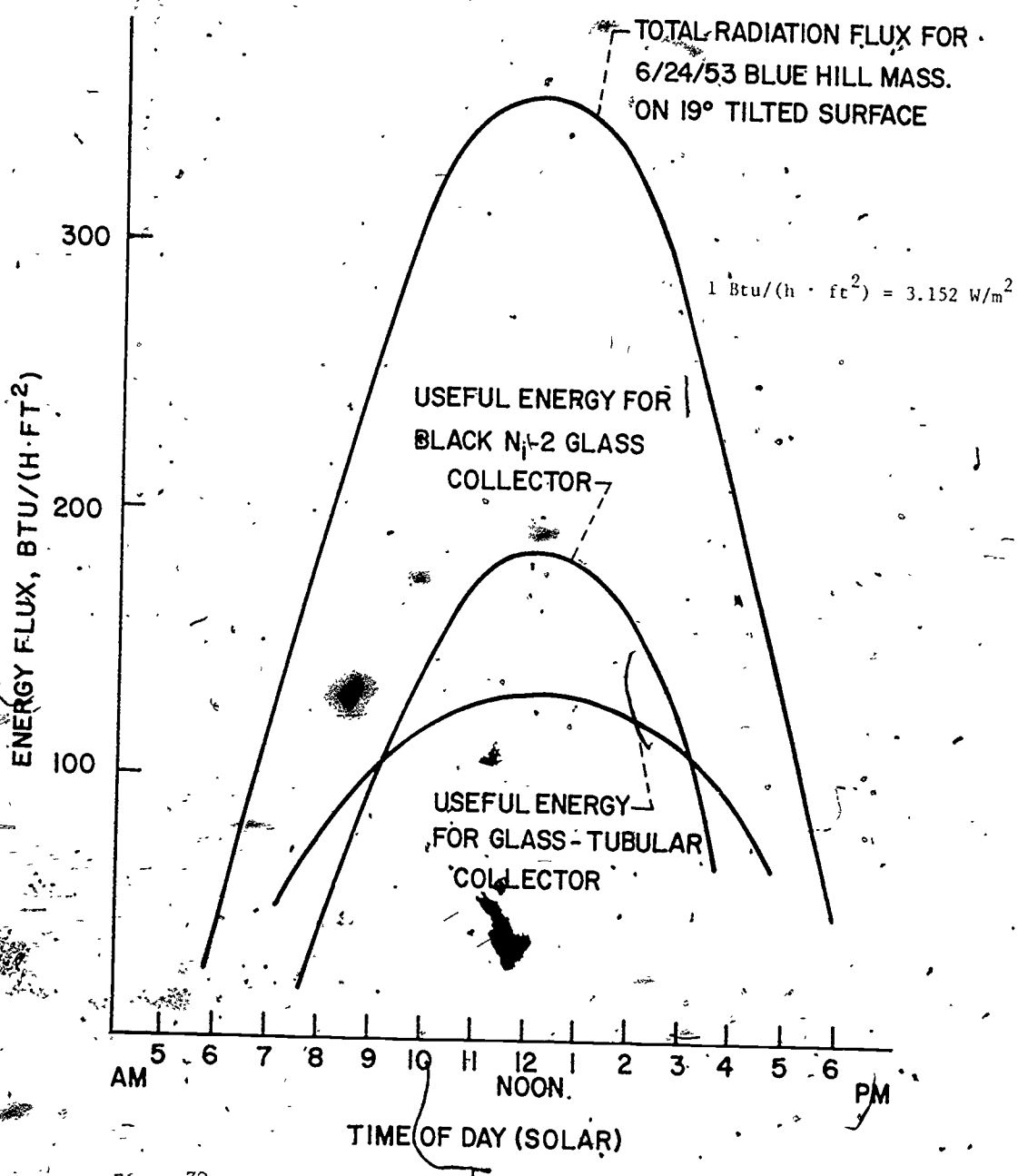


Figure 72 Predicted Daily Performance for an Evacuated Cylindrical Solar Collector and a Double-Glazed Flat-Plate Solar Collector, Both with Selectively Coated Absorbers [75]

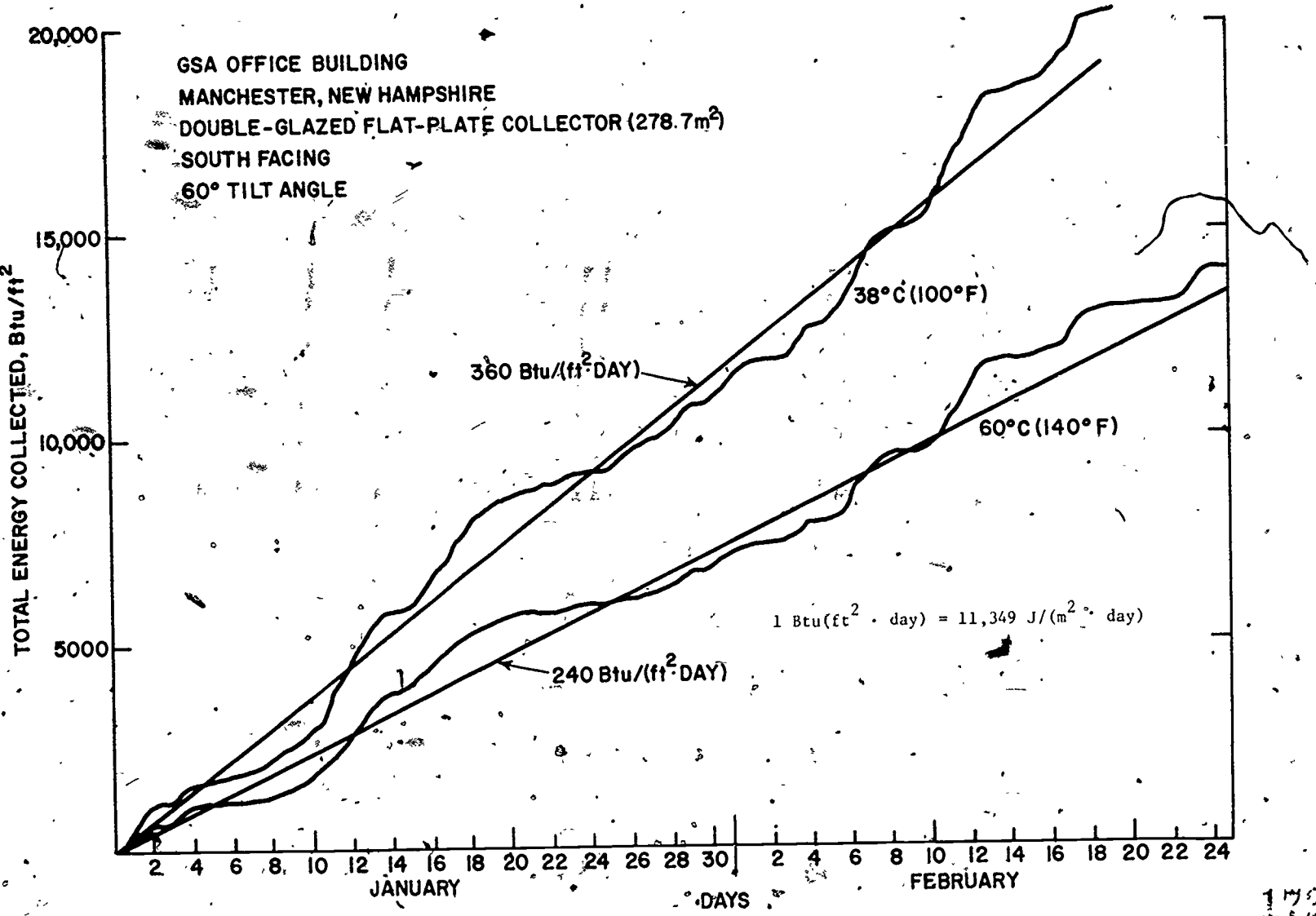


Figure 73 Predicted Output for a Double-Glazed Liquid-Heating Flat-Plate Solar Collector in Manchester, New Hampshire [125]

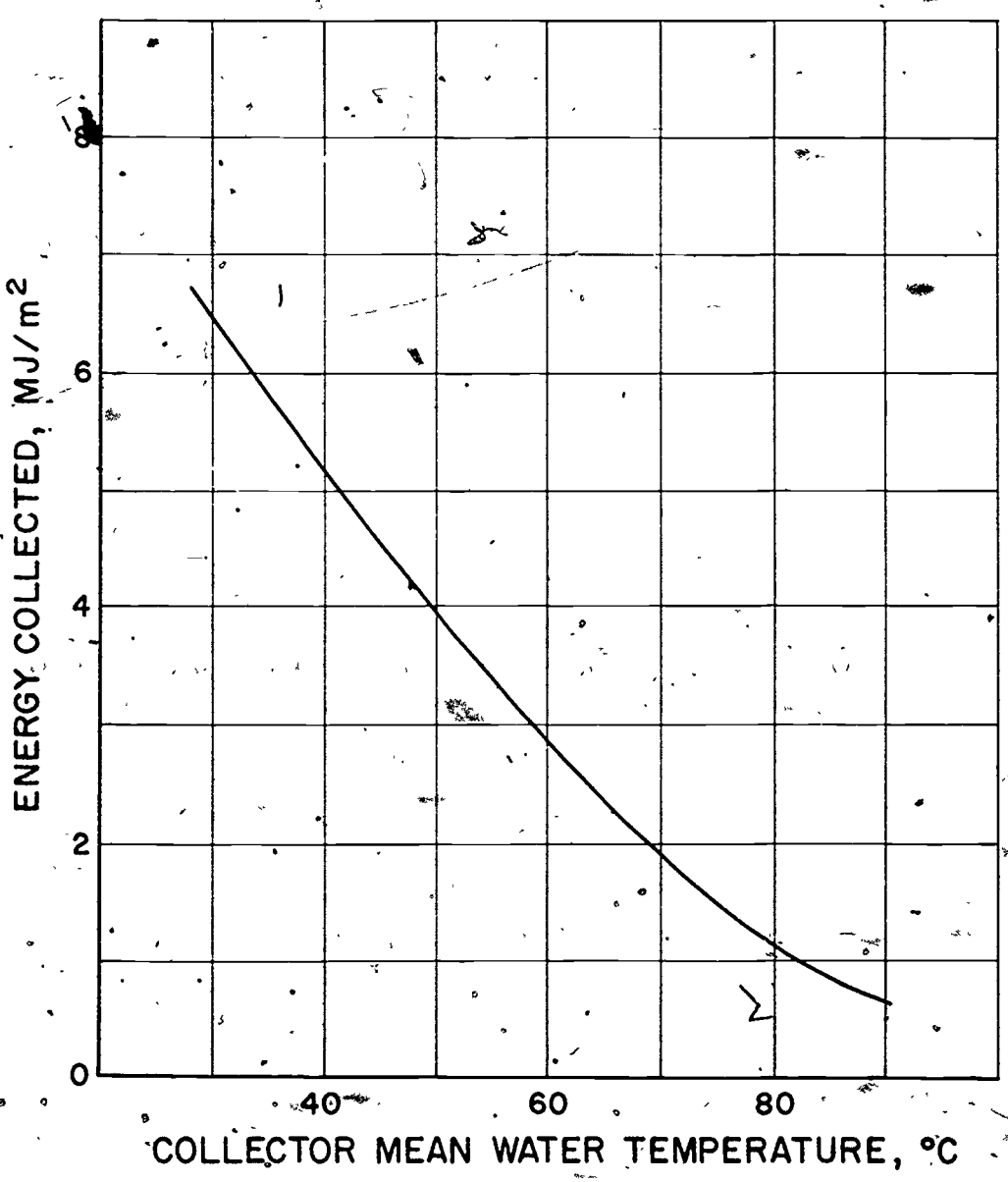


Figure 74 Daily Energy Collected as a Function of Collector Operating Temperature for a Single-Glazed Liquid-Heating Solar Collector in Australia [128]

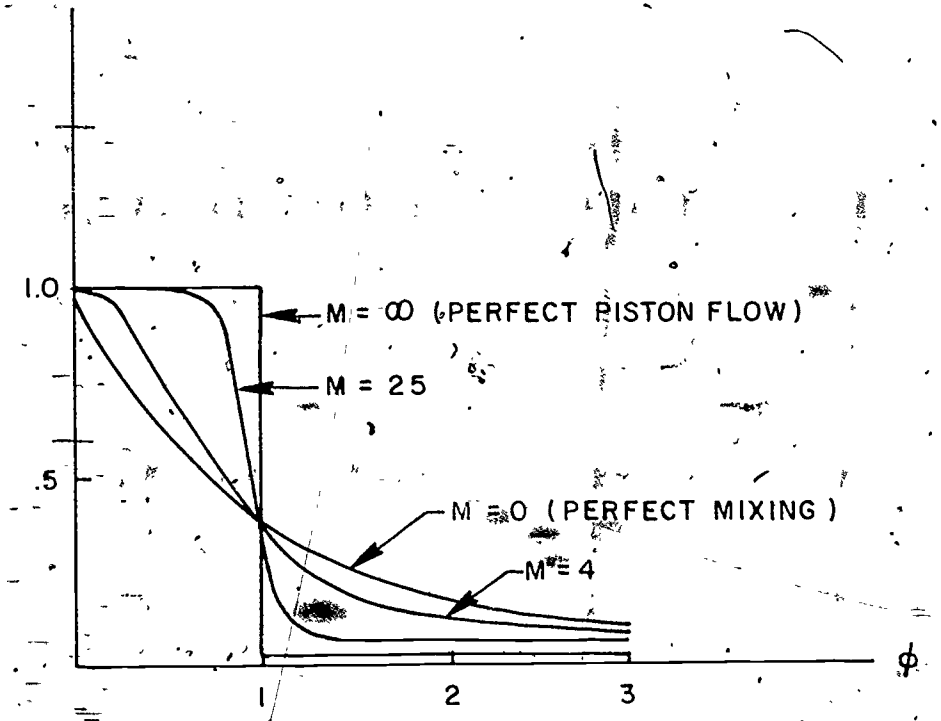


Figure 75 —~~Indicial~~ Response Function for the Outlet Temperature of a Water Tank when there is a Unit Step Rise in the Inlet Temperature

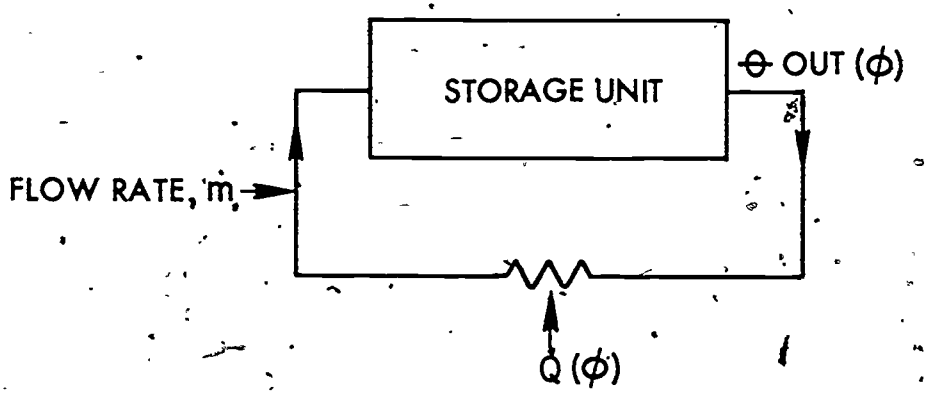


Figure 76 Schematic Representation of the Testing Configuration for a Thermal Storage Unit when the Driving Force is a Time Dependent Heat Flux

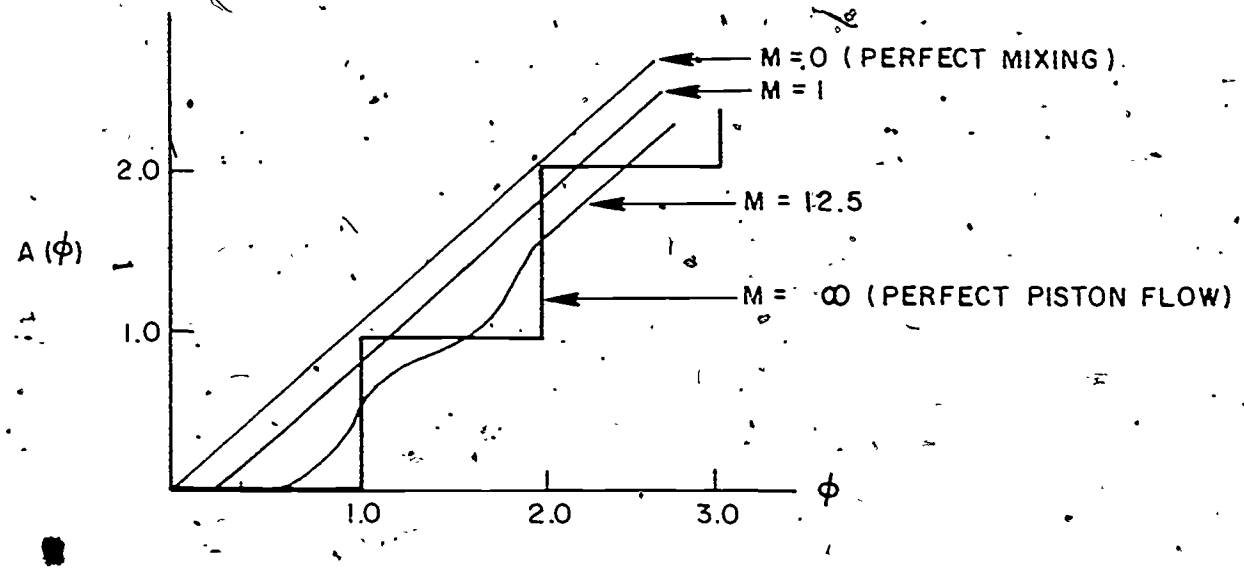


Figure 77 Indicial Response Function of a Thermal Storage Unit for Different Values of the Mixing Parameter M

## 6. Appendix A

## Methods of Testing for Rating Solar Collectors Based on Thermal Performance

### SECTION 1. PURPOSE

1.1 The purpose of this standard is to provide test methods for determining the thermal performance of solar collectors which heat fluids and are used in systems to provide the thermal requirements for heating, cooling, and the generation of domestic hot water in buildings.

### SECTION 2. SCOPE

2.1 This standard applies to solar collectors in which a fluid enters the device through a single inlet and leaves the device through a single outlet. The collector containing more than one inlet and/or outlet can be tested according to this standard provided that the external piping can be connected in such a way as to effectively provide a single inlet and/or outlet for the determination of the bulk properties of the fluid entering and leaving the collector. The fluid can be either a gas or liquid but not a mixture of the two. The collector can be a concentrating collector provided that the aperture or interception area for the device can be determined. The collector may have the capability of rotating so as to track the sun.

2.2 This standard is not applicable to those configurations in which the flow into the collector and out of the collector cannot be reduced effectively to one inlet and one outlet. This standard is not applicable to those collectors in which the thermal storage unit is an integral part of the collector such that the collection process and storage process cannot be separated for the purpose of making measurements.

2.3 This standard does not address factors relating to cost or consideration of requirements for interfacing with a specific heating and cooling system.

2.4 The present version of the standard provides test methods for determining the steady-state efficiency of solar collectors. The transient response of solar collectors cannot be determined with the test methods outlined herein.

## SECTION 3. DEFINITIONS

### 3.1 AMBIENT AIR

Ambient air is the outdoor air in the vicinity of the solar collector being tested.

### 3.2 ABSORBER

The absorber is that part of the solar collector that receives the incident solar radiation and transforms it into thermal energy. It is usually a solid surface through which energy is transferred to the transfer fluid; however, the transfer fluid itself could be the absorber in the case of a "black liquid".

### 3.3 APERTURE

The aperture is the opening or projected area of a solar collector through which the unconcentrated solar energy is admitted and directed to the absorber.

### 3.4 CONCENTRATING COLLECTOR

A concentrating collector is a solar collector that contains reflectors, lenses, or other optical elements to concentrate the energy falling on the aperture onto a heat exchanger of surface area smaller than the aperture.

### 3.5 CONCENTRATOR

The concentrator is that part of a concentrating collector which directs the incident solar radiation onto the absorber.

### 3.6 COVER PLATE

The cover plate designates the diathermanous material or materials covering the aperture and most directly exposed to the solar radiation. These materials are generally used to reduce the heat loss from the absorber to the surroundings and to protect the absorber.

### 3.7 FLAT-PLATE COLLECTOR

A flat-plate collector is a solar collector in which the solid surface absorbing the incident solar radiation is essentially flat and employs no concentration.

3.8 GROSS CROSS-SECTIONAL AREA

Gross cross-sectional area is the overall or outside area of a flat-plate collector. It is usually slightly larger than the absorber area since it includes the framework required to hold the absorber.

3.9 INCIDENT ANGLE

The incident angle is the angle between the sun's rays and the outward drawn normal from the solar collector.

3.10 INSOLATION

Insolation is the rate of solar radiation received by a unit surface area in unit time ($W/m^2$, $Btu/(h \cdot ft^2)$).

3.11 INSTANTANEOUS EFFICIENCY

The instantaneous efficiency of a solar collector is defined as the amount of energy removed by the transfer fluid per unit of transparent frontal area over a given 15 minute period divided by the total incident solar radiation onto the collector per unit area for the 15 minute period.

3.12 INTEGRATED AVERAGE INSOLATION

The integrated average insolation is the total energy per unit area received by a surface for a specified time period divided by the time period ($W/m^2$, $Btu/(h \cdot ft^2)$).

3.13 PYRANOMETER

A pyranometer is a radiometer used to measure the total incident solar energy per unit time per unit area upon a surface which includes the beam radiation from the sun, the diffuse radiation from the sky, and the shortwave radiation reflected from the foreground.

3.14 PYRHELIOMETER

A pyrheliometer is a radiometer used to measure the direct or beam radiation on a surface normal to the sun's rays.

3.15 QUASISTEADY

Quasisteady is the term used in this document to describe the state of the solar collector test when the flow rate and temperature of the fluid entering the collector is constant but the exit fluid temperature changes "gradually" due to the normal change in insolation that occurs with time for clear sky conditions.

3.16 SOLAR COLLECTOR

A solar collector is a device designed to absorb incident solar radiation and to transfer the energy to a fluid passing in contact with it.

3.17 TOTAL INCIDENT INSOLATION

Total incident insolation is the total energy received by a unit surface area for a specified time period ($J/m^2$).

3.18 TRANSFER FLUID

The transfer fluid is the medium such as air, water, or other fluid which passes through or in contact with the solar collector and carries the thermal energy away from the collector.

3.19 TRANSPARENT FRONTAL AREA

The transparent frontal area is the area of the transparent frontal surface for flat-plate collectors.

3.20 STANDARD AIR

Standard air is air weighing 1.2 $kg/m^3$ (0.075 $lb/ft^3$), and is equivalent in density to dry air at a temperature of 21.1°C (70°F) and a barometric pressure of $1.01 \times 10^5$ $N/m^2$ (29.92 in of Hg)

3.21 STANDARD BAROMETRIC PRESSURE

$1.01 \times 10^5$ $N/m^2$ (29.92 in. of Hg)

## SECTION 4. CLASSIFICATIONS

4.1 Solar collectors may be classified according to their collecting characteristics, the way in which they are mounted, and the type of transfer fluid they employ.

4.1.1 Collecting Characteristics. A non-concentrating or "flat-plate" collector is one in which the absorbing surface for solar radiation is essentially flat with no means for concentrating the incoming solar radiation. A concentrating or "focusing" collector is one which usually contains reflectors or employs other optical means to concentrate the energy falling on the aperture onto a heat exchanger of surface area smaller than the aperture.

4.1.2 Mounting. A collector can be mounted to remain stationary, be adjustable as to tilt angle (measured from the horizontal) to follow the change in solar declination, or be designed to track the sun. Tracking is done by employing either an equatorial mount or an altazimuth mounting, for the purpose of increasing the absorption of the daily solar irradiation.

4.1.3 Type of Fluid. A collector will usually use either a liquid or a gas as the transfer fluid. The most common liquids are water or a water-ethylene glycol solution. The most common gas is air.

## SECTION 5. REQUIREMENTS

5.1 Solar collectors shall be tested for rating in accordance with the provisions set forth below and in Section 8.

5.1.1 The size of collector tested shall be large enough so that the performance characteristics determined will be indicative of those that would occur when the collector is part of an installed system. If the collector is modular and the test is being done on one module, it should be mounted and insulated in such a way that the back and edge losses will be characteristic of those that will occur during operation on a structure.

5.1.2 The collector shall be mounted in a location such that there will be no significant energy reflected or reradiated onto the collector from surrounding buildings or any other surfaces in the vicinity of the test stand for the duration of the test(s). This will be satisfied if the ground and immediately adjacent surfaces are diffuse with a reflectance of less than 0.20. If significant reflection will occur, provision shall be made to shield the collector by the use of a non-reflective shield. In addition, the test stand shall be located so that a shadow will not be cast onto the collector at any time during the test period.

5.1.3 The test(s) shall be conducted on days having weather conditions such that the 15 minute integrated average insolation measured in the plane of the collector or aperture, reported, and used for the computation of instantaneous efficiency values shall be a minimum of 630 $W/m^2$ (199.8 $Btu/(h.ft^2)$). Specific values that can be expected for clear sky conditions are shown in Tables A1 through A6 taken from reference [1]. More accurate estimates can be made using the tables in conjunction with clearness numbers*.

5.1.4 The orientation of the collector shall be such that the incident angle (measured from the normal to the collector surface or aperture) is less than 45° during the period in which test data is being taken. Angles of incidence can be estimated from Tables A7 through A12 taken from reference [2]. More accurate estimates can be made using the procedures outlined in references [3], p. 393 or [4], pp. 283-292.

5.1.5 The air velocity across the collector surface of a flat-plate collector or aperture of a concentrating collector during the test(s) shall be measured. The measurement shall be made at a distance of approximately 1 m (3.3 ft) from the collector along the direction it faces and at a height corresponding to the center of the collector panel.

5.1.6 The range of ambient temperatures for all reported test points comprising the "efficiency curve" shall be less than 30°C (54°F).

5.1.7 The transfer fluid used in the solar collector shall have a known specific heat which varies by less than 0.5% over the temperature range of the fluid during a particular 15 minute test period.

## SECTION 6. INSTRUMENTATION

### 6.1 SOLAR RADIATION MEASUREMENT

6.1.1 A pyranometer shall be used to measure the total short-wave radiation from both the sun and the sky. The instrument shall have the following characteristics [5]:

---

* Reference [3], p. 394, Figure 4.

6.1.1.1 Change of Response Due to Variation in Ambient Temperature. The instrument shall either be equipped with a built-in temperature compensation circuit and have a temperature sensitivity of less than ± 1 percent over the range of ambient temperature encountered during the test(s) or have been tested in a temperature-controlled chamber over the same temperature range so that its temperature coefficient has been determined in accordance with reference [5].

6.1.1.2 Variation in Spectral Response. Errors caused by a departure from the required spectral response of the sensor shall not exceed ± 2 percent over the range of interest*.

6.1.1.3 Nonlinearity of Response. Unless the pyranometer was supplied with a calibration curve relating the output to the insolation, its response shall be within ± 1 percent of being linear over the range of insolation existing during the tests.

6.1.1.4 Time Response of Pyranometer. The time constant of the pyranometer shall be less than 5 s.

6.1.1.5 Variation of Response With Attitude. The calibration factor of a pyranometer can change when the instrument is used in other than the orientation for which it was calibrated. The instruments' calibration factor (including corrections) shall change less than ± 0.5 percent compared with the calibrated orientation when placed in the orientation used during the test(s).

6.1.1.6 Variation of Response With Angle of Incidence. Ideally the response of the receiver is proportional to the cosine of the zenith angle of the solar beam and is constant at all azimuth angles. The pyranometer's deviation from a true cosine response shall be less than ± 1 percent for the incident angles encountered during the test(s).

---

* Pyranometer thermopiles which are "all black" and which are coated with Parson's black or 3M 101C10 velvet black paint and which have selected optical grade hemispheres usually satisfy this requirement [5]. Note: Identification of commercial materials does not imply recommendation or endorsement by the National Bureau of Standards.

6.1.2 The pyranometer shall be calibrated within six months of the collector test(s) against other pyranometers whose calibration uncertainty relative to recognized measurement standards is known*.

## 6.2 TEMPERATURE MEASUREMENTS

6.2.1 Temperature measurements shall be made in accordance with ASHRAE Standard 41-66, Part 1 [6].

6.2.2 Temperature Difference Measurements Across the Solar Collector. The temperature difference of the transfer fluid across the solar collector shall be measured with:

a. Thermopile (air or water as the transfer fluid)

b. Calibrated resistance thermometers connected in two arms of a bridge circuit (only when a liquid is the transfer fluid)

6.2.3 The accuracy and precision of the instruments and their associated readout devices shall be within the limits as follows:

| | Instrument Accuracy** | Instrument Precision*** |
|---|---|---|
| Temperature | ± 0.5°C (± 0.9°F) | ± 0.2°C (± 0.4°F) |
| Temperature Difference | ± 0.1°C (± 0.2°F) | ± 0.1°C (± 0.2°F) |

One nationally recognized calibration center is the Eppley Laboratory in Newport, Rhode Island. The calibration data are commonly expressed in cal/(cm$^2$· min) or in Langleys/min. In some meteorological services, calibration data are supplied in milliwatt/cm$^2$. The following equivalent units shall be used:

$$1 \text{ cal}/(\text{cm}^2 \cdot \text{min}) = 1 \text{ ly/min} = .001434 \text{ W/m}^2$$

$$1 \text{ mW/cm}^2 = 0.1 \text{ W/m}^2$$

** The ability of the instrument to indicate the true value of the measured quantity.

*** Closeness of agreement among repeated measurements of the same physical quantity.

6.2.4 In no case should the smallest scale division of the instrument or instrument system exceed 2 1/2 times the specified precision. For example, if the specified precision is ± 0.1°C (± 0.2°F), the smallest scale division shall not exceed 0.25°C (0.5°F).

6.2.5 The instruments shall be configured and used in accordance with Section 7. of this standard.

6.2.6 When using thermopiles, they shall be constructed in accordance with ANSI Standard C96.1-1964 (R 1969) [7].

## 6.3 LIQUID FLOW MEASUREMENTS

6.3.1 The accuracy of the liquid flow rate measurement using the calibration, if furnished shall be equal to or better than ± 1.0% of the measured value.

## 6.4 INTEGRATORS AND RECORDERS

6.4.1 Strip chart recorders used shall have an accuracy equal to or better than ± 0.5% of the temperature difference and/or voltage measured and have a time constant of 1 s or less.

6.4.2 Electronic integrators used shall have an accuracy equal to or better than ± 1.0% of the measured value.

## 6.5 AIR FLOW MEASUREMENTS

When air is used as the transfer fluid, air flow rate shall be determined as described in Section 7.

## 6.6 PRESSURE MEASUREMENTS

6.6.1 Nozzle Throat Pressure. The pressure measurement at the nozzle throat shall be made with instruments which shall permit measurements of pressure to within ± 2.0% absolute and whose smallest scale division shall not exceed 2 1/2 times the specified accuracy [11].

6.6.2 Air Flow Measurements. The static pressure across the nozzle and the velocity pressure at the nozzle throat shall be measured with manometers which have been calibrated to have an accuracy to within ± 1.0% of the reading. The smallest manometer scale division shall not exceed 2.0% of the reading [11].

6.6.3 Pressure Drop Across Collector. The static pressure drop across the solar collector shall be measured with a manometer having an accuracy of 2.49 $N/m^2$ (0.01 in. of water).

6.7 TIME AND MASS MEASUREMENTS

Time measurements and mass measurements shall be made to an accuracy of ± 0.20% [11].

6.8 WIND VELOCITY

The wind velocity shall be measured with an instrument and associated readout device that can determine the integrated average wind velocity for each 15 minute test period to an accuracy of ± 0.08 m/s (1.8 mph).

## SECTION 7. APPARATUS AND METHOD OF TESTING

### 7.1 LIQUID AS THE TRANSFER FLUID

The test configuration for the solar collector employing liquid as the transfer fluid is shown in Figure A1*.

7.1.1 Solar Collector. The solar collector should be mounted in its rigid frame at the predetermined tilt angle (for stationary collectors) or movable frame (for movable collectors) and anchored rigidly enough to a foundation so that the collector can hold its selected angular position against a strong gust of wind.

7.1.2 Ambient Temperature. The ambient temperature sensor shall be housed in a well-ventilated instrumentation shelter with its bottom 1.25 m (4.1 ft) above the ground and with its door facing north, so that the sun's direct beam cannot fall upon the sensor when the door is opened. The instrument shelter shall be painted white outside and shall not be closer to any obstruction than twice the height of the obstruction itself (i.e., trees, fences, buildings, etc.) [15].

7.1.3 Pyranometer. The pyranometer shall be mounted on the surface parallel to the collector surface in such a manner that it does not cast a shadow onto the collector plate. Precautions should be always taken to avoid subjecting the instrument to mechanical shocks or vibration during the installation. The pyranometer should be oriented so that the emerging leads or the connector are located north of the receiving surface (in the Northern Hemisphere) or are in some other manner shaded. This minimizes heating of the electrical connections by the sun.

Care should also be taken to minimize reflected and reradiated energy from the solar collector onto the pyranometer. Some pyranometers come supplied with shields. This should be adjusted so that the highest point on the shield lies parallel to and just below the plane of the thermopile. Some pyranometers not supplied with a shield may be susceptible to error due to reflections by radiation that originates below the plane of the thermopile. Precautions can be taken by constructing a cylindrical shield, the top of which should be coplaner with the thermopile [5].

---

* The recommended apparatus consists of a closed loop configuration. An open loop configuration is an acceptable alternative provided that the test conditions specified herein can be satisfied.

7.1.4 Temperature Measurement Across the Solar Collector. The temperature difference of the transfer fluid between entering and leaving the solar collector shall be measured using either two calibrated resistance thermometers connected in two arms of a bridge or a thermopile made from calibrated, type T thermocouple wire all taken from a single spool. The thermopile shall contain any even number of junctions constructed according to the recommendations in reference [7]. Each resistance thermometer or each end of the thermopile is to be inserted into a well [8] located as shown in Figure A1. To insure good thermal contact, the wells shall be filled with light oil. The wells should be located just downstream of a right angle bend to insure proper mixing [6].

To minimize temperature measurement error, each probe should be located as close as possible to the inlet or outlet of the solar collector device. In addition, the piping between the wells and the collector shall be insulated in such a manner that the calculated heat loss or gain from the ambient air would not cause a temperature change for any test of more than 0.05°C (0.09°F) between each well and the collector.

7.1.5 Additional Temperature Measurements. The temperature of the transfer fluid at the two positions cited above shall also be measured by inserting appropriate sensors into the wells. Reference [6] should be followed in making these measurements.

7.1.6 Pressure Drop Across the Solar Collector. The pressure drop across the solar collector shall be measured using static pressure tap holes and a manometer. The edges of the holes on the inside surface of the pipe should be free of burrs and should be as small as practicable and not exceeding 1.6 mm (1/16 inch) diameter [12]. The thickness of the pipe wall should be 2 1/2 times the hole diameter [12].

7.1.7 Reconditioning Apparatus. As shown in Figure A1, a heat exchanger is used to cool the transfer fluid to simulate the building load and an adjustable electric resistance heater is used to control the inlet temperature to the prescribed test value. This combination of equipment or equivalent shall control the temperature of the fluid entering the solar collector to within ± 0.5°C (± 0.9°F) at all times during the tests.

7.1.8 Additional Equipment. A pressure gauge, a pump, and a means of adjusting the flow rate of the transfer fluid shall be provided at the relative locations shown in Figure A1. Depending upon the test apparatus design, an additional throttle valve may be required in the line just preceding the solar collector for proper control. An expansion tank and

a pressure relief valve should be installed to allow the transfer fluid to freely expand and contract in the apparatus*. In addition, filters should be installed within the apparatus as well as a sight glass to insure that the transfer fluid passing through the collector is free of contaminants including air bubbles.

7.2 AIR AS THE TRANSFER FLUID

The test configuration for the solar collector employing air as the transfer fluid is shown in Figure A2**.

7.2.1 Solar Collector. The solar collector should be mounted in its rigid frame at the predetermined tilt angle (for stationary collectors) or movable frame (for movable collectors) and anchored rigidly enough to a foundation so that the collector can hold its selected angular position against a strong gust of wind.

7.2.2 Ambient Temperature. The ambient temperature sensor shall be housed in a well-ventilated instrumentation shelter with its bottom 1.25 m (4.1 ft) above the ground and with its door facing north, so that the sun's direct beam cannot fall upon the sensor when the door is opened. The instrument shelter shall be painted white outside and shall not be closer to any obstruction than twice the height of the obstruction itself (i.e., trees, fences, buildings, etc.) [15].

7.2.3 Pyranometer. The pyranometer shall be mounted on the surface parallel to the collector surface in such a manner that it does not cast a shadow onto the collector plate. Precautions should be always taken to avoid subjecting the instrument to mechanical shocks or vibration during the installation. The pyranometer should be oriented so that the emerging leads or the connector are located north of the receiving surface (in the Northern Hemisphere) or are in some other manner shaded. This minimizes heating of the electrical connections by the sun.

---

* Figure A1 should not be interpreted to mean that the relief valve and expansion tank necessarily be located below the solar collector.

** The recommended apparatus consists of a closed loop configuration. An open loop configuration is an acceptable alternative provided that the test conditions specified herein can be satisfied.

Care should also be taken to minimize reflected and reradiated energy from the solar collector onto the pyranometer. Some pyranometers come supplied with shields. This should be adjusted to be parallel to and to lie just below the plane of the thermopile. Some pyranometers not supplied with a shield may be susceptible to error due to reflections by radiation that originates below the plane of the thermopile. Precautions can be taken by constructing a cylindrical shield, the top of which should be coplaner with the thermopile [5].

7.2.4 Test Ducts. The air inlet duct, between the air flow measuring apparatus and the solar collector, shall have the same cross-sectional dimensions as the inlet manifold to the solar collector. The air outlet duct, between the solar collector and the reconditioning apparatus, shall have the same cross-sectional dimensions as the outlet manifold from the solar collector*.

7.2.5 Temperature Measurement Across the Solar Collector. A thermopile shall be used to measure the difference between the inlet air temperature and outlet air temperature of the solar collector. It shall be constructed from calibrated type T thermocouple wire all taken from a single spool. No extension wires are to be used in either its fabrication or installation. The wire diameter must be no larger than 0.51mm (24 AWG) and the thermopile shall be fabricated as shown in Figure A3. There shall be a minimum of six junctions in the air inlet test duct and six junctions in the air outlet test duct. These junctions shall be located at the center of equal cross-sectional areas.

During all tests, the variation in temperature at a given cross section of the air inlet and air outlet test ducts shall be less than $\pm$ 0.5°C ($\pm$ 0.9°F) at the location of the thermopile junctions. The variation shall be checked prior to testing utilizing instrumentation and procedures outlined in reference [6]. If the variation exceeds the limits above, mixing devices shall be installed to achieve this degree of temperature uniformity. Reference [16] discusses the positioning and performance of several types of air mixers.

The ends of the thermopile should be located as near as possible to the inlet and outlet of the solar collector. The air inlet and air outlet ducts shall be insulated in such a manner that the calculated heat loss or gain to or from the ambient air would not cause a temperature change for any test

---

*The performance of air heaters is expected to be affected by the ductwork entering and leaving the solar collector considerably more so than in the case of solar collectors using a liquid as the transfer fluid.

of more than 0.05°C (0.09°F) between the temperature measuring locations and the collector.

7.2.6 Temperature Measurements. Sensors and read-out devices meeting the accuracy requirements of Section 6. and giving a continuous reading shall be used to measure the temperature at the locations in the air inlet and air outlet ducts shown in Figure A2. Reference [6] should be followed in making these measurements.

7.2.7 Duct Pressure Measurements. The static pressure drop across the solar collector shall be measured using a manometer as shown in Figures A2 and A4 [11]. Each side of the manometer shall be connected to four externally manifolded pressure taps on the air inlet and air outlet ducts. The pressure taps should consist of 6.4 mm (1/4 inch) nipples soldered to the duct and centered over 1 mm (0.040 inch) diameter holes. The edges of these holes on the inside surfaces of the ducts should be free of burrs and other surface irregularities [12].

7.2.8 Air Flow Measuring Apparatus. Where the air flow rate is sufficiently large, it shall be measured with the nozzle apparatus discussed in Section 7. of reference [11]. As shown in Figure A5, this apparatus consists basically of a receiving chamber, a discharge chamber and an air flow measuring nozzle. The distance from the center of the nozzle to the side walls shall not be less than 1 1/2 times the nozzle throat diameter, and the diffusion baffles shall be installed in the receiving chamber at least 1 1/2 nozzle throat diameters upstream of the nozzle and 2 1/2 nozzle throat diameters downstream of the nozzle. The apparatus should be designed so that the nozzle can be easily changed and the nozzle used on each test shall be selected so that the throat velocity is between 15 m/s (2960 fpm) and 35 m/s (6900 fpm). When nozzles are constructed in accordance with Figure A6 and installed in accordance with Section 7.2.9 of this Standard, the discharge coefficient may be assumed to be as follows:

| Reynolds Number, $N_{Re}$ | Coefficient of Discharge, C |
|---|---|
| 20,000 | 0.96 |
| 50,000 | 0.97 |
| 100,000 | 0.98 |
| 150,000 | 0.98 |
| 200,000 | 0.99 |
| 250,000 | 0.99 |
| 300,000 | 0.99 |
| 400,000 | 0.99 |
| 500,000 | 0.99 |

If the throat diameter of the nozzle is 0.13 m (5 in.) or larger, the discharge coefficient may be assumed to be 0.99. For nozzles smaller than 0.05 m (2 in.) and where a more precise discharge coefficient than given above is desired, the nozzle should be calibrated. The area of the nozzle shall be determined by measuring its diameter to an accuracy of ± 0.20% in four places approximately 45 degrees apart around the nozzle in each of two planes through the nozzle throat, one at the outlet and the other in the straight section near the radius [11].

Where the nozzle apparatus is used, an exhaust fan capable of providing the desired flow rates through the solar collector shall be installed in the end wall of the discharge chamber rather than separate from the air flow measuring apparatus as shown in Figure A2. The dry and wet bulb temperature of the air entering the nozzle shall be measured in accordance with reference [6]. The velocity of the air passing through the nozzle shall be determined by either measuring the velocity head by means of a commercially available pitot tube or by measuring the static pressure drop across the nozzle with a manometer. If the latter method is used, one end of the manometer shall be connected to a static pressure tap located flush with the inner wall of the discharge chamber, or preferably, several taps in each chamber should be manifolded to a single manometer. A means shall also be provided for measuring the absolute pressure of the air in the nozzle throat.

Where the air flow rate is sufficiently small so that a nozzle constructed and installed in accordance with the requirements above would have a throat diameter of smaller than 0.025 m (1 in.), the above configuration should not be used and the air flow measuring apparatus as shown in Fig-

ure A2 should consist of a calibrated flow element* where at least 10 pipe diameters of upstream and downstream pipe section have been included in the calibration**.

7.2.9 Air Leakage. Air leakage through the air flow measuring apparatus, air inlet test duct, the solar collector and the air outlet test duct shall not exceed ± 1.0% of the measured air flow.

7.2.10 Air Reconditioning Apparatus. The reconditioning apparatus shall control the dry bulb temperature of the transfer medium entering the solar collector to within ± 1.0°C (± 1.8°F) of the desired test values at all times during the tests. Its heating and cooling capacity shall be selected so that dry bulb temperature of the air entering the reconditioning apparatus may be raised or lowered the required amount to meet the applicable test conditions in Section 8.

## SECTION 8. TEST PROCEDURE AND CALCULATIONS

### 8.1 GENERAL

The performance of the solar collector is determined by obtaining values of instantaneous efficiency for a large combination of values of incident insolation, ambient temperature, and inlet fluid temperature. This requires experimentally measuring the rate of incident solar radiation onto the solar collector as well as the rate of energy addition to the transfer fluid as it passes through the collector, all under quasi-steady conditions.

### 8.2 INSTANTANEOUS EFFICIENCY

It has been shown and discussed by a number of investigators [17, 18, 19 and 20] that the performance of flat plate solar collector operating under steady conditions can be successfully described by the following relationship:

---

* Usually an orifice, venturi, or flow nozzle.

** For small flow elements, the discharge coefficients associated with elements varies considerably from those associated with the larger elements. In addition, for small pipe or duct sizes, the ratio of pipe circumference to pipe area becomes large and the characteristics of the upstream and downstream pipe sections affect the behavior of the element itself.

$$\frac{q_u}{A} = I\,(\tau\alpha)_e - U_L\,(t_p - t_a) \qquad (1)$$

A very similar equation can be used to describe the performance of concentrating collectors [21, 22 and 23]. Equation (1) becomes modified as follows [21]:

$$\frac{q_u}{A_a} = I\,(\tau\alpha)_e\,\rho\,\gamma - U_L\,\frac{A_r}{A_a}\,(t_r - t_a) \qquad (2)$$

To assist in obtaining detailed information about the performance of collectors and to prevent the necessity of determining some average surface temperature, it has been convenient to introduce a parameter F' where

$$F' \equiv \frac{\text{actual useful energy collected}}{\text{useful energy collected if the entire collector surface were at the average fluid temperature}}$$

Introducing this factor into equation (1) results in

$$\frac{q_u}{A} = F'\left[I\,(\tau\alpha)_e - U_L\left(\frac{t_{f,i} + t_{f,e}}{2} - t_a\right)\right] \qquad (3)$$

If the solar collector efficiency can be defined as

$$\eta \equiv \frac{\text{actual useful energy collected}}{\text{solar energy incident upon or intercepted by the collector}}$$

or in equation form

$$\eta = \frac{q_u/A}{I} \qquad (4)$$

then the efficiency of the flat-plate collector is given by:

$$\eta = F' (\tau\alpha)_e - F' U_L \frac{\left(\frac{t_{f,i} + t_{f,e}}{2}\right) - t_a}{I} \qquad (5)$$

Equation (5) indicates that if the efficiency is plotted against an appropriate $\frac{\Delta t}{I}$, a straight line will result where the slope is some function of $U_L$ and the y intercept is some function of $(\tau\alpha)_e$. In reality $U_L$ is not a constant but rather a function of the temperature of the collector and of the ambient weather conditions. In addition, the product $(\tau\alpha)_e$ varies with incident angle to the collector.

The procedures outlined in this document have been developed in an attempt to control the test conditions so that a well defined efficiency "curve" can be obtained with a minimum of scatter. Figure A7 shows typical test results taken from reference [24] for two flat-plate collectors using air as the transfer fluid. The collector tests were conducted outside and the scatter about the two lines in each figure indicates "... apart from experimental errors, the order of variation on account of the variations in heat loss coefficient $U_L$, and the parameter F' due to variations in ambient wind speed and sky temperatures". Figure A10 was taken from reference [25] and is for a flat-plate collector using water as the transfer fluid. There is less scatter due to the fact that the tests were conducted indoors using a "solar simulator".

The curves shown in Figures A7 and A10 are duplicates of those reported in references [24] and [25], respectively. The abscissa in the first case is in metric units and in the second, english units. The curves to be presented in the test report described herein should be done so the abscissa is either in the SI units of $(°C \cdot m^2)/W$ (as in Figures A8 and A11) or as shown in Figures A9 and A12. Here the experimentally determined temperature difference has been divided by the difference in temperature between the boiling point and freezing point on the respective scale (100°C, 180°F) and the insolation has been divided by the solar constant, $I_{SC}$ (1353 $W/m^2$), in appropriate units [26]. The result is an abscissa whose units are dimensionless.

It is expected that a "straight-line" representation will suffice for most conventional flat-plate collectors but that an attempt to represent the performance of a concentrating collector on such a plot will require the use of a "higher-order fit" due to the larger variation in $U_L$ and the product $(\tau\alpha)_e$.

## 8.3 TESTING PROCEDURE

The testing of the solar collector shall be conducted in such a way that an "efficiency curve" is determined for the collector under test conditions described in Section 5. and 8.3. At least four different values of inlet fluid temperature shall be used to obtain the values of $\Delta t/I$. Ideally the inlet fluid temperature should correspond to 10, 30, 50, and 70°C (18, 54, 90, and 126°F) above the ambient temperature; however the values that can realistically be used will depend upon the particular collector design and the environmental conditions at the location and time of year when the collector is being tested. Consequently, the four different inlet fluid temperatures selected should be as close to the above values as is feasible. At least four "data points" shall be taken for each value of $t_{f,i}$; two during the time period preceding solar noon and two in the period following solar noon, the specific periods being chosen so that the data points represent times symmetrical to solar noon. This latter requirement is made so that any "transient effects" that may be present will not bias the test results when they are used for design purposes. All test data shall be reported in addition to the fitted curve (see Section 9.) so that any difference in efficiency due solely to the operating temperature level of the collector can be discerned in the test report. The curve shall be established by "data points" that represent 15 minute integrated efficiency values. In other words, the integrated value of incident solar energy will be divided into the integrated value of energy obtained from the collector to obtain the efficiency value for that "instant". Care should be taken to insure that the incident solar energy is steady for each 15 minute segment during which an efficiency value is calculated. Either electronic integrators or continuous pen strip chart recorders may be used to determine the integrated values of incident solar radiation and temperature rise across the collector. However, a strip chart recorder with a recommended chart speed of 30.cm/hr must always be used to monitor the output of the pyranometer to insure that the incident radiation has remained steady during the 15 minute segment. Figures A13 and A14 show a strip chart recording of incident solar radiation on a horizontal surface at the National Bureau of Standards site in Gaithersburg, Maryland. Whereas the conditions of Figure A13 would be perfectly acceptable for obtaining efficiency values, those of Figure A14 would not be*.

---

* One or two "blips" of 10 s or less occurring during the 15 minute period such as at 12:18 in Figure A11 is acceptable.

The surface of the collector cover plate (if present) as well as exposed envelope of the pyranometer should be wiped clean and dry prior to the tests. If local pollution or sand has formed a deposit on the transparent surfaces, the wiping should be carried out very gently, preferably after blowing off most of the loose material or after wetting it a little, in order to prevent scratching of the surface. This is particularly important for the pyranometer since such abrasive action can appreciably alter the original transmission properties of the enclosing envelope.

The pyranometer shall be checked prior to testing to see if there is any accumulation of water vapor enclosed within the glass cover. The use of "wet" pyranometers (where moisture is visible) shall not be allowed.

In order to obtain sufficiently good "quasi-steady" conditions for the solar collection process, the collector should stand in the sun under no flow conditions until the contained fluid heats up to a temperature equivalent to or slightly greater than the inlet fluid temperature for the test. The transfer fluid should then be circulated through the collector at the appropriate temperature level for at least 30 minutes* prior to the period in which data will be taken to calculate the efficiency values. During this period, a check should be made to insure that the flow rate of the transfer fluid does not vary by more than + 1% and that the incident solar radiation is steady as described above.

The flow rate of transfer fluid through the collector shall be standardized at one value for all data points. The recommended value of flow rate per unit area (transparent frontal or aperture) for tests are 0.02 kg/(s·m$^2$) (14.7 lbm/(h · ft$^2$)) when a liquid is the transfer fluid and 0.01 m$^3$/(s·m$^2$) (1.96 cfm per ft$^2$) of standard are when the transfer fluid is air. It is recognized that in some cases the collector will have been designed for a flow rate much different than specified above. In such cases, the design flow rate should be used.

In order to determine and report the fraction of the incident solar radiation that is diffuse for each efficiency value, the sensing element of the pyranometer shall be shaded from the direct beam of sun just prior and just following each 15 minute testing

---

* 30 minutes is felt to be sufficient for typical tube and sheet type solar collectors using water as the transfer fluid. For those collectors having higher thermal capacity, a longer time period may be necessary.

period and the value of the incident radiation determined*. This shall be accomplished by using a small disk attached to a slender rod held on a direct line between the pyranometer and the sun. The disk should be just large enough to shade the sensing element alone. In reference [5], this is accomplished by a disk 100 mm in diameter and held at a distance of 1 m from the sensing element**.

## 8.4 CALCULATION OF INSTANTANEOUS EFFICIENCY

For each 15 minute segment for which an efficiency value is to be determined, the value is calculated using the equation:

$$\eta = \frac{\left[\dot{m}\, c_p \int_{\tau_1}^{\tau_2} (t_{f,e} - t_{f,i})\, d\tau\right]/A_a}{\int_{\tau_1}^{\tau_2} I\, d\tau} \qquad (6)$$

The quantities $\dot{m}$ and $c_p$ have been taken out of the integration in the numerator since they remain essentially constant during the test. Note that the collector area used for the calculation is not the absorbing surface area but rather the transparent frontal area or aperture area.

At least sixteen data points shall be obtained for the establishment of the "efficiency curve" and an equation for the curve shall be obtained using the standard technique of a least-squares fit to a second-order polynomial***.

## 8.5 AN EXPERIMENTAL CHECK

As an independent check on the experimental results, the inlet temperature, $t_{f,i}$, and the outlet temperature, $t_{f,e}$, of the collector shall be recorded on continuous pen strip chart recorders. The

---

* A normal incidence pyrheliometer can be used in lieu of shading the sensing element of the pyranometer.

** This was when using a Moll-Gorszynski Pyranometer made by Kipp and Zonen.

*** One should consult any standard text discussing analysis of experimental data for a presentation of this technique (i.e., [27] and [28]).

quantity $\int_{\tau_1}^{\tau_2} (t_{f,e} - t_{f,i})\, d\tau$ shall be approximated using these recordings and compared with the identical quantity obtained by using the primary method which measures the temperature difference directly.

## 8.6 CALCULATION OF AIR FLOW RATE

The air flow rate through the nozzle is calculated by the following equations:

$$Q_{mi} = 1.41\ C\ A_n\ (P_v\ v'_n)^{0.5} \quad (7)$$

$$v'_n = 10.1 \times 10^{-4}\ v_n/P_n\ (1 + W_n) \quad (8)$$

The air flow rate of standard air is then:

$$Q_s = Q_{mi}/(1.2\ v'_n) \quad (9)$$

## 8.7 CALCULATION OF NOZZLE REYNOLDS NUMBER

The Reynolds number is calculated as follows:

$$N_{Re} = f.V_a\ D \quad (10)$$

The temperature factor is as follows:

| Temperature, °C | Factor, f |
|---|---|
| -6.7 | 78275 |
| +4.4 | 72075 |
| +15.6 | 67425 |
| +26.7 | 62775 |
| +37.8 | 58125 |
| +48.9 | 55025 |
| +60.0 | 51925 |
| +71.1 | 48825 |

## 8.8 CALCULATION OF THEORETICAL POWER REQUIREMENTS

In order to calculate the theoretical power required to move the transfer fluid through the solar collector, the following equation shall be used:

$$P_{th} \doteq \dot{m} \Delta P / \rho \qquad (11)$$

## SECTION 9. DATA TO BE RECORDED AND TEST REPORT

### 9.1 TEST DATA

Table A13 lists the measurements which are to be made at the beginning of the testing day and during the individual tests to obtain an efficiency "data point".

### 9.2 TEST REPORT

Table A14 specifies the data and information that shall be reported in testing the solar collector.

## SECTION 10. NOMENCLATURE

| | |
|---|---|
| $A$ | cross-sectional area, $m^2$ |
| $A_a$ | transparent frontal area for a flat-plate collector or aperture for a concentrating collector, $m^2$ |
| $A_n$ | area of nozzle, $m^2$ |
| $A_r$ | absorbing or receiving area of the concentrating solar collector, $m^2$ |
| $C$ | nozzle coefficient of discharge |
| $c_p$ | specific heat of the transfer fluid, J/(kg·°C) |
| $D$ | nozzle throat diameter, m |
| $f$ | temperature factor for the calculation of nozzle $N_{Re}$ |
| $F'$ | solar collector efficiency factor |
| $h$ | outside surface heat transfer coefficient (includes radiation and convection) for the solar collector, $W/(m^2 \cdot °C)$ |
| $I$ | total solar energy incident upon the plane of the solar collector per unit time per unit area, $W/m^2$ |
| $I_d$ | diffuse solar energy incident upon the plane of the solar collector per unit time per unit area, $W/m^2$ |
| $I_{sc}$ | solar constant, 1353 $W/m^2$ |

| | |
|---|---|
| $\dot{m}$ | mass flow rate of the transfer fluid, kg/s |
| $N_{Re}$ | Reynolds number |
| $P_n$ | absolute pressure at the nozzle throat, $N/m^2$ |
| $P_{th}$ | theoretical power required to move the transfer fluid through the solar collector, W |
| $P_v$ | velocity pressure at the nozzle throat or the static pressure difference across the nozzle, $N/m^2$ |
| $\Delta P$ | pressure drop across the solar collector, $N/m^2$ |
| $Q_{mi}$ | measured air flow rate, $m^3/s$ |
| $Q_s$ | standard air flow rate, $m^3/s$. |
| $q_u$ | rate of useful energy extraction from the solar collector, W |
| $t_a$ | ambient air temperature, $^oC$ |
| $t_{bp}$ | temperature of the boiling point on a temperature scale, $^oC$ or $^oF$ |
| $t_{f,e}$ | temperature of the fluid leaving the collector, $^oC$ |
| $t_{f,i}$ | temperature of the fluid entering the collector, $^oC$ |
| $t_{fp}$ | temperature of freezing point on a temperature scale, $^oC$ or $^oF$ |
| $t_p$ | average temperature of the absorber surface of the solar collector, $^oC$ |
| $t_r$ | average temperature of the absorber surface of the concentrating solar collector, $^oC$ |
| $\Delta t$ | temperature difference, $^oC$ |
| $U_L$ | heat transfer loss coefficient for the solar collector, $W/m^2 \cdot ^oC$) |
| $V_a$ | velocity of the air at the nozzle throat, m/s |
| $v_n$ | specific volume of the air at dry and wet bulb temperature conditions existing at the nozzle but at standard barometric pressure, $m^3/kg$ dry air |
| $v_{n,}$ | specific volume of the air at the nozzle, $m^3/kg$ dry air |
| $W_n$ | humidity ratio at the nozzle, kg $H_2O$/kg dry air |
| $\alpha$ | absorptance of the solar collector absorbing surface to solar radiation |
| $\gamma$ | the fraction of specularly reflected radiation from the reflector which is intercepted by the solar collector absorbing surface |

$\eta$ solar collector efficiency, %

$\rho$ specular reflectance of the solar collector reflector, or density, $kg/m^3$

$\tau$ time, s, or transmittance of the solar collector cover plate

$(\tau\alpha)_e$ effective transmission-absorptance factor for the solar collector

$\tau_1$ time at the beginning of a 15 minute test period, s

$\tau_2$ time at the end of a 15 minute test period, s

## SECTION 11. REFERENCES


1. Morrison, C. A., and E. A. Farber, "Development and Use of Insolation Data for South Facing Surfaces in Northern Latitudes", paper presented at the ASHRAE Symposium, Solar Energy Applications, Montreal, Canada, June 22, 1974.

2. Personal communication with J. I. Yellott, Arizona State University, Tempe, Arizona, data to be published in 1975 revised edition of the ASHRAE publication, Low Temperature Engineering Application of Solar Energy.

3. ASHRAE Handbook of Fundamentals, American Society of Heating, Refrigerating and Air-Conditioning Engineers, Inc., 345 East 47th Street, New York, N. Y. 10017, 1972.

4. Threlkeld, J. L., Thermal Environmental Engineering, Prentice-Hall, Englewood Cliffs, New Jersey, Second Edition, 1970.

5. Latimer, J. R., "Radiation Measurement", International Field Year for the Great Lakes, Technical Manual Series, No. 2, The Secretariet, Canadian National Committee for the International Hydrological Decade, No. 8 Building, Carling Avenue, Ottawa, Canada, 1971.

6. "Standard Measurements Guide: Section on Temperature Measurements", ASHRAE Standard 41-66, Part 1, American Society of Heating, Refrigerating and Air-Conditioning Engineers, Inc., 345 East 47th Street, New York, N. Y. 10017, January, 1966.

7. "American Standard for Temperature Measurement, Thermocouples C96.1-1964" (R 1969), American National Standards Institute, 1969.

8. "Instruments and Apparatus, Part 3, Temperature Measurement", Supplement to the ASME Power Test Codes, American Society of Mechanical Engineers, 345 East 47th Street, New York, N. Y. 10017, March, 1961.

9. Davis, J. C., "Radiation Errors in Air Ducts Under Isothermal Conditions Using Thermocouples, Thermistors, and a Resistance Thermometer", NBS Building Science Series 26, November, 1969. (Available from the Superintendent of Documents, U. S. Government Printing Office, Washington, D. C. 20402 - order by SD Catalog No. C 13.29/2:26, $0.25.)

10. Davis, J. C., Faison, T. K., and P. R. Achenbach, "Errors in Temperature Measurement of Moving Air Under Isothermal Conditions Using Thermocouples, Thermistors, and Thermometers", ASHRAE Transactions, Vol. 72, Part 1, 1966.

11. "Methods of Testing for Rating Unitary Air Conditioning and Heat Pump Equipment", ASHRAE Standard 37-69, American Society of Heating, Refrigerating and Air-Conditioning Engineers, Inc., 345 East 47th Street, New York, N. Y. 10017, April, 1969.

12. "Instruments and Apparatus, Part 2, Pressure Measurement", Supplement to the ASME Power Test Codes, American Society of Mechanical Engineers, 345 East 47th Street, New York, N. Y. 10017, July, 1964.

13. "Instruments and Apparatus, Part 5, Measurement of Quantity of Materials, Chapter 4, Flow Measurement", Supplement to the ASME Power Test Codes, American Society of Mechanical Engineers, 345 East 47th Street, New York, N. Y. 10017, February, 1959.

14. "Fluid Meters, Their Theory and Application", 5th edition, American Society of Mechanical Engineers, 345 East 47th Street, New York, N. Y. 10017, 1959.

15. "Instructions for Climatological Observations, Circular B", United States Weather Bureau Service, 11th edition, January, 1962.

16. Faison, T. K., Davis, J. C., and P. R. Achenbach, "Performance of Louvered Devices as Air Mixers, NBS Building Science Series 27, March, 1970. (Available from the Superintendent of Documents, U. S. Government Printing Office, Washington, D. C. 20402 - order by SD Catalog No. C 13.29/2:27, $0.30.)

17. Hottel, H. C., and B. B. Woertz, "The Performance of Flat-Plate Solar-Heat Collectors", ASME Transactions, Vol. 64, p. 91, 1942.

18. Hottel, H. C., and A. Whillier, "Evaluation of Flat-Plate Collector Performance", Transactions of the Conference on the Use of Solar Energy, Vol. 2, Part I, p. 74, University of Arizona Press, 1958.

19. Bliss, R. W., "The Derivation of Several 'Plate-Efficiency Factors' Useful in the Design of Flat-Plate Solar Heat Collectors", Solar Energy, Vol. 3, No. 4, p. 55, 1959.

20. Whillier, A., "Design Factors Influencing Collector Performance", Low Temperature Engineering Application of Solar Energy, American Society of Heating, Refrigerating and Air-Conditioning Engineers, Inc., 345 East 47th Street, New York, N. Y. 10017, 1967.

21. Duffie, J. A., and W. A. Beckman, Solar Energy Thermal Processes, John Wiley and Sons, 1974.

22. Nevins, R. G., and P. E. McNall, "A High-Flux Low-Temperature Solar Collector", ASHRAE Transactions, Vol. 64, pp. 69-82, 1958.

23. Löf, G. O. G., Fester, D. A., and J. A. Duffie, "Energy Balance on a Parabolic Cylinder Solar Reflector", ASME Transactions, Vol. 84A, p. 24, 1962.

24. Gupta, C. L., and H. P. Garg, "Performance Studies on Solar Air Heaters", Solar Energy, Vol. 11, No. 1, 1967.

25. Simon, F. F., and P. Harlament, "Flat-Plate Collector Performance Evaluation: The Case for a Solar Simulator Approach", NASA TM X-71427, October, 1973.

26. Thekaekara, M. P., "Solar Energy Outside the Earth's Atmosphere", Solar Energy, Vol. 14, No. 2, p. 109, 1973.

27. Holman, J. P., Experimental Methods for Engineers, McGraw-Hill, Second Edition, 1971.

28. Bevington, P.R., Data Reduction and Error Analysis for the Physical Sciences, McGraw-Hill, 1969.

# TABLE A1 .., SOLAR POSITION AND INSOLATION VALUES FOR 24 DEGREES NORTH LATITUDE

| DATE | SOLAR TIME AM | SOLAR TIME PM | SOLAR POSITION ALT | SOLAR POSITION AZM | BTUH/SQ. FT. TOTAL INSOLATION ON SURFACES NORMAL | HORIZ | SOUTH FACING SURFACE ANGLE WITH HORIZ. 14 | 24 | 34 | 44 | 90 |
|---|---|---|---|---|---|---|---|---|---|---|---|
| JAN 21 | 7 | 5 | 4.8 | 65.6 | 71 | 10 | 17 | 21 | 25 | 28 | 31 |
| | 8 | 4 | 16.9 | 58.3 | 239 | 83 | 110 | 126 | 137 | 145 | 127 |
| | 9 | 3 | 27.9 | 48.8 | 288 | 151 | 188 | 207 | 221 | 228 | 176 |
| | 10 | 2 | 37.2 | 36.1 | 308 | 204 | 246 | 268 | 282 | 287 | 207 |
| | 11 | 1 | 43.6 | 19.6 | 317 | 237 | 287 | 306 | 319 | 324 | 226 |
| | 12 | | 46.0 | 0.0 | 320 | 249 | 296 | 319 | 332 | 336 | 232 |
| | SURFACE DAILY TOTALS | | | | 2766 | 1622 | 1984 | 2174 | 2300 | 2369 | 1766 |
| FEB 21 | 7 | 5 | 9.3 | 74.6 | 152 | 35 | 44 | 49 | 53 | 56 | 46 |
| | 8 | 4 | 22.3 | 67.2 | 263 | 116 | 135 | 145 | 150 | 151 | 102 |
| | 9 | 3 | 34.4 | 57.6 | 298 | 187 | 213 | 225 | 230 | 228 | 141 |
| | 10 | 2 | 45.1 | 44.2 | 314 | 241 | 273 | 288 | 291 | 287 | 169 |
| | 11 | 1 | 53.0 | 25.0 | 321 | 276 | 310 | 324 | 328 | 323 | 185 |
| | 12 | | 56.0 | 0.0 | 324 | 288 | 323 | 337 | 341 | 335 | 191 |
| | SURFACE DAILY TOTALS | | | | 3036 | 1909 | 2276 | 2396 | 2446 | 2424 | 1476 |
| MAR 21 | 7 | 5 | 13.7 | 83.3 | 104 | 60 | 63 | 64 | 62 | 59 | 27 |
| | 8 | 4 | 27.2 | 76.8 | 267 | 141 | 156 | 152 | 149 | 142 | 64 |
| | 9 | 3 | 40.2 | 67.9 | 295 | 212 | 226 | 229 | 225 | 214 | 95 |
| | 10 | 2 | 52.3 | 54.8 | 309 | 266 | 285 | 288 | 283 | 270 | 120 |
| | 11 | 1 | 61.9 | 33.4 | 315 | 300 | 322 | 326 | 320 | 305 | 135 |
| | 12 | | 66.0 | 0.0 | 317 | 312 | 334 | 339 | 333 | 317 | 140 |
| | SURFACE DAILY TOTALS | | | | 3078 | 2270 | 2428 | 2456 | 2412 | 2298 | 1022 |
| APR 21 | 6 | 6 | 4.7 | 100.6 | 40 | 7 | 5 | 4 | 4 | 3 | 2 |
| | 7 | 5 | 18.3 | 94.9 | 203 | 83 | 77 | 70 | 62 | 51 | 19 |
| | 8 | 4 | 32.0 | 89.0 | 256 | 169 | 157 | 149 | 137 | 122 | 16 |
| | 9 | 3 | 45.6 | 81.9 | 280 | 227 | 227 | 220 | 206 | 186 | 41 |
| | 10 | 2 | 59.0 | 71.8 | 292 | 278 | 282 | 275 | 259 | 237 | 68 |
| | 11 | 1 | 71.1 | 51.6 | 298 | 310 | 316 | 309 | 293 | 269 | 74 |
| | 12 | | 77.6 | 0.0 | 299 | 321 | 328 | 321 | 305 | 280 | 79 |
| | SURFACE DAILY TOTALS | | | | 3036 | 2454 | 2458 | 2374 | 2228 | 2016 | 489 |
| MAY 21 | 6 | 6 | 8.0 | 108.4 | 86 | 22 | 15 | 10 | 9 | 9 | 5 |
| | 7 | 5 | 21.2 | 103.2 | 203 | 98 | 85 | 73 | 59 | 44 | 12 |
| | 8 | 4 | 34.6 | 98.5 | 248 | 171 | 159 | 145 | 127 | 106 | 15 |
| | 9 | 3 | 48.3 | 93.6 | 269 | 233 | 224 | 210 | 190 | 165 | 16 |
| | 10 | 2 | 62.0 | 87.7 | 280 | 281 | 275 | 261 | 239 | 211 | 22 |
| | 11 | 1 | 75.5 | 76.9 | 286 | 311 | 307 | 293 | 270 | 240 | 34 |
| | 12 | | 86.0 | 0.0 | 288 | 322 | 317 | 304 | 281 | 250 | 37 |
| | SURFACE DAILY TOTALS | | | | 3032 | 2556 | 2447 | 2286 | 2072 | 1800 | 246 |
| JUN 21 | 6 | 6 | 9.3 | 111.6 | 97 | 29 | 20 | 12 | 12 | 11 | 7 |
| | 7 | 5 | 22.3 | 106.8 | 201 | 103 | 87 | 73 | 58 | 41 | 13 |
| | 8 | 4 | 35.5 | 102.6 | 242 | 173 | 158 | 142 | 122 | 99 | 16 |
| | 9 | 3 | 49.0 | 98.7 | 263 | 234 | 221 | 204 | 182 | 155 | 18 |
| | 10 | 2 | 62.6 | 95.0 | 274 | 280 | 269 | 253 | 229 | 199 | 18 |
| | 11 | 1 | 76.3 | 90.8 | 279 | 309 | 300 | 283 | 259 | 227 | 19 |
| | 12 | | 89.4 | 0.0 | 281 | 319 | 310 | 294 | 269 | 236 | 22 |
| | SURFACE DAILY TOTALS | | | | 2994 | 2574 | 2422 | 2230 | 1992 | 1700 | 204 |

| DATE | SOLAR TIME AM | SOLAR TIME PM | SOLAR POSITION ALT | SOLAR POSITION AZM | BTUH/SQ. FT. TOTAL INSOLATION ON SURFACES NORMAL | HORIZ | SOUTH FACING SURFACE ANGLE WITH HORIZ. 14 | 24 | 34 | 44 | 90 |
|---|---|---|---|---|---|---|---|---|---|---|---|
| JUL 21 | 6 | 6 | 8.2 | 109.0 | 81 | 23 | 16 | 11 | 10 | 9 | 6 |
| | 7 | 5 | 21.4 | 103.8 | 195 | 98 | 85 | 73 | 59 | 44 | 17 |
| | 8 | 4 | 34.8 | 99.2 | 239 | 169 | 157 | 143 | 125 | 104 | 16 |
| | 9 | 3 | 48.4 | 94.5 | 261 | 231 | 221 | 207 | 187 | 161 | 18 |
| | 10 | 2 | 62.1 | 89.0 | 272 | 278 | 270 | 256 | 235 | 206 | 21 |
| | 11 | 1 | 75.7 | 79.2 | 278 | 307 | 302 | 287 | 265 | 235 | 32 |
| | 12 | | 86.6 | 0.0 | 280 | 317 | 312 | 298 | 275 | 245 | 36 |
| | SURFACE DAILY TOTALS | | | | 2932 | 2526 | 2412 | 2250 | 2036 | 1766 | 246 |
| AUG 21 | 6 | 6 | 5.0 | 101.3 | 35 | 7 | 5 | 4 | 4 | 4 | 2 |
| | 7 | 5 | 18.5 | 95.6 | 186 | 82 | 76 | 69 | 60 | 50 | 11 |
| | 8 | 4 | 32.2 | 89.7 | 241 | 158 | 154 | 146 | 134 | 118 | 16 |
| | 9 | 3 | 45.9 | 82.9 | 265 | 223 | 222 | 214 | 200 | 181 | 39 |
| | 10 | 2 | 58.3 | 73.0 | 278 | 273 | 275 | 268 | 252 | 230 | 58 |
| | 11 | 1 | 71.6 | 53.2 | 284 | 304 | 309 | 301 | 285 | 261 | 71 |
| | 12 | | 78.3 | 0.0 | 286 | 315 | 320 | 313 | 296 | 272 | 75 |
| | SURFACE DAILY TOTALS | | | | 2864 | 2408 | 2402 | 2316 | 2168 | 1958 | 470 |
| SEP 21 | 7 | 5 | 13.7 | 83.8 | 173 | 57 | 60 | 60 | 59 | 56 | 26 |
| | 8 | 4 | 27.2 | 76.8 | 248 | 136 | 144 | 146 | 143 | 136 | 62 |
| | 9 | 5 | 40.2 | 67.9 | 278 | 205 | 218 | 221 | 217 | 206 | 93 |
| | 10 | 2 | 52.3 | 54.8 | 292 | 258 | 275 | 278 | 273 | 261 | 116 |
| | 11 | 1 | 61.9 | 33.4 | 299 | 291 | 311 | 315 | 309 | 295 | 131 |
| | 12 | | 66.0 | 0.0 | 301 | 302 | 323 | 327 | 321 | 306 | 136 |
| | SURFACE DAILY TOTALS | | | | 2878 | 2194 | 2342 | 2366 | 2322 | 2212 | 992 |
| OCT 21 | 7 | 5 | 9.1 | 74.1 | 138 | 32 | 40 | 45 | 48 | 50 | 42 |
| | 8 | 4 | 22.0 | 66.7 | 247 | 111 | 129 | 139 | 144 | 145 | 99 |
| | 9 | 3 | 34.1 | 57.1 | 284 | 180 | 206 | 217 | 223 | 221 | 138 |
| | 10 | 2 | 44.7 | 43.8 | 301 | 234 | 265 | 277 | 282 | 279 | 169 |
| | 11 | 1 | 52.5 | 24.7 | 309 | 268 | 301 | 315 | 319 | 314 | 182 |
| | 12 | | 55.5 | 0.0 | 311 | 279 | 314 | 328 | 332 | 327 | 188 |
| | SURFACE DAILY TOTALS | | | | 2868 | 1928 | 2198 | 2314 | 2364 | 2346 | 1442 |
| NOV 21 | 7 | 5 | 4.9 | 65.8 | 67 | 10 | 16 | 20 | 24 | 27 | 29 |
| | 8 | 4 | 17.0 | 58.4 | 232 | 82 | 108 | 123 | 135 | 142 | 124 |
| | 9 | 3 | 28.0 | 48.9 | 282 | 150 | 186 | 205 | 217 | 224 | 172 |
| | 10 | 2 | 37.3 | 36.3 | 303 | 203 | 244 | 265 | 278 | 283 | 204 |
| | 11 | 1 | 43.8 | 19.7 | 312 | 236 | 280 | 302 | 316 | 320 | 222 |
| | 12 | | 46.2 | 0.0 | 315 | 247 | 293 | 315 | 328 | 332 | 228 |
| | SURFACE DAILY TOTALS | | | | 2706 | 1610 | 1962 | 2146 | 2268 | 2324 | 1730 |
| DEC 21 | 7 | 5 | 3.2 | 62.6 | 30 | 3 | 7 | 9 | 11 | 12 | 14 |
| | 8 | 4 | 14.9 | 55.3 | 225 | 71 | 99 | 116 | 129 | 139 | 130 |
| | 9 | 3 | 25.5 | 46.6 | 281 | 137 | 176 | 198 | 214 | 223 | 184 |
| | 10 | 2 | 34.3 | 33.7 | 304 | 189 | 234 | 258 | 275 | 283 | 217 |
| | 11 | 1 | 40.4 | 18.2 | 314 | 221 | 270 | 295 | 312 | 320 | 236 |
| | 12 | | 42.6 | 0.0 | 317 | 232 | 282 | 308 | 325 | 332 | 243 |
| | SURFACE DAILY TOTALS | | | | 2624 | 1474 | 1852 | 2058 | 2204 | 2286 | 1808 |

NOTE: 1) BASED ON DATA IN TABLE 1, P. 387 IN REF. [3]; 0% GROUND REFLECTANCE; 1.0 CLEARNESS FACTOR.
2) SEE FIG. 4, P. 394 IN [3] FOR TYPICAL REGIONAL CLEARNESS FACTORS.
3) GROUND REFLECTION NOT INCLUDED ON NORMAL OR HORIZONTAL SURFACES.

1 BTUH/SQ. FT. = 3.152 W/m$^2$

# TABLE A2 ... SOLAR POSITION AND INSOLATION VALUES FOR 32 DEGREES NORTH LATITUDE

| DATE | SOLAR TIME AM | SOLAR TIME PM | SOLAR POSITION ALT | SOLAR POSITION AZM | BTUH/SQ. FT. TOTAL INSOLATION ON SURFACES NORMAL | HORIZ. | SOUTH FACING SURFACE ANGLE WITH HORIZ. 22 | 32 | 42 | 52 | 90 |
|---|---|---|---|---|---|---|---|---|---|---|---|
| JAN 21 | 7 | 5 | 1.4 | 65.2 | 1 | 0 | 0 | 0 | 0 | 1 | 1 |
| | 8 | 4 | 12.5 | 56.5 | 203 | 56 | 93 | 106 | 116 | 123 | 115 |
| | 9 | 3 | 22.5 | 46.0 | 269 | 118 | 175 | 193 | 206 | 212 | 181 |
| | 10 | 2 | 30.6 | 33.1 | 295 | 167 | 235 | 256 | 269 | 274 | 221 |
| | 11 | 1 | 36.1 | 17.5 | 306 | 198 | 273 | 295 | 308 | 312 | 245 |
| | 12 | | 38.0 | 0.0 | 310 | 209 | 285 | 308 | 321 | 324 | 253 |
| | SURFACE DAILY TOTALS | | | | 2458 | 1288 | 1838 | 2008 | 2118 | 2166 | 1779 |
| FEB 21 | 7 | 5 | 7.1 | 73.5 | 121 | 22 | 34 | 37 | 40 | 42 | 38 |
| | 8 | 4 | 19.0 | 64.4 | 247 | 95 | 127 | 136 | 140 | 141 | 108 |
| | 9 | 3 | 29.9 | 53.4 | 288 | 161 | 206 | 217 | 222 | 220 | 158 |
| | 10 | 2 | 39.1 | 39.4 | 306 | 212 | 266 | 278 | 283 | 279 | 193 |
| | 11 | 1 | 45.6 | 21.4 | 315 | 244 | 304 | 317 | 321 | 315 | 214 |
| | 12 | | 48.0 | 0.0 | 317 | 255 | 316 | 330 | 334 | 328 | 222 |
| | SURFACE DAILY TOTALS | | | | 2872 | 1724 | 2188 | 2300 | 2345 | 2322 | 1644 |
| MAR 21 | 7 | 5 | 12.7 | 81.9 | 185 | 54 | 60 | 60 | 59 | 56 | 32 |
| | 8 | 4 | 25.1 | 73.0 | 266 | 129 | 146 | 147 | 144 | 137 | 78 |
| | 9 | 3 | 36.8 | 62.1 | 290 | 194 | 222 | 224 | 220 | 209 | 119 |
| | 10 | 2 | 47.3 | 47.5 | 304 | 245 | 280 | 283 | 278 | 265 | 150 |
| | 11 | 1 | 55.0 | 26.8 | 311 | 277 | 317 | 321 | 315 | 300 | 170 |
| | 12 | | 58.0 | 0.0 | 313 | 287 | 329 | 333 | 327 | 312 | 177 |
| | SURFACE DAILY TOTALS | | | | 3012 | 2084 | 2378 | 2403 | 2358 | 2246 | 1276 |
| APR 21 | 6 | 6 | 6.1 | 99.9 | 66 | 14 | 9 | 6 | 6 | 5 | 3 |
| | 7 | 5 | 18.8 | 92.2 | 206 | 86 | 78 | 71 | 62 | 51 | 10 |
| | 8 | 4 | 31.5 | 84.0 | 259 | 158 | 156 | 148 | 136 | 120 | 35 |
| | 9 | 3 | 43.9 | 74.2 | 278 | 220 | 225 | 217 | 203 | 183 | 68 |
| | 10 | 2 | 55.7 | 60.3 | 290 | 267 | 279 | 272 | 256 | 234 | 95 |
| | 11 | 1 | 65.4 | 37.5 | 295 | 297 | 313 | 306 | 290 | 265 | 112 |
| | 12 | | 69.6 | 0.0 | 297 | 307 | 325 | 318 | 301 | 276 | 118 |
| | SURFACE DAILY TOTALS | | | | 3076 | 2390 | 2444 | 2356 | 2206 | 1994 | 764 |
| MAY 21 | 6 | 6 | 10.4 | 107.2 | 119 | 36 | 21 | 13 | 13 | 12 | 9 |
| | 7 | 5 | 22.8 | 100.1 | 211 | 107 | 88 | 75 | 60 | 44 | 13 |
| | 8 | 4 | 35.4 | 92.9 | 250 | 175 | 159 | 145 | 127 | 105 | 15 |
| | 9 | 3 | 48.1 | 84.7 | 269 | 233 | 223 | 209 | 188 | 163 | 53 |
| | 10 | 2 | 60.6 | 73.3 | 280 | 277 | 273 | 259 | 237 | 208 | 56 |
| | 11 | 1 | 72.0 | 51.9 | 285 | 305 | 305 | 290 | 268 | 237 | 72 |
| | 12 | | 78.0 | 0.0 | 286 | 315 | 315 | 301 | 278 | 247 | 77 |
| | SURFACE DAILY TOTALS | | | | 3112 | 2582 | 2454 | 2284 | 2064 | 1788 | 469 |
| JUN 21 | 6 | 6 | 12.2 | 110.2 | 131 | 45 | 26 | 16 | 15 | 14 | 9 |
| | 7 | 5 | 24.3 | 103.4 | 210 | 115 | 91 | 76 | 59 | 41 | 14 |
| | 8 | 4 | 36.9 | 96.8 | 245 | 180 | 159 | 143 | 122 | 99 | 16 |
| | 9 | 3 | 49.6 | 89.4 | 264 | 236 | 221 | 204 | 181 | 153 | 19 |
| | 10 | 2 | 62.2 | 79.7 | 274 | 279 | 268 | 251 | 227 | 197 | 41 |
| | 11 | 1 | 74.2 | 60.9 | 279 | 306 | 299 | 282 | 257 | 224 | 56 |
| | 12 | | 81.5 | 0.0 | 280 | 315 | 309 | 292 | 267 | 234 | 60 |
| | SURFACE DAILY TOTALS | | | | 3084 | 2634 | 2436 | 2234 | 1990 | 1690 | 370 |

| DATE | SOLAR TIME AM | SOLAR TIME PM | SOLAR POSITION ALT | SOLAR POSITION AZM | BTUH/SQ. FT. TOTAL INSOLATION ON SURFACES NORMAL | HORIZ. | SOUTH FACING SURFACE ANGLE WITH HORIZ. 22 | 32 | 42 | 52 | 90 |
|---|---|---|---|---|---|---|---|---|---|---|---|
| JUL 21 | 6 | 6 | 10.7 | 107.7 | 113 | 37 | 22 | 14 | 13 | 12 | 8 |
| | 7 | 5 | 23.1 | 100.6 | 203 | 107 | 87 | 75 | 60 | 44 | 14 |
| | 8 | 4 | 35.7 | 93.6 | 241 | 174 | 158 | 143 | 125 | 104 | 16 |
| | 9 | 3 | 48.4 | 85.5 | 261 | 231 | 220 | 205 | 185 | 159 | 31 |
| | 10 | 2 | 60.9 | 74.3 | 271 | 274 | 269 | 254 | 232 | 204 | 54 |
| | 11 | 1 | 72.4 | 53.3 | 277 | 302 | 300 | 285 | 262 | 232 | 69 |
| | 12 | | 78.6 | 0.0 | 279 | 311 | 310 | 296 | 273 | 242 | 74 |
| | SURFACE DAILY TOTALS | | | | 3012 | 2558 | 2422 | 2250 | 2030 | 1754 | 458 |
| AUG 21 | 6 | 6 | 6.5 | 100.5 | 59 | 14 | 9 | 7 | 6 | 6 | 4 |
| | 7 | 5 | 19.1 | 92.8 | 190 | 85 | 77 | 69 | 60 | 50 | 12 |
| | 8 | 4 | 31.8 | 84.7 | 240 | 156 | 152 | 144 | 132 | 116 | 33 |
| | 9 | 3 | 44.3 | 75.0 | 263 | 216 | 220 | 212 | 197 | 178 | 65 |
| | 10 | 2 | 56.1 | 61.3 | 276 | 262 | 272 | 264 | 249 | 226 | 91 |
| | 11 | 1 | 66.0 | 38.4 | 282 | 292 | 305 | 298 | 281 | 257 | 107 |
| | 12 | | 70.3 | 0.0 | 284 | 302 | 317 | 309 | 292 | 268 | 113 |
| | SURFACE DAILY TOTALS | | | | 2902 | 2352 | 2388 | 2296 | 2144 | 1934 | 736 |
| SEP 21 | 7 | 5 | 12.7 | 81.9 | 163 | 51 | 56 | 56 | 55 | 52 | 30 |
| | 8 | 4 | 25.1 | 73.0 | 240 | 124 | 140 | 141 | 138 | 131 | 75 |
| | 9 | 3 | 36.8 | 62.1 | 272 | 188 | 213 | 215 | 211 | 201 | 114 |
| | 10 | 2 | 47.3 | 47.5 | 287 | 237 | 270 | 273 | 268 | 255 | 145 |
| | 11 | 1 | 55.0 | 26.8 | 294 | 268 | 306 | 309 | 303 | 289 | 164 |
| | 12 | | 58.0 | 0.0 | 296 | 278 | 318 | 321 | 315 | 300 | 171 |
| | SURFACE DAILY TOTALS | | | | 2808 | 2014 | 2288 | 2308 | 2264 | 2154 | 1226 |
| OCT 21 | 7 | 5 | 6.8 | 73.1 | 99 | 19 | 29 | 32 | 34 | 36 | 32 |
| | 8 | 4 | 18.7 | 64.0 | 229 | 90 | 120 | 128 | 133 | 134 | 104 |
| | 9 | 3 | 29.5 | 53.0 | 273 | 155 | 198 | 208 | 213 | 212 | 153 |
| | 10 | 2 | 38.7 | 39.1 | 293 | 204 | 257 | 269 | 273 | 270 | 188 |
| | 11 | 1 | 45.1 | 21.1 | 302 | 236 | 294 | 307 | 311 | 306 | 209 |
| | 12 | | 47.5 | 0.0 | 304 | 247 | 306 | 320 | 324 | 318 | 217 |
| | SURFACE DAILY TOTALS | | | | 2696 | 1654 | 2100 | 2208 | 2252 | 2232 | 1598 |
| NOV 21 | 7 | 5 | 1.5 | 65.4 | 2 | 0 | 0 | 0 | 1 | 1 | 1 |
| | 8 | 4 | 12.7 | 56.6 | 196 | 55 | 91 | 104 | 113 | 119 | 111 |
| | 9 | 3 | 22.6 | 46.1 | 263 | 118 | 173 | 190 | 202 | 208 | 176 |
| | 10 | 2 | 30.8 | 33.2 | 289 | 166 | 233 | 252 | 265 | 270 | 217 |
| | 11 | 1 | 36.2 | 17.6 | 301 | 197 | 270 | 291 | 303 | 307 | 241 |
| | 12 | | 38.2 | 0.0 | 304 | 207 | 282 | 304 | 316 | 320 | 249 |
| | SURFACE DAILY TOTALS | | | | 2406 | 1280 | 1816 | 1980 | 2084 | 2130 | 1742 |
| DEC 21 | 8 | 4 | 10.3 | 53.8 | 176 | 41 | 77 | 90 | 101 | 108 | 107 |
| | 9 | 3 | 19.8 | 43.6 | 257 | 102 | 161 | 180 | 195 | 204 | 183 |
| | 10 | 2 | 27.6 | 31.2 | 288 | 150 | 221 | 244 | 259 | 267 | 226 |
| | 11 | 1 | 32.7 | 16.4 | 301 | 180 | 259 | 282 | 298 | 305 | 251 |
| | 12 | | 34.6 | 0.0 | 304 | 190 | 271 | 295 | 311 | 318 | 259 |
| | SURFACE DAILY TOTALS | | | | 2348 | 1136 | 1704 | 1888 | 2016 | 2086 | 1794 |

NOTE: 1) BASED ON DATA IN TABLE 1, P. 387 IN REF. [3]; 0% GROUND REFLECTANCE; 1.0 CLEARNESS FACTOR.

2) SEE FIG. 4, P. 394 IN [3] FOR TYPICAL REGIONAL CLEARNESS FACTORS.

3) GROUND REFLECTION NOT INCLUDED ON NORMAL OR HORIZONTAL SURFACES.

1 BTUH/SQ. FT. = 3.152 W/m$^2$

# TABLE A3 .... SOLAR POSITION AND INSOLATION VALUES FOR 40 DEGREES NORTH LATITUDE

| DATE | SOLAR TIME AM | SOLAR TIME PM | SOLAR POSITION ALT | SOLAR POSITION AZM | BTUH/SQ. FT. TOTAL INSOLATION ON SURFACES NORMAL | HORIZ | SOUTH FACING SURFACE ANGLE WITH HORIZ. 30 | 40 | 50 | 60 | 90 |
|---|---|---|---|---|---|---|---|---|---|---|---|
| JAN 21 | 8 | 4 | 8.1 | 55.5 | 142 | 28 | 65 | 74 | 81 | 85 | 84 |
| | 9 | 3 | 16.8 | 44.0 | 239 | 83 | 155 | 172 | 182 | 187 | 171 |
| | 10 | 2 | 23.8 | 30.9 | 274 | 127 | 218 | 237 | 249 | 254 | 223 |
| | 11 | 1 | 28.4 | 16.0 | 289 | 154 | 257 | 277 | 290 | 293 | 253 |
| | 12 | | 30.0 | -0.0 | 294 | 164 | 270 | 291 | 303 | 306 | 263 |
| | SURFACE DAILY TOTALS | | | | 2182 | 948 | 1660 | 1810 | 1906 | 1944 | 1726 |
| FEB 21 | 7 | 5 | 4.8 | 72.7 | 69 | 10 | 19 | 21 | 23 | 24 | 22 |
| | 8 | 4 | 15.4 | 62.2 | 224 | 73 | 114 | 122 | 126 | 127 | 107 |
| | 9 | 3 | 25.0 | 50.2 | 274 | 132 | 195 | 205 | 209 | 208 | 167 |
| | 10 | 2 | 32.8 | 35.9 | 295 | 178 | 256 | 267 | 271 | 267 | 210 |
| | 11 | 1 | 38.1 | 18.9 | 305 | 206 | 293 | 306 | 310 | 304 | 236 |
| | 12 | | 40.0 | 0.0 | 308 | 216 | 306 | 319 | 323 | 317 | 245 |
| | SURFACE DAILY TOTALS | | | | 2640 | 1414 | 2060 | 2162 | 2202 | 2176 | 1730 |
| MAR 21 | 7 | 5 | 11.4 | 80.2 | 171 | 46 | 55 | 55 | 54 | 51 | 35 |
| | 8 | 4 | 22.5 | 69.6 | 250 | 114 | 140 | 141 | 138 | 131 | 89 |
| | 9 | 3 | 32.8 | 57.3 | 282 | 173 | 215 | 217 | 213 | 202 | 138 |
| | 10 | 2 | 41.6 | 41.9 | 297 | 218 | 273 | 276 | 271 | 258 | 176 |
| | 11 | 1 | 47.7 | 22.6 | 305 | 247 | 310 | 313 | 307 | 293 | 200 |
| | 12 | | 50.0 | 0.0 | 307 | 257 | 322 | 326 | 320 | 305 | 208 |
| | SURFACE DAILY TOTALS | | | | 2916 | 1552 | 2308 | 2330 | 2284 | 2174 | 1484 |
| APR 21 | 6 | 6 | 7.4 | 98.9 | 89 | 20 | 11 | 8 | 7 | 7 | 4 |
| | 7 | 5 | 18.9 | 84.6 | 206 | 92 | 77 | 70 | 61 | 50 | 12 |
| | 8 | 4 | 30.3 | 79.3 | 252 | 152 | 153 | 145 | 133 | 117 | 53 |
| | 9 | 3 | 41.3 | 67.2 | 274 | 207 | 221 | 213 | 199 | 179 | 93 |
| | 10 | 2 | 51.2 | 51.4 | 286 | 250 | 275 | 267 | 252 | 229 | 126 |
| | 11 | 1 | 58.7 | 29.2 | 292 | 277 | 308 | 301 | 285 | 260 | 147 |
| | 12 | | 61.6 | 0.0 | 293 | 287 | 320 | 313 | 296 | 271 | 154 |
| | SURFACE DAILY TOTALS | | | | 3092 | 2274 | 2412 | 2320 | 2168 | 1956 | 1022 |
| MAY 21 | 5 | 7 | 1.9 | 114.7 | 1 | 0 | 0 | 0 | 0 | 0 | 0 |
| | 6 | 6 | 12.7 | 105.6 | 144 | 49 | 25 | 15 | 14 | 13 | 9 |
| | 7 | 5 | 24.0 | 96.6 | 216 | 89 | 76 | 60 | 44 | 33 | 13 |
| | 8 | 4 | 35.4 | 87.2 | 250 | 175 | 158 | 144 | 125 | 104 | 25 |
| | 9 | 3 | 46.8 | 76.0 | 267 | 227 | 221 | 206 | 186 | 160 | 60 |
| | 10 | 2 | 57.5 | 60.9 | 277 | 267 | 270 | 255 | 233 | 205 | 89 |
| | 11 | 1 | 66.2 | 37.1 | 283 | 293 | 301 | 287 | 264 | 234 | 108 |
| | 12 | | 70.0 | 0.0 | 284 | 301 | 312 | 297 | 274 | 243 | 114 |
| | SURFACE DAILY TOTOLS | | | | 3160 | 2552 | 2442 | 2264 | 2060 | 1760 | 724 |
| JUN 21 | 5 | 7 | 4.2 | 117.3 | 22 | 4 | 3 | 3 | 2 | 2 | 1 |
| | 6 | 6 | 14.8 | 108.4 | 155 | 60 | 30 | 18 | 17 | 16 | 10 |
| | 7 | 5 | 26.0 | 99.7 | 216 | 123 | 92 | 77 | 59 | 41 | 14 |
| | 8 | 4 | 37.4 | 90.7 | 246 | 182 | 159 | 142 | 121 | 97 | 16 |
| | 9 | 3 | 48.8 | 80.2 | 263 | 233 | 219 | 202 | 179 | 151 | 47 |
| | 10 | 2 | 59.8 | 65.8 | 272 | 272 | 266 | 248 | 224 | 194 | 74 |
| | 11 | 1 | 69.2 | 41.9 | 277 | 296 | 296 | 278 | 253 | 221 | 92 |
| | 12 | | 73.5 | 0.0 | 279 | 304 | 306 | 289 | 263 | 230 | 98 |
| | SURFACE DAILY TOTALS | | | | 3180 | 2648 | 2434 | 2224 | 1974 | 1670 | 610 |

| DATE | SOLAR TIME AM | SOLAR TIME PM | SOLAR POSITION ALT | SOLAR POSITION AZM | BTUH/SQ. FT. TOTAL INSOLATION ON SURFACES NORMAL | HORIZ | SOUTH FACING SURFACE ANGLE WITH HORIZ. 30 | 40 | 50 | 60 | 90 |
|---|---|---|---|---|---|---|---|---|---|---|---|
| JUL 21 | 5 | 7 | 2.3 | 115.2 | 2 | 0 | 0 | 0 | 0 | 0 | 0 |
| | 6 | 6 | 13.1 | 106.1 | 138 | 50 | 26 | 17 | 15 | 14 | 9 |
| | 7 | 5 | 24.3 | 97.2 | 208 | 114 | 89 | 75 | 60 | 44 | 14 |
| | 8 | 4 | 35.8 | 87.8 | 241 | 174 | 157 | 142 | 124 | 102 | 24 |
| | 9 | 3 | 47.2 | 76.7 | 259 | 225 | 218 | 203 | 182 | 152 | 58 |
| | 10 | 2 | 57.9 | 61.7 | 269 | 265 | 266 | 251 | 229 | 200 | 86 |
| | 11 | 1 | 66.2 | 37.9 | 275 | 290 | 295 | 281 | 258 | 228 | 104 |
| | 12 | | 70.6 | 0.0 | 276 | 298 | 307 | 292 | 269 | 238 | 111 |
| | SURFACE DAILY TOTALS | | | | 3062 | 2534 | 2409 | 2230 | 2006 | 1728 | 709 |
| AUG 21 | 6 | 6 | 7.9 | 99.5 | 81 | 21 | 12 | 9 | 8 | 7 | 5 |
| | 7 | 5 | 19.3 | 90.0 | 191 | 87 | 76 | 69 | 60 | 49 | 12 |
| | 8 | 4 | 30.7 | 79.9 | 237 | 150 | 150 | 141 | 129 | 113 | 50 |
| | 9 | 3 | 41.8 | 67.9 | 260 | 205 | 216 | 207 | 193 | 173 | 89 |
| | 10 | 2 | 51.7 | 52.1 | 272 | 246 | 267 | 259 | 244 | 221 | 120 |
| | 11 | 1 | 59.9 | 29.7 | 278 | 273 | 300 | 292 | 276 | 252 | 140 |
| | 12 | | 62.3 | 0.0 | 280 | 282 | 311 | 303 | 287 | 262 | 147 |
| | SURFACE DAILY TOTALS | | | | 2916 | 2244 | 2354 | 2258 | 2104 | 1894 | 978 |
| SEP 21 | 7 | 5 | 11.4 | 80.2 | 169 | 43 | 51 | 51 | 49 | 47 | 32 |
| | 8 | 4 | 22.5 | 69.6 | 230 | 109 | 133 | 134 | 131 | 124 | 84 |
| | 9 | 3 | 32.8 | 57.3 | 263 | 167 | 206 | 208 | 203 | 193 | 132 |
| | 10 | 2 | 41.6 | 41.9 | 280 | 211 | 262 | 265 | 260 | 247 | 168 |
| | 11 | 1 | 47.7 | 22.6 | 287 | 239 | 298 | 301 | 295 | 281 | 192 |
| | 12 | | 50.0 | 0.0 | 290 | 249 | 310 | 313 | 307 | 292 | 200 |
| | SURFACE DAILY TOTALS | | | | 2708 | 1788 | 2210 | 2228 | 2182 | 2074 | 1416 |
| OCT 21 | 7 | 5 | 4.5 | 72.3 | 48 | 7 | 14 | 15 | 17 | 17 | 16 |
| | 8 | 4 | 15.0 | 61.9 | 204 | 68 | 106 | 113 | 117 | 118 | 100 |
| | 9 | 3 | 24.5 | 49.8 | 257 | 126 | 185 | 195 | 200 | 198 | 160 |
| | 10 | 2 | 32.4 | 35.6 | 280 | 170 | 245 | 257 | 261 | 257 | 203 |
| | 11 | 1 | 37.6 | 18.7 | 291 | 199 | 283 | 295 | 299 | 294 | 229 |
| | 12 | | 39.5 | 0.0 | 294 | 208 | 295 | 308 | 312 | 306 | 238 |
| | SURFACE DAILY TOTALS | | | | 2454 | 1348 | 1962 | 2060 | 2098 | 2074 | 1654 |
| NOV 21 | 8 | 4 | 8.2 | 59.4 | 136 | 28 | 63 | 72 | 78 | 82 | 81 |
| | 9 | 3 | 17.0 | 44.1 | 232 | 82 | 152 | 167 | 178 | 183 | 167 |
| | 10 | 2 | 24.0 | 31.0 | 268 | 126 | 215 | 233 | 245 | 249 | 219 |
| | 11 | 1 | 28.6 | 16.1 | 283 | 153 | 254 | 273 | 285 | 288 | 248 |
| | 12 | | 30.2 | -0.0 | 288 | 163 | 287 | 287 | 298 | 301 | 258 |
| | SURFACE DAILY TOTALS | | | | 2128 | 942 | 1636 | 1778 | 1870 | 1908 | 1586 |
| DEC | 8 | 4 | 5.5 | 53.0 | 89 | 14 | 39 | 45 | 50 | 54 | 56 |
| | 9 | 3 | 14.0 | 41.9 | 217 | 65 | 135 | 152 | 164 | 171 | 163 |
| | 10 | 2 | 20.7 | 29.4 | 261 | 107 | 200 | 221 | 235 | 242 | 221 |
| | 11 | 1 | 25.0 | 15.2 | 280 | 134 | 239 | 262 | 276 | 283 | 252 |
| | 12 | | 26.6 | 0.0 | 285 | 143 | 253 | 275 | 290 | 296 | 263 |
| | SURFACE DAILY TOTALS | | | | 1978 | 782 | 1480 | 1634 | 1740 | 1796 | 1646 |

NOTE: 1) BASED ON DATA IN TABLE 1, P. 387 IN REF. [3]; 0% GROUND REFLECTANCE; 1.0 CLEARNESS FACTOR.

2) SEE FIG. 4, P. 394 IN [3] FOR TYPICAL REGIONAL CLEARNESS FACTORS.

3) GROUND REFLECTION NOT INCLUDED ON NORMAL OR HORIZONTAL SURFACES.

1 BTUH/SQ. FT. = 3.152 $W/m^2$

# TABLE A4 ... SOLAR POSITION AND INSOLATION VALUES FOR 48 DEGREES NORTH LATITUDE

| DATE | SOLAR TIME AM | SOLAR TIME PM | SOLAR POSITION ALT | SOLAR POSITION AZM | BTUH/SQ. FT. TOTAL INSOLATION ON SURFACES NORMAL | HORIZ. | SOUTH FACING SURFACE ANGLE WITH HORIZ. 38 | 48 | 58 | 68 | 90 |
|---|---|---|---|---|---|---|---|---|---|---|---|
| JAN 21 | 8 | 4 | 3.5 | 54.6 | 37 | 4 | 17 | 19 | 21 | 22 | 22 |
| | 9 | 3 | 11.0 | 42.6 | 185 | 46 | 120 | 132 | 140 | 145 | 139 |
| | 10 | 2 | 16.9 | 29.4 | 239 | 83 | 190 | 206 | 216 | 220 | 206 |
| | 11 | 1 | 20.7 | 15.1 | 261 | 107 | 231 | 249 | 260 | 263 | 243 |
| | 12 | | 22.0 | 0.0 | 267 | 115 | 245 | 264 | 275 | 278 | 255 |
| | SURFACE DAILY TOTALS | | | | 1710 | 596 | 1360 | 1478 | 1550 | 1578 | 1478 |
| FEB 21 | 7 | 5 | 2.4 | 72.2 | 12 | 1 | 3 | 4 | 4 | 4 | 4 |
| | 8 | 4 | 11.6 | 60.5 | 188 | 49 | 95 | 102 | 105 | 106 | 96 |
| | 9 | 3 | 19.7 | 47.7 | 251 | 140 | 178 | 187 | 191 | 190 | 167 |
| | 10 | 2 | 26.2 | 33.3 | 278 | 159 | 240 | 251 | 255 | 251 | 217 |
| | 11 | 1 | 30.5 | 17.2 | 290 | 165 | 278 | 290 | 294 | 288 | 247 |
| | 12 | | 32.0 | 0.0 | 293 | 173 | 291 | 304 | 307 | 301 | 258 |
| | SURFACE DAILY TOTALS | | | | 2330 | 1080 | 1880 | 1972 | 2024 | 1978 | 1720 |
| MAR 21 | 7 | 5 | 10.0 | 78.7 | 153 | 37 | 49 | 49 | 47 | 45 | 35 |
| | 8 | 4 | 19.5 | 66.8 | 236 | 96 | 137 | 132 | 129 | 122 | 96 |
| | 9 | 3 | 28.2 | 53.4 | 270 | 147 | 205 | 207 | 203 | 193 | 152 |
| | 10 | 2 | 35.4 | 37.8 | 287 | 187 | 263 | 266 | 261 | 248 | 195 |
| | 11 | 1 | 40.3 | 19.8 | 295 | 212 | 300 | 303 | 297 | 283 | 223 |
| | 12 | | 42.0 | 0.0 | 298 | 220 | 312 | 315 | 309 | 294 | 232 |
| | SURFACE DAILY TOTALS | | | | 2780 | 1578 | 2208 | 2228 | 2182 | 2074 | 1632 |
| APR 21 | 6 | 6 | 8.6 | 97.8 | 108 | 27 | 13 | 9 | 8 | 7 | 5 |
| | 7 | 5 | 18.6 | 86.7 | 205 | 85 | 76 | 69 | 59 | 48 | 21 |
| | 8 | 4 | 28.5 | 74.9 | 247 | 142 | 149 | 141 | 129 | 113 | 69 |
| | 9 | 3 | 37.8 | 61.2 | 268 | 191 | 218 | 208 | 194 | 174 | 115 |
| | 10 | 2 | 45.8 | 44.6 | 280 | 228 | 268 | 260 | 245 | 223 | 152 |
| | 11 | 1 | 51.5 | 24.0 | 286 | 252 | 301 | 294 | 278 | 254 | 177 |
| | 12 | | 53.6 | 0.0 | 288 | 260 | 313 | 305 | 289 | 264 | 185 |
| | SURFACE DAILY TOTALS | | | | 3076 | 2106 | 2358 | 2266 | 2114 | 1902 | 1262 |
| MAY 21 | 5 | 7 | 5.2 | 114.3 | 41 | 9 | 4 | 4 | 4 | 3 | 2 |
| | 6 | 6 | 14.7 | 103.7 | 162 | 61 | 27 | 16 | 15 | 13 | 10 |
| | 7 | 5 | 24.6 | 93.0 | 219 | 118 | 89 | 75 | 60 | 43 | 13 |
| | 8 | 4 | 34.7 | 81.6 | 248 | 171 | 156 | 142 | 123 | 101 | 45 |
| | 9 | 3 | 44.3 | 68.3 | 264 | 217 | 217 | 202 | 182 | 156 | 88 |
| | 10 | 2 | 53.0 | 51.3 | 274 | 252 | 265 | 251 | 229 | 200 | 120 |
| | 11 | 1 | 59.5 | 28.6 | 279 | 274 | 296 | 281 | 258 | 228 | 141 |
| | 12 | | 62.0 | 0.0 | 280 | 281 | 306 | 292 | 269 | 238 | 149 |
| | SURFACE DAILY TOTALS | | | | 3254 | 2482 | 2418 | 2234 | 2010 | 1728 | 982 |
| JUN 21 | 5 | 7 | 7.9 | 116.5 | 77 | 21 | 9 | 9 | 8 | 7 | 5 |
| | 6 | 6 | 17.2 | 106.2 | 172 | 74 | 33 | 19 | 18 | 16 | 12 |
| | 7 | 5 | 27.0 | 95.8 | 220 | 129 | 93 | 77 | 59 | 39 | 15 |
| | 8 | 4 | 37.1 | 84.6 | 246 | 181 | 157 | 140 | 119 | 95 | 35 |
| | 9 | 3 | 46.9 | 71.6 | 261 | 225 | 216 | 198 | 175 | 147 | 79 |
| | 10 | 2 | 55.8 | 54.8 | 269 | 259 | 262 | 244 | 220 | 189 | 105 |
| | 11 | 1 | 62.7 | 31.2 | 274 | 280 | 291 | 273 | 248 | 216 | 126 |
| | 12 | | 65.5 | 0.0 | 275 | 287 | 301 | 283 | 258 | 225 | 133 |
| | SURFACE DAILY TOTALS | | | | 3312 | 2626 | 2420 | 2204 | 1950 | 1644 | 874 |

| DATE | SOLAR TIME AM | SOLAR TIME PM | SOLAR POSITION ALT | SOLAR POSITION AZM | BTUH/SQ. FT. TOTAL INSOLATION ON SURFACES NORMAL | HORIZ. | SOUTH FACING SURFACE ANGLE WITH HORIZ. 38 | 48 | 58 | 68 | 90 |
|---|---|---|---|---|---|---|---|---|---|---|---|
| JUL 21 | 5 | 7 | 5.7 | 114.7 | 43 | 10 | 5 | 5 | 4 | 4 | 3 |
| | 6 | 6 | 15.2 | 104.1 | 156 | 62 | 28 | 18 | 16 | 15 | 11 |
| | 7 | 5 | 25.1 | 93.5 | 211 | 118 | 89 | 75 | 59 | 42 | 14 |
| | 8 | 4 | 35.1 | 82.1 | 240 | 171 | 154 | 140 | 121 | 99 | 43 |
| | 9 | 3 | 44.8 | 68.8 | 256 | 215 | 214 | 199 | 178 | 153 | 83 |
| | 10 | 2 | 53.5 | 51.9 | 266 | 250 | 261 | 246 | 224 | 195 | 116 |
| | 11 | 1 | 60.1 | 29.0 | 271 | 272 | 291 | 276 | 253 | 223 | 137 |
| | 12 | | 62.6 | 0.0 | 272 | 279 | 301 | 286 | 263 | 232 | 144 |
| | SURFACE DAILY TOTALS | | | | 3158 | 2474 | 2386 | 2200 | 1974 | 1694 | 956 |
| AUG 21 | 6 | 6 | 9.1 | 98.3 | 99 | 28 | 14 | 10 | 9 | 8 | 6 |
| | 7 | 5 | 19.1 | 87.2 | 190 | 85 | 75 | 67 | 58 | 47 | 20 |
| | 8 | 4 | 29.0 | 75.4 | 232 | 142 | 145 | 137 | 125 | 109 | 65 |
| | 9 | 3 | 38.4 | 61.8 | 254 | 189 | 210 | 201 | 187 | 168 | 110 |
| | 10 | 2 | 46.4 | 45.1 | 266 | 225 | 260 | 252 | 237 | 214 | 146 |
| | 11 | 1 | 52.2 | 24.3 | 272 | 248 | 293 | 285 | 268 | 244 | 169 |
| | 12 | | 54.3 | 0.0 | 274 | 256 | 304 | 296 | 279 | 255 | 177 |
| | SURFACE DAILY TOTALS | | | | 2898 | 2086 | 2300 | 2200 | 2046 | 1836 | 1208 |
| SEP 21 | 7 | 5 | 10.0 | 78.7 | 131 | 35 | 44 | 44 | 43 | 40 | 31 |
| | 8 | 4 | 19.5 | 66.8 | 215 | 92 | 124 | 124 | 121 | 115 | 90 |
| | 9 | 3 | 28.2 | 53.4 | 251 | 142 | 196 | 197 | 193 | 183 | 143 |
| | 10 | 2 | 35.4 | 37.8 | 269 | 181 | 251 | 254 | 248 | 236 | 185 |
| | 11 | 1 | 40.3 | 19.8 | 278 | 205 | 287 | 289 | 284 | 269 | 212 |
| | 12 | | 42.0 | 0.0 | 280 | 213 | 299 | 302 | 296 | 281 | 221 |
| | SURFACE DAILY TOTALS | | | | 2568 | 1522 | 2102 | 2118 | 2070 | 1966 | 1546 |
| OCT 21 | 7 | 5 | 2.0 | 71.9 | 4 | 0 | 1 | 1 | 1 | 1 | 1 |
| | 8 | 4 | 11.2 | 60.2 | 165 | 44 | 86 | 91 | 95 | 95 | 87 |
| | 9 | 3 | 19.3 | 47.4 | 233 | 94 | 167 | 176 | 180 | 178 | 157 |
| | 10 | 2 | 25.7 | 33.1 | 262 | 133 | 228 | 239 | 242 | 239 | 207 |
| | 11 | 1 | 30.0 | 17.1 | 274 | 157 | 266 | 277 | 281 | 276 | 237 |
| | 12 | | 31.5 | 0.0 | 278 | 166 | 279 | 291 | 294 | 288 | 247 |
| | SURFACE DAILY TOTALS | | | | 2154 | 1022 | 1774 | 1860 | 1890 | 1866 | 1626 |
| NOV 21 | 8 | 4 | 3.6 | 54.7 | 36 | 5 | 17 | 19 | 21 | 22 | 22 |
| | 9 | 3 | 11.2 | 42.4 | 179 | 46 | 117 | 129 | 137 | 141 | 135 |
| | 10 | 2 | 17.1 | 29.5 | 233 | 83 | 186 | 202 | 212 | 215 | 201 |
| | 11 | 1 | 20.9 | 15.1 | 255 | 107 | 227 | 245 | 255 | 258 | 238 |
| | 12 | | 22.2 | 0.0 | 261 | 115 | 241 | 259 | 270 | 272 | 250 |
| | SURFACE DAILY TOTALS | | | | 1668 | 596 | 1336 | 1448 | 1518 | 1544 | 1442 |
| DEC 21 | 9 | 3 | 8.0 | 40.9 | 140 | 27 | 87 | 98 | 105 | 110 | 109 |
| | 10 | 2 | 13.6 | 28.2 | 214 | 63 | 164 | 180 | 192 | 197 | 190 |
| | 11 | 1 | 17.3 | 14.4 | 242 | 86 | 207 | 226 | 239 | 244 | 231 |
| | 12 | | 18.6 | 0.0 | 250 | 94 | 222 | 241 | 254 | 260 | 244 |
| | SURFACE DAILY TOTALS | | | | 1444 | 446 | 1136 | 1250 | 1326 | 1384 | 1304 |

NOTE: 1) BASED ON DATA IN TABLE 1, P. 387 IN REF. [3]; 0% GROUND REFLECTANCE; 1.0 CLEARNESS FACTOR.
2) SEE FIG. 4, P. 394 IN [3] FOR TYPICAL REGIONAL CLEARNESS FACTORS.
3) GROUND REFLECTION NOT INCLUDED ON NORMAL OR HORIZONTAL SURFACES.

1 BTUH/SQ. FT. = 3.152 W/m$^2$

# TABLE A5 .... SOLAR POSITION AND INSOLATION VALUES FOR 56 DEGREES NORTH LATITUDE

| DATE | SOLAR TIME AM | SOLAR TIME PM | SOLAR POSITION ALT | SOLAR POSITION AZM | BTUH/SQ. FT. TOTAL INSOLATION ON SURFACES NORMAL | HORIZ. | SOUTH FACING SURFACE ANGLE WITH HORIZ. 46 | 56 | 66 | 76 | 90 |
|---|---|---|---|---|---|---|---|---|---|---|---|
| JAN 21 | 9 | 3 | 5.0 | 41.8 | 78 | 11 | 50 | 55 | 59 | 60 | 60 |
| | 10 | 2 | 9.9 | 28.5 | 170 | 39 | 135 | 146 | 154 | 156 | 155 |
| | 11 | 1 | 12.9 | 14.5 | 207 | 58 | 183 | 197 | 206 | 208 | 201 |
| | 12 | | 14.0 | 0.0 | 217 | 65 | 198 | 214 | 222 | 225 | 217 |
| | SURFACE DAILY TOTALS | | | | 1126 | 282 | 936 | 1010 | 1058 | 1079 | 1044 |
| FEB 21 | 8 | 4 | 7.6 | 59.4 | 129 | 25 | 65 | 69 | 72 | 72 | 69 |
| | 9 | 3 | 14.2 | 45.9 | 214 | 65 | 151 | 159 | 162 | 161 | 151 |
| | 10 | 2 | 19.4 | 31.5 | 250 | 98 | 215 | 225 | 228 | 224 | 208 |
| | 11 | 1 | 22.8 | 16.1 | 266 | 119 | 254 | 265 | 268 | 263 | 243 |
| | 12 | | 24.0 | 0.0 | 270 | 126 | 268 | 279 | 282 | 276 | 255 |
| | SURFACE DAILY TOTALS | | | | 1986 | 740 | 1640 | 1716 | 1742 | 1716 | 1595 |
| MAR 21 | 7 | 5 | 8.3 | 77.5 | 128 | 28 | 80 | 80 | 79 | 77 | 72 |
| | 8 | 4 | 15.2 | 64.4 | 215 | 75 | 119 | 120 | 117 | 111 | 97 |
| | 9 | 3 | 23.3 | 50.3 | 253 | 118 | 192 | 193 | 189 | 180 | 154 |
| | 10 | 2 | 29.0 | 34.9 | 272 | 151 | 249 | 251 | 246 | 234 | 195 |
| | 11 | 1 | 32.7 | 17.9 | 282 | 172 | 285 | 288 | 282 | 268 | 225 |
| | 12 | | 34.0 | 0.0 | 284 | 179 | 297 | 300 | 294 | 279 | 234 |
| | SURFACE DAILY TOTALS | | | | 2586 | 1268 | 2066 | 2084 | 2040 | 1938 | 1720 |
| APR 21 | 5 | 7 | 1.4 | 108.3 | 0 | 0 | 0 | 0 | 0 | 0 | 0 |
| | 6 | 6 | 9.6 | 96.5 | 122 | 32 | 14 | 9 | 8 | 7 | 6 |
| | 7 | 5 | 18.0 | 84.1 | 201 | 81 | 74 | 66 | 57 | 46 | 29 |
| | 8 | 4 | 26.1 | 70.9 | 239 | 123 | 143 | 135 | 123 | 108 | 82 |
| | 9 | 3 | 33.6 | 56.3 | 260 | 169 | 208 | 200 | 186 | 167 | 133 |
| | 10 | 2 | 39.9 | 39.7 | 272 | 201 | 259 | 251 | 236 | 214 | 174 |
| | 11 | 1 | 44.1 | 20.7 | 278 | 220 | 292 | 284 | 268 | 245 | 200 |
| | 12 | | 45.6 | 0.0 | 280 | 227 | 303 | 295 | 279 | 255 | 209 |
| | SURFACE DAILY TOTALS | | | | 3024 | 1892 | 2282 | 2186 | 2038 | 1838 | 1858 |
| MAY 21 | 4 | 8 | 1.2 | 125.5 | 0 | 0 | 0 | 0 | 0 | 0 | 0 |
| | 5 | 7 | 8.5 | 113.4 | 93 | 25 | 10 | 9 | 8 | 7 | 6 |
| | 6 | 6 | 16.5 | 101.5 | 175 | 71 | 28 | 17 | 15 | 13 | 11 |
| | 7 | 5 | 24.8 | 89.3 | 219 | 119 | 88 | 74 | 58 | 41 | 16 |
| | 8 | 4 | 33.1 | 76.3 | 244 | 163 | 153 | 138 | 119 | 98 | 69 |
| | 9 | 3 | 40.9 | 61.6 | 259 | 201 | 212 | 197 | 176 | 151 | 109 |
| | 10 | 2 | 47.6 | 44.2 | 268 | 231 | 259 | 244 | 222 | 194 | 146 |
| | 11 | 1 | 52.3 | 23.4 | 273 | 248 | 288 | 274 | 251 | 222 | 170 |
| | 12 | | 54.0 | 0.0 | 275 | 255 | 299 | 284 | 261 | 231 | 176 |
| | SURFACE DAILY TOTALS | | | | 3340 | 2574 | 2374 | 2188 | 1962 | 1692 | 1218 |
| JUN 21 | 4 | 8 | 4.2 | 127.2 | 21 | 4 | 2 | 2 | 2 | 2 | 1 |
| | 5 | 7 | 11.4 | 115.3 | 122 | 40 | 14 | 13 | 11 | 10 | 8 |
| | 6 | 6 | 19.3 | 103.6 | 185 | 86 | 34 | 19 | 17 | 15 | 12 |
| | 7 | 5 | 27.6 | 91.7 | 222 | 132 | 92 | 76 | 57 | 38 | 15 |
| | 8 | 4 | 35.9 | 78.8 | 243 | 175 | 154 | 137 | 116 | 92 | 59 |
| | 9 | 3 | 43.8 | 64.1 | 257 | 212 | 211 | 193 | 170 | 143 | 98 |
| | 10 | 2 | 50.7 | 46.4 | 265 | 240 | 255 | 238 | 216 | 184 | 133 |
| | 11 | 1 | 55.6 | 24.9 | 269 | 258 | 284 | 267 | 242 | 210 | 156 |
| | 12 | | 57.5 | 0.0 | 271 | 264 | 294 | 278 | 251 | 219 | 164 |
| | SURFACE DAILY TOTALS | | | | 3438 | 2562 | 2388 | 2166 | 1910 | 1606 | 1120 |

| DATE | SOLAR TIME AM | SOLAR TIME PM | SOLAR POSITION ALT | SOLAR POSITION AZM | BTUH/SQ. FT. TOTAL INSOLATION ON SURFACES NORMAL | HORIZ. | SOUTH FACING SURFACE ANGLE WITH HORIZ. 46 | 56 | 66 | 76 | 90 |
|---|---|---|---|---|---|---|---|---|---|---|---|
| JUL 21 | 4 | 8 | 1.7 | 125.8 | 0 | 0 | 0 | 0 | 0 | 0 | 0 |
| | 5 | 7 | 9.0 | 113.7 | 91 | 27 | 11 | 10 | 9 | 8 | 6 |
| | 6 | 6 | 17.6 | 101.6 | 169 | 72 | 34 | 18 | 16 | 14 | 12 |
| | 7 | 5 | 25.5 | 89.7 | 212 | 119 | 83 | 74 | 58 | 41 | 15 |
| | 8 | 4 | 33.6 | 76.7 | 237 | 159 | 151 | 139 | 117 | 96 | 61 |
| | 9 | 3 | 41.4 | 62.8 | 252 | 201 | 208 | 193 | 173 | 147 | 106 |
| | 10 | 2 | 48.2 | 44.6 | 261 | 235 | 254 | 239 | 217 | 189 | 142 |
| | 11 | 1 | 52.9 | 23.7 | 265 | 248 | 283 | 268 | 245 | 216 | 165 |
| | 12 | | 54.6 | 0.0 | 267 | 254 | 293 | 278 | 255 | 225 | 173 |
| | SURFACE DAILY TOTALS | | | | 3240 | 2372 | 2342 | 2162 | 1926 | 1645 | 1186 |
| AUG 21 | 5 | 7 | 2.0 | 109.2 | 1 | 0 | 0 | 0 | 0 | 0 | 0 |
| | 6 | 6 | 10.2 | 97.6 | 112 | 34 | 16 | 11 | 10 | 9 | 7 |
| | 7 | 5 | 18.5 | 84.5 | 187 | 82 | 73 | 65 | 55 | 45 | 28 |
| | 8 | 4 | 26.7 | 71.3 | 225 | 128 | 140 | 131 | 119 | 104 | 78 |
| | 9 | 3 | 34.3 | 56.7 | 246 | 166 | 202 | 186 | 164 | 139 | 105 |
| | 10 | 2 | 40.5 | 40.9 | 258 | 192 | 252 | 232 | 207 | 176 | 126 |
| | 11 | 1 | 44.8 | 20.8 | 264 | 228 | 282 | 259 | 235 | 201 | 151 |
| | 12 | | 46.3 | 0.0 | 266 | 235 | 293 | 269 | 245 | 209 | 160 |
| | SURFACE DAILY TOTALS | | | | 2839 | 1839 | 2718 | 2488 | 2188 | 1860 | 1392 |
| SEP 21 | 7 | 5 | 8.3 | 77.5 | 107 | 26 | 56 | 56 | 54 | 52 | 48 |
| | 8 | 4 | 16.2 | 64.4 | 184 | 72 | 111 | 111 | 108 | 102 | 89 |
| | 9 | 3 | 23.3 | 50.3 | 233 | 134 | 181 | 182 | 178 | 168 | 147 |
| | 10 | 2 | 29.0 | 34.9 | 253 | 186 | 238 | 237 | 232 | 221 | 193 |
| | 11 | 1 | 32.7 | 17.9 | 263 | 226 | 271 | 273 | 267 | 254 | 223 |
| | 12 | | 34.0 | 0.0 | 266 | 173 | 285 | 285 | 279 | 265 | 233 |
| | SURFACE DAILY TOTALS | | | | 2368 | 1229 | 1950 | 1962 | 1928 | 1820 | 1596 |
| OCT 21 | 8 | 4 | 7.1 | 59.1 | 104 | 20 | 53 | 57 | 59 | 59 | 52 |
| | 9 | 3 | 13.6 | 45.7 | 193 | 70 | 132 | 145 | 148 | 147 | 138 |
| | 10 | 2 | 18.0 | 31.3 | 231 | 92 | 201 | 210 | 213 | 210 | 195 |
| | 11 | 1 | 20.5 | 16.0 | 248 | 112 | 244 | 259 | 263 | 258 | 241 |
| | 12 | | 21.5 | 0.0 | 253 | 119 | 253 | 263 | 266 | 261 | 241 |
| | SURFACE DAILY TOTALS | | | | 1804 | 688 | 1516 | 1588 | 1612 | 1588 | 1482 |
| NOV 21 | 9 | 3 | 5.2 | 42.5 | 70 | 12 | 49 | 54 | 57 | 59 | 58 |
| | 10 | 2 | 10.0 | 28.5 | 165 | 35 | 127 | 143 | 149 | 152 | 148 |
| | 11 | 1 | 13.1 | 14.5 | 201 | 58 | 179 | 193 | 201 | 203 | 196 |
| | 12 | | 14.2 | 0.0 | 211 | 65 | 198 | 209 | 217 | 219 | 211 |
| | SURFACE DAILY TOTALS | | | | 1094 | 289 | 914 | 986 | 1032 | 1046 | 1016 |
| DEC 21 | 9 | 3 | 1.5 | 40.5 | 3 | 0 | 3 | 4 | 4 | 4 | 4 |
| | 10 | 2 | 6.6 | 27.5 | 113 | 19 | 86 | 96 | 101 | 104 | 103 |
| | 11 | 1 | 9.5 | 13.9 | 166 | 37 | 141 | 154 | 163 | 167 | 164 |
| | 12 | | 10.6 | 0.0 | 180 | 43 | 159 | 175 | 182 | 186 | 182 |
| | SURFACE DAILY TOTALS | | | | 748 | 156 | 620 | 678 | 716 | 734 | 722 |

NOTE: 1) BASED ON DATA IN TABLE 1, P. 387 IN REF. [3]; 0% GROUND REFLECTANCE; 1.0 CLEARNESS FACTOR.

2) SEE FIG. 4, P. 394 in [3] FOR TYPICAL REGIONAL CLEARNESS FACTORS.

3) GROUND REFLECTION NOT INCLUDED ON NORMAL OR HORIZONTAL SURFACES.

1 BTUH/SQ. FT. = 3.152 W/m$^2$

TABLE A6 ... SOLAR POSITION AND INSOLATION VALUES FOR 64 DEGREES NORTH LATITUDE

| DATE | SOLAR TIME AM | SOLAR TIME PM | SOLAR POSITION ALT | SOLAR POSITION AZM | BTUH/SQ. FT. TOTAL INSOLATION ON SURFACES — SOUTH FACING SURFACE ANGLE FROM HORIZ: NORMAL | HORIZ | 54 | 64 | 74 | 84 | 90 |
|---|---|---|---|---|---|---|---|---|---|---|---|
| JAN 21 | 10 | 2 | 2.8 | 28.1 | 22 | 2 | 17 | 19 | 20 | 21 | 21 |
| | 11 | 1 | 5.2 | 14.1 | 91 | 12 | 72 | 77 | 81 | 83 | 83 |
| | 12 | | 6.0 | 0.0 | 130 | 15 | 91 | 98 | 102 | 103 | 103 |
| | SURFACE DAILY TOTALS | | | | 506 | 45 | 268 | 296 | 322 | 336 | 336 |
| FEB 21 | 8 | 4 | 3.4 | 58.7 | 55 | 9 | 37 | 39 | 39 | 39 | 39 |
| | 9 | 3 | 8.6 | 44.8 | 142 | 31 | 103 | 108 | 111 | 112 | 112 |
| | 10 | 2 | 12.6 | 30.3 | 199 | 55 | 151 | 158 | 162 | 158 | 158 |
| | 11 | 1 | 15.1 | 15.3 | 222 | 71 | 212 | 223 | 223 | 219 | 219 |
| | 12 | | 16.0 | 0.0 | 228 | 77 | 225 | 235 | 237 | 232 | 226 |
| | SURFACE DAILY TOTALS | | | | 1432 | 500 | 1295 | 1286 | 1322 | 1292 | 1279 |
| MAR 21 | 7 | 5 | 6.5 | 75.5 | 45 | 15 | 30 | 28 | 28 | 27 | 25 |
| | 8 | 4 | 20.7 | 62.6 | 135 | 54 | 101 | 102 | 99 | 94 | 89 |
| | 9 | 3 | 18.1 | 48.1 | 207 | 87 | 171 | 172 | 168 | 160 | 150 |
| | 10 | 2 | 22.3 | 32.7 | 245 | 112 | 227 | 229 | 224 | 213 | 203 |
| | 11 | 1 | 25.9 | 16.6 | 260 | 129 | 252 | 255 | 248 | 238 | 226 |
| | 12 | | 26.9 | 0.0 | 265 | 134 | 274 | 277 | 271 | 259 | 246 |
| | SURFACE DAILY TOTALS | | | | 2296 | 933 | 1956 | 1893 | 1838 | 1734 | 1636 |
| APR 21 | 5 | 7 | 3.0 | 108.5 | 27 | 5 | 2 | 2 | 2 | 1 | 1 |
| | 6 | 6 | 13.4 | 95.1 | 133 | 35 | 15 | 9 | 8 | 7 | 6 |
| | 7 | 5 | 17.0 | 81.6 | 194 | 76 | 70 | 65 | 54 | 45 | 37 |
| | 8 | 4 | 23.3 | 67.5 | 228 | 112 | 136 | 128 | 115 | 102 | 91 |
| | 9 | 3 | 29.0 | 52.3 | 245 | 141 | 157 | 139 | 124 | 152 | 145 |
| | 10 | 2 | 33.5 | 36.3 | 250 | 153 | 246 | 233 | 218 | 203 | 188 |
| | 11 | 1 | 36.6 | 18.4 | 256 | 162 | 288 | 270 | 255 | 233 | 215 |
| | 12 | | 37.6 | 0.0 | 258 | 190 | 289 | 284 | 265 | 243 | 225 |
| | SURFACE DAILY TOTALS | | | | 2982 | 1548 | 2176 | 2022 | 1856 | 1656 | 1522 |
| MAY 21 | 4 | 8 | 05.5 | 125.1 | 21 | 11 | 5 | 4 | 4 | 3 | 3 |
| | 5 | 7 | 11.5 | 112.1 | 132 | 42 | 33 | 11 | 10 | 9 | 8 |
| | 6 | 6 | 17.9 | 99.1 | 195 | 73 | 26 | 15 | 14 | 12 | 12 |
| | 7 | 5 | 23.5 | 85.7 | 218 | 117 | 86 | 72 | 56 | 39 | 22 |
| | 8 | 4 | 30.9 | 71.5 | 255 | 152 | 143 | 133 | 115 | 94 | 89 |
| | 9 | 3 | 36.8 | 56.1 | 282 | 182 | 206 | 190 | 170 | 145 | 128 |
| | 10 | 2 | 41.6 | 38.9 | 281 | 205 | 248 | 235 | 213 | 189 | 157 |
| | 11 | 1 | 44.9 | 20.1 | 265 | 219 | 278 | 259 | 242 | 223 | 199 |
| | 12 | | 46.0 | 0.0 | 267 | 228 | 288 | 274 | 253 | 222 | 201 |
| | SURFACE DAILY TOTALS | | | | 3409 | 2236 | 2317 | 2129 | 1898 | 1678 | 1495 |
| JUN 21 | 3 | 9 | 4.2 | 139.4 | 21 | 4 | 2 | 2 | 2 | 2 | 1 |
| | 4 | 8 | 9.0 | 126.4 | 93 | 27 | 10 | 9 | 8 | 7 | 6 |
| | 5 | 7 | 14.7 | 113.6 | 158 | 68 | 15 | 15 | 13 | 11 | 10 |
| | 6 | 6 | 21.0 | 100.8 | 198 | 96 | 24 | 19 | 17 | 15 | 13 |
| | 7 | 5 | 27.5 | 87.5 | 221 | 132 | 91 | 74 | 58 | 36 | 23 |
| | 8 | 4 | 34.0 | 73.3 | 239 | 166 | 150 | 135 | 112 | 88 | 73 |
| | 9 | 3 | 39.9 | 57.8 | 251 | 195 | 208 | 187 | 168 | 137 | 115 |
| | 10 | 2 | 44.9 | 40.4 | 258 | 217 | 247 | 230 | 206 | 177 | 157 |
| | 11 | 1 | 48.3 | 20.9 | 262 | 231 | 275 | 258 | 233 | 202 | 181 |
| | 12 | | 49.5 | 0.0 | 263 | 235 | 284 | 267 | 242 | 211 | 189 |
| | SURFACE DAILY TOTALS | | | | 3650 | 2488 | 2342 | 2118 | 1882 | 1558 | 1356 |

NOTE: 1) BASED ON DATA IN TABLE 1, P. 387 IN REF. [3]; 0% GROUND REFLECTANCE; 1.0 CLEARNESS FACTOR.

2) SEE FIG. 4, P. 394 IN [3] FOR TYPICAL REGIONAL CLEARNESS FACTORS.

3) GROUND REFLECTION NOT INCLUDED ON NORMAL OR HORIZONTAL SURFACES.

1 BTUH/SQ. FT. = 3.152 W/m$^2$

# TABLE A7 LATITUDE 24°N. INCIDENT ANGLES FOR HORIZONTAL AND SOUTH-FACING TILTED SURFACES

Dates: (Decl.)
Dec. 21 (-23.45)

| | | Horiz. | L - 10 | Lat. | Lat. + 10 | Lat. + 20 | Vert. |
|---|---|---|---|---|---|---|---|
| 7 | 5 | 66.8 | 60.5 | 26.3 | 72.4 | 68.9 | 62.6 |
| 8 | 4 | 75.1 | 67.5 | 62.7 | 58.6 | 55.4 | 56.6 |
| 9 | 3 | 64.5 | 55.3 | 49.6 | 44.9 | 41.8 | 51.1 |
| 10 | 2 | 55.7 | 44.5 | 37.4 | 31.6 | 28.0 | 46.6 |
| 11 | 1 | 49.6 | 36.5 | 27.6 | 19.6 | 14.3 | 43.6 |
| 12 | | 47.4 | 33.4 | 23.5 | 13.5 | 3.4 | 42.5 |

Jan. 21 (-19.9)
Nov. 21 (-19.9)

| | | Horiz. | L - 10 | Lat. | Lat. + 10 | Lat. + 20 | Vert. |
|---|---|---|---|---|---|---|---|
| 7 | 5 | 85.2 | 79.6 | 75.9 | 72.6 | 69.8 | 65.7 |
| 8 | 4 | 73.1 | 66.2 | 62.0 | 58.5 | 56.0 | 59.8 |
| 9 | 3 | 62.1 | 53.5 | 48.4 | 44.5 | 42.2 | 54.4 |
| 10 | 2 | 52.8 | 42.1 | 35.5 | 30.6 | 28.2 | 50.0 |
| 11 | 1 | 46.4 | 33.4 | 24.8 | 17.6 | 14.1 | 47.0 |
| 12 | | 44.0 | 30.0 | 20.0 | 10.0 | 0.0 | 46.0 |

Feb. 21 (-10.6)
Oct. 21 (-10.7)

| | | Horiz. | L - 10 | Lat. | Lat. + 10 | Lat. + 20 | Vert. |
|---|---|---|---|---|---|---|---|
| 7 | 5 | 80.7 | 77.2 | 75.2 | 73.7 | 72.6 | 74.8 |
| 8 | 4 | 67.7 | 62.9 | 60.5 | 59.0 | 58.5 | 69.0 |
| 9 | 3 | 55.6 | 49.0 | 45.9 | 44.3 | 44.5 | 63.8 |
| 10 | 2 | 44.9 | 35.9 | 31.5 | 29.5 | 30.6 | 59.6 |
| 11 | 1 | 37.0 | 25.0 | 18.0 | 14.8 | 17.6 | 56.9 |
| 12 | | 34.0 | 20.0 | 10.0 | 0.0 | 10.0 | 56.0 |

Mar. 21 (0.0)
Sep. 21 (0.0)

| | | Horiz. | L - 10 | Lat. | Lat. + 10 | Lat. + 20 | Vert. |
|---|---|---|---|---|---|---|---|
| 7 | 5 | 76.3 | 75.2 | 75.0 | 75.2 | 75.9 | 84.0 |
| 8 | 4 | 62.8 | 60.5 | 60.0 | 60.5 | 62.0 | 78.3 |
| 9 | 3 | 49.8 | 45.9 | 45.0 | 45.9 | 48.4 | 73.3 |
| 10 | 2 | 37.7 | 31.5 | 30.0 | 31.5 | 35.5 | 69.4 |
| 11 | 1 | 28.1 | 18.0 | 15.0 | 18.0 | 24.8 | 66.9 |
| 12 | | 24.0 | 10.0 | 0.0 | 10.0 | 20.0 | 66.0 |

Apr. 21 (+11.9)
Aug. 21 (+12.1)

| | | Horiz. | L - 10 | Lat. | Lat. + 10 | Lat. + 20 | Vert. |
|---|---|---|---|---|---|---|---|
| 6 | 6 | 85.3 | 88.0 | 90.0 | 92.0 | 93.9 | 100.6 |
| 7 | 5 | 71.7 | 73.5 | 75.3 | 77.6 | 80.2 | 94.6 |
| 8 | 4 | 58.0 | 58.9 | 60.7 | 63.4 | 67.0 | 89.1 |
| 9 | 3 | 44.4 | 44.2 | 46.2 | 49.7 | 54.4 | 84.4 |
| 10 | 2 | 31.0 | 29.5 | 32.0 | 36.8 | 43.2 | 80.7 |
| 11 | 1 | 18.9 | 14.8 | 18.9 | 26.2 | 34.9 | 78.4 |
| 12 | | 12.4 | 1.6 | 11.6 | 21.6 | 31.6 | 77.6 |

May 21 (+20.3)
Jul 21 (+20.5)

| | | Horiz. | L - 10 | Lat. | Lat. + 10 | Lat. + 20 | Vert. |
|---|---|---|---|---|---|---|---|
| 6 | 6 | 82.0 | 86.0 | 90.0 | 93.4 | 96.7 | 108.2 |
| 7 | 5 | 68.8 | 72.6 | 75.9 | 79.6 | 83.6 | 102.3 |
| 8 | 4 | 55.5 | 58.5 | 62.0 | 66.2 | 71.1 | 97.0 |
| 9 | 3 | 41.7 | 44.5 | 48.4 | 53.5 | 59.5 | 92.4 |
| 10 | 2 | 28.0 | 30.6 | 35.5 | 42.1 | 49.6 | 88.9 |
| 11 | 1 | 14.5 | 17.6 | 24.8 | 33.4 | 42.6 | 86.7 |
| 12 | | 4.0 | 10.0 | 20.0 | 30.0 | 40.0 | 86.0 |

Jun. 21 (+23.45)

| | | Horiz. | L - 10 | Lat. | Lat. + 10 | Lat. + 20 | Vert. |
|---|---|---|---|---|---|---|---|
| 6 | 6 | 80.7 | 86.0 | 90.0 | 94.0 | 97.8 | 111.3 |
| 7 | 5 | 67.7 | 72.4 | 76.3 | 80.5 | 85.0 | 105.5 |
| 8 | 4 | 54.5 | 58.6 | 62.7 | 67.5 | 72.8 | 100.2 |
| 9 | 3 | 41.0 | 44.9 | 49.6 | 55.8 | 61.7 | 95.7 |
| 10 | 2 | 27.4 | 31.6 | 37.4 | 44.5 | 52.4 | 92.3 |
| 11 | 1 | 13.7 | 19.7 | 27.6 | 36.5 | 45.9 | 90.2 |
| 12 | | 0.6 | 13.4 | 23.4 | 33.4 | 43.4 | 89.4 |

# TABLE A8. LATITUDE 32°N. INCIDENT ANGLES FOR HORIZONTAL AND SOUTH-FACING TILTED SURFACES

Dates (Decl.)
Dec. 21 (-23.45

| | | Horiz. | L - 10 | Lat. | Lat. + 10 | Lat. + 20 | Vert. |
|---|---|---|---|---|---|---|---|
| 8 | 4 | 79.7 | 67.5 | 62.7 | 58.6 | 55.4 | 54.5 |
| 9 | 3 | 70.2 | 55.3 | 49.6 | 44.9 | 41.8 | 47.1 |
| 10 | 2 | 62.4 | 44.5 | 37.4 | 31.6 | 28.0 | 40.7 |
| 11 | 1 | 57.3 | 36.5 | 27.6 | 19.6 | 14.3 | 36.2 |
| 12 | | 55.4 | 33.4 | 23.4 | 13.5 | 3.5 | 34.5 |

Jan. 21 (-19.9)
Nov. 21 (-19.9)

| | | Horiz. | L - 10 | Lat. | Lat. + 10 | Lat. + 20 | Vert. |
|---|---|---|---|---|---|---|---|
| 7 | 5 | 88.6 | 79.6 | 75.9 | 72.6 | 69.8 | 65.2 |
| 8 | 4 | 77.5 | 66.2 | 62.0 | 58.5 | 56.0 | 57.4 |
| 9 | 3 | 67.5 | 53.5 | 48.4 | 44.5 | 42.2 | 50.0 |
| 10 | 2 | 59.4 | 42.1 | 35.5 | 30.6 | 28.2 | 43.8 |
| 11 | 1 | 53.9 | 33.4 | 24.8 | 17.6 | 14.1 | 39.6 |
| 12 | | 52.9 | 30.0 | 20.0 | 10.0 | 0.0 | 38.0 |

Feb. 21 (-10.6)
Oct. 21 (-10.7)

| | | Horiz. | L - 10 | Lat. | Lat. + 10 | Lat. + 20 | Vert. |
|---|---|---|---|---|---|---|---|
| 7 | 5 | 82.9 | 77.2 | 75.2 | 73.7 | 72.6 | 73.6 |
| 8 | 4 | 71.0 | 62.9 | 60.5 | 59.0 | 58.5 | 65.9 |
| 9 | 3 | 60.1 | 49.0 | 45.9 | 44.3 | 44.5 | 58.9 |
| 10 | 2 | 50.9 | 35.9 | 31.5 | 29.5 | 30.6 | 53.2 |
| 11 | 1 | 44.4 | 25.0 | 18.0 | 14.8 | 17.6 | 49.4 |
| 12 | | 42.0 | 20.0 | 10.0 | 0.0 | 10.0 | 48.0 |

Mar. 21 (0.0)
Sep. 21 (0.0)

| | | Horiz. | L - 10 | Lat. | Lat. + 10 | Lat. + 20 | Vert. |
|---|---|---|---|---|---|---|---|
| 7 | 5 | 77.3 | 75.2 | 75.0 | 75.2 | 75.9 | 82.1 |
| 8 | 4 | 64.9 | 60.5 | 60.0 | 60.5 | 62.0 | 74.6 |
| 9 | 3 | 53.2 | 45.9 | 45.0 | 45.9 | 48.4 | 68.0 |
| 10 | 2 | 42.7 | 31.5 | 30.0 | 31.5 | 35.5 | 62.7 |
| 11 | 1 | 35.0 | 18.0 | 15.0 | 18.0 | 24.8 | 59.2 |
| 12 | | 32.0 | 10.0 | 0.0 | 10.0 | 20.0 | 58.0 |

Apr. 21 (+11.9)
Aug. 21 (+12.1)

| | | Horiz. | L - 10 | Lat. | Lat. + 10 | Lat. + 20 | Vert. |
|---|---|---|---|---|---|---|---|
| 6 | 6 | 83.9 | 88.0 | 90.0 | 92.0 | 93.9 | 99.8 |
| 7 | 5 | 71.2 | 73.5 | 75.3 | 77.6 | 80.2 | 92.1 |
| 8 | 4 | 58.5 | 58.9 | 60.7 | 63.4 | 67.0 | 84.9 |
| 9 | 3 | 46.1 | 44.2 | 46.2 | 49.2 | 54.4 | 78.7 |
| 10 | 2 | 34.3 | 29.5 | 32.0 | 36.8 | 43.2 | 73.8 |
| 11 | 1 | 24.6 | 14.8 | 18.9 | 26.2 | 34.9 | 70.7 |
| 12 | | 20.4 | 1.6 | 11.6 | 21.6 | 31.6 | 69.6 |

May 21 (+20.3)
Jul. 21 (+20.5)

| | | Horiz. | L - 10 | Lat. | Lat. + 10 | Lat. + 20 | Vert. |
|---|---|---|---|---|---|---|---|
| 6 | 6 | 79.6 | 86.6 | 90.0 | 93.4 | 96.7 | 106.9 |
| 7 | 5 | 67.2 | 72.6 | 75.9 | 79.6 | 83.6 | 99.3 |
| 8 | 4 | 54.6 | 58.5 | 62.0 | 66.2 | 71.1 | 92.4 |
| 9 | 3 | 41.9 | 44.5 | 48.4 | 53.5 | 59.5 | 86.4 |
| 10 | 2 | 29.4 | 30.6 | 35.5 | 42.1 | 49.6 | 81.9 |
| 11 | 1 | 18.0 | 17.6 | 24.8 | 33.4 | 42.6 | 79.0 |
| 12 | | 12.0 | 10.0 | 20.0 | 30.0 | 40.0 | 78.0 |

Jun. 21 (+23.45)

| | | Horiz. | L - 10 | Lat. | Lat. + 10 | Lat. + 20 | Vert. |
|---|---|---|---|---|---|---|---|
| 6 | 6 | 77.8 | 86.0 | 90.0 | 94.0 | 97.8 | 109.7 |
| 7 | 5 | 65.7 | 72.4 | 76.3 | 80.5 | 85.0 | 102.2 |
| 8 | 4 | 53.1 | 58.6 | 62.7 | 67.5 | 72.8 | 95.4 |
| 9 | 3 | 40.4 | 44.9 | 49.6 | 55.3 | 61.7 | 89.6 |
| 10 | 2 | 27.8 | 31.6 | 37.4 | 44.5 | 52.4 | 85.2 |
| 11 | 1 | 15.8 | 19.6 | 27.6 | 36.5 | 45.8 | 82.4 |
| 12 | | 8.6 | 13.4 | 23.4 | 33.4 | 43.4 | 81.4 |

# TABLE A9 LATITUDE 40°N. INCIDENT ANGLES FOR HORIZONTAL AND SOUTH-FACING TILTED SURFACES

Date: (Decl.)
Dec. 21 (-23.45)

| | | Horiz. | L - 10 | Lat. | Lat. + 10 | Lat. + 20 | Vert. |
|---|---|---|---|---|---|---|---|
| 8 | 4 | 84.5 | 67.5 | 62.7 | 58.6 | 55.4 | 53.2 |
| 9 | 3 | 76.0 | 55.3 | 49.6 | 44.9 | 41.8 | 43.8 |
| 10 | 2 | 69.3 | 44.5 | 37.4 | 31.6 | 28.0 | 35.4 |
| 11 | 1 | 65.0 | 36.5 | 27.6 | 19.6 | 14.3 | 29.0 |
| 12 | | 63.4 | 33.4 | 23.4 | 13.5 | 3.5 | 26.6 |

Jan. 21 (-19.9)
Nov. 21 (-19.9)

| | | Horiz. | L - 10 | Lat. | Lat. + 10 | Lat. + 20 | Vert. |
|---|---|---|---|---|---|---|---|
| 8 | 4 | 81.9 | 66.2 | 62.0 | 58.5 | 56.0 | 55.7 |
| 9 | 3 | 73.2 | 53.5 | 48.4 | 44.5 | 42.2 | 46.4 |
| 10 | 2 | 66.2 | 42.1 | 35.5 | 30.6 | 28.2 | 38.3 |
| 11 | 1 | 61.6 | 33.4 | 24.8 | 17.6 | 14.1 | 32.3 |
| 12 | | 60.0 | 30.0 | 20.0 | 10.0 | 0.0 | 30.0 |

Feb. 21 (-10.6)
Oct. 21 (-10.7)

| | | Horiz. | L - 10 | Lat. | Lat. + 10 | Lat. + 20 | Vert. |
|---|---|---|---|---|---|---|---|
| 7 | 5 | 85.2 | 77.2 | 75.2 | 73.7 | 72.6 | 72.7 |
| 8 | 4 | 74.6 | 62.9 | 60.5 | 59.0 | 58.5 | 63.3 |
| 9 | 3 | 65.0 | 49.0 | 45.9 | 44.3 | 44.5 | 59.5 |
| 10 | 2 | 57.2 | 35.9 | 31.5 | 29.5 | 30.6 | 47.1 |
| 11 | 1 | 51.9 | 25.0 | 18.0 | 14.8 | 17.6 | 41.9 |
| 12 | | 50.0 | 20.0 | 10.0 | 0.0 | 10.0 | 40.0 |

Mar. 21 (0.0)
Sep. 21 (0.0)

| | | Horiz. | L - 10 | Lat. | Lat. + 10 | Lat. + 20 | Vert. |
|---|---|---|---|---|---|---|---|
| 7 | 5 | 78.6 | 75.2 | 75.0 | 75.2 | 75.9 | 80.4 |
| 8 | 4 | 67.5 | 60.5 | 60.0 | 60.5 | 62.0 | 71.3 |
| 9 | 3 | 57.2 | 45.9 | 45.0 | 45.9 | 48.4 | 63.0 |
| 10 | 2 | 48.4 | 31.5 | 30.0 | 31.5 | 35.5 | 56.2 |
| 11 | 1 | 42.3 | 18.0 | 15.0 | 18.0 | 24.8 | 51.6 |
| 12 | | 40.0 | 10.0 | 0.0 | 10.0 | 20.0 | 50.0 |

Apr. 21 (+11.9)
Aug. 21 (+12.1)

| | | Horiz. | L - 10 | Lat. | Lat. + 10 | Lat. + 20 | Vert. |
|---|---|---|---|---|---|---|---|
| 6 | 6 | 82.6 | 88.0 | 90.0 | 92.0 | 93.9 | 98.9 |
| 7 | 5 | 71.1 | 73.5 | 75.3 | 77.6 | 80.2 | 89.5 |
| 8 | 4 | 59.7 | 58.9 | 60.7 | 63.4 | 67.0 | 80.7 |
| 9 | 3 | 48.7 | 44.2 | 46.2 | 49.7 | 54.4 | 73.1 |
| 10 | 2 | 38.8 | 29.5 | 32.0 | 36.8 | 43.2 | 67.0 |
| 11 | 1 | 31.3 | 14.8 | 18.9 | 26.2 | 34.9 | 63.0 |
| 12 | | 28.4 | 1.6 | 11.6 | 21.6 | 31.6 | 61.6 |

May 21 (+20.3)
Jul. 21 (+20.5)

| | | Horiz. | L - 10 | Lat. | Lat. + 10 | Lat. + 20 | Vert. |
|---|---|---|---|---|---|---|---|
| 5 | 7 | 88.1 | 100.4 | 104.1 | 107.4 | 110.2 | 114.7 |
| 6 | 6 | 77.3 | 86.6 | 90.0 | 93.4 | 96.7 | 105.2 |
| 7 | 5 | 66.0 | 72.6 | 75.9 | 79.6 | 83.6 | 96.1 |
| 8 | 4 | 54.6 | 58.5 | 62.0 | 66.2 | 71.1 | 87.7 |
| 9 | 3 | 43.2 | 44.5 | 48.4 | 53.5 | 59.5 | 80.5 |
| 10 | 2 | 32.5 | 30.6 | 35.5 | 42.1 | 49.6 | 74.9 |
| 11 | 1 | 23.8 | 17.6 | 24.8 | 33.4 | 42.6 | 71.2 |
| 12 | | 20.0 | 10.0 | 20.0 | 30.0 | 40.0 | 70.0 |

Jun. 21 (+23.45)

| | | Horiz. | L - 10 | Lat. | Lat. + 10 | Lat. + 20 | Vert. |
|---|---|---|---|---|---|---|---|
| 5 | 7 | 85.8 | 99.5 | 103.7 | 107.6 | 111.1 | 117.2 |
| 6 | 6 | 75.2 | 86.0 | 90.0 | 94.0 | 97.8 | 107.7 |
| 7 | 5 | 64.0 | 72.4 | 76.3 | 80.5 | 85.0 | 98.8 |
| 8 | 4 | 52.6 | 58.6 | 62.7 | 67.5 | 72.8 | 90.6 |
| 9 | 3 | 41.2 | 44.9 | 49.6 | 55.3 | 61.7 | 83.6 |
| 10 | 2 | 30.2 | 31.6 | 37.4 | 44.5 | 52.4 | 78.1 |
| 11 | 1 | 20.8 | 19.6 | 27.6 | 36.5 | 45.8 | 74.6 |
| 12 | | 16.6 | 13.4 | 23.4 | 33.4 | 43.4 | 73.4 |

# TABLE A10 LATITUDE 48°N. INCIDENT ANGLES FOR HORIZONTAL AND SOUTH-FACING TILTED SURFACES

Dec. 21 (-23.45)

| | | Horiz. | L - 10 | Lat. | Lat. + 10 | Lat. + 20 | Vert. |
|---|---|---|---|---|---|---|---|
| 9 | 3 | 82.0 | 55.3 | 49.6 | 44.9 | 41.8 | 41.6 |
| 10 | 2 | 76.4 | 44.5 | 37.4 | 31.6 | 28.0 | 31.1 |
| 11 | 1 | 72.7 | 36.5 | 27.6 | 19.6 | 14.3 | 22.4 |
| 12 | | 71.4 | 33.4 | 23.4 | 13.5 | 3.5 | 18.5 |

Jan. 21 (-19.9)
Nov. 21 (-19.9)

| | | Horiz. | L - 10 | Lat. | Lat. + 10 | Lat. + 20 | Vert. |
|---|---|---|---|---|---|---|---|
| 8 | 4 | 86.5 | 66.2 | 62.0 | 58.5 | 56.0 | 54.7 |
| 9 | 3 | 79.0 | 53.5 | 48.4 | 44.5 | 42.2 | 43.7 |
| 10 | 2 | 73.1 | 42.1 | 35.5 | 30.6 | 28.2 | 33.5 |
| 11 | 1 | 69.3 | 33.4 | 24.8 | 17.6 | 14.1 | 25.4 |
| 12 | | 68.0 | 30.0 | 20.0 | 10.0 | 0.0 | 22.0 |

Feb 21* (-10.6)
Oct. 21 (-10.7)

| | | Horiz. | L - 10 | Lat. | Lat. + 10 | Lat. + 20 | Vert. |
|---|---|---|---|---|---|---|---|
| 7 | 5 | 87.6 | 77.2 | 75.2 | 73.7 | 72.6 | 72.2 |
| 8 | 4 | 78.4 | 62.9 | 60.5 | 59.0 | 58.5 | 61.2 |
| 9 | 3 | 70.3 | 49.0 | 45.9 | 44.3 | 44.5 | 50.7 |
| 10 | 2 | 63.3 | 35.9 | 31.5 | 29.5 | 30.6 | 41.4 |
| 11 | 1 | 59.5 | 25.0 | 18.0 | 14.8 | 17.6 | 34.6 |
| 12 | | 58.0 | 20.0 | 10.0 | 0.0 | 10.0 | 32.0 |

Mar 21 (0.0)
Sep. 21 (0.0)

| | | Horiz. | L - 10 | Lat. | Lat. + 10 | Lat. + 20 | Vert. |
|---|---|---|---|---|---|---|---|
| 7 | 5 | 80.0 | 75.2 | 75.0 | 75.2 | 75.9 | 78.9 |
| 8 | 4 | 70.5 | 60.5 | 60.0 | 60.5 | 62.0 | 68.2 |
| 9 | 3 | 61.8 | 45.9 | 45.0 | 45.9 | 48.4 | 58.3 |
| 10 | 2 | 54.6 | 31.5 | 30.0 | 31.5 | 35.5 | 49.9 |
| 11 | 1 | 49.7 | 18.0 | 15.0 | 18.0 | 24.8 | 44.4 |
| 12 | | 48.0 | 10.0 | 0.0 | 10.0 | 20.0 | 42.0 |

Apr. 21 (+11.9)
Aug. 21 (+12.1)

| | | Horiz. | L - 10 | Lat. | Lat. + 10 | Lat. + 20 | Vert. |
|---|---|---|---|---|---|---|---|
| 6 | 6 | 81.4 | 88.0 | 90.0 | 92.0 | 93.9 | 97.7 |
| 7 | 5 | 71.4 | 73.5 | 75.3 | 77.6 | 80.2 | 86.9 |
| 8 | 4 | 61.5 | 58.9 | 60.7 | 63.4 | 67.0 | 76.7 |
| 9 | 3 | 52.2 | 44.2 | 46.2 | 49.7 | 54.4 | 67.7 |
| 10 | 2 | 44.2 | 29.5 | 32.0 | 36.8 | 43.2 | 60.3 |
| 11 | 1 | 38.5 | 16.8 | 18.9 | 26.2 | 34.9 | 55.3 |
| 12 | | 36.4 | 1.6 | 11.6 | 21.6 | 31.6 | 53.6 |

May 21 (+20.3)
Jul. 21 (+20.5)

| | | Horiz. | L - 10 | Lat. | Lat. + 10 | Lat. + 20 | Vert. |
|---|---|---|---|---|---|---|---|
| 5 | 7 | 84.8 | 100.4 | 104.1 | 107.4 | 110.2 | 114.2 |
| 6 | 6 | 75.1 | 86.6 | 90.0 | 93.4 | 96.7 | 103.2 |
| 7 | 5 | 66.4 | 72.0 | 75.9 | 79.6 | 83.6 | 92.8 |
| 8 | 4 | 55.4 | 58.5 | 62.0 | 66.2 | 71.1 | 83.1 |
| 9 | 3 | 45.7 | 44.5 | 48.4 | 53.5 | 59.5 | 74.6 |
| 10 | 2 | 37.0 | 30.6 | 35.5 | 42.1 | 49.6 | 67.9 |
| 11 | 1 | 30.5 | 17.6 | 24.8 | 33.4 | 42.6 | 63.5 |
| 12 | | 28.0 | 10.0 | 20.0 | 30.0 | 40.0 | 62.0 |

Jun. 21 (+23.45)

| | | Horiz. | L - 10 | Lat. | Lat. + 10 | Lat. + 20 | Vert. |
|---|---|---|---|---|---|---|---|
| 5 | 7 | 82.1 | 99.5 | 103.7 | 107.6 | 111.1 | 116.3 |
| 6 | 6 | 72.8 | 86.0 | 90.0 | 94.0 | 97.8 | 105.4 |
| 7 | 5 | 61.0 | 72.4 | 76.3 | 80.5 | 85.0 | 95.2 |
| 8 | 4 | 52.9 | 58.6 | 62.7 | 67.6 | 72.8 | 85.7 |
| 9 | 3 | 43.1 | 44.9 | 49.6 | 55.3 | 61.7 | 77.5 |
| 10 | 2 | 34.2 | 31.6 | 37.4 | 44.5 | 52.4 | 71.1 |
| 11 | 1 | 27.3 | 19.6 | 27.6 | 36.5 | 45.8 | 66.9 |
| 12 | | 24.6 | 11.4 | 23.4 | 33.4 | 43.3 | 65.4 |

# TABLE A11 LATITUDE 56°N. INCIDENT ANGLES FOR HORIZONTAL AND SOUTH-FACING TILTED SURFACES

| | | | Horiz. | L - 10 | Lat. | Lat. + 10 | Lat. + 20 | Vert. |
|---|---|---|---|---|---|---|---|---|
| Dec. 21 (-23.45) | 9 | 3 | 89.1 | 55.3 | 49.6 | 44.9 | 41.8 | 40.5 |
| | 10 | 2 | 83.4 | 44.5 | 37.4 | 31.6 | 28.0 | 28.2 |
| | 11 | 1 | 80.5 | 36.5 | 27.6 | 19.6 | 14.3 | 16.8 |
| | 12 | | 79.4 | 33.4 | 23.4 | 13.5 | 3.4 | 10.5 |

| | | | Horiz. | L - 10 | Lat. | Lat. + 10 | Lat. + 20 | Vert. |
|---|---|---|---|---|---|---|---|---|
| Jan. 21 (-19.9) Nov. 21 (-19.9) | 9 | 3 | 85.0 | 53.5 | 48.4 | 44.5 | 42.2 | 42.1 |
| | 10 | 2 | 80.1 | 42.1 | 35.5 | 30.6 | 28.2 | 30.0 |
| | 11 | 1 | 77.1 | 33.4 | 24.8 | 17.6 | 14.1 | 19.3 |
| | 12 | | 76.0 | 30.0 | 20.0 | 10.0 | 0.0 | 14.0 |

| | | | Horiz. | L - 10 | Lat. | Lat. + 10 | Lat. + 20 | Vert. |
|---|---|---|---|---|---|---|---|---|
| Feb. 21 (-10.6) Oct. 21 (-10.7) | 8 | 4 | 82.5 | 62.9 | 60.5 | 59.0 | 58.5 | 59.6 |
| | 9 | 3 | 75.3 | 49.0 | 45.9 | 44.3 | 44.5 | 47.6 |
| | 10 | 2 | 70.6 | 35.9 | 31.5 | 29.5 | 30.6 | 36.5 |
| | 11 | 1 | 67.2 | 25.0 | 18.0 | 14.8 | 17.6 | 27.7 |
| | 12 | | 66.0 | 20.0 | 10.0 | 0.0 | -10.0 | 24.0 |

| | | | Horiz. | L - 10 | Lat. | Lat. + 10 | Lat. + 20 | Vert. |
|---|---|---|---|---|---|---|---|---|
| Mar. 21 (0.0) Sep. 21 (0.0) | 7 | 5 | 81.2 | 75.2 | 75.0 | 75.2 | 75.9 | 77.6 |
| | 8 | 4 | 73.9 | 60.5 | 60.0 | 60.5 | 62.0 | 66.0 |
| | 9 | 3 | 66.7 | 45.9 | 45.0 | 45.9 | 48.4 | 54.1 |
| | 10 | 2 | 61.0 | 31.5 | 30.0 | 31.5 | 35.5 | 44.1 |
| | 11 | 1 | 57.3 | 18.0 | 15.0 | 18.0 | 24.8 | 36.8 |
| | 12 | | 56.0 | 10.0 | 0.0 | 10.0 | 20.0 | 34.0 |

| | | | Horiz. | L - 10 | Lat. | Lat. + 10 | Lat. + 20 | Vert. |
|---|---|---|---|---|---|---|---|---|
| Apr. 21 (+11.9) Aug. 21 (+12.1) | 5 | 7 | 83.6 | 102.4 | 104.7 | 106.5 | 107.9 | 108.8 |
| | 6 | 6 | 80.4 | 88.0 | 90.0 | 92.0 | 93.9 | 96.5 |
| | 7 | 5 | 72.0 | 73.5 | 75.3 | 77.6 | 80.2 | 84.4 |
| | 8 | 4 | 63.9 | 58.9 | 60.7 | 63.4 | 67.0 | 72.9 |
| | 9 | 3 | 56.4 | 44.2 | 46.2 | 49.7 | 54.4 | 62.5 |
| | 10 | 2 | 50.1 | 29.5 | 32.0 | 36.8 | 43.2 | 53.8 |
| | 11 | 1 | 45.9 | 16.8 | 18.9 | 26.2 | 34.9 | 47.8 |
| | 12 | | 44.4 | 1.6 | 11.6 | 21.6 | 31.6 | 45.6 |

| | | | Horiz. | L - 10 | Lat. | Lat. + 10 | Lat. + 20 | Vert. |
|---|---|---|---|---|---|---|---|---|
| May 21 (+20.3) Jul. 21 (+20.5) | 4 | 8 | 88.8 | 113.8 | 118.0 | 121.5 | 124.0 | 125.5 |
| | 5 | 7 | 81.5 | 100.4 | 104.1 | 107.4 | 110.2 | 113.1 |
| | 6 | 6 | 73.5 | 86.6 | 90.4 | 93.4 | 96.7 | 101.0 |
| | 7 | 5 | 65.2 | 72.6 | 75.9 | 79.6 | 83.6 | 89.4 |
| | 8 | 4 | 56.9 | 58.5 | 62.0 | 66.2 | 71.1 | 78.6 |
| | 9 | 3 | 49.1 | 44.5 | 48.4 | 53.5 | 59.5 | 68.9 |
| | 10 | 2 | 42.4 | 30.6 | 35.5 | 42.1 | 49.6 | 61.1 |
| | 11 | 1 | 37.2 | 17.6 | 24.8 | 33.4 | 42.6 | 55.9 |
| | 12 | | 36.0 | 10.0 | 20.0 | 30.0 | 40.0 | 54.0 |

| | | | Horiz. | L - 10 | Lat. | Lat. + 10 | Lat. + 20 | Vert. |
|---|---|---|---|---|---|---|---|---|
| Jun. 21 (+23.45) | 4 | 8 | 85.8 | 112.5 | 117.3 | 121.4 | 124.6 | 127.1 |
| | 5 | 7 | 78.6 | 99.5 | 103.7 | 107.6 | 111.1 | 114.8 |
| | 6 | 6 | 70.7 | 86.0 | 90.0 | 94.0 | 97.8 | 102.9 |
| | 7 | 5 | 62.4 | 72.4 | 76.3 | 80.5 | 85.0 | 91.5 |
| | 8 | 4 | 54.1 | 58.6 | 62.7 | 67.5 | 72.8 | 80.9 |
| | 9 | 3 | 46.2 | 44.9 | 49.6 | 55.3 | 61.7 | 71.6 |
| | 10 | 2 | 39.3 | 31.6 | 37.4 | 44.5 | 52.4 | 64.1 |
| | 11 | 1 | 34.4 | 19.6 | 27.6 | 36.5 | 45.8 | 59.2 |
| | 12 | | 32.6 | 13.4 | 23.4 | 33.4 | 43.4 | 57.4 |

TABLE A12 LATITUDE 64°N, INCIDENT ANGLES FOR HORIZONTAL AND SOUTH-FACING TILTED SURFACES

| | | | Horiz. | L - 10 | Lat. | Lat. + 10 | Lat. + 20 | Vert. |
|---|---|---|---|---|---|---|---|---|
| Dec. 21 (-23.45) | 11 | 1 | 88.2 | 36.5 | 27.6 | 19.6 | 14.3 | 13.9 |
| | 12 | | 87.4 | 33.4 | 23.4 | 13.5 | 3.4 | 2.5 |

| | | | Horiz. | L - 10 | Lat. | Lat. + 10 | Lat. + 20 | Vert. |
|---|---|---|---|---|---|---|---|---|
| Jan. 21 (-19.9) Nov. 21 (-19.9) | 10 | 2 | 87.2 | 42.1 | 35.5 | 30.6 | 28.2 | 28.2 |
| | 11 | 1 | 84.8 | 33.4 | 24.8 | 17.6 | 14.1 | 15.0 |
| | 12 | | 64.0 | 30.0 | 20.0 | 10.0 | 0.0 | 4.0 |

| | | | Horiz. | L - 10 | Lat. | Lat. + 10 | Lat. + 20 | Vert. |
|---|---|---|---|---|---|---|---|---|
| Feb. 21 (-10.6) Oct. 21 (-10.7) | 8 | 4 | 86.6 | 69.9 | 60.5 | 59.0 | 58.5 | 58.8 |
| | 9 | 3 | 81.4 | 49.2 | 45.9 | 44.3 | 44.5 | 45.4 |
| | 10 | 2 | 77.4 | 35.9 | 31.5 | 29.5 | 30.6 | 32.6 |
| | 11 | 1 | 74.9 | 25.0 | 18.0 | 14.8 | 17.6 | 21.4 |
| | 12 | | 74.0 | 20.0 | 10.0 | 0.0 | 10.0 | 16.0 |

| | | | Horiz | L - 10 | Lat. | Lat. + 10 | Lat. + 20 | Vert. |
|---|---|---|---|---|---|---|---|---|
| Mar. 21 (0.0) Sep. 21 (0.0) | 7 | 5 | 83.5 | 75.2 | 75.0 | 75.2 | 75.9 | 76.5 |
| | 8 | 4 | 77.3 | 60.5 | 60.0 | 60.5 | 62.0 | 63.3 |
| | 9 | 3 | 71.9 | 45.9 | 45.0 | 45.9 | 48.4 | 50.5 |
| | 10 | 2 | 67.7 | 31.5 | 30.0 | 31.5 | 35.5 | 38.9 |
| | 11 | 1 | 64.9 | 18.0 | 15.0 | 18.0 | 24.8 | 29.8 |
| | 12 | | 64.0 | 10.0 | 0.0 | 10.0 | 20.0 | 26.0 |

| | | | Horiz. | L - 10 | Lat. | Lat. + 10 | Lat. + 20 | Vert. |
|---|---|---|---|---|---|---|---|---|
| Apr. 21 (+11.9) Aug. 21 (+12.1) | 5 | 7 | 86.0 | 102.4 | 104.2 | 106.5 | 107.9 | 108.4 |
| | 6 | 6 | 79.6 | 88.0 | 90.0 | 92.0 | 93.9 | 95.1 |
| | 7 | 5 | 73.0 | 73.5 | 75.3 | 77.6 | 80.2 | 82.0 |
| | 8 | 4 | 66.7 | 58.9 | 60.7 | 63.4 | 67.0 | 69.4 |
| | 9 | 3 | 61.0 | 44.2 | 46.2 | 49.7 | 54.4 | 57.7 |
| | 10 | 2 | 56.5 | 29.5 | 32.0 | 36.8 | 43.2 | 47.6 |
| | 11 | 1 | 53.5 | 14.8 | 18.9 | 26.2 | 34.9 | 40.3 |
| | 12 | | 52.4 | 1.6 | 13.6 | 21.6 | 31.6 | 37.6 |

| | | | Horiz. | L - 10 | Lat. | Lat. + 10 | Lat. + 20 | Vert. |
|---|---|---|---|---|---|---|---|---|
| May 21 (+20.3) Jul. 21 (+20.5) | 4 | 8 | 84.2 | 113.8 | 118.0 | 121.5 | 124.0 | 124.9 |
| | 5 | 7 | 78.4 | 100.4 | 104.1 | 107.4 | 110.2 | 111.6 |
| | 6 | 6 | 72.1 | 86.6 | 90.0 | 93.4 | 96.7 | 98.6 |
| | 7 | 5 | 65.5 | 72.6 | 75.9 | 79.6 | 83.6 | 86.1 |
| | 8 | 4 | 59.1 | 58.5 | 62.0 | 66.2 | 71.1 | 74.2 |
| | 9 | 3 | 53.2 | 44.5 | 48.4 | 53.5 | 59.5 | 63.4 |
| | 10 | 2 | 48.4 | 30.6 | 35.5 | 42.1 | 49.6 | 54.4 |
| | 11 | 1 | 45.3 | 17.6 | 24.8 | 33.4 | 42.6 | 48.3 |
| | 12 | | 44.0 | 10.0 | 20.0 | 30.0 | 40.0 | 46.0 |

| | | | Horiz. | L - 10 | Lat. | Lat. + 10 | Lat. + 20 | Vert. |
|---|---|---|---|---|---|---|---|---|
| Jun. 21 (+23.45) | 3 | 9 | 85.8 | 124.7 | 130.4 | 135.1 | 138.2 | 139.2 |
| | 4 | 8 | 81.0 | 112.5 | 117.3 | 121.4 | 124.6 | 125.9 |
| | 5 | 7 | 75.3 | 99.5 | 103.7 | 107.6 | 111.1 | 112.8 |
| | 6 | 6 | 69.0 | 86.0 | 90.0 | 94.0 | 97.8 | 100.0 |
| | 7 | 5 | 62.5 | 72.4 | 76.3 | 80.5 | 85.0 | 87.8 |
| | 8 | 4 | 56.0 | 58.6 | 62.7 | 67.5 | 72.8 | 76.2 |
| | 9 | 3 | 50.1 | 44.9 | 49.6 | 55.6 | 61.7 | 65.9 |
| | 10 | 2 | 45.1 | 31.6 | 37.4 | 44.5 | 52.4 | 57.3 |
| | 11 | 1 | 41.7 | 19.6 | 27.6 | 36.5 | 45.8 | 51.5 |
| | 12 | | 40.6 | 13.5 | 23.4 | 33.4 | 43.4 | 49.5 |

Table A13- Test Data to be Recorded

| Item | Test Involving Air as the Transfer Fluid | Test Involving a Liquid as the Transfer Fluid |
|---|---|---|
| Date | X | X |
| Observer(s) | X | X |
| Equipment name plate data | X | X |
| Collector tilt angle | X | X |
| Collector azimuth angle (as a function of time if movable) | X | X |
| Collector aperture area or frontal transparent area | X | X |
| Local standard time, at the beginning of collector warm-up and at the beginning and end of each 15 minute test period | X | X |
| Barometric pressure | X | |
| Ambient air temperature (at the beginning and end of each 15 minute test period) | X | X |
| $\Delta t = t_{f,e} - t_{f,i}$ across solar collector (either as a continuous function of time or as a 15 minute integrated quantity) | X | X |
| Inlet temperature, $t_{f,i}$ (as a continuous function of time | X | X |
| Outlet temperature, $t_{f,e}$ (as a continuous function of time | X | X |

Table A13 - continued

| Item | Test Involving Air as the Transfer Fluid | Test Involving a Liquid as the Transfer Fluid |
|---|---|---|
| Liquid flow rate | | X |
| Gauge pressure at solar collector inlet | | X |
| Gauge pressure at nozzle throat | X | |
| Nozzle throat diameter | X | |
| Velocity pressure at nozzle throat or static pressure difference across nozzle | X | |
| Dry bulb temperature at nozzle throat | X | |
| Wet bulb temperature at nozzle throat | X | |
| Pressure drop across solar collector | X | X |
| Height of the collector outlet above the collector inlet | X | X |
| Wind velocity near the collector surface or aperture (15 minute average) | X | X |
| I, the incident solar radiation onto the collector (as a continuous function of time and as a 15 minute integrated quantity if desired) | X | X |
| $I_d$, the diffuse component of the solar radiation onto the collector (at the beginning of the 15 minute period and after the completion of the 15 minute period) | X | X |

Table A14 Data to be Reported

General Information

Manufacturer or Project Name . . . . . .
Collector Model No. . . . . .
Construction details of the collector

gross dimensions and area . . . . . .
area of absorbing surface . . . . . .
cover plate*, dimensions, materials, optical properties (if known) . . .
reflector*, dimensions and shape, materials, optical properties (if known) . . . . . .
absorber plate, dimensional layout and configuration of flow path, absorptivity to short wave radiation (if known), emissivity for long wave radiation (if known), description of coating (including maximum allowable temperature if known) . . . . . .
air space(s)*, thickness and description of contained gas or construction . . . . . .
insulation*, material, thickness, thermal properties . . . . . .

Transfer fluid used and its properties . . . . . .

Weight of collector per $m^2$ of gross cross-sectional area . . . . . .

Volumetric capacity of the collector per $m^2$ of gross cross-sectional area if designed to operate with a liquid as the transfer fluid . . . .

Normal operating temperature range . . . . . .

Minimum transfer fluid flow rate . . . . . .

Maximum transfer fluid flow rate . . . . . .

Maximum operating pressure . . . . . .

Description of apparatus, including flow configuration and instrumentation used in testing (include photographs) . . . . . .

Description of the mounting of the collector for testing . . . . . .

Location of tests (longitude, latitude, and elevation above see level)

Efficiency Tests

A plot of the efficiency versus $\left(\frac{t_{f,i} + t_{f,e}}{2} - t_a\right)/I$ . . . . . .

* if applicable

An equation for the efficiency curve . . . . . .

For each "data point"

$\dot{m}$ . . . . . .

$c_p$ . . . . . .

$\int_{\tau_1}^{\tau_2} (t_{f,e} - t_{f,i})\, d\tau$ . . . . . .

$\int_{\tau_1}^{\tau_2} I\, d\tau$ . . . . . .

pressure drop across the solar collector . . . . . .
collector tilt angle . . . . . .
collector azimuth angle (as a function of time if movable) . . . . . .
incident angle . . . . . .
inlet fluid temperature, $t_{f,i}$ . . . . . .
percentage of incident radiation that is diffuse . . . . . .
wind speed near the collector surface or aperture . . . . . .

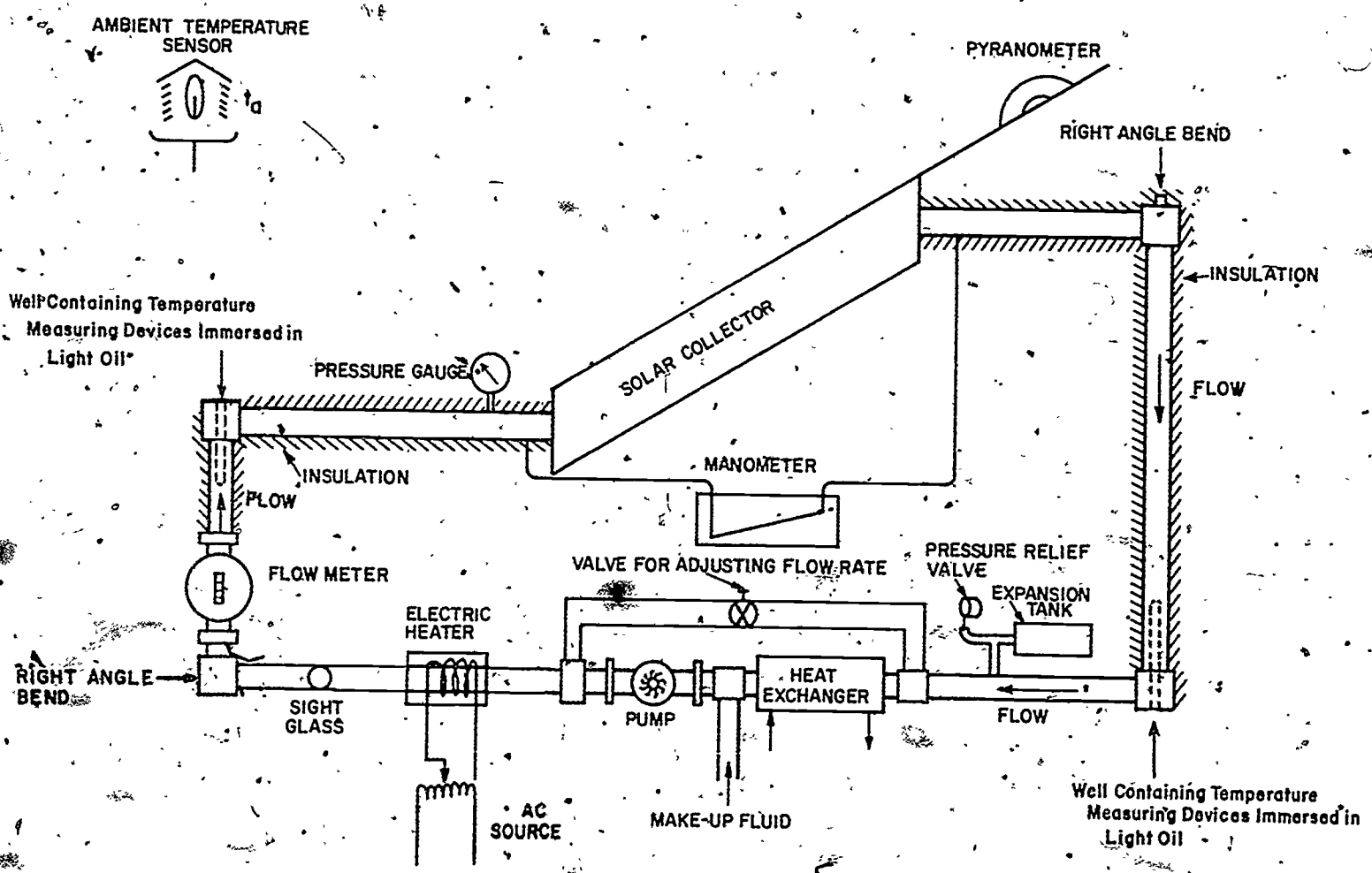


Figure A1 - Testing Configuration for the Solar Collector When the Transfer Fluid is a Liquid

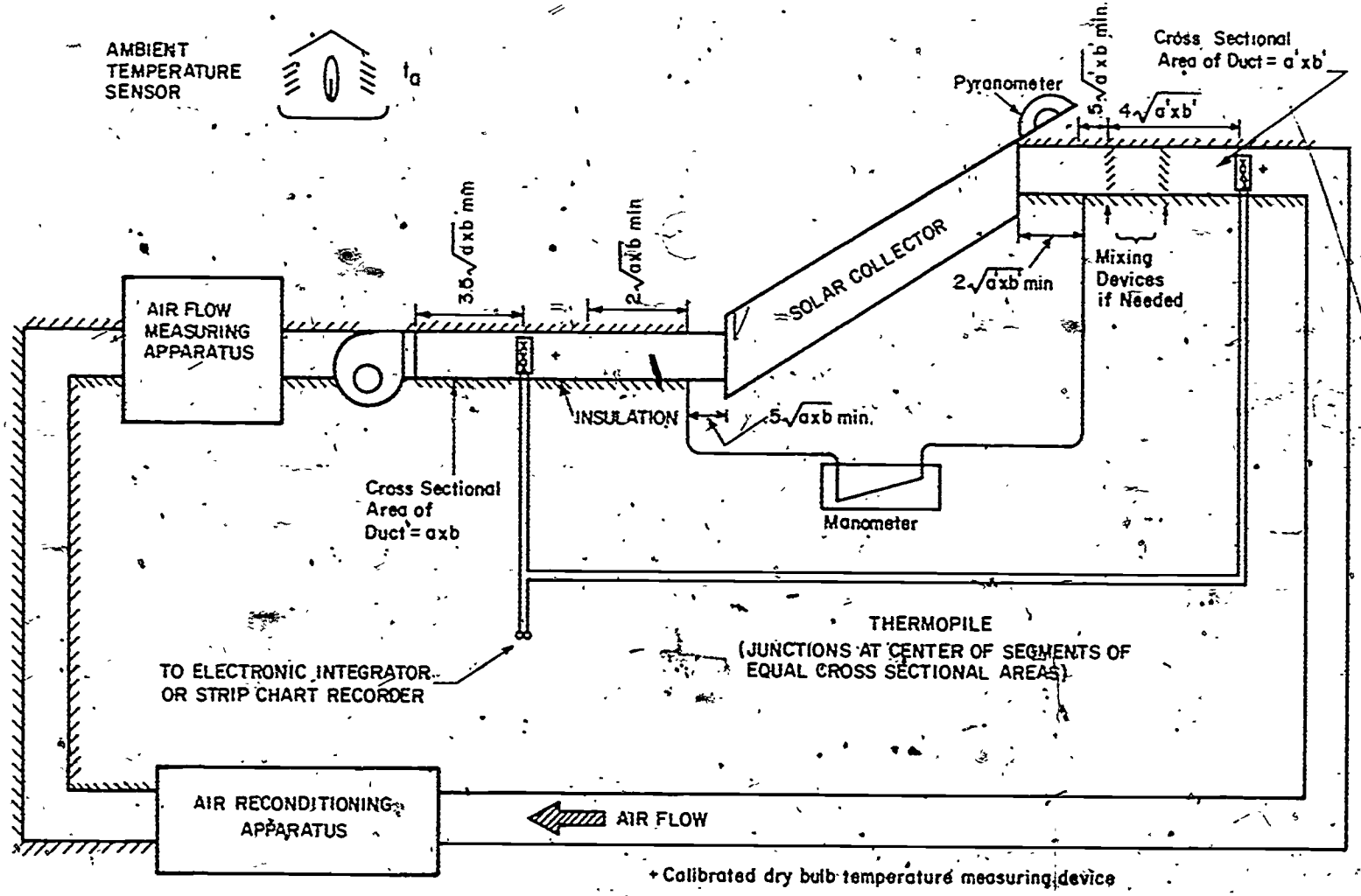


Figure A2 Testing Configuration for the Solar Collector When the Transfer Fluid is Air

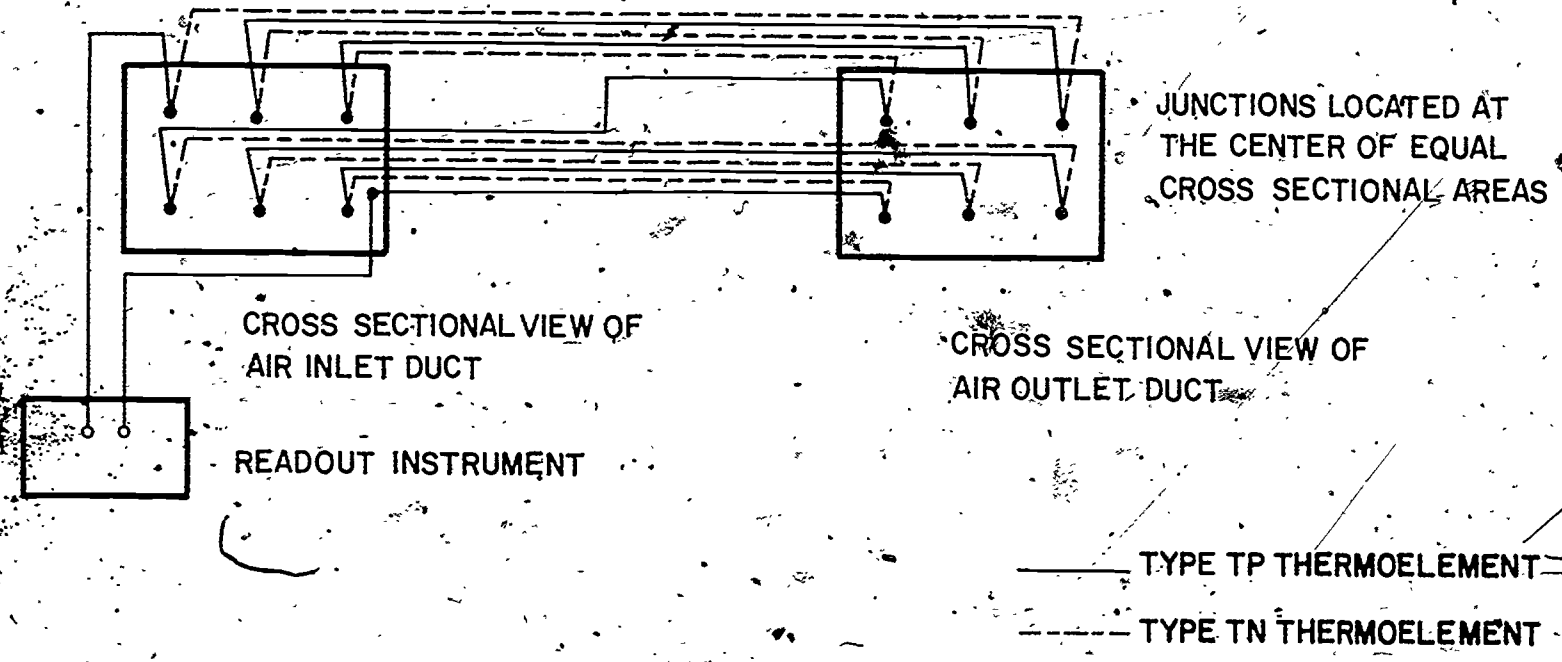


Figure A3 Schematic of the Thermopile Arrangement Used to Measure the Temperature Difference Across the Solar-Collector

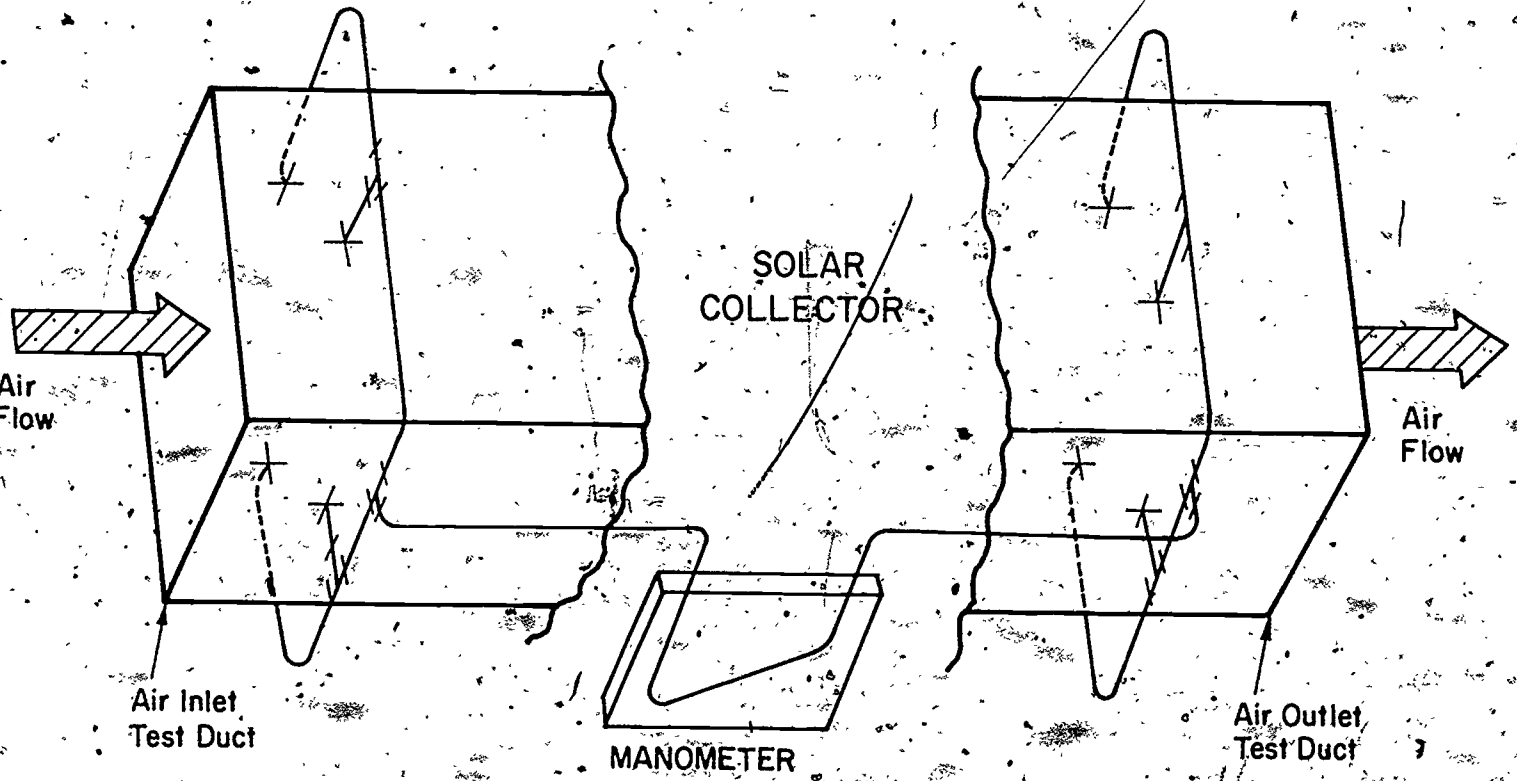


Figure A4 Schematic Representation of the Measurement of Pressure Drop Across the Solar Collector When Air is the Transfer Fluid

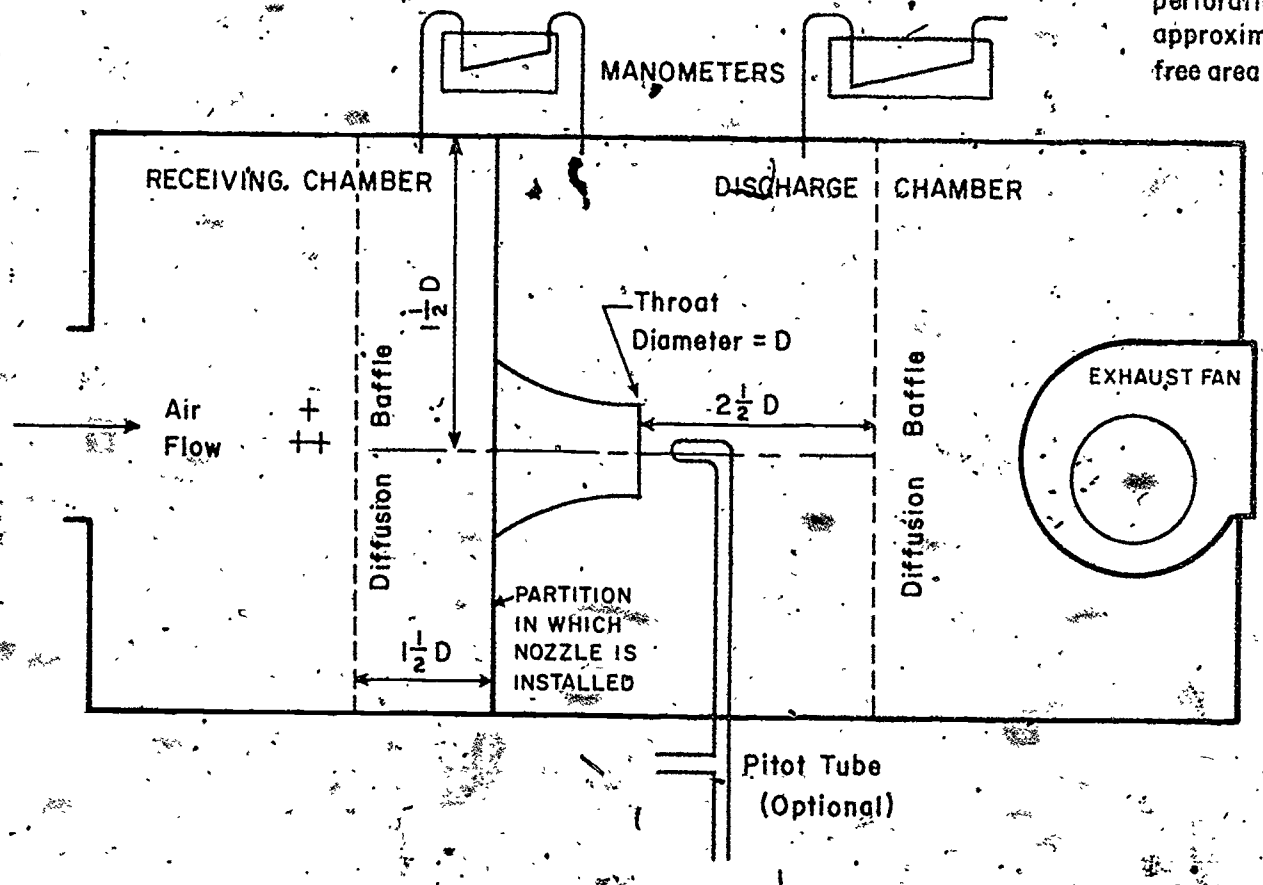


Figure A5 Nozzle Apparatus for Measuring Air Flow Rate

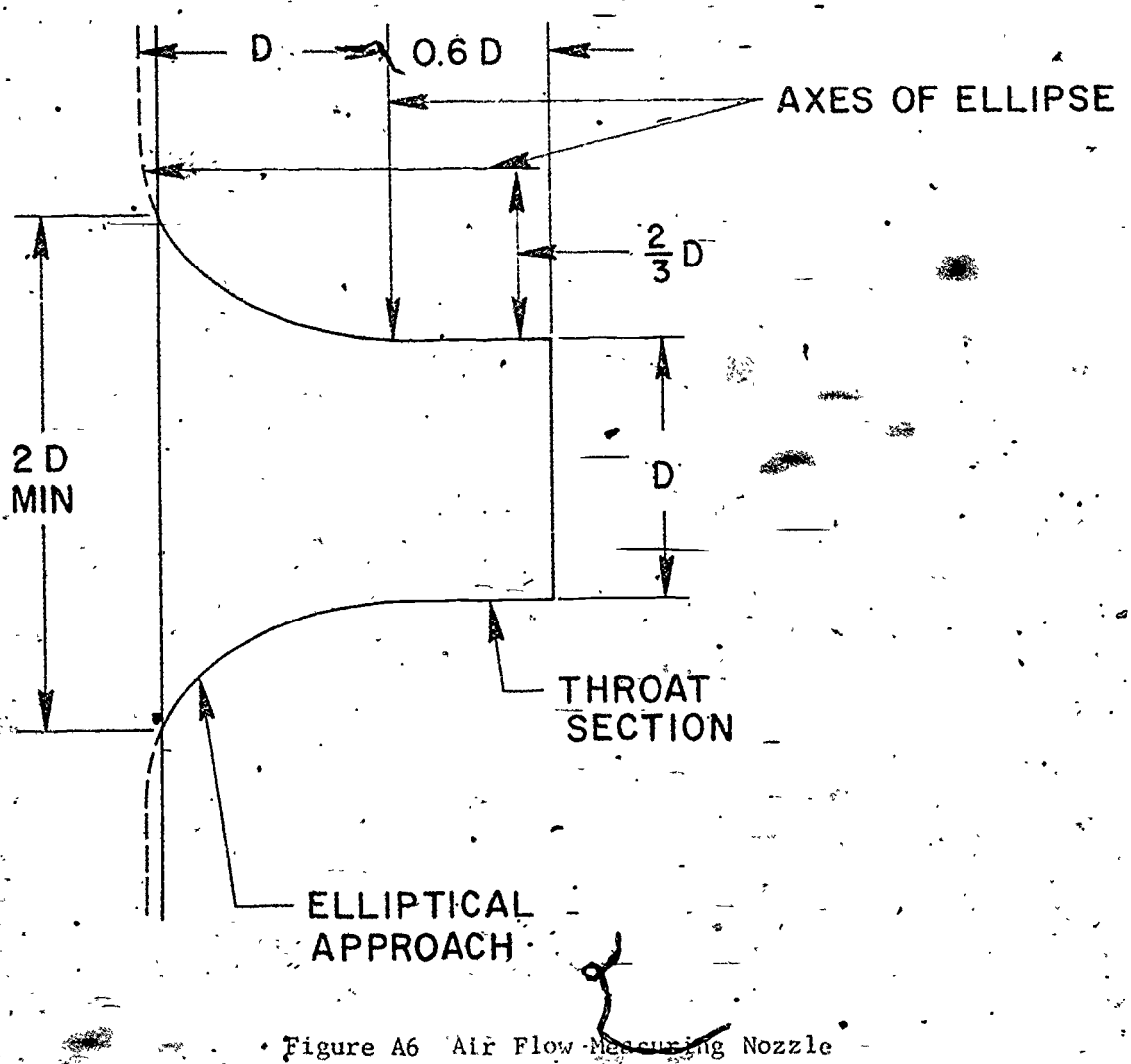


Figure A6 Air Flow-Measuring Nozzle

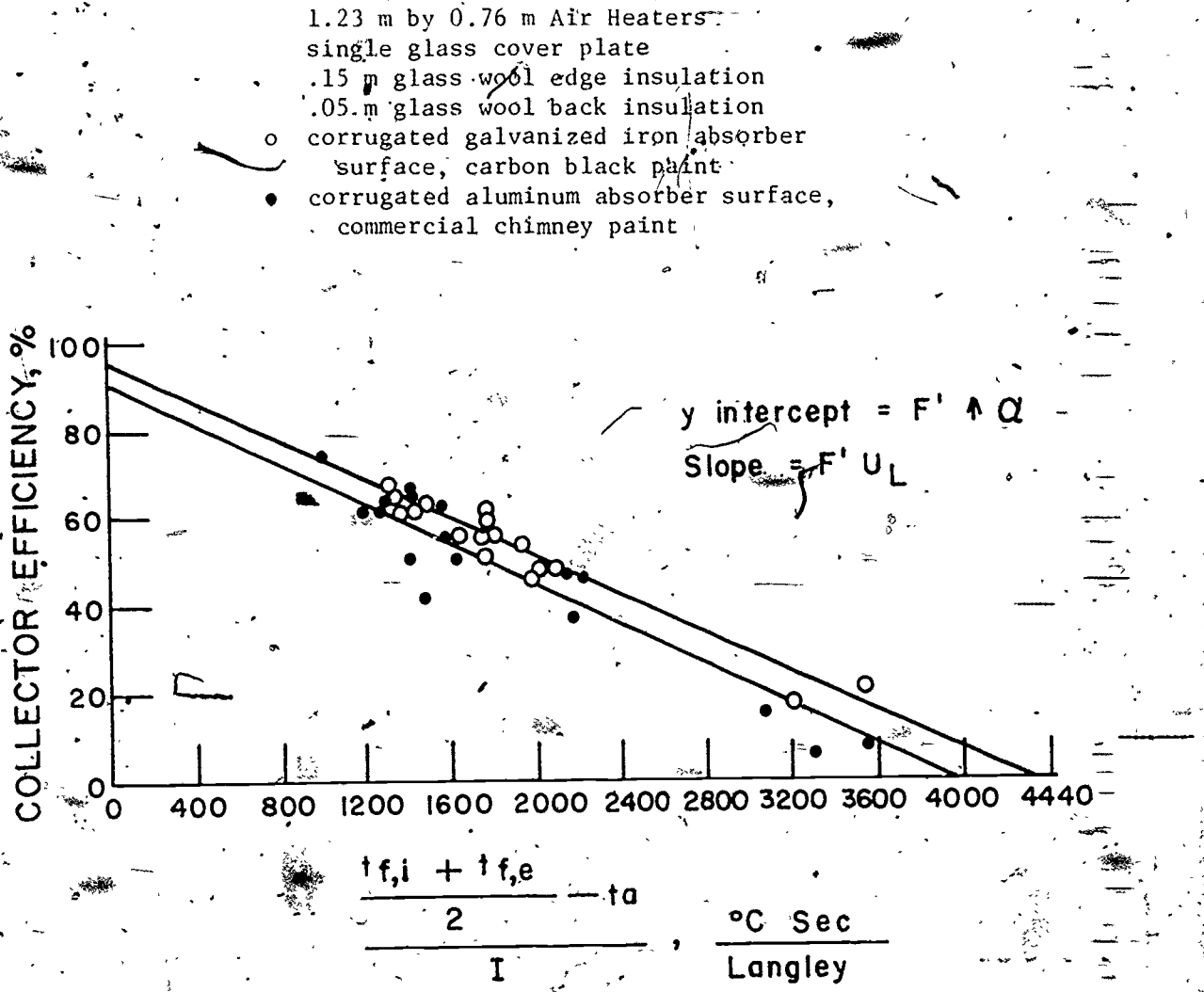


Figure A7 Efficiency Curves for Two Flat-Plate Collectors Using Air as the Transfer Fluid (reference [24])

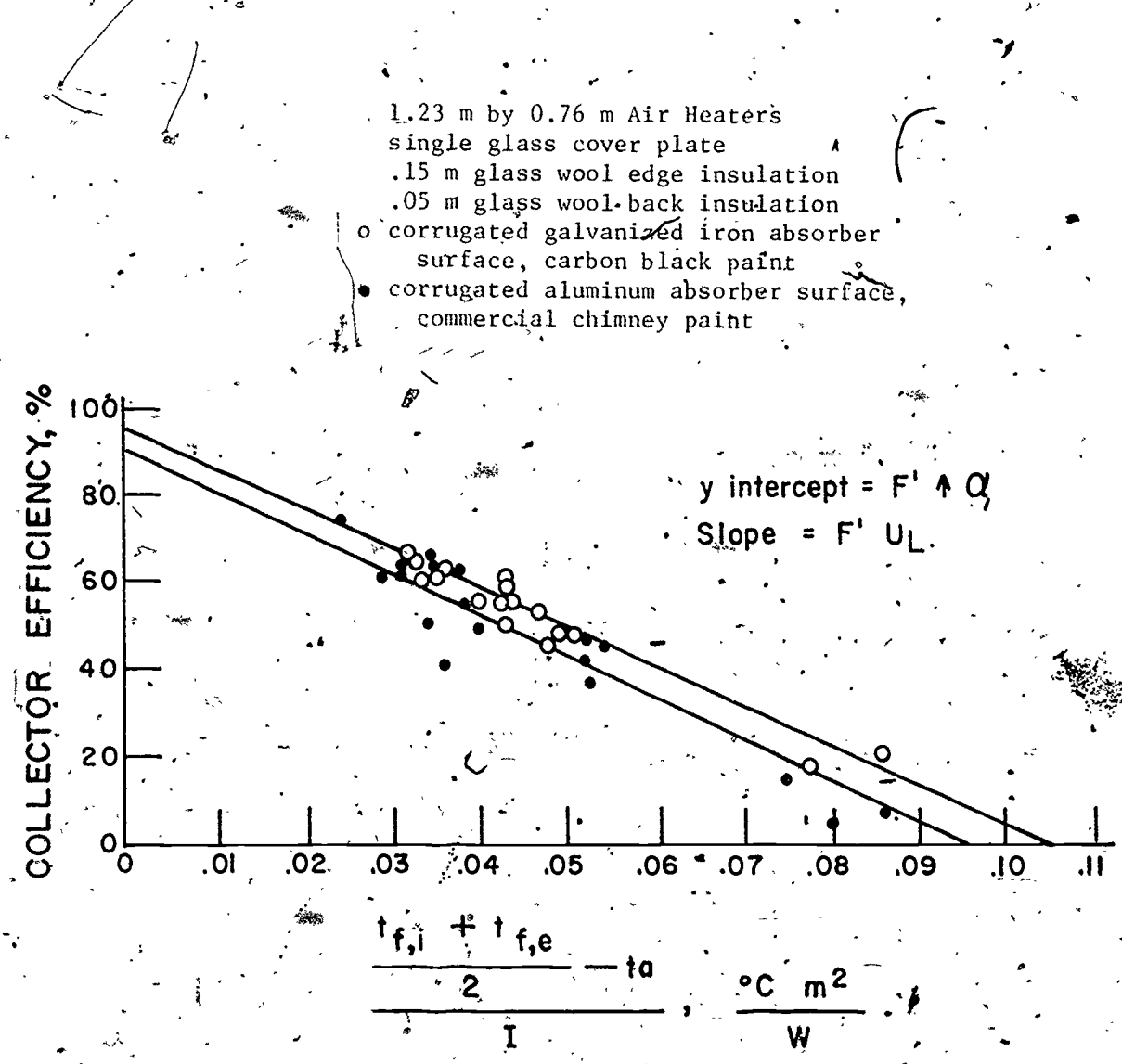


Figure A8 Efficiency Curves for Two Flat-Plate Collectors Using Air as the Transfer Fluid (reference [24])

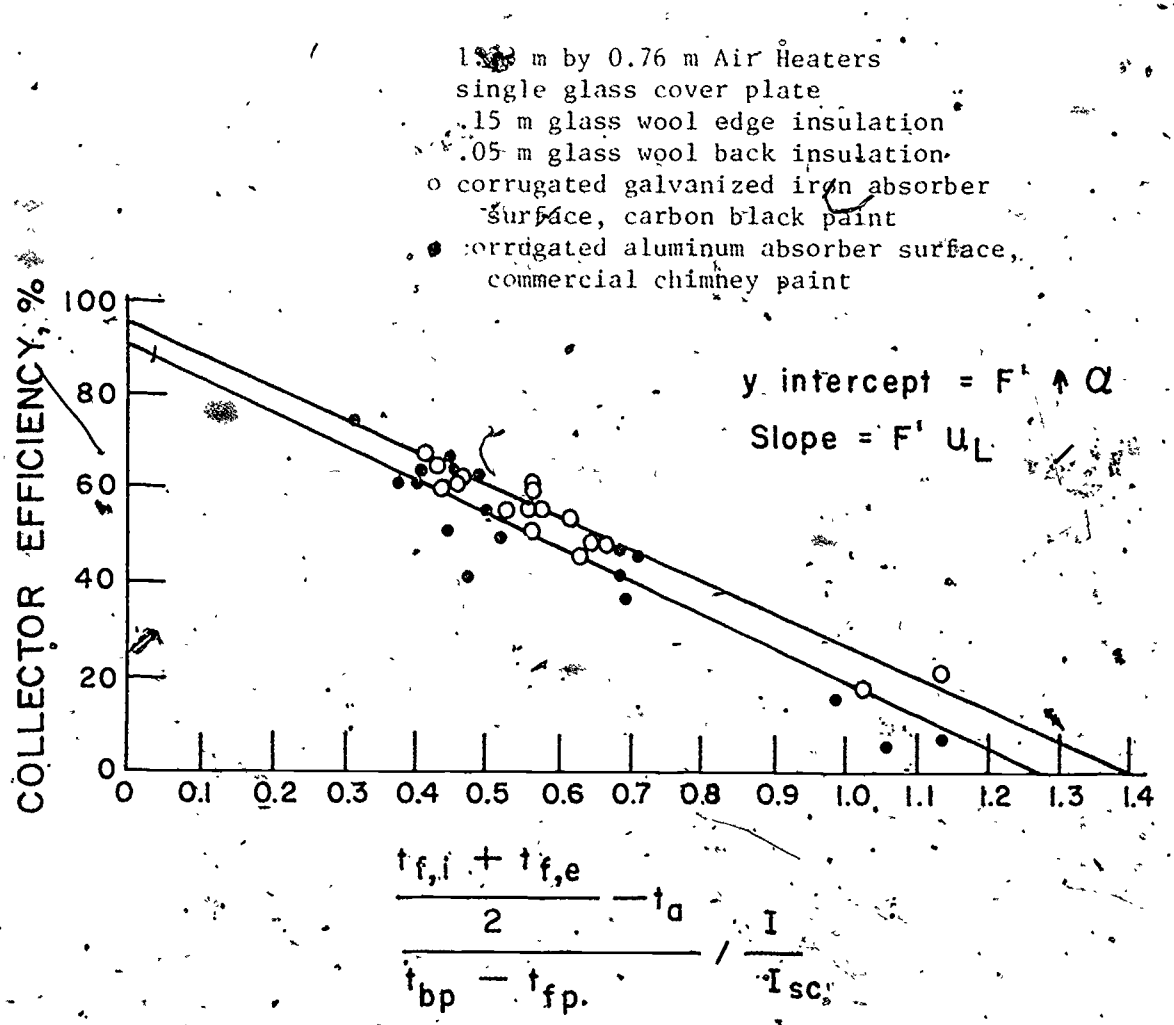


Figure A9 Efficiency Curves for Two Flat-Plate Collectors Using Air as the Transfer Fluid (reference [24])

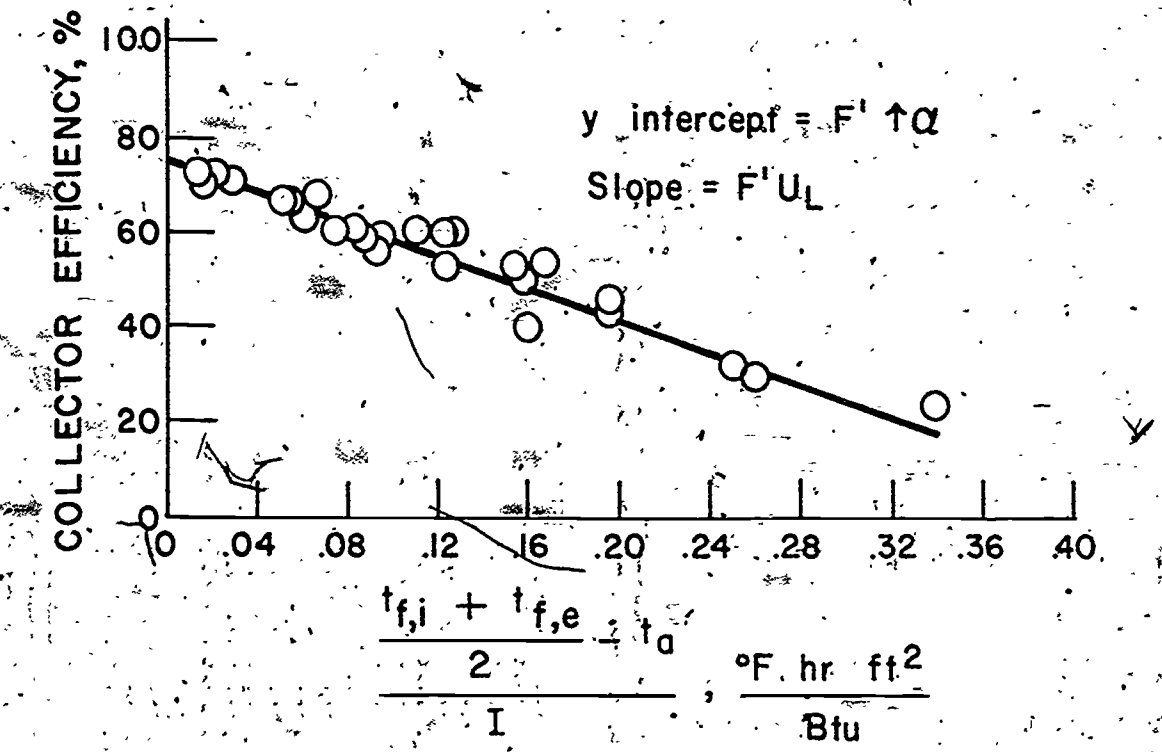


Figure A10 - Efficiency Curve for a Flat-Plate Collector Using Water as the Transfer Fluid (reference [25])

0.3 m by 0.3 m Flat-Plate Collector
single glass cover plate
.15 m styrofoam edge insulation
.15 m styrofoam back insulation
copper tube on copper plate absorber surface, carbon black-silicon dioxide paint

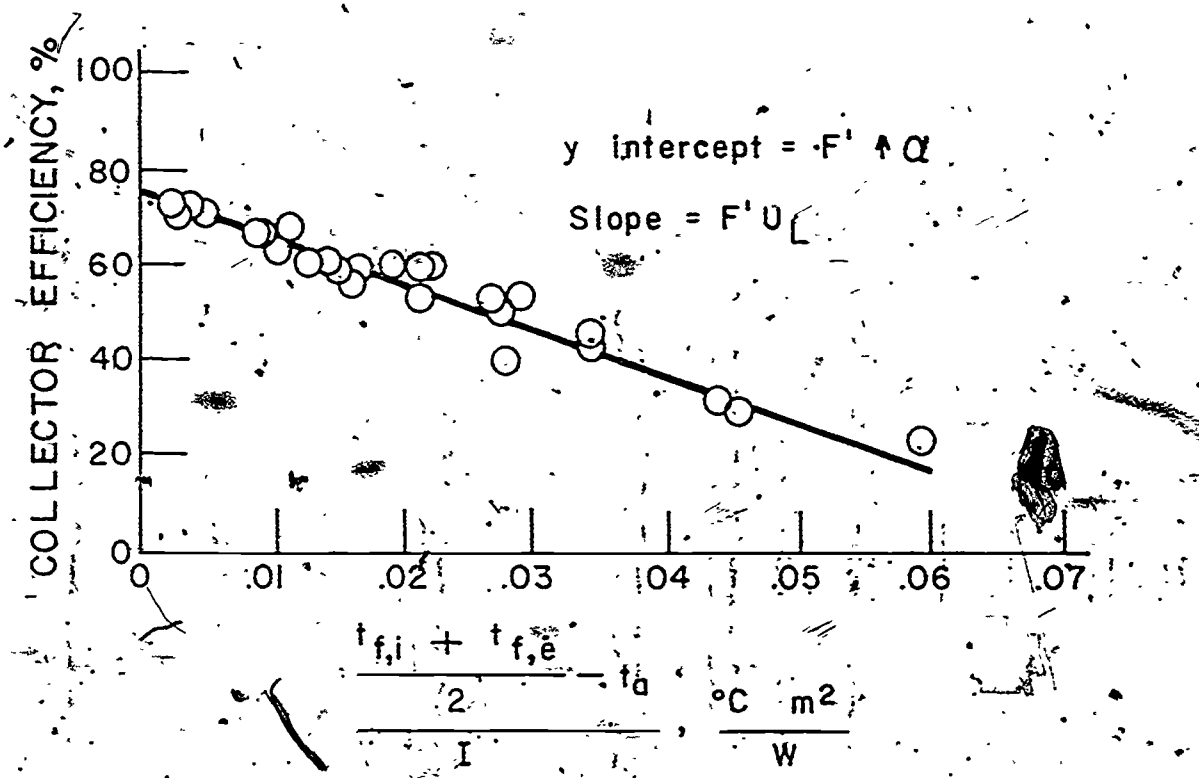


Figure A11 Efficiency Curve for a Flat-Plate Collector Using Water as the Transfer Fluid (reference [25])

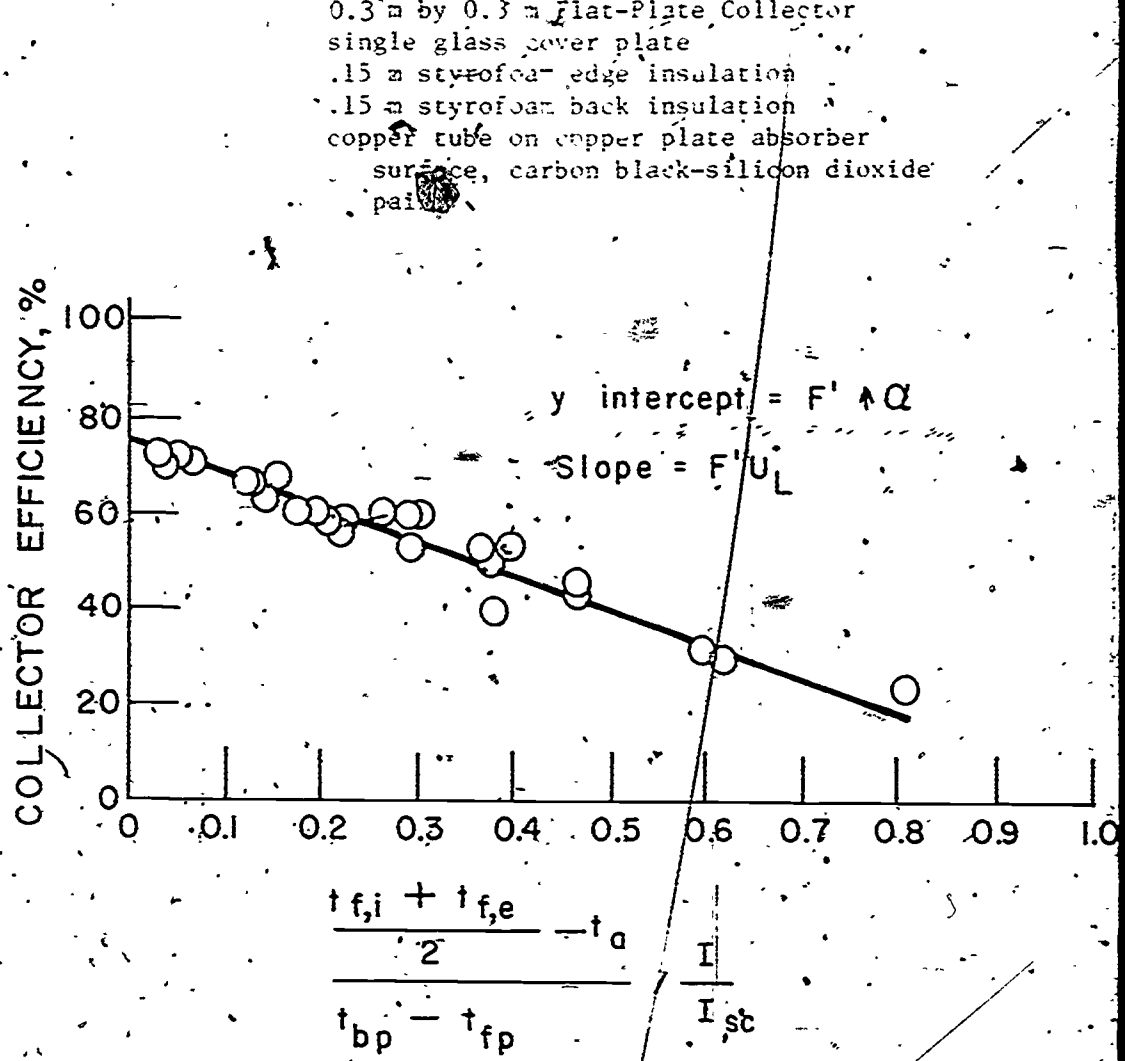


Figure XI2 Efficiency Curve for a Flat-Plate Collector Using Water as the Transfer Fluid (reference [25])

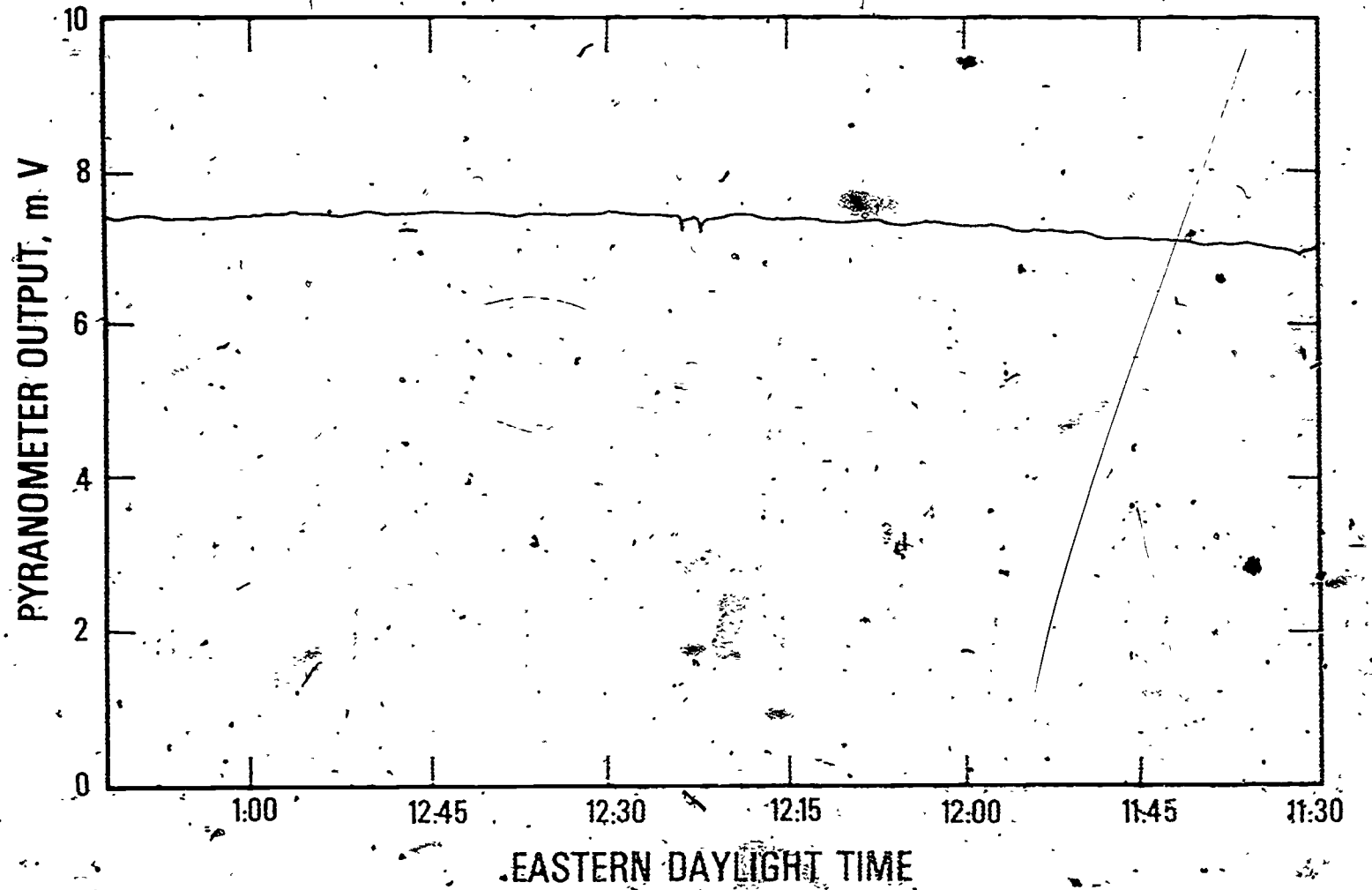


Figure A13 Incident Solar Radiation on a Horizontal Surface at the National Bureau of Standards Site in Gaithersburg, Maryland, March 13, 1974

0.3 m by 0.3 m Flat-Plate Collector
single glass cover plate
.15 m styrofoam edge insulation
.15 m styrofoam back insulation
copper tube on copper plate absorber surface, carbon black-silicon dioxide paint

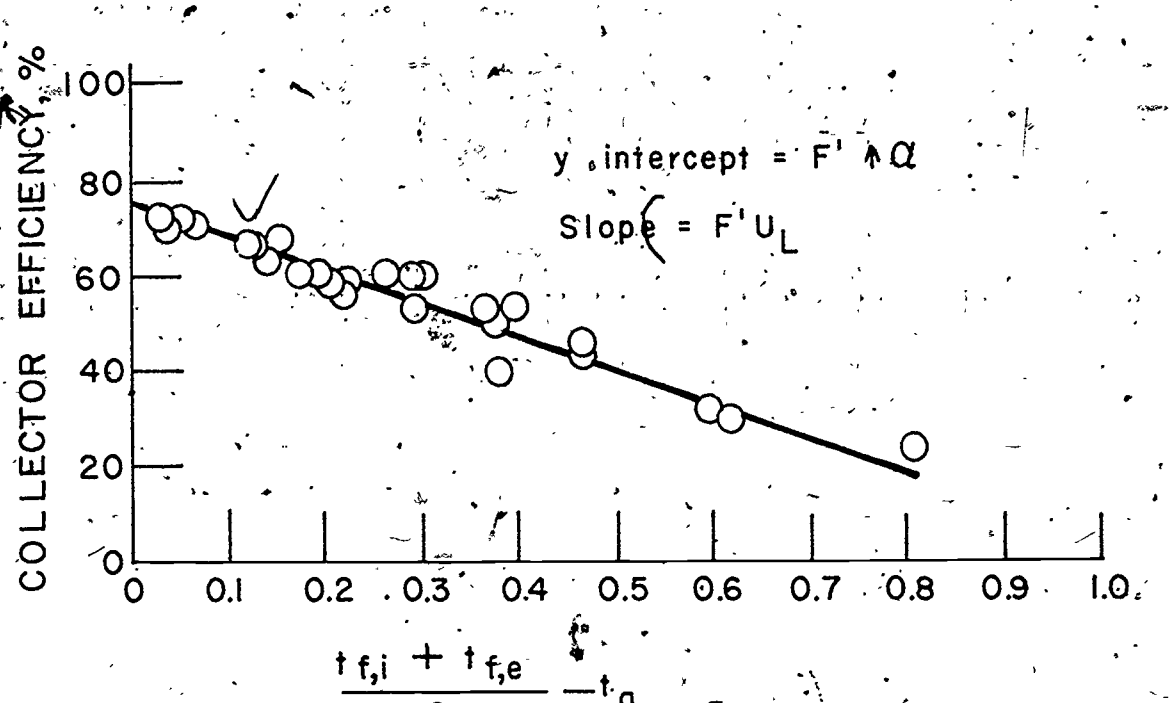


Figure A12 Efficiency Curve for a Flat-Plate Collector Using Water as the Transfer Fluid (reference [25])

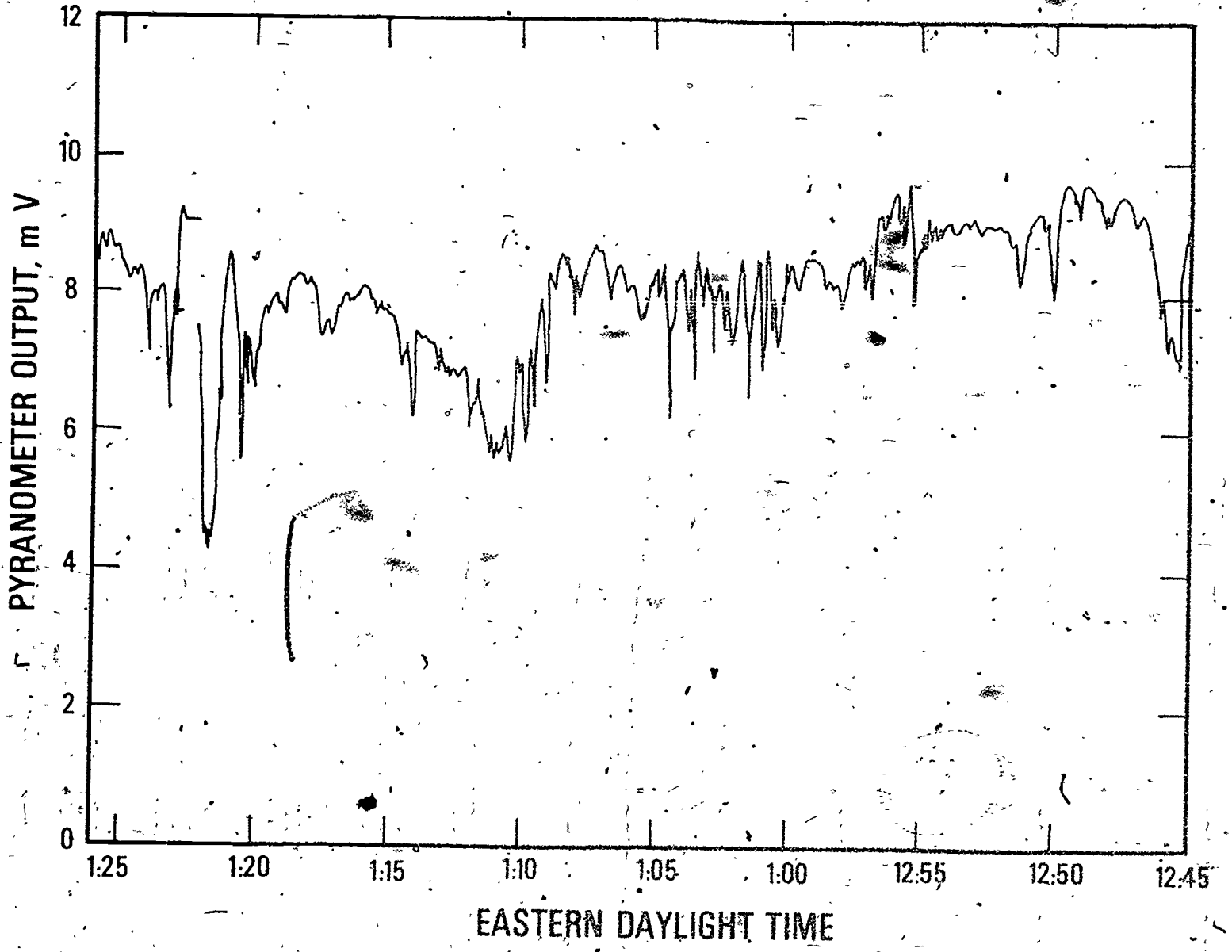


Figure A14. Incident Solar Radiation on a Horizontal Surface at the National Bureau of Standards Site in Gaithersburg, Maryland, March 11, 1974.

## 7. Appendix B

### Method of Testing for Rating Thermal Storage Devices Based on Thermal Performance

### SECTION 1. PURPOSE

1.1 The purpose of this standard is to provide a standard procedure for determining the thermal performance of thermal energy storage devices that are used in systems to provide the thermal requirements for heating, cooling, and the generation of domestic hot water in buildings.

### SECTION 2. SCOPE

2.1 This standard applies to sensible-heat and latent-heat type thermal energy storage systems. In addition, it is limited to those storage devices in which a fluid enters the device through a single inlet and leaves the device through a single outlet. Storage devices having more than one inlet and/or outlet may be tested according to this standard, but each flow configuration involving a single inlet and a single outlet must be tested separately. This standard is not applicable to those configurations in which there is simultaneous flow into the storage device through more than one inlet or simultaneous flow out of the storage device through more than one outlet. The fluid can be either a gas or liquid but not a mixture of the two.

2.2 This standard does not address factors relating to cost or consideration of requirements for interfacing with a specific heating and cooling system. Consequently, the test results do not provide all the information required for a complete evaluation of the thermal energy storage system.

2.3 The test procedure and equipment outlined in this standard are most easily adaptable to thermal energy storage system having capacities on the order of $10^3$ J ($10^6$ Btu) or less.

### SECTION 3. DEFINITIONS

3.1 AMBIENT AIR

Ambient air is the air in the space surrounding the thermal energy storage system.

3.2 CYCLING

Cycling of a latent-heat type storage device is a process in which the temperature of the system is raised and lowered in a cyclic manner and the phase of the storage medium is changed twice in each temperature cycle.

## 3.3 EFFECTIVE CAPACITY FOR HEAT REMOVAL

The effective capacity for heat removal is the amount of heat that can be removed from the storage system during a period of time equal to the fill time and for a specific set of values for $t_i$, the initial temperature of the storage system; $\Delta t$, the temperature difference between $t_i$ and the temperature of the entering fluid; and $\dot{m}$, the mass flow rate of the fluid through the storage system.

## 3.4 EFFECTIVE CAPACITY FOR HEAT STORAGE

The effective capacity for heat storage is the amount of heat that can be stored in the storage system during a period of time equal to the fill time and for a specific set of parameters $t_i$, $\Delta t$ and $\dot{m}$.

## 3.5 FILL TIME

The fill time is the duration of a single transient test as specified in Section 8 in which energy is either added or extracted from the storage system.

## 3.6 RATE OF HEAT LOSS

The heat loss rate is the rate that heat is lost from the storage system per degree temperature difference between the storage medium temperature and the average ambient air temperature.

## 3.7 STORAGE CAPACITY

The storage capacity of a thermal energy storage system is defined as the heat that can be stored in a system undergoing a $\Delta t$ increase in temperature from its initial value $t_i$.

## 3.8 PERFORMANCE COEFFICIENT FOR HEAT REMOVAL

The performance coefficient for heat removal is the ratio of the effective capacity for heat removal to the amount of heat that could be removed from an equal volume of water in an ideal water tank under the same conditions.

3.9 PERFORMANCE COEFFICIENT FOR HEAT STORAGE

The performance coefficient for heat storage is the ratio of the effective capacity for heat storage to the amount of heat that could be stored in an equal volume of water in an ideal water tank under the same conditions.

3.10 STANDARD AIR

Standard air is air weighing 1.2 kg/$m^3$ (0.075 lb/$ft^3$), and is equivalent in density to dry air at a temperature of 21.1°C (70°F) and a barometric pressure of 1.01 X $10^5$ N/$m^2$ (29.92 in. of Hg.).

3.11 STANDARD BAROMETRIC PRESSURE

1.01 X $10^5$ N/$m^2$ (29.92 in. of Hg.).

3.12 STORAGE MEDIUM

The storage medium is the material in the storage system in which the major portion of the energy is stored.

3.13 STORAGE SYSTEM

The storage system is defined as the container(s) plus all contents of the container(s) used for storing thermal energy in a system. The transfer fluid and other accessories such as heat exchangers within the thermal storage container(s) are considered as part of the storage system.

3.14 SPECIFIC HEAT

The specific heat of a substance is the quantity of energy necessary to produce a unit change in temperature of a unit mass.

3.15 TRANSFER FLUID

The transfer fluid is the fluid that carries energy in and out of the storage system.

## SECTION 4. CLASSIFICATIONS

4.1 In this standard thermal energy storage systems are classified according to the method they use to store energy and the type of transfer fluid they employ.

4.1.1 Sensible heat storage systems are those in which the heat absorbed by or removed from the system results in an increase or decrease in the temperature of the storage medium and there is no change of phase of any portion of the storage medium. Typical systems employ pressurized water, unpressurized water, rock, brick or concrete as the storage medium.

Latent-heat storage systems are those involving a change of phase of the storage medium. In this type of system, most of the heat added to or removed from the system goes into changing the enthalpy of the storage medium during a change of phase process. Some heat is also stored as sensible heat, since charging and discharging of the storage device usually involves a finite change in the temperature of the system.

4.1.2 A storage system will use either a liquid or a gas as the transfer fluid. The most common liquids are water or a water-ethylene glycol solution. The most common gas is air.

## SECTION 5. REQUIREMENTS

5.1 This standard covers only those thermal energy storage systems that can be treated as black boxes and that do not alter the phase or composition of the transfer fluid passing through them.

5.2 Latent-heat type storage systems evaluated under this standard shall have been cycled (see definition of cycling) through their change of phase at least 30 times prior to being tested.

5.3 The transfer fluid used in evaluating the performance of a thermal energy storage system shall have a known specific heat that varies by less than +-0.5% over the temperature range encountered during a test.

5.4 The room where the testing of the storage system is performed shall have its temperature controlled to the extent that the average ambient air temperature $t_a$, determined by the average of the four temperatures measured as specified in Section 8.9, varies between extremes by less than $\pm$ 1.0°C ($\pm$ 1.8°F) during a test.

## SECTION 6. INSTRUMENTATION

### 6.1 TEMPERATURE MEASUREMENTS

6.1.1 Temperature measurements shall be made in accordance with ASHRAE Standard 41-66, Part 1 [1].

6.1.2 Temperature Difference Measurements Across the Thermal Storage System: The temperature difference of the transfer fluid across the thermal storage system shall be measured with:

a. Thermopile (air or liquid as the transfer fluid)

b. Calibrated resistance thermometers connected in two arms of a bridge circuit (only when a liquid is the transfer fluid)

6.1.3 The accuracy and precision of the instruments and their associated readout devices shall be within the limits as follows:

| | Instrument Accuracy[a] | Instrument Precision[b] |
|---|---|---|
| Temperature | ± 0.5°C (± 0.9°F) | ± 0.2°C (± 0.4°F) |
| Temperature Difference | ± 0.1°C (± 0.2°F) | ± 0.1°C (± 0.2°F) |

6.1.4 In no case shall the smallest scale division of the instrument or instrument system exceed 2 P/2 times the specified precision. For example, if the specified precision is ± 0.1°C (± 0.2°F), the smallest scale division shall not exceed 0.25°C (0.5°F).

6.1.5 The instruments shall be configured and used in accordance with Section 7. of this standard.

6.1.6 When thermopiles are used, they shall be constructed in accordance with ANSI Standard C96.1-1964 (R 1969) [2].

---

[a] The ability of the instrument to indicate the true value of the measured quantity.

[b] Closeness of agreement among repeated measurements of the same physical quantity.

## 6.2 LIQUID FLOW MEASUREMENTS

6.2.1 The accuracy of the meter including a calibration, if furnished, shall be equal to or better than ± 1.0% of the measured value.

## 6.3 RECORDERS AND INTEGRATORS

6.3.1 Strip chart recorders used shall have an accuracy equal to or better than ± 0.5% of the temperature difference and/or voltage measured for each test with the exception of the heat loss rate test. In the test to determine the heat loss rate, the accuracy of the strip chart recorder shall be equal to or better than ± 2.0%.

6.3.2 Electronic integrators used shall have an accuracy equal to or better than ± 1.0% of the measured value for each test with the exception of the heat loss rate test. In the test to determine the heat loss rate, the accuracy of the electronic integrator shall be equal to or better than ± 4.0%.

## 6.4 AIR FLOW MEASUREMENTS

When air is used as the transfer fluid, air flow rate shall be determined as described in Section 7.

## 6.5 PRESSURE MEASUREMENTS

6.5.1 Nozzle Throat Pressure. The pressure measurement at the nozzle throat shall be made with instruments that shall permit measurements of pressure to within ± 2.0% absolute and whose smallest scale division shall not exceed 2 1/2 times the specified accuracy [3].

6.5.2 Air Flow Measurements. The static pressure across the nozzle and the velocity pressure at the nozzle throat shall be measured with manometers that have been calibrated and are accurate to within ± 1.0% of the reading. The area of the nozzle shall be determined by measuring its diameter to an accuracy of ± 0.20% in four places approximately 45 degrees apart around the nozzle in each of two planes through the nozzle throat, one at the outlet and the other in the straight section near the radius [3].

6.5.3 Pressure Drop Across the Thermal Storage System. The static pressure drop across the thermal storage system shall be measured with a manometer having an accuracy of 2.49 $N/m^2$ (0.01 in. of water).

## 6.6 TIME AND MASS MEASUREMENTS

Time measurements and mass measurements shall be made to an accuracy of ± 0.20% [3].

# SECTION 7. APPARATUS AND METHOD OF TESTING

## 7.1 AIR AS THE TRANSFER FLUID

The relative position of the thermal energy storage system, the temperature measuring instrumentation, the air flow measuring apparatus and the reconditioning apparatus is shown in Figure B1[a].

7.1.1 Test Ducts. The air inlet test duct, between the air flow measuring apparatus and the thermal energy storage system, shall have the same cross-sectional dimensions as the inlet to the storage device. The air outlet test duct, between the thermal energy storage system and the reconditioning apparatus, shall have the same cross-sectional dimensions as the outlet of the storage device.

7.1.2 Temperature Measurement Across the Storage System. A thermopile shall be used to measure the difference between the inlet air temperature and outlet air temperature of the thermal energy storage system. It shall be constructed from calibrated type T thermocouple wire all taken from a single spool of wire. No extension wires are to be used in either its fabrication or installation. The wire diameter must be no larger than 0.51 mm (24 AWG) and the thermopile shall be fabricated as shown in Figure B2. There shall be a minimum of six junctions in the air inlet test duct and six junctions in the air outlet test duct. These junctions shall be located at the center of equal cross-sectional areas.

[a] The recommended apparatus consists of a closed loop configuration. An open loop configuration is an acceptable alternative provided that the test conditions specified herein can be satisfied.

During all tests, the variation in temperature across the air inlet and air outlet test ducts shall be less than ± 0.5°C (± 0.9°F) at the location of the thermopile junctions. The variation shall be checked prior to testing utilizing instrumentation and procedures outlined in reference [1]. If the variation exceeds the limits above, mixing devices shall be installed to achieve this degree of temperature uniformity. Reference [4] discusses the positioning and performance of several types of air mixers.

The measuring junctions of the thermopile should be located as near as possible to the inlet and outlet of the thermal energy storage system. The air inlet and air outlet ducts shall be insulated in such a manner that the calculated heat loss from these ducts to the ambient air would not result in a temperature change for any test of more than 0.05°C (0.09°F) between the temperature measuring locations and the storage system.

7.1.3 Dry and Wet Bulb Temperature Measurements. Thermocouples or other devices giving a continuous reading shall be used to measure the wet and dry bulb temperature at the locations in the air inlet and air outlet ducts shown in Figure B1. ASHRAE Standard 41-66, Part I [1] shall be followed in making these measurements.

7.1.4 Duct Pressure Measurements. The static pressure drop across the thermal energy storage system shall be measured using a manometer as shown in Figures B1 and B3. Each side of the manometer shall be connected to four pressure taps that are connected to an external manifold on the air inlet and air outlet ducts. The pressure taps should consist of 6.4 mm (1/4 in.) nipples soldered to the duct and centered over 1 mm (0.040 in.) diameter holes. The edges of these holes on the inside surfaces of the ducts should be free of burrs and other surface irregularities [5].

7.1.5 Air Flow Measuring Apparatus. The air flow shall be measured with the nozzle apparatus discussed in Section 7 of ASHRAE Standard 37-69 [3]. As shown in Figure B4, this apparatus consists basically of a receiving chamber, a discharge chamber and an air flow measuring nozzle. The distance from the center of the nozzle to the side walls shall not be less than 1 1/2 times the nozzle throat diameter, and diffusers shall be installed in the receiving chamber at least 1 1/2 nozzle throat diameters upstream of the nozzle and 2 1/2 nozzle throat diameters downstream of the nozzle. The apparatus should be designed so that the nozzle can be easily changed and the nozzle used on each test shall be selected so that the throat velocity is between 15 m/s (2960 fpm) and 35 m/s (6900 fpm). Details on nozzle construction and discharge coefficients that may be used are contained in Section 7.3 of ASHRAE Standard 37-69 [3].

An exhaust fan capable of providing the desired flow rates through the thermal energy storage system shall be installed in the end wall of the discharge chamber. The dry and wet bulb temperature of the air entering the nozzle shall be measured in accordance with ASHRAE Standard 41-66, Part I [1]. The velocity of the air passing through the nozzle shall be determined by either measuring the velocity head by means of a commercially available pitot tube or by measuring the static pressure drop across the nozzle with a manometer. If the latter method is used, one end of the manometer shall be connected to a static pressure tap located flush with the inner wall of the receiving chamber and the other end to a static pressure tap located flush with the inner wall of the discharge chamber, or preferably, several taps in each chamber should be connected through a manifold to a single manometer. A means shall also be provided for measuring the absolute pressure of the air in the nozzle throat.

7.1.6 Air Leakage. Air leakage through the air flow measuring apparatus, air inlet test duct, the thermal energy storage system and the air outlet test duct shall not exceed ± 1.0% of the measured air flow.

7.1.7 Air Reconditioning Apparatus. The reconditioning apparatus shall control the dry bulb temperature of the air entering the storage system to within ± 1.0°C (± 1.8°F) of the desired test values at all times during the tests. Its heating and cooling capacity shall be selected so that dry bulb temperature of the air entering the reconditioning apparatus may be raised or lowered by an amount equal to the largest required in Section 8.

## 7.2 LIQUID AS THE TRANSFER FLUID

The test setup for thermal energy storage systems employing liquid as a transfer fluid is shown in Figure B5[a].

7.2.1 Temperature Measurement Across the Storage System. The temperature difference between the transfer fluid entering and leaving the storage system shall be measured using either two calibrated resistance thermometers connected in two arms of a bridge or a thermopile made from calibrated, type T thermocouple wire all taken from a single spool of wire. The thermopile shall contain any even number of junctions constructed according to the recommendations in ANSI Standard C96.1-1964 (R 1969) [2].

[a] The recommended apparatus consists of a closed loop configuration. An open loop configuration is an acceptable alternative provided that the test conditions specified herein can be satisfied.

Each resistance thermometer or each end of the thermopile is to be inserted into a well [6] located as shown in Figure B5. To insure good thermal contact, the wells shall be filled with light oil. The wells should be located just downstream of a right angle bend to insure proper mixing [1].

To minimize temperature measurement error, the wells should be located as close as possible to the inlet or outlet of the storage device. In addition, the piping shall be insulated in such a manner that the calculated heat loss from this piping to the ambient air would not cause a temperature change for any test of more than 0.05°C (0.09°F) between each well and the storage system.

7.2.2 Additional Temperature Measurements. The temperature of the transfer fluid at the two locations cited above shall also be measured by inserting appropriate sensors into the wells. ASHRAE Standard 41-66, Part I [1] shall be followed in making these measurements.

7.2.3 Pressure Drop Across the Storage System. The pressure drop across the thermal energy storage system shall be measured using static pressure tap holes and a manometer. The edges of the holes on the inside surfaces of the pipe should be free of burrs and should be as small as practicable but not exceeding 1.6 mm (1/16 in.) diameter [5]. The thickness of the pipe wall should be 2 1/2 times the hole diameter [5].

7.2.4 Liquid Transfer Fluid Reconditioning Apparatus. The reconditioning apparatus shall control the temperature of the transfer fluid entering the storage system to within ± 1.0°C (± 1.8°F) of the desired test values at all times during the tests. Its heating and cooling capacity shall be selected so that the temperature of the liquid entering the reconditioning apparatus may be raised or lowered by an amount equal to the largest required in Section 8.

7.2.5 Additional Equipment. A pressure gauge, a pump and a means of adjusting the flow rate of the transfer fluid shall be provided at the relative locations shown in Figure B5. In addition, a pressure relief valve and an expansion tank should be installed to allow the transfer fluid to expand and contract freely in the apparatus[a].

---

[a] Figure B5 should not be interpreted to mean that the relief valve and expansion tank necessarily be located below the thermal energy storage unit.

## SECTION 8. TEST PROCEDURE AND CALCULATIONS

### 8.1 GENERAL

The method that has been most commonly employed in testing of water storage tanks in Japan [11, 12, 13] is to cause the transfer fluid entering the storage device to undergo a step change in temperature and to measure the temperature of the transfer fluid leaving the storage unit. By integrating the difference in temperature between the inlet and outlet over the testing period and multiplying the result by the transfer fluids' mass flow rate and specific heat, one can determine the amount of heat added or removed during this time period[a]. This energy balance is shown conceptually in Figure B6 where the area under the curve represents the energy absorbed during the time period shown. If the time period chosen for the test were some characteristic time depending upon the size of the storage device chosen, the heat storage capability of different devices could be compared. This will be illustrated by citing typical results taken from reference [14].

Yang and Lee [14] performed an analysis to determine the nature of the transient heat transfer between a heat storage unit and a circulating or transfer fluid due to variations in the inlet temperature of the transfer fluid. The configurations chosen for analysis are shown in Figures B7, B8, and B9. Figure B7 shows a specific-heat type storage device in which a liquid storage medium is heated or cooled by a fluid passing through thin tubes inside the container. Figure B8 shows a pebble-bed type unit in which the transfer fluid comes in direct contact with the storage medium. Figure B9 shows as in Figure B7, a heat-exchanger type storage device except in this case, the transfer fluid is circulated around tubes which encapsulate a latent-heat type material such as a salt hydrate.

The basic one-dimensional transient equations governing the temperature distribution of both the transfer fluid and storage medium are presented and solved using the Laplace transformation technique. Yang and Lee point out that the boundary conditions most appropriate to simulate a real storage device would be some arbitrary variation of inlet fluid temperature with time.

---

[a] This is strictly true only if the losses from the outside of the storage unit are negligible. Otherwise, the losses must be accounted for in the energy balance.

However, since it is impractical to calculate the system response for every possible inlet variation and since the storage system is described by linear equations, its dynamic characteristics may be conveniently investigated by using a step input or a sinusoidal input. Solutions are given in [14] for both the step input and sinusoidal input for the configurations of Figures B7 and B8 but only for the step input for the latent-heat type device.

Typical results are shown in Figures B10 and B11 for a water tank in which water is also circulated through the heat exchanger as the transfer fluid and the input is a step function. Figure B10 shows the temperature distribution of the transfer fluid as a function of position down the tube and time. Figure B11 shows the same thing for the storage medium or water in the tank. These results were for the case of negligible resistance to heat transfer at the interface between the tubes and the storage medium. One should note that it has been possible to present the results in dimensionless form. The temperature difference between the fluid and the initial value is divided by the difference between the inlet value and the initial value (step function) to get $t^*$. The space dimension is divided by the total path length through the storage device to get $x^*$ and time has been made dimensionless by dividing it by the time required for a fluid particle to travel through the system of length $\ell$, $\ell/u$, where $u$ is the flow velocity. The process of normalizing the results has been possible due to the fact that the system behavior is described by linear equations. In reality, the response of storage devices will only approximate a linear behavior. Consequently the testing procedure included herein has been written in such a way as to determine the response of the system to different step inputs and for both heat storage and heat removal processes even though the results of the linear theory would indicate this is unnecessary.

To demonstrate how different storage devices can be compared based on their response to a step function input, the results of reference [14] have been used to plot the curves in Figure B12. The curves are plots of dimensionless temperature difference

between the inlet and outlet of a storage tank configured as in Figure B7. Both curves are for the same flow rate of water (transfer fluid) through the storage device. The only difference between the two is that on one hand there is a finite resistance to heat transfer on the outside of the pipes ($h_o$ = 56.7 W/($m^2$ · $^oK$) typical of natural convection in the tank and on the other, there is negligible resistance ($h_o = \infty$). The area under the curve is proportional to the amount of energy transferred into or away from the storage unit. As can be seen, the device with the smallest resistance to heat transfer is clearly the more effective one for absorbing or releasing the energy.

Up until this point, emphasis has been placed on discussing the comparison of storage devices based on their response to a step increase in inlet fluid temperature. Other possibilities exist.

A second method that could be employed would be to subject the transfer fluid entering the storage unit to a constant influx of heat, Q. This would result in raising the temperature of the entering transfer fluid (assuming the specific heat of the transfer fluid is constant) by a fixed number of degrees above the outlet temperature. By measuring the time dependent outlet temperature one could obtain information that would be useful in designing collector-storage systems. While this method simulates more closely the real interaction between a collector and a storage device, it has the disadvantage that one cannot measure the energy storage and removal capability of the unit. This is due to the fact that if one measured the heat absorbed by the storage unit over a period of time, it would just be equal to Q x the test period or the amount of energy added to the system. Thus the only way of comparing different storage devices would be to compare plots of outlet temperature versus time for different values of Q choosen so as to take into account the different sizes of the storage units being compared. The storage device with the lowest average outlet temperature would probably be considered best because this would tend to maximize the efficiency of a collector.

A third method would be to use a time varying $\dot{Q}$ and to measure the outlet temperature as a function of time during the testing period. This would allow one to simulate the output of a collector over one or more days and to determine the response of the storage device. If the time dependence of $\dot{Q}$ resulted in an oscillating inlet temperature, one would also be able to look at the degree of stratification attained in the storage unit. This method has the same disadvantage as the second method in that it would be very difficult to compare the performance of different storage devices. In addition, one has the problem of deciding on what is the typical cycle for $\dot{Q}$; not an easy task when one considers that the output of the collector depends not only on the weather but on the particular storage unit employed. The major advantage of this method would be that by inserting an array of thermocouples in the storage medium, the experimenter could measure the temperature stratification in the unit.

Stratification, which in water tanks results from different temperature water seeking its own density level, is a desirable characteristic for operation in a solar heating and cooling system when the inlet fluid temperature varies up and down with time. If large stratification results when the inlet temperature is either constant or a monotonic (increasing or decreasing) function of time, it is probably a result of short circuiting flow (i.e. dead space in a water tank). This short circuiting of the flow could result in higher fluid temperatures to the collector and thus decreased efficiency, which could easily off-set the advantages of stratification.

To test the transient response of the storage unit, the first method of measuring the response of outlet temperature to a step change in inlet temperature, was chosen as a basis for the test. This method was selected because:

a) it permits the determination of effective storage capacity and thus allows an easy comparison of different types of storage units,

b) it appears to be the most fundamental approach since linear theory shows that the outlet temperature response to a constant or variable heat flux $\dot{Q}$ can be predicted if one knows how the outlet temperature changes with a step change in inlet temperature, and

c) it is felt that the relative performance of storage devices using this method will be the same if either of the other procedures were used.

## 8.2 STORAGE CAPACITY, FILL TIME, EFFECTIVE CAPACITY FOR HEAT STORAGE, EFFECTIVE CAPACITY FOR HEAT REMOVAL

The storage capacity SC $(t_i, \Delta t)$ of a thermal energy storage system is defined as the energy that can be stored in a system undergoing a $\Delta t$ increase in temperature from its initial value $t_i$. The value SC $(t_i, \Delta t)$ shall be calculated by adding up the amount of heat absorbed by the individual components in the storage system (storage medium, tank, heat exchanger, insulation, etc.) in raising their temperature from $t_i$ to $(t_i + \Delta t)$. If there is an uncertainty in the heat storage ability of the storage medium, a representative sample shall be tested in a calorimeter to determine the amount of heat required to raise its temperature from $t_i$ to $(t_i + \Delta t)$.

The concept of fill time as introduced in this test procedure is used for the purpose of specifying the time of the transient tests. Recall that in the analysis of Yang and Lee [14], it was possible to present the response characteristics of the thermal storage unit in terms of a dimensionless time where real time is divided by some characteristic time $\ell/u$, the effective path length of the transfer fluid divided by the effective transfer fluid velocity. This allows a convenient way of comparing storage units of the same basic design but of different sizes. However, if one is going to compare, for example, a water storage tank where the transfer fluid and the storage medium are the same with a storage tank and embedded heat exchanger where the volume of water in the heat exchanger (transfer fluid) at any instant is only 1/10 of the volume of the water in the storage tank (storage medium), then comparing the response of the two over the same time period $\ell/u$ would be unfair. The device with the embedded heat exchanger would appear to have something on the order of 10% of the storage capacity of the other device when compared over the same number of time periods $\ell/u$. Consequently, a different time scale is introduced herein that will allow storage units of entirely different designs to be compared on an equitable basis.

If a storage unit has a specified thermal capacity or storage capacity SC $(t_i, \Delta t)$, and the transfer fluid of specific heat $c_{tf}(t_i)$ is flowing through the device at a constant flow rate $\dot{m}$ and has an inlet temperature $\Delta t$, above the initial temperature of the storage device, then the fill time is defined by

$$\tau_F = \frac{SC(t_i, \Delta t)}{\dot{m}\, c_{tf}(t_i)\, \Delta t} \qquad (1)$$

In the testing procedure, all storage units are tested for the same fill time and then the thermal responses compared.

In other words, if two different sensible-heat devices had the same ultimate storage capacity and were being tested over the same $\Delta t$ but one used water (water tank) and the other air (pebble-bed type) as the transfer fluid, and the flow rates were such that the fluid dwell times (determined by $\ell/u$) were identical, it would be unfair to compare the response of the two units over the same real time period. One would be able to charge the water tank with considerably more energy over the same time period (approximately by the ratio of $((\dot{m}\, c_{tf})_{water})/((\dot{m}\, c_{tf})_{air}$). The recommendation here would be to test the two units for the same fill time as defined by equation (1). Consequently, the flow rates would be adjusted so that $((\dot{m}\, c_{tf})_{water})/((\dot{m}\, c_{tf})_{air}) = 1$. In other words, the flow rates for the different devices are adjusted so that the amount of energy entering the device (or leaving for an energy removal test) per unit thermal storage capacity is identical for the two devices.[a]

The fill time $\tau_F$ and the flow rate of the transfer fluid $\dot{m}$ are related in an inverse manner according to equation (1). One possibility for specifying the test conditions of the transient tests would be to specify the $\Delta t$ to be used, allow the experimenter to select an $\dot{m}$, and then, depending upon the properties of the transfer fluid ($c_{tf}$) and storage capacity of the unit, conduct the tests for some fraction or integral of the fill time. However, the experimenter who was concerned about the optimum performance of his unit would no doubt select a flow rate where the relationship between the energy transfer rate and pressure drop (or power required to push the fluid through the device) was an optimum. In actual installations, the flow rate through and $\Delta t$ across the storage device is controlled by the flow rate through and $\Delta t$ across the collector and/or building heating and cooling system. The flow rate is usually proportional to the collector size and in turn the storage capacity is usually proportional to the collector size. Consequently, the ratio of $SC/\dot{m}$ is constant within certain limits which means according to equation (1), the fill time is constant within certain limits. As a result, in the test procedure, two different fill times are specified that are felt to be typical of installed systems, the $\Delta t$'s are specified according to whether a liquid or air is the transfer fluid[b], and the flow rate to be used is

---

[a] One should recognize that for an ideal water-tank where there is entirely piston-type flow, the above definition of fill time is identical with the fluid dwell time.

[b] Air heating collectors impose a much higher $\Delta t$ on the storage device than do liquid heating collectors.

calculated according to equation (1).

The effective capacity for heat storage $EC_{hs}$ $(t_i, \Delta t, \tau_F)$ is defined as the net amount of heat flowing into a storage system during the time period $(\tau_o, \tau_o + \tau_F)$ when the entering transfer fluid, that is initially at temperature $t_i$, undergoes at $\Delta t$ step increase in temperature at time $\tau_o$. It may be calculated using the equation:

$$EC_{hs}\ (t_i, \Delta t, \tau_F) = \dot{m}\ c_{tf}\ (t_i) \int_{\tau_o}^{\tau_o + \tau_F} \delta t\ (\tau)\ d\tau$$

$$= L\ \tau_F\ [t_i + \frac{\Delta t}{2} - t_a] \qquad (2)$$

where $\delta t\ (\tau) = [t_{in}\ (\tau) - t_{out}\ (\tau)]$ is the difference between the inlet temperature $t_{in}$ and the outlet temperature $t_{out}$ at time $\tau$, $t_a$ is the average ambient air temperature, and $\dot{m}$ has the value specified in Section 8.6.

The effective capacity for heat removal $EC_{hr}$ $(t_i + \Delta t, -\Delta t, \tau_F)$ is defined as the net amount of heat removed from a storage system during the time period $(\tau'_o, \tau'_o + \tau_F)$ when the entering transfer fluid, which is initially at temperature $(t_i + \Delta t)$, undergoes a $\Delta t$ step decrease in temperature at time $\tau'_o$. It may be determined using the formula:

$$EC_{hr}\ (t_i + \Delta t, -\Delta t, \tau_F) = \dot{m}\ c_{tf}\ (t_i) \int_{\tau'_o}^{\tau'_o + \tau_F} |\delta t\ (\tau)|\ d\tau \qquad (3)$$

## 8.3 GENERAL TEST REQUIREMENTS

All of the tests require that the temperature of the storage medium, prior to the start of data taking, be uniform at the desired temperature and that there exist steady flow of the transfer fluid through the storage system during a test. To achieve the former, the transfer fluid shall be circulated through the testing apparatus until steady state conditions are achieved and the inlet and outlet temperatures vary by less than $\pm$ 0.5°C ($\pm$ 0.9°F) during a one hour period. The initial temperature is then defined to be the arithmetic average of the inlet and outlet temperatures. Steady flow of the transfer fluid shall be considered achieved if the flow rate varies by less than $\pm$ 1.0% during a test.

For all tests, with the exception of the one to determine the heat loss rate, the temperature of the storage medium shall remain within the normal operating range of the storage medium. For latent heat type storage systems this means that the storage medium shall undergo a change of phase as the temperature of the storage medium is both increased and decreased by $\Delta t$ in the manner discussed in Section 8.1.

During tests involving air as the transfer fluid, the dry bulb temperature of the transfer fluid shall remain above the dew point temperature of the transfer fluid, and the inlet dew point temperature shall equal the outlet dew point temperature and both shall remain constant. The latter shall be considered accomplished if the inlet and outlet dew point temperatures vary be less than $\pm$ 0.5 °C ($\pm$ 0.9 °F) during a test.

## 8.4 TESTS TO BE PERFORMED

The first test to be performed on a thermal energy storage system is the determination of the heat loss rate, L. The test method for doing this is discussed in Section 8.5. After this is completed, additional tests are required to evaluate $EC_{hs}$ $(t_i, \Delta t, \tau_F)$ and $EC_{hr}$ $(t_i + \Delta t, -\Delta t, \tau_F)$ for a specific $t_i$ and a given pair of parameters $\tau_F$ and $\Delta t$. The set of parameters $\tau_F$ and $\Delta t$ are to be chosen depending on the type of thermal energy storage system, so that all of the following combinations of the variables $\tau_F$ and $\Delta t$ are tested:

$\tau_F$ = 2 hr, 4 hr and $\Delta t$ = 16°C (28.8°F), 8°C (14.4°F) for thermal energy storage systems using a liquid transfer fluid,

$\tau_F$ = 2 hr, 4 hr and $\Delta t$ = 50°C (90°F), 28°C (50.4°F) for thermal energy storage systems using air as the transfer fluid.

When a phase-change type thermal storage system is being tested that has been designed to be "charged" or "discharged" over a specific time period, this time period shall be used as the fill time for testing in lieu of the above specification.

The value of $t_i$ to be used shall be chosen based on the intended application for the thermal energy storage system. The performance of these tests is discussed in Section 8.6.

## 8.5 METHOD FOR DETERMINING THE HEAT LOSS RATE

The flow rate of the transfer fluid shall be adjusted to the value (see equation (1)):

$$\dot{m} = \frac{SC\ (t_a, 25^\circ C)}{(c_{tf}\ (t_a + 25^\circ C))\ (1\ hr)\ (25^\circ C)} \qquad (4)$$

and the temperature of the transfer fluid entering the storage system shall be raised 25°C (45°F) above the average ambient air temperature $t_a$. After the storage system has reached a uniform, steady-state temperature, the average value of $\delta t$ shall be determined over a one hour period. This average, that will be called $\overline{\delta t}$, is to be obtained by integrating $\delta t$ over this time period and then dividing by the time period. The rate of heat loss L from the storage system shall then be determined from

$$L = \frac{\dot{m}\ c_{tf}\ (t_a + 25^\circ C)\ \overline{\delta t}}{25^\circ C} \qquad (5)$$

## 8.6 PERFORMANCE OF A TEST INVOLVING A $\Delta t$ STEP CHANGE IN TEMPERATURE AND A $\tau_F$ FILL TIME

The test described in this section is to be performed on both sensible and latent heat-type storage systems. However, because the performance of a latent heat-type storage system is usually affected by its immediate past temperature history, the test herein described shall be performed twice on this kind of storage system. After the test has been completed once, the storage system shall be allowed to reach a uniform temperature and the test is then to be repeated. Only data collected on this second test shall be reduced and reported as discussed in this section and in Section 9.

After the storage medium has reached a uniform initial temperature $t_i$, the flow rate shall be adjusted to the value:

$$\dot{m} = \frac{SC\ (t_i, \Delta t)}{c_{tf}\ (t_i)\ \Delta t\ \tau_F} \qquad (6)$$

The temperature of the transfer fluid entering the storage system shall be increased in a step-like manner to the new value $t_i + \Delta t$ at some time $\tau_o$. During the time period $(\tau_o, \tau_F)$, the difference between the temperature of the transfer fluid entering and leaving the storage system, $\delta t\ (\tau) = [t_{in}\ (\tau) - t_{out}\ (\tau)]$, shall either be recorded on a strip chart recorder or integrated over time using an electronic integrator. If a strip chart recorder is used, $\delta t\ (\tau)$ shall be manually integrated over time after the test is completed. The integrated value

$$\int_{\tau_o}^{\tau_o + \tau_F} \delta t\ (\tau)\, d\tau$$

plus a knowledge of $\dot{m}$ and $c_{tf}\ (t_i)$ will allow determination of the effective storage capacity $EC_{hs}\ (t_i, \Delta t, \tau_F)$ by means of equation (2).

The last phase of the test involves a step-like decrease in the temperature of the transfer fluid entering the reconditioning apparatus. The temperature of the entering transfer fluid shall be maintained at $t_i + \Delta t$ until the temperature of the transfer fluid leaving the storage system is no longer changing with time. Following this, the temperature of the entering transfer fluid shall be reduced from $(t_i + \Delta t)$ to $t_i$. Assuming this step-change takes place at $\tau_o'$, the quantity

$$\int_{\tau_o'}^{\tau_o' + \tau_F} \delta t\ (\tau)\, d\tau$$

is to be evaluated over the time period $(\tau_o', \tau_o' + \tau_F)$ either by direct electronic integration or by recording $\delta t\ (\tau)$ on a strip chart recorder and then manually integrating. Equation (3) is then to be used to find the effective heat removal capacity $EC_{hr}$ $(t_i + \Delta t, -\Delta t, \tau_F)$.

## 8.7 AN INDEPENDENT CHECK ON THE INTEGRAL OF $\delta t$

As an independent check, the inlet temperature, $t_{in}$, and the outlet temperature, $t_{out}$, of the transfer fluid shall be recorded on strip chart recorders. The quantities

$$\int_{\tau_o}^{\tau_o + \tau_F} \delta t\ (-)\, d\tau \quad \text{and} \quad \int_{\tau_o'}^{\tau_o' + \tau_F'} \delta t\ (-)\, d\tau \text{ shall be calculated using these}$$

recordings and compared with the identical quantities that are obtained by using the primary method which measures $\delta t\ (\tau) = [t_{in}\ (\tau) - t_{out}\ (\tau)]$ directly. In order for a test to be valid, the values obtained on the check must be within $\pm$ 10% of the results obtained using the primary method.

## 8.8 AIR FLOW RATE CALCULATIONS

The air flow rate through the nozzle is calculated by the following equations:

$$Q_{mi} = 1.41\ C\ A_n\ (P_v\ v'_n)^{0.5} \qquad (7a)$$

$$v'_n = 10.1 \times 10^4\ v_n / P_n\ (1 + W_n) \qquad (7b)$$

The air flow rate of standard air is then:

$$Q_s = Q_{mi} / (1.2\ v'_n) \qquad (7c)$$

## 8.9 MEASUREMENT OF AMBIENT AIR TEMPERATURE

The ambient air temperature $t_a$ shall be the arithmetic average temperature of the test area, determined by four calibrated, temperature sensors. ASHRAE Standard 41-66, Part I [1] shall be followed in making these measurements. The sensors shall lie in a horizontal plane approximately at the vertical midpoint of the storage system and shall be approximately 0.6 m (23.6 in.) from the sides of the storage system.

## 8.10 ESTIMATION OF POWER REQUIREMENTS

In order to estimate the power required to move the transfer fluid through the thermal energy storage system, the following equation shall be used:

$$P = \dot{m}\,\Delta P / \rho \qquad (8)$$

# SECTION 9. DATA TO BE RECORDED AND TEST REPORT

## 9.1 TEST DATA

Table B1 lists the measurements that are to be made during the various tests.

## 9.2 TEST REPORT

Table B2 specifies the data to be reported in testing a thermal energy storage system. The performance coefficient for heat storage, $PC_{hs}$, is defined in Table B2 by the formula:

$$PC_{hs} = \frac{EC_{hs}(t_i, \Delta t, \tau_F)/V}{\Delta t\, c_{H_2O}\, \rho_{H_2O}} \qquad (9)$$

where $c_{H_2O}$ and $\rho_{H_2O}$ are the specific heat and density, respectively, of water at the temperature $t_i + \Delta t/2$. The performance coefficient for heat removal is similarly defined by:

$$PC_{hr} = \frac{EC_{hr}(t_i + \Delta t, -\Delta t, \tau_F)/V}{\Delta t\, c_{H_2O}\, \rho_{H_2O}} \qquad (10)$$

The performance coefficients for heat storage and heat removal, as defined above, compare the performance of a thermal energy storage system with the theoretical performance of an ideal water tank of equal volume and having perfect piston-type flow and zero heat loss.

Both $PC_{hs}$ and $PC_{hr}$ are to be calculated for each of the eight tests that determine the effective heat storage and removal capacities for a specific $t_i$. In addition, a single plot is to be provided showing the time variation in outlet temperature of the transfer fluid for these eight tests. The quantity

$$\frac{t_{out}(\tau) - t_i}{\Delta t}$$

shall be plotted as the ordinate, while the abscissa shall show the time periods $(\tau_o, \tau_o + \tau_F)$ and $(\tau'_o, \tau'_o + \tau_F)$.

## SECTION 10. NOMENCLATURE

| | |
|---|---|
| $A_n$ | area of nozzle, $m^2$ |
| C | nozzle coefficient of discharge |
| $c_{H_2O}$ | specific heat of water, J/(kg · °C) |
| $c_{tf}(t_i)$ | specific heat of transfer fluid at $t_i$, J/(kg · °C) |
| D | nozzle throat diameter, m |
| $EC_{hs}(t_i, \Delta t, \tau_F)$ | effective capacity for heat storage, J |
| $EC_{hr}(t_i + \Delta t, -\Delta t, \tau_F)$ | effective capacity for heat removal, J |
| $SC(t_i, \Delta t)$ | storage capacity, J |
| L | heat loss rate, W/°C |
| $\dot{m}$ | mass flow rate of transfer medium, kg/s |
| $PC_{hr}$ | performance coefficient for heat removal |
| $PC_{hs}$ | performance coefficient for heat storage |
| $P_n$ | absolute pressure at nozzle throat, $N/m^2$ |
| P | estimated power required to move the transfer fluid through the thermal energy storage system, W |
| $P_v$ | velocity pressure or static pressure difference across nozzle, $N/m^2$ |
| $Q_{mi}$ | measured air flow, $m^3/s$ |

| | |
|---|---|
| $Q_s$ | standard air flow, $m^3/s$ |
| $t_i$ | initial temperature of storage system, °C |
| $t_{in}$ | temperature of transfer fluid at inlet, °C |
| $t_a$ | average ambient air temperature, °C |
| $t_{out}$ | temperature of transfer fluid at outlet, °C |
| $v_n$ | specific volume of air at dry and wet-bulb temperature conditions existing at the nozzle but at standard barometric pressure, $m^3$/kg dry air |
| $v_n'$ | specific volume of air at the nozzle, $m^3$/kg dry air |
| V | volume of the storage system, $m^3$ |
| W | total mass of storage system, kg |
| $W_n$ | humidity ratio at nozzle, kg $H_2O$/kg dry air |
| $\Delta P$ | pressure drop across storage system, $N/m^2$ |
| $\Delta t$ | step change in temperature, °C |
| $\delta t\ (\tau)$ | inlet temperature, $t_{in}$, minus outlet temperature, $t_{out}$, °C |
| $\overline{\delta t}$ | average of $\delta t\ (t)$ during test for L, °C |
| $\rho$ | density of the transfer fluid, $kg/m^3$ |
| $\rho_{H_2O}$ | density of water, $kg/m^3$ |
| $\tau$ | time |
| $\tau_F$ | fill time, s |
| $\tau_o$ | initial time |
| $\tau_o'$ | time at which temperature of transfer fluid is decreased from $t_i + \Delta t$ to $t_i$ |

## SECTION 11. REFERENCES


1. "Standard Measurements Guide: Section on Temperature Measurements", ASHRAE Standard 41-66, Part 1, American Society of Heating, Refrigerating and Air-Conditioning Engineers, Inc., 345 East 47th Street, New York, N.Y. 10017, January, 1966.

2. "American Standard for Temperature Measurement Thermocouples C96.1-1964" (R 1969), American National Standards Institute, 1969.

3. "Methods of Testing for Rating Unitary Air Conditioning and Heat Pump Equipment", ASHRAE Standard 37-69, American Society of Heating, Refrigerating and Air-Conditioning Engineers, Inc., 345 East 47th Street, New York, N.Y. 10017, April, 1969.

4. Faison, T.K., Davis, J.C., and P.R. Achenbach, "Performance of Louvered Devices as Air Mixers, NBS Building Science Series 27, March, 1970. (Available from the Superintendent of Documents, U.S. Government Printing Office, Washington, D.C. 20402 - order by SD Catalog No. C 13.29/2:27, $0.30.)

5. "Instruments and Apparatus, Part 2, Pressure Measurement", Supplement to the ASME Power Test Codes, American Society of Mechanical Engineers, 345 East 47th Street, New York, N.Y. 10017, July, 1964.

6. "Instruments and Apparatus, Part 3, Temperature Measurement", Supplement to the ASME Power Test Codes, American Society of Mechanical Engineers, 345 East 47th Street, New York, N.Y. 10017, March, 1961.

7. Davis, J.C., "Radiation Errors in Air Ducts Under Isothermal Conditions Using Thermocouples, Thermistors, and a Resistance Thermometer", NBS Building Science Series 26, November, 1969. (Available from the Superintendent of Documents, U.S. Government Printing Office, Washington, D.C. 20402 - order by SD Catalog No. C 13.29/2:26, $0.25.)

8. Davis, J.C., Faison, T.K., and P.R. Achenbach, "Errors in Temperature Measurement of Moving Air Under Isothermal Conditions Using Thermocouples, Thermistors, and Thermometers, ASHRAE Transactions, Vol. 72, Part 1, 1966.

9. "Fluid Meters, Their Theory and Application", 5th edition, American Society of Mechanical Engineers, 345 East 47th Street, New York, N.Y. 10017, 1959.

10. "Instruments and Apparatus, Part 5, Measurement of Quantity of Materials, Chapter 4, Flow Measurement", Supplement to the ASME Power Test Codes, American Society of Mechanical Engineers, 345 East 47th Street, New York, N.Y. 10017, February, 1959.

11. Nakajima, Y., "Studies on the Weighting Functions of Thermal Storage Water-Tanks, Part I", Transactions of the Japanese Architectural Society, Vol. 199, pp. 37-47, September, 1972 (Japanese).

12. Nakajima, Y., "Studies on the Weighting Functions of Thermal Storage Water Tanks, Part II", Transactions of the Japanese Architectural Society, Vol. 200, pp. 75-83, October, 1972 (Japanese).

13. Matsudaira, H., and Y. Sakakura, "Analysis on the Thermal Capacity of Heat Storage Water Tanks, Part I", Journal of the Society of Heating, Air-Conditioning, and Sanitary Engineers of Japan, Vol. 46, No. 4, pp. 11-17, April, 1972 (Japanese).

14. Yang, W.J., and C.P. Lee, "Dynamic Response of Solar Heat Storage Systems", ASME paper 74-WA/HT-22, presented at the ASME Winter Annual Meeting, New York, 1974.

Table B1 Test Data to be Recorded

| Item | Tests Involving Air as the Transfer Medium | Tests Involving a Liquid as the Transfer Medium |
|---|---|---|
| Date | X | X |
| Observer | X | X |
| Equipment Name Plate Data | X | X |
| $\delta t$ ($\tau$) Across Storage System | X | X |
| Inlet Temperature, $t_{in}$ | X | X |
| Outlet Temperature, $t_{out}$ | X | X |
| Inlet Wet Bulb Temperature | X | |
| Outlet Wet Bulb Temperature | X | |
| Times | X | X |
| Liquid Flow Rate | | X |
| Barometric Pressure | X | X |
| Gauge Pressure at Inlet | | X |
| Gauge Pressure at Nozzle Throat | X | |
| Nozzle Throat Diameter | X | |
| Velocity Pressure at Nozzle Throat or Static Pressure Difference Across Nozzle | X | |
| Dry Bulb Temperature at Nozzle Throat | X | |
| Wet Bulb Temperature at Nozzle Throat | X | |
| Pressure Drop Across Storage System | X | X |
| Ambient Air Temperature | X | X |
| Initial Temperature $t_i$ | X | X |
| Step Change $\Delta t$ | X | X |

Table B2 Data to be Reported

General Information

Manufacturer . . . . . .

Model # . . . . . .

Serial # . . . . . .

Storage Medium . . . . . .

Transfer Fluid . . . . . .

Weight of Storage System, W . . . . . .

Volume of Storage System, V . . . . . .

Normal Operating Temperature Range . . . . . .

Minimum Transfer Fluid Flow Rate . . . . . .

Maximum Transfer Fluid Flow Rate . . . . . .

Maximum Operating Pressure . . . . . .

Flow Configuration Tested . . . . . (picture)

Heat Loss Rate Test

$t_a$ . . . . . .

SC $(t_a, 25^{\circ}C)$ . . . . . .

$\overline{\delta(t)}$ . . . . . .

$\dot{m}$ . . . . . .

$c_{tf}(\overline{t_{in}})$ . . . . . .

$$L = \frac{\dot{m}\, c_{tf}(\overline{t_{in}})\, \overline{\delta t}}{t_{in} - t_a} \quad \ldots\ldots$$

Table B2 (continued)

Transient Tests

$t_a$ . . . . . .

$t_i$ . . . . . .

$\Delta t$ . . . . . .

$\tau_F$ . . . . . .

$\dot{m}$ . . . . . .

$\Delta P$ . . . . . .

$P$ . . . . . .

$c_{tf}\ (t_i)$ . . . . . .

$SC\ (t_i, \Delta t)$ . . . . . .

$EC_{hs}\ (t_i, \Delta t, \tau_F)$ . . . . . .

$EC_{hr}\ (t_i + \Delta t, -\Delta t, \tau_F)$ . . . . . .

$$PC_{hs} = \frac{EC_{hs}\ (t_i, \Delta t, \tau_F)/V}{\Delta t \quad c_{H_2O}\ \rho_{H_2O}} \quad . \quad . \quad . \quad . \quad . \quad .$$

$$PC_{hr} = \frac{EC_{hr}\ (t_i + \Delta t, -\Delta t, \tau_F)/V}{\Delta t \quad c_{H_2O}\ \rho_{H_2O}}$$

USCOMM-NBS-DC

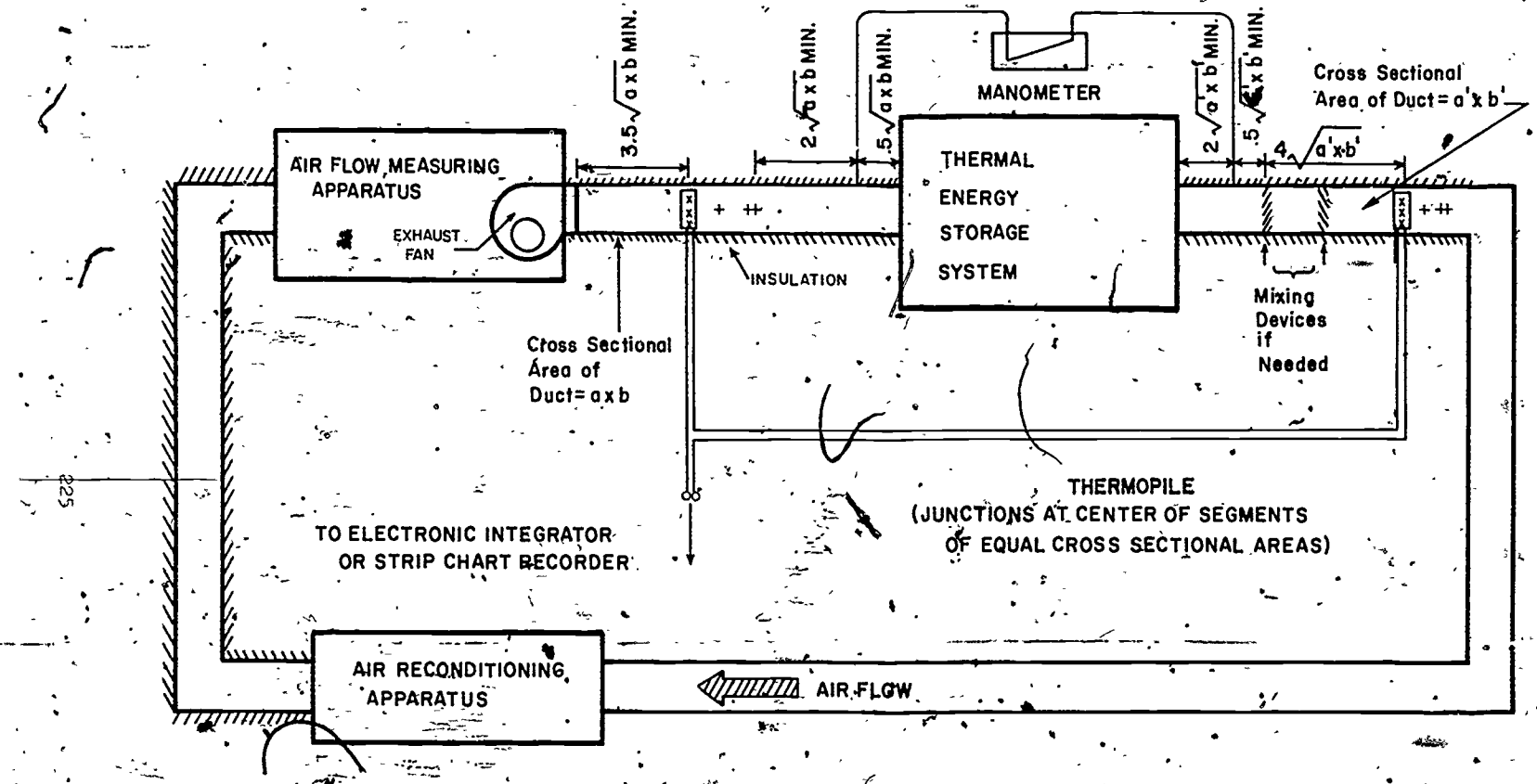


Figure B1 Testing Configuration for the Thermal Storage System When the Transfer Fluid is Air

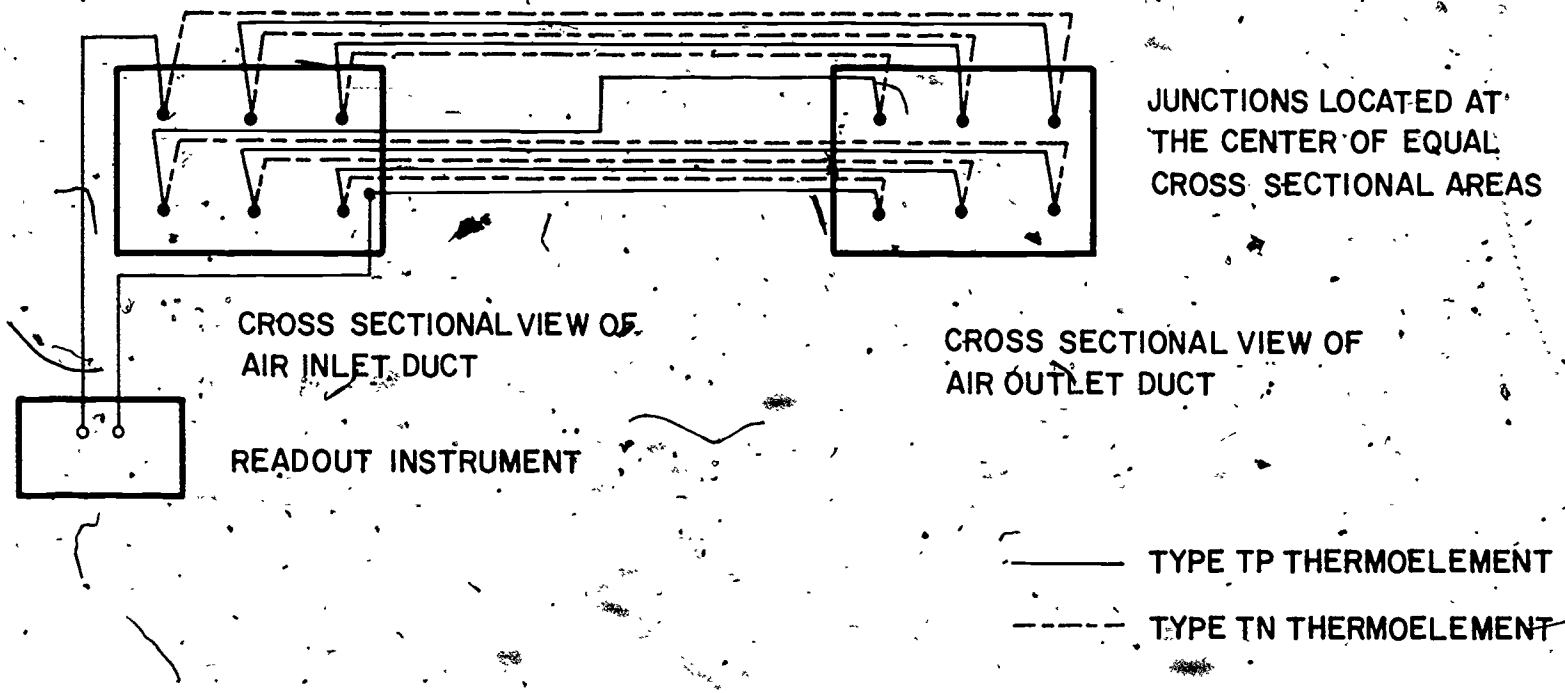


Figure B2 Schematic of the Thermopile Arrangement Used to Measure the Temperature Difference Across the Thermal Storage System

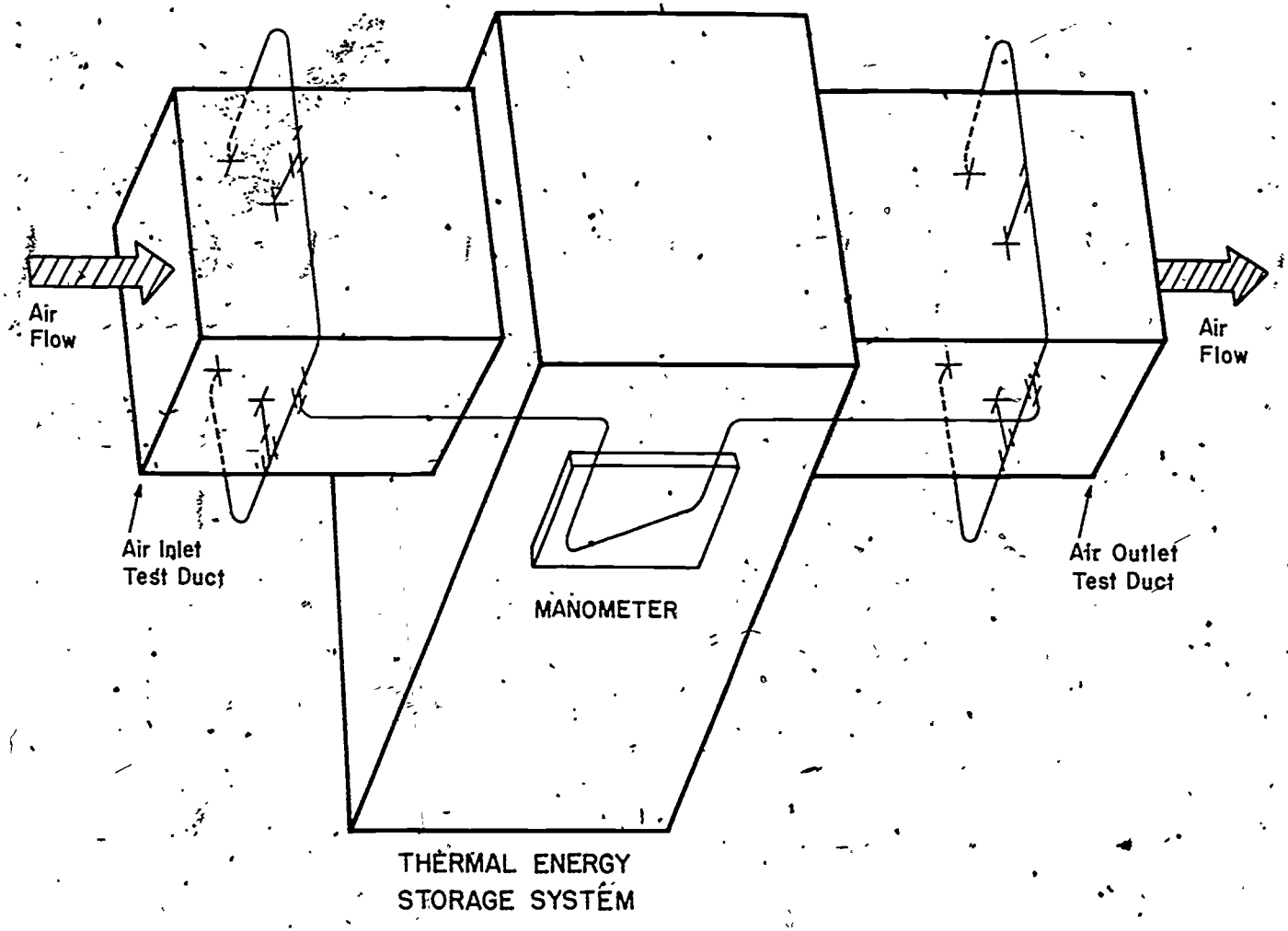


Figure B3 Schematic Representation of the Measurement of Pressure Drop Across the Thermal Storage System When Air is the Transfer Fluid

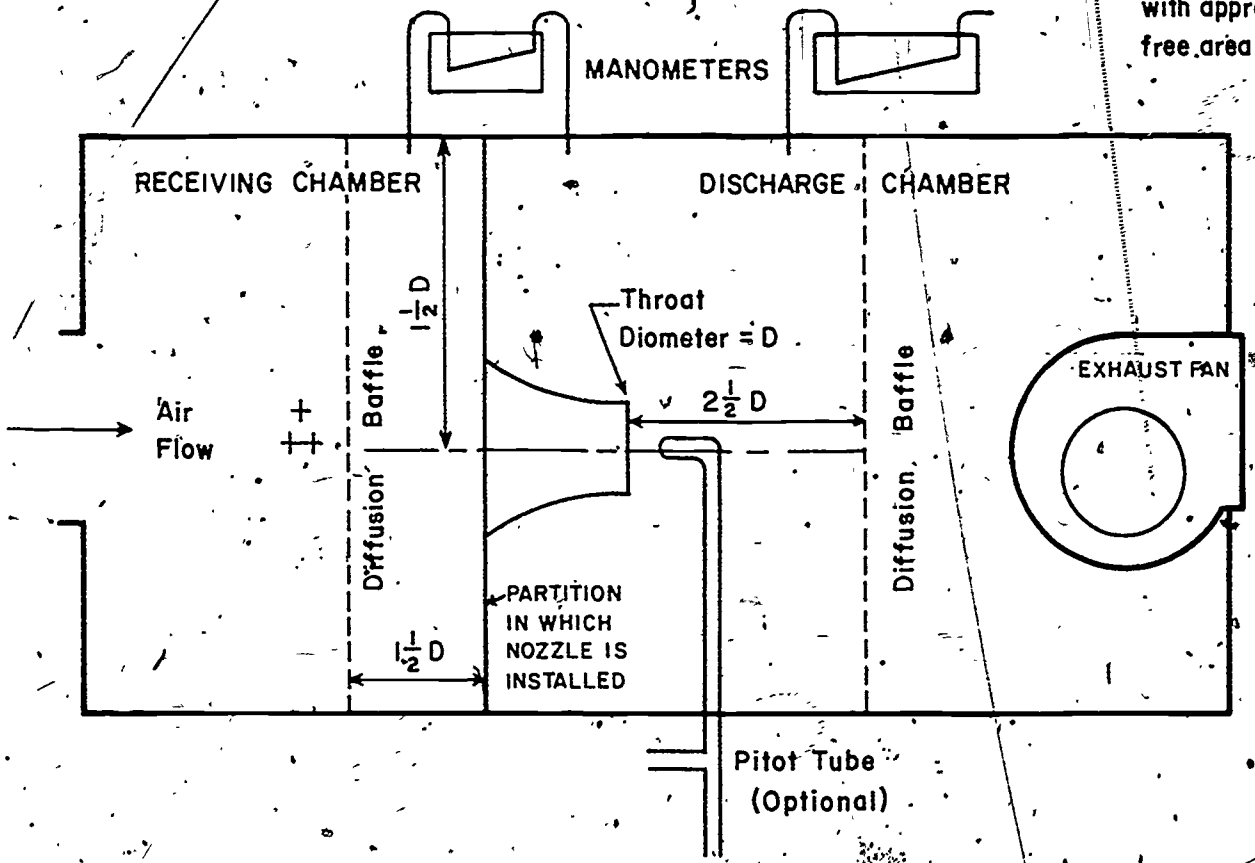


Note: Diffusion Baffles should have uniform perforation with approximately 40% free area

\+ CALIBRATED THERMOCOUPLE OR THERMISTOR

++ CALIBRATED WET BULB TEMPERATURE MEASURING DEVICE

Figure B4 Nozzle Apparatus for Measuring Air Flow Rate

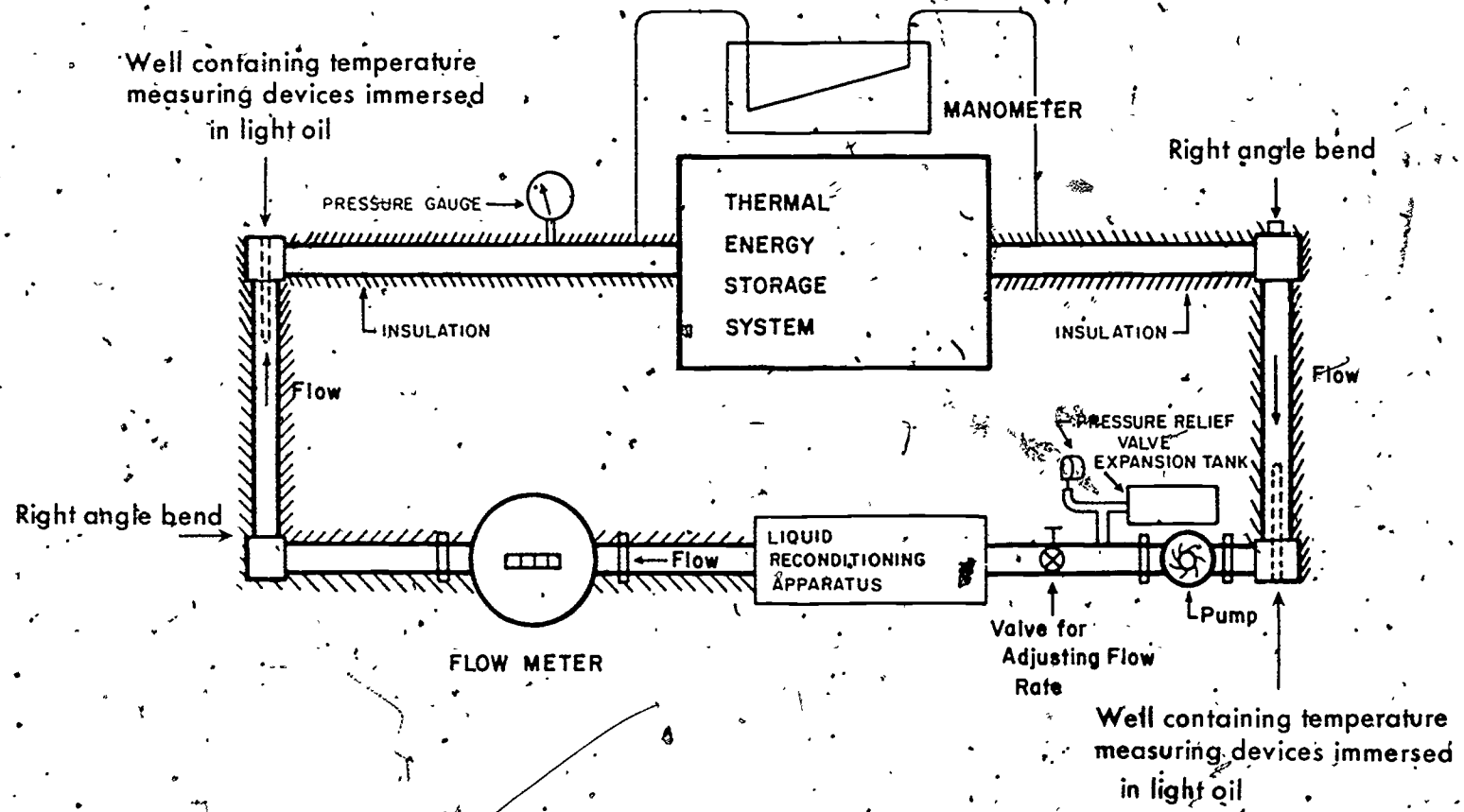


Figure B5 Testing Configuration for the Thermal Storage System When the Transfer Fluid is a Liquid

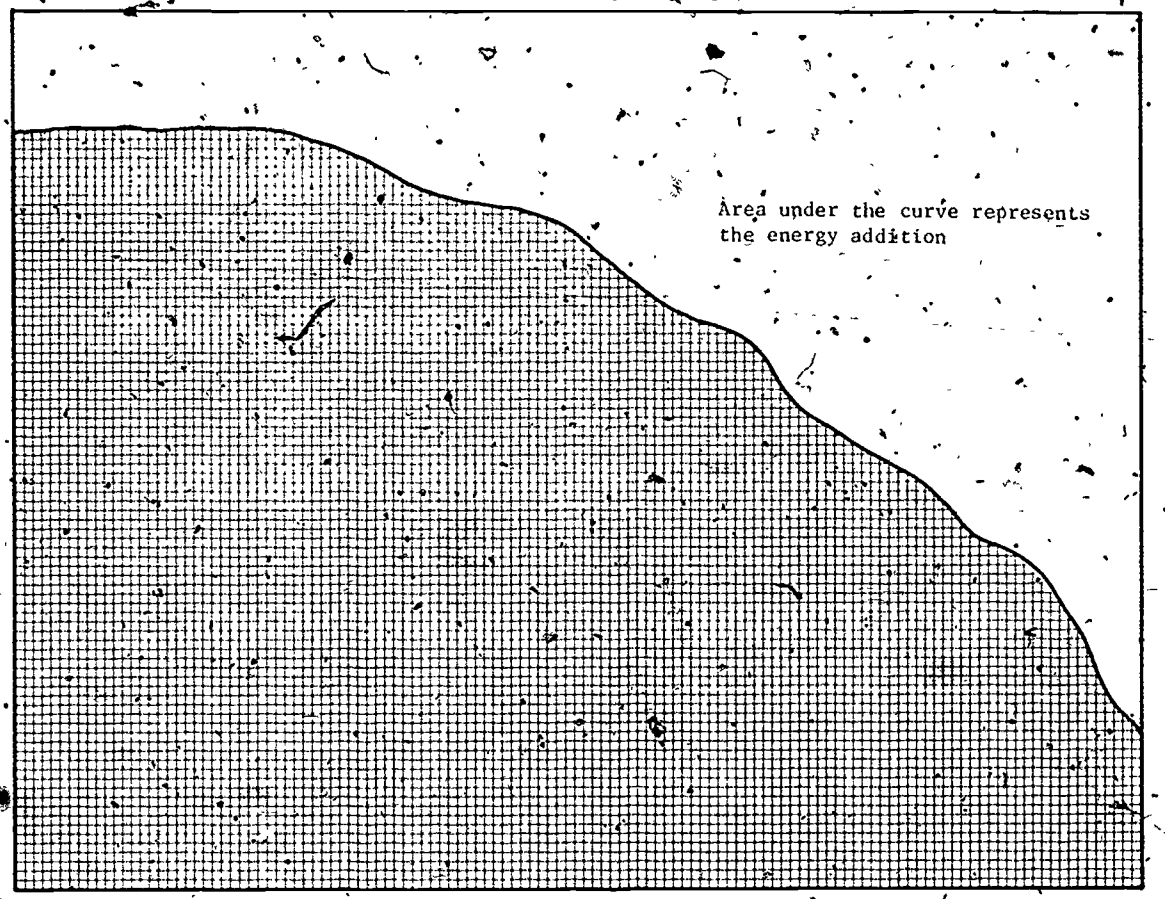


Figure B6 Schematic Representation of Energy Transfer into a Thermal Storage System as a Function of Time When the Inlet Temperature is a Step Function

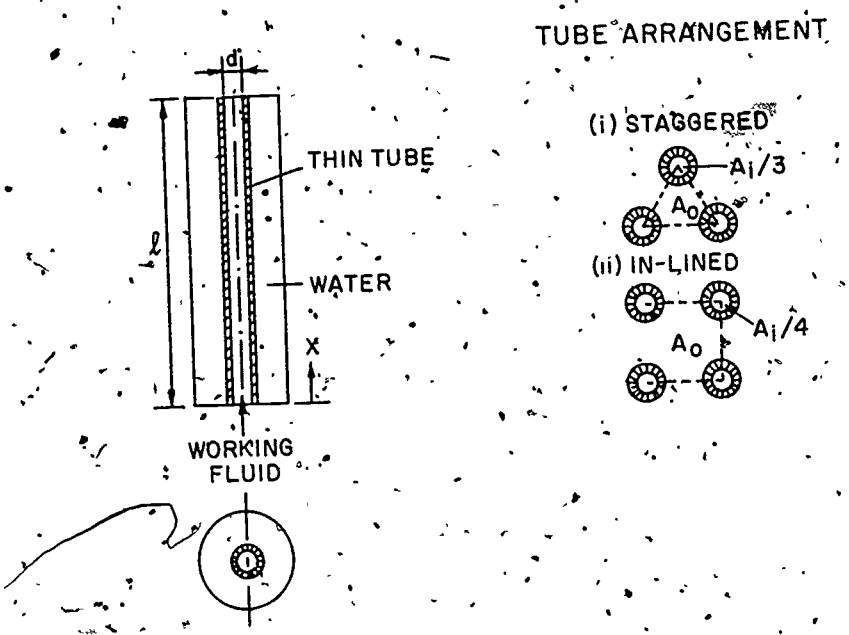


Figure B7 Schematic Representation of a Heat Exchanger-Type Thermal Storage Unit from Reference [14]

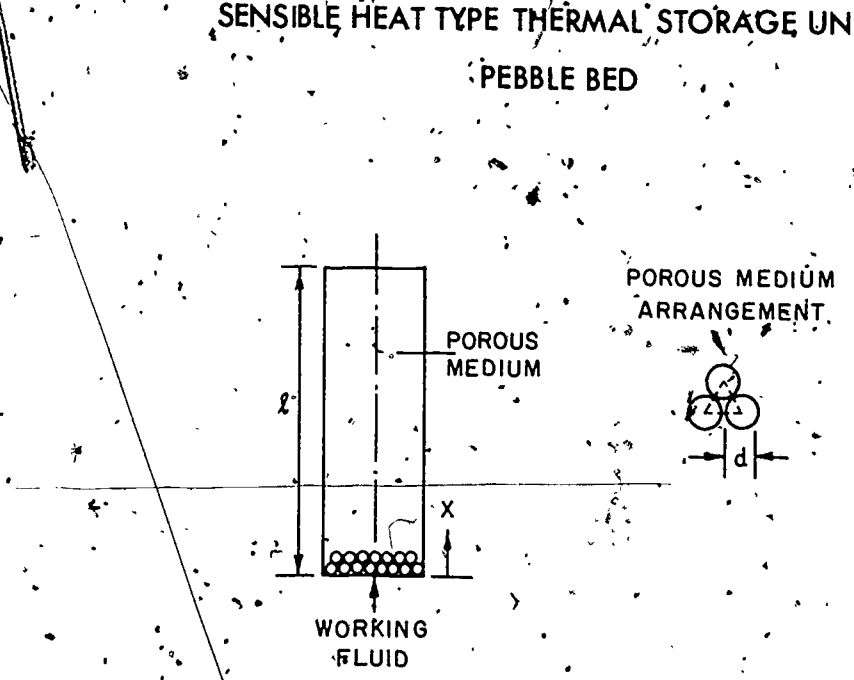


Figure B8. Schematic Representation of a Pebble Bed-Type Thermal Storage Unit from Reference [14].

LATENT HEAT TYPE THERMAL STORAGE UNIT

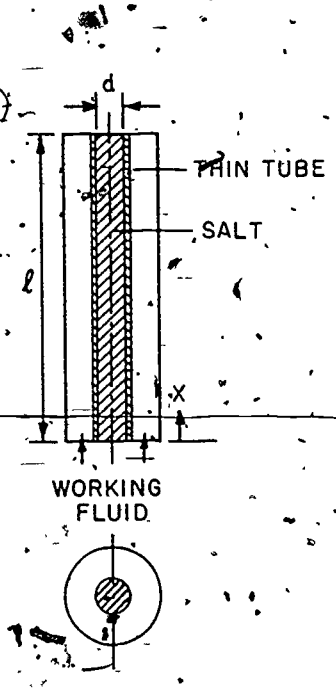


Figure B9 Schematic Representation of a Latent Heat-Type Thermal Storage Unit from Reference [14]

# HEAT EXCHANGER TYPE THERMAL STORAGE UNIT
## TRANSFER FLUID TRANSIENT TEMPERATURE DISTRIBUTION

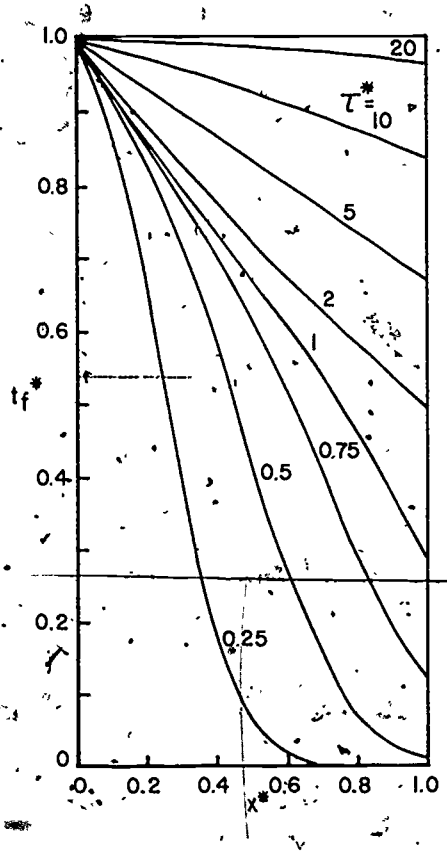


$$t_f^* = \frac{t_f - t_o}{t_{fo} - t_o}$$

$t_f$ = transfer fluid temperature
$t_o$ = initial temperature
$t_{fo}$ = temperature at inlet

$$x^* = x/\ell$$

$$\tau^* = \frac{\tau u}{\ell}$$

- transfer fluid-water
- storage medium-water

$$\frac{\dot{m} c_{tf}}{UA} = 1.1$$

$h_o = \infty$

$d = 1.27\text{cm}$

$A_o/A_i = 4$

Figure B10 Transient Temperature Distribution for the Transfer Fluid in a Heat Exchanger-Type Thermal Storage Unit from Reference [14]

# HEAT EXCHANGER TYPE THERMAL STORAGE UNIT

## STORAGE MEDIUM TRANSIENT TEMPERATURE DISTRIBUTION

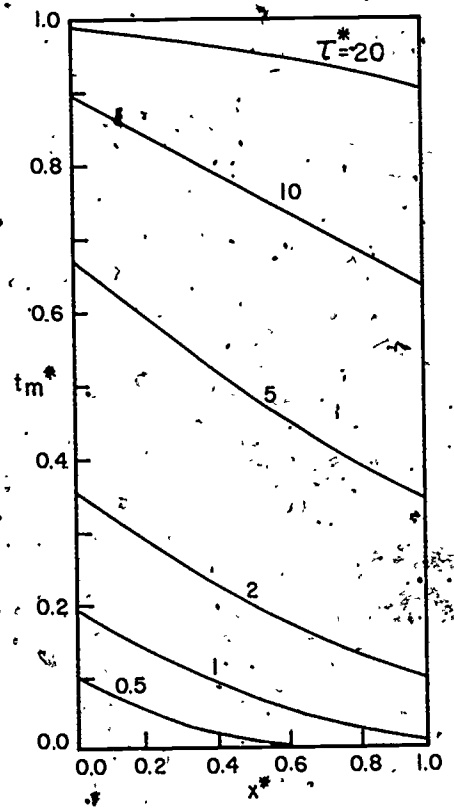


$$t_m^* = \frac{t_m - t_o}{t_{fo} - t_o}$$

$t_m$ = storage medium temperature
$t_o$ = initial temperature
$t_{fo}$ = temperature at inlet

$$x^* = x/\ell$$

$$\tau^* = \frac{\tau u}{\ell}$$

transfer fluid - water

storage medium - water

$$\frac{\dot{m} c_{tf}}{UA} = 1.1$$

$$h_o = \infty$$

$d = 1.27$ cm

$$A_o/A_i = 4$$

Figure B11 Transient Temperature Distribution for the Storage Medium in a Heat Exchanger-Type Thermal Storage Unit from Reference [14]

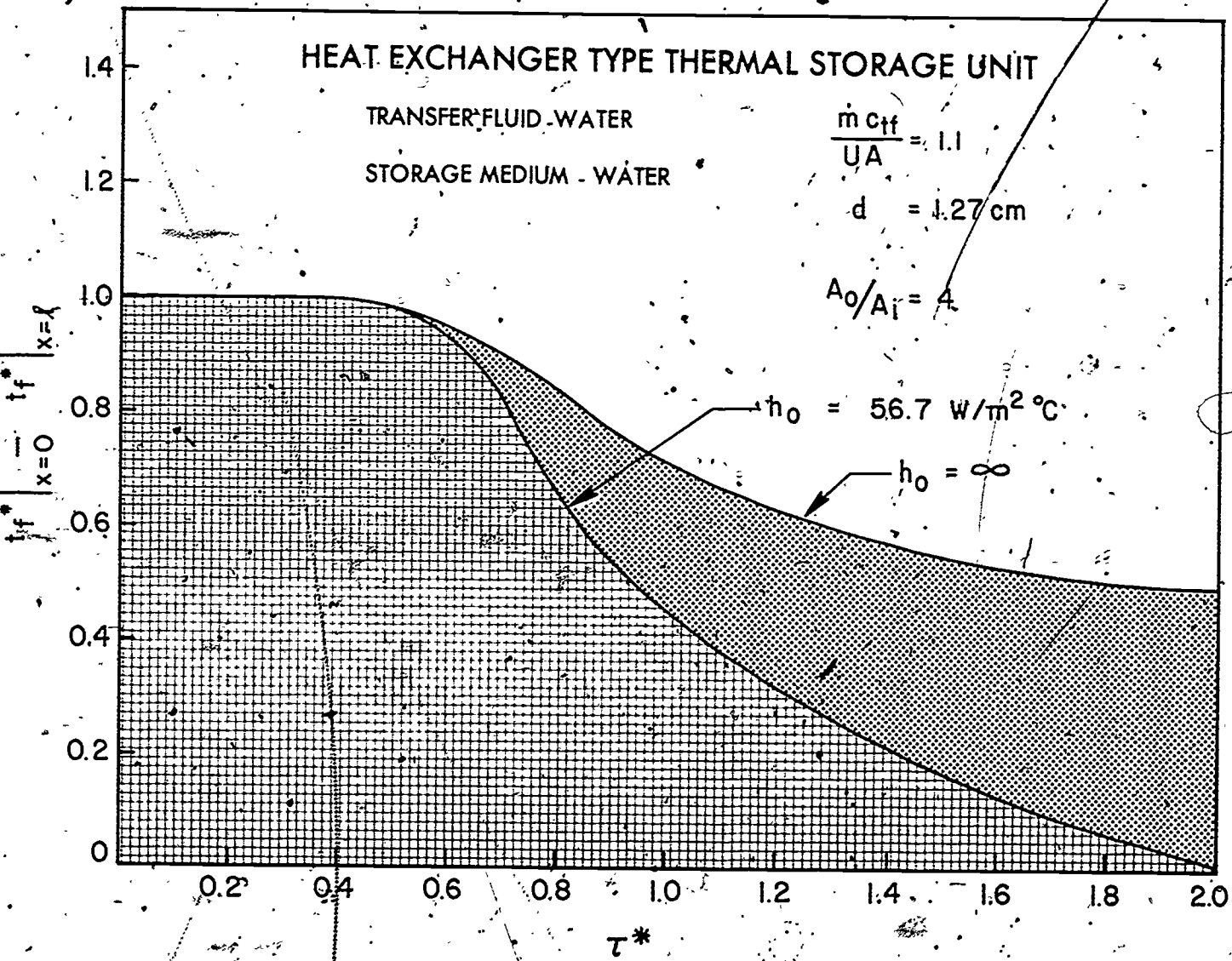


Figure B12 Comparison of the Transient Storage Capacity for Two Heat Exchanger-Type Thermal Storage Units from Reference [14]

## 8. Appendix C

## Radiometry and Its Relationship to the Characterization of Solar Collectors

### INTRODUCTION

The purpose of this Appendix is to describe (1) the radiometric quantities that must be measured for solar energy utilization programs, (2) the sources of error affecting measurements of these quantities, and (3) procedures for accurately performing these measurements. Since procedures will be described that require equipment that has not yet been developed, this Appendix will define both the state-of-the-art and current problem areas in solar conversion radiometry. This material is general enough to apply to photo-conversion as well as thermal conversion, but the emphasis is on the latter.

The role of radiometry in support of solar power utilization has been examined in Reference [1][a]. Three distinct tasks that make somewhat different demands upon radiometry have been identified: (1) convertor design, (2) competitive selection among convertors, and (3) optimization of performance of operational convertors. The present material is written with these tasks in mind, but specific procedures for each task will not be described. There are two reasons for this omission. First, such an approach probably requires that both the solar convertor and the instrumentation used to characterize it be treated in a unified manner as elements of a single system. This of course, is well beyond the scope of this Appendix. Second, such an approach is premature at the present state-of-the-art in radiometry. This field has the dubious distinction of being an area of measurement science that is characterized by surprisingly low accuracy. One percent is rarely achieved, and one quarter of one percent has been bettered only in relative measurements (measurements of the ratios of a given quantity), never in absolute measurements (measurements of quantities with units such as $W/m^2$). Typically, five percent radiometry, if not pushing the state-of-the-art, is at least very near it. This is in marked contrast to electrical measurements, where five percent is typically two orders of magnitude from the state-of-the-art. Furthermore, radiometry is presently undergoing a conceptual and technological revolution that promises to completely transform the field over the next five years. Thus, this material can serve only as a basis for interim, rather than long range, planning and recommendations.

The material is organized as follows. In the next section, the concepts that are necessary for understanding what follows are defined. They include the key radiometric quantities for solar conversion which are the relative angular and spectral response of the converter and the effective irradiance. In the following section, various sources of error affecting measurements of these and related quantities are described. In the final section, various measurement procedures and the accuracy that can be expected of their results are given.

---

[a] References are listed at the end of this Appendix.

## CONCEPTUAL DEFINITIONS

Various radiometric quantities of importance to solar conversion will be defined in this section. With reference to Figure C1, surface S that includes a point p, and a solid angle Ω that includes a direction m which makes an angle θ with the normal n to S at p are shown. The spectral radiance is defined as

$$L(m,p,\lambda,t) = \lim_{\substack{A\to 0\\ \omega\to 0\\ \Delta\lambda\to 0}} \frac{P}{A\cos\theta\omega\Delta\lambda} \qquad (1)$$

where P is the quantity of radiant power with wavelengths in the interval between λ and λ+Δλ that is incident on the surface S from the directions included in Ω, where A is the area of S, and where ω is the measure of Ω. The spectral radiance is defined for each direction m at each point p in space. It is a function of seven variables, the two coordinates that define the direction m, the three that locate the point p, wavelength λ, and time t.

Reversing the process, the power incident on a surface S, from a specified solid angle Ω is given by

$$P = \int_S \int_\lambda \int_\Omega L(m,p,\lambda,t)\ m\cdot n\ d\omega_m\ d\lambda\ dA_p \qquad (2)$$

The inner most integral in equation (2) is the spectral irradiance (at the point p from the solid angle Ω) defined as

$$E(\Omega,p,\lambda,t) = \lim_{\substack{A\to 0\\ \Delta\lambda\to 0}} \frac{P}{A\ \Delta\lambda} \qquad (3)$$

again with reference to Figure C1. The inner most double integral in equation (2) is the integral of spectral irradiance with respect to wavelength. It is called the total irradiance or just irradiance. It is defined as

$$E(\Omega,p,t) = \lim_{A\to 0} \frac{P}{A} \qquad (4)$$

again with reference to Figure C1.

If S in equation (2) were the surface of a solar collector and Ω were the portion of the sky that was viewed by the collector, then P would be the solar power, insolation, or rate of energy incident on the collector. In general, the useful power output $P_o$ is not simply related to P but rather it is a functional of the spectral radiance distribution function [a]. For simplicity (and because it is a good assumption), it is assumed that there exists some function of a single variation f(x) such that the power conversion process can be described by

$$P_o = f(E^*[n,p,t]) \qquad (5)$$

where

$$E^*(n,p,t) = \frac{1}{A}\int_S \int_\lambda \int_\Omega \alpha(m\cdot n,\lambda)\ L(m,p,\lambda,t)\ m\cdot n\ d\omega_m\ d\lambda\ dA_p \qquad (6)$$

[a] For a discussion of functionals see reference [2], p. 106.

is called the effective irradiance, $\alpha(\cos\theta,\lambda)$ is the relative spectral, directional response of the convertor, normalized to unity at the wavelength and direction of maximum response, and A is the area of the collector surface S. For all practical purposes the spectral radiance can be assumed to be independent of p over areas at least as large as solar collectors, so

$$E^*(n,p,t) = \int_\lambda \int_\Omega L(m,p,\lambda,t)\ m\cdot n\ d\omega_m\ d\lambda\ dA_p \qquad (7)$$

Furthermore, it is convenient to choose the specific functional form of f(x) such that

$$P_o/A = \beta(E^*[m,p,t])\ E^*(n,p,t) \qquad (8)$$

The physical interpretation of this equation is that the effective irradiance is converted into useful power output per unit collector area with an efficiency $\beta(E^*)$ that depends upon the effective irradiance E*. Furthermore, different spectral radiance distributions that give rise to the same effective irradiance of a given collector, also give rise to the same useful power output from that collector. Finally, since the collector for the special case of monochromatic, uni-directional incident power concentrated at the wavelength and direction of maximum response, the function $\beta(E^*)$ is just the maximum efficiency with which radiant power can be converted into useful power by the particular convertor when its effective irradiance is E*. This is all very nice, but it is crucially dependent upon the validity of equation (5). Thus, it is worthwhile to investigate its physical significance. Essentially, it states that all variations in spectral and directional response arise from optical effects. Once the incident radiant power has been absorbed it is treated exactly the same by the convertor, independent of the wavelength or direction of the radiant power that gave rise to it. The possibility that the processing of the absorbed power is non-linear is allowed, but none of the optical effects preceding or accompanying absorption may be non-linear. Actually these are quite reasonable assumptions, and they reduce the complexity of the problem immensely.

Finally two more definitions are required. First, the scaler irradiance defined by

$$\bar{E}(\Omega,p,t) = \int_\lambda \int_\Omega L(m,p,\lambda,t)\ d\omega_m\ d\lambda \qquad (9)$$

is a useful concept because it is proportional to the energy density of the radiation field, and therefore sets an upper limit for the rate at which energy can be extracted from the field per unit area. The actual rate, of course, depends upon $\beta(E^*)\ E^*$. Since the only difference between $\bar{E}(\Omega,p,t)$ and $E(\Omega,p,t)$, the inner most double integral in equation (2), is the presence or absence of the m·n (i.e. $\cos\theta$) factor, one is led to define the collection efficiency of a surface in a given direction as the ratio of the area of the projection of the surface in the given direction to the total area of the surface. This rather trivial concept is of importance in the discussion of sources of error in the next section for the following reason. In solar collectors, area costs money, so area must be minimized. The surface that provides the best collection efficiency averaged over all directions (i.e. for isotropic flux) is a plane; however, the collection efficiency of a plane is not uniform with direction, varying as it does proportionally to $\cos\theta$.

## SOURCES OR ERROR

Perhaps the most serious source of error in solar conversion radiometry is the tremendous variability with time of the directional distribution of the spectral radiance in the sky above a solar convertor. The problem is that the relative directional response,

$$\alpha(\cos\theta) = \int \alpha(\cos\theta,\lambda)\, d\lambda \qquad (10)$$

of practical solar collectors varies significantly among the different types. This is illustrated in Figure C2 where typical curves are shown for two different types of flat-plate collectors[a]. Also shown are typical curves for some different types of commercially available pyranometers [4, 5]. All of the curves have been normalized to unity at 0°.

Two hypotheses are suggested by the data of Figure C2. First, below thirty or forty degrees from the normal, all flat-plate collectors have very similar relative directional responses; so it is the radiant power incident from beyond approximately forty degrees that is the source of error in effective irradiance measurements. Second, no commercially available pyranometer, nor any single type of pyranometer will by itself be able to accurately determine the effective irradiance for different types of flat-plate collectors.

The limits of the error that can arise from this effect for flat-plate collectors will be estimated. It will be necessary to estimate the ratio[b]

$$R = \frac{\int_t E^*(\Omega_{40°-90°},p,t)\, dt}{\int_t E^*(2\pi,p,t)\, dt} \qquad (11)$$

for various different types of flat-plate collectors, where $E^*(\Omega,p,t)$ is the contribution to the effective irradiance that arises from directions contained in $\Omega$. The ratios R for different relative response functions in Figure C2 are critically dependent upon the temporal and directional distribution of the solar spectral radiance, so a cursory review of this distribution will be made prior to making some plausible estimates of its time average behavior.

On overcast days, the sky to a first approximation is of uniform radiance. However, the significant quantities of energy produced by most flat-plate collectors will not occur on these days due to the normally low values of insolation. Therefore for this analysis, the considerations are restricted to days on which more than half the sky is cloud free. The daily and yearly variation of sun position in the sky must be considered. Figure C3 is a projection (looking upward) of the hemisphere whose normal is perpendicular to the average surface of the earth at 37° latitude. On the projection are traced the paths of the sun at the summer solstice (lower curve), winter solstice (upper curve), and the equinoxes (middle curve). Consider a flat-plate collector of fixed orientation with its normal toward the solar zenith at the equinoxes. The portion of the diagram between the dashed lines is the portion of the sky that is within forty degrees of the normal to the collector. Of the time that it is within ninety degrees to the normal of the collector, the sun spends about 45% of this time within forty degrees of the normal to the collector.

Next the fact that some of the incident solar radiation comes from parts of the sky other than the solar disc due to atmospheric scattering must be considered. Somewhere between ten and thirty percent of the incident solar energy on clear days will come from regions of the sky other than the immediate neighborhood of the solar disc [6]. If it is

---

[a] The curves for the flat-plate collectors were obtained by calculating the transmittance of a glass plate as a function of angle of incidence using the Fresnel formulae [3].

[b] This ratio is rigorously applicable only in the case of linear convertors, but is indicative of the magnitude of the problem for all systems.

assumed that this radiation is distributed uniformly over the sky, then R can be estimated by

$$R_a = \frac{[0.80 + 0.10]\ IP(40°) + [0.20 \quad 0.10]\ IS(40°)}{[0.80 \pm 0.10]\ IP(0°) + [0.20. \quad 0.10]\ IS(0°)} \qquad (12)$$

for each of the relative response functions in Figure C2, where

$$IP(\theta) = \int_{\theta}^{90°} \alpha(\cos\theta)\ \cos\theta\ d\theta \qquad (13)$$

which is an estimate of the average quantity of solar energy that is incident from directions between θ and 90° to the surface of the collector due to variable location of the sun in the sky, and where

$$IS(\theta) = \int_{\theta}^{90°} (\cos\theta)\ \cos\theta\ \sin\theta\ d\theta \qquad (14)$$

which is an estimate of the average quantity of solar energy that is incident between θ and 90° to the surface of the collector from parts of the sky not near the solar disc. The results of this analysis are summarized in Table C1:

Two effects that tend to compensate for one another have been ignored in obtaining the estimates in Table C1. The first of these is that at the higher angles of incidence the direct solar irradiance is decreased beyond the effect predicted by the collection efficiency of the surface (cosine effect) due to the increased mass of atmosphere through which the radiation must pass. This would tend to reduce all of the percentages in Table C1. On the other hand, the effect of clouds has been neglected. Their effect would be to increase all of the percentages in Table C1, and to increase the uncertainties significantly.

Another factor that has been ignored in preparing Table C1, is the fact that the absorption and scattering coefficients of the atmosphere vary significantly with wavelength. Since the solar radiation must pass through differing masses of atmosphere when the sun is in different parts of the sky, the net spectral attenuation varies with solar locations, as well as with meteorological conditions. Thus the spectral distribution of solar radiation is subject to temporal variations that interact with the non-uniformities of spectral response in some types of collectors and pyranometers. For the purposes of this section, flat-plate thermal collectors and thermopile pyranometers can be considered to be spectrally non-selective. However, this is not the case with silicon cell pyranometers. For this type of instrument the effect is shown in Figure 11 of [5], where the interaction of the spectral distribution of solar radiation with the spectral response of a silicon cell pyranometer (sol-a-meter) has been investigated under clear sky conditions in Phoenix, Arizona in 1962. This study showed small effects of variation in spectral response, the conclusion being "....with proper calibration and adequate attention to the effects caused by solar altitude, a temperature-compensated silicon-cell pyrheliometer can be used with confidence to measure direct, total, and diffuse solar radiation with an accuracy of at least ±3 percent." Unfortunately, this conclusion is based upon sky conditions that are much cleaner, and less humid than prevail in much of the U.S. Furthermore, the sun is much higher in the sky on the average in Phoenix than in most other parts of the U.S. Thus this conclusion cannot be extrapolated to the U.S. as a whole without further investigation.

The purpose of Table C1 is to give an estimate of the size of the errors that can be expected to occur in solar conversion radiometry due to different directional response functions. The entries in the table should by no means be considered as limits of error but rather as guiding estimates. When it is recalled that the useful power output of a convertor is generally not proportional to the effective irradiance, that materials other than glass might be used as the cover plate on flat-plate collectors, that the effect of dirt films on the relative response has been ignored, as have the effects of clouds and spectral distribution, it is clear that the uncertainties in predicting the useful power output from a solar convertor, given some effective irradiance measurements, could be two or three times as large as the uncertainties shown in the table.

Up to now consideration has been given to sources of error that arise from the nature of the radiation that is to be measured and how it is to be weighted spectrally and directionally. One must additionally consider the sources of error that are associated with the instruments that will be used for the measurements. These are:

1. alignment of the instruments
2. stability of the instrument's calibration
3. changes in the instrument's response due to variations in ambient temperature
4. non-linearity in the instrument's response

Latimer [4] has estimated the errors in the calibration of pyranometers for meteorological applications for the latter three effects. The root mean-sum of the squares of these estimates ranges from 2.1% to 3% for the pyranometers he considered. Latimer has also estimated the errors arising from the temporal variations in the directional distribution of the solar radiation. However, all of his estimates are based upon measurements of the total solar irradiance, rather than the effective irradiance of a particular solar convertor. The errors arising from the temporal variations in the solar radiance distribution would tend to be larger for measurements of effective than for measurements of total irradiance. A comparison of the estimates here (Table C1) with those of Latimer show them to be of comparable magnitude. However, it is important to realize that his estimates are considerably more solid than ours. Measurements of effective irradiance must account for a response function that varies from collector to collector and that is not present in total irradiance measurements. Measurements of the maximum efficiency of a collector must account for possible variations of this quantity with the effective irradiance. This also is not a factor in total irradiance measurements. The impact of a less solid uncertainty figure will be addressed in the following section.

One final problem that is much more severe with effective irradiance measurements than with total irradiance measurements is the first source of error listed above, alignment. Generally in total irradiance measurements the pyranometer is to be oriented parallel with the average surface of the earth at the location in question. This is easily achieved with the spirit level that is generally affixed to the instrument, provided that the level has been set parallel to the pyranometer receiver. However, in the case of effective irradiance measurements for flat-plate collectors, it will be necessary to accurately align the plane of the receiver with the plane of the collector. This could conceivably present some practical problems.

A final source of error that must at least be mentioned is miscalibration. Error of this nature can arise either from human mistakes, or from calibration on different scales. As an example of the former, consider the possibility of making irradiance measurements with comercially available laser power meters. Some of these instruments have nominal 1 $cm^2$ aperture areas, and could be suitable for irradiance measurements. This is true only if all of the flux that passes through the aperture is incident on the active area of the receiver, and only if the area of the receiver is known. It is important to avoid the temptation to report an irradiance of X watts/$cm^2$ where a power X watts has been measured unless independent measurements yield an aperture area of 1 $cm^2$.

With reference to calibrations of difference scales, the U.S. has signed the "Treaty-of-the-Metre" and thereby has agreed to report measurements of power in the appropriate SI unit, the watt. The U.S. has also signed the treaty setting up the World Meteorological Organization, which has recommended that all measurements of radiant power for meteorological applications be reported on the International Pyrheliometric Scale, 1956, whose units are called W/$cm^2$. However, it has been shown [7] that the IPS 1956 W/$cm^2$ is about two percent lower than the SI W/$cm^2$. Moreover, it can be argued [8] that the IPS 1956 is not precisely defined at all and therefore is really meaningless.

## RECOMMENDED MEASUREMENT PROCEDURES

In this section some recommended measurement procedures will be described and the uncertainties associated with them given. The procedures will be described starting from the primary calibration. It should not be assumed that all parts of the procedure must be carried out at the same time or even by the same personnel or organizations. These decisions involve trade-offs that cannot be anticipated at this time. Also, some of the procedures involve equipment that is not available commercially. Clearly, such instruments would have to be developed and their commercial exploitation be encouraged and/or subsidized before all these procedures could be adopted.

The procedures that will be described as follows:

1. Characterization of spectrally non-selective focusing converters,
2. Characterization of spectrally non-selective flat-plate converters

The primary instrument for the two procedures is an electrically calibrated pyrheliometer of modern design. Such an instrument is an radiometer that measures the irradiance from a small (3 degree half angle) solid angle about the sun. The principal of operation is the alternate comparison of the temperature rise in the instruments' receiver due to radiant heating with that due to electrical heating by a measured quantity of electrical power. Errors arising from variation in the instruments' responsivity due to non-linearity and changes in ambient temperatures are eliminated. Also eliminated are problems with calibration against standard sources of radiation such as blackbodies or lamps which were in turn calibrated against a blackbody. There is considerable evidence that these instruments are capable of producing measurements of the total irradiance from a small solid angle about the sun ~~with~~ errors of less than 0.5 percent of the measured value. A definitive statement on this question will be available shortly. There are at least two different types of this instrument that are presently available from commercial sources.

### 1. Characterization of Spectrally Non-Selective Focusing Converters

#### Procedure 1.1

In this procedure, the simplest to be described, the irradiance from the sky in a small region around the solar disc is measured with an electrically calibrated pyrheliometer of modern design that has a nominally 5 degree field of view. Only two sources of error are significant in this procedure. They are the possibility that the pyrheliometer weights the radiation from the circumsolar sky differently than does the focusing converter, and the validity of the assumption of spectral non-selectivity.

If the pyrheliometer weights the radiation from the circumsolar sky more heavily than does the converter, then the first effect cannot produce errors larger than a few percent on days that are clear enough for focusing systems to be operating. If this is not the case, a detailed comparison of the exact weighting of the circumsolar radiation by the converter and the pyrheliometer must be undertaken. It may also be desirable to adopt Procedure 1.2.

If the spectral response of the converter is known to be flat to within $\pm$ X percent between 0.3 $\mu$ m and 2.5 $\mu$ m, then $\pm$ X percent is a very conservative limit on the error that could be introduced by this assumption. Tighter limits on this error could be produced by calculating the change in effective irradiance due to changes in spectral distribution of the radiation from the solar disc. It should be emphasized that knowledge of the spectral response of the converter that is accurate enough for this procedure is probably available only for systems that are relatively spectrally non-selective over the 0.3 $\mu$ m to 2.5 $\mu$ m wavelength range, that is systems with black absorbers and simple optics entirely of glass or quartz. If this is not the case, a more elaborate procedure should be adopted.

Simultaneous measurements of the effective irradiance $E^*$ and the useful power output $P_0$ allow the maximum efficiency $\beta(E^*)$ to be determined as a function of $E^*$.

Procedure 1.2

This procedure is identical to the preceding one, except that the geometry of the view limiting aperture of the pyrheliometer is modified so that the radiation from the circumsolar sky is weighted identically by the focusing converter and the pyrheliometer. With this procedure, measurements of the effective irradiance of spectrally non-selective, focusing converters with uncertainties approaching ± 0.5 percent should be achievable. The effect of imperfect spectral non-selectivity is identical to that described under Procedure 1.1.

Procedure 1.3

This procedure involves use of a solar simulator to characterize a focusing converter. It is recommended because the detailed source geometry will differ radically from that of the solar disc and circumsolar sky, and might introduce uncertainties that are difficult to quantify.

Comments

In the first two procedures, it has been assumed that the pyrheliometer is precisely aimed at the solar disc. If this is not the case, errors that are difficult to quantify (in the general case, specific examples can be handled readily) will be incurred. Precise aiming can be achieved by simple mechanical means, and precise aiming has already been incorporated into the focusing converter. Therefore, it is recommended that procedures and mechanics be adopted that reduce the uncertainty due to this source of error to a level significantly below the uncertainties that arise from the assumption of spectral non-selectivity and the effect of the circumsolar sky.

2. Characterization of Spectrally Non-Selective Flat-Plate Converters

The primary instrument for these procedures is the same as above, an electrically calibrated pyrheliometer of modern design. However, in the following procedures, the pyrheliometer will not be used to characterize a flat-plate collector, but rather to calibrate another type of instrument that can more closely follow the directional response of the converter.

Pyranometers are commercially available instruments that more closely follow the directional response of flat-plate converters than do pyrheliometers. Their design goal is a relative directional response that is independent of direction and a collection efficiency of a plane surface ($\cos\theta$, where $\theta$ is the angle of incidence relative to some reference direction). It is commonly assumed in measurements of total solar irradiance with this instrument that errors of less than 5 percent can be achieved if great care is taken.

There are other types of instruments that would be of more use to solar conversion radiometry than are pyranometers. For instance, a pyranometer-like instrument whose relative directional response could be changed to simulate the relative response of various common types of flat-plate collectors would be useful. Another type of potentially useful device would be a pyranometer-like instrument whose field of view could be adjusted. From Figure C3, it is concluded that useful fields of view might be 0° to 40°, 40° to 60°, 60° to 70°, and 70° to 80° about the normal to the instrument. Actually both of these requirements could be satisfied by a single instrument. A conceptual diagram is shown in Figure C4.

Notice that this instrument has flat windows rather than the domed window of the conventional pyranometer. The windows are removable so that single window and double window collectors with other window materials as well as glass could be characterized. The removable top plate limits the instruments' field of view. For the instrument shown in the figure, the field of view is nominally 70° to 80° about the normal, but the finite size of the receiver degrades the directional response function from the ideal. A smaller receiver would improve this situation. Another useful feature would be electrical calibration. This would not eliminate the requirement for calibration with an electrically calibrated pyrheliometer, since the effect of the windows would still need to be determined. It would however eliminate

errors arising from non-proportional response, temperature coefficient of response, and variations of response with orientation. Such an instrument could be called an electrically calibrated, flat-plate pyranometer.

Prior to discussing the characterization procedures, the way in which one or more conventional or flat-plate pyranometers could be calibrated will be described.

Pyranometer Calibration Procedure 1

The pyranometers are calibrated following the procedure of Latimer [4] using the sun, sky, an occulting disc as the source of radiation, and an electrically calibrated pyrheliometer of modern design to measure the irradiance from a small solid angle about the sun. It is recommended that the pyrheliometer readout be in SI $W/cm^2$ rather than in IPS 1956 $W/cm^2$. Latimer's estimates of the accuracy should be valid.

Pyranometer Calibration Procedure 2

The pyranometers are calibrated with a solar simulator that uses a well filtered zenon arc as a source of radiation, and an electrically calibrated pyrheliometer of modern design to measure the irradiance from the solar simulator. Care must be taken to assure that the field of view of the pyrheliometer is larger than the angular extent of the radiation from the simulator, and that interreflections off of walls, people, etc. do not interfere with the measurement. Recommended practices for using solar simulators are available. This procedure has the potential to produce more accurate results than the preceding procedure due to the fact that much greater control of the experimental parameters is available. However, a considerable amount of careful work must be performed before this potential can be realized.

Characterization Procedure 2.1

1. Choose the most linear conventional pyranometer with the smallest temperature coefficient available.
2. Calibrate it or have it calibrated following the procedures above.
3. Carefully orient the pyranometer so that its receiver is parallel to the surface of the collector, being sure that nothing obstructs the field of view of either the collector or the pyranometer. (If the collector is mounted in a location where a wall of tower or any other permanent object obstructs its field of view, the object must be considered a part of the converter that modifies its directional response).
4. Use the measured values of irradiance to estimate the effective irradiance of the collector.

This procedure is probably insufficient because of large time dependent errors that are difficult to quantify[a].

Procedure 2.2

Steps 1, 2, and 3 are identical to the steps in Procedure 2.1. Step 4 above should be replaced with the following: Calculate the effective irradiance from measured values of the total irradiance on the collector and theoretical values of the directional response of the collector using astronomical and meteorological data to model the time dependence of the radiance distribution of the sky as in the previous major section of this Appendix[b].

There are four major sources of error affecting this procedure. First, the astronomical and meteorological model of the time dependent radiance distribution of the sky may be faulty. It is difficult to estimate limits of the error that could arise from this source. Second, the theoretical values of the directional response of the collector may be in error due to

[a] This is the procedure that has been adopted in the current version of the collector test procedure.

[b] Perhaps even more sophisticated meteorological techniques should be used.

unknown factors affecting the materials or construction of the device. It is also difficult to estimate limits of the error that could arise from this source. Third, measurements of total irradiance with pyranometers are typically subject to errors at the ± 5 percent level. Fourth, any dependence of the maximum conversion efficiency as a function of the effective irradiance $\beta(E^*)$ upon $E^*$ would interact in an unpredictable way with the errors arising from the first three sources to produce more error.

It is very difficult to obtain reliable uncertainties for this procedure. Twenty to forty percent does not seem pessimistic, yet the actual error could be well below these limits. Only careful investigations of a rather substantial nature could produce reliable uncertainties.

Procedure 2.3

1. Choose an electrically calibrated flat-plate pyranometer with the same type of windows as the flat-plate collector that is to be characterized.
2. Calibrate the pyranometer or have it calibrated following the procedures given previously.
3. This step is identical to step 3 of Procedure 2.1.
4. Use the measured values of the effective irradiance of the pyranometer as estimates of the effective irradiance of the collector.

This is somewhat of a half-way measure. It does eliminate the first and third source of error affecting Procedure 2.2, but the second and fourth errors are still present. Reliable uncertainties are still difficult to obtain.

Procedure 2.4

1. Choose four electrically calibrated flat-plate pyranometers with the same type of windows as the flat-plate collector that is to be calibrated.
2. Calibrate each of the pyranometers or have them calibrated following the procedures given previously. Try to get some data for near normal incidence. This may require tilting the pyranometer at an accurately measured angle toward the sun. Verify that all four instruments have identical directional response.
3. Affix a 0° to 40°, 40° to 60°, 60° to 70°, and 70° to 80° view limiting aperture to the four pyranometers, respectively.
4. This procedure is identical to step 3 of Procedure 2.1.
5. Fit the measured values of useful output power $P_o$ from the solar converter to the equation

$$P_o = f\left(\sum_{i=1}^{4} A_i E_i^*\right)$$

where $f(x)$ is a low power polynomial or other function that is appropriate for describing the non-linear behavior of the converter, where $E_i^*$ is the effective irradiance measured by the $i^{th}$ instrument, and where $A_i$ are unknown constants to be determined by the fitting procedure.

If all $A_i$ are identical, then the directional response of the converter is identical to that of the pyranometers, any one of which may then be used to measure the effective irradiance of the converter with its view limiting aperture removed following Procedure 2.3. If the $A_i$ are significantly but not drastically different, the directional response of the converter can be approximated by a smooth curve drawn through the points

$(0°, R(1))$,

$(50°, A_2 R(\cos 50°)/A_1)$,

$(65°, A_3 R(\cos 65°)/A_1)$,

and $(75°, A_4 R(\cos 75°)/A_1)$

where $R(\cos\theta)$ is the relative response function of the flat-plate pyranometer obtained from step 2. If the $A_i$ are drastically different, determine the cause of the difference in relative response between the flat-plate collector and pyranometers, and appropriately modify the pyranometers (adding or changing a window for instance). Repeat Procedure 2.4 with the modified pyranometers.

This procedure eliminates or at least drastically reduces all of the errors present with Procedure 2.2. Uncertainties considerably smaller than $\pm$ 5 percent should be obtainable. That this procedure should produce effective irradiance data of higher accuracy than that of the total irradiance data obtained from pyranometers should not be surprising. The procedure is based on electrically calibrated instruments which eliminate two of the largest sources of error in pyranometers (variations of responsivity with ambient temperature, and non-proportional response). A number of instruments with limited fields of view have been used to decrease the effect of the third large source of error. Furthermore, power available near grazing incidence is less heavily weighted in the effective irradiance than in the total irradiance.

## CONCLUSIONS AND RECOMMENDATIONS

It is premature to describe procedures for measuring the effective irradiance of spectrally selective converters. Further study must be done to determine whether effective irradiance is indeed the concept to be used.

An investigation of the uncertainty associated with Procedure 2.2 should be undertaken by NOAA and/or supported by ERDA. It would consist of a comparison of the effective irradiance of some flat-plate pyranometers as measured by Procedure 2.3 and as calculated from Procedure 2.2 using the measured relative directional response of the pyranometer obtained in Procedure 2.3. The flat-plate pyranometers would be chosen to simulate the relative directional response of typical flat-plate converters, and the theoretical and measured relative directional responses of the pyranometer could be compared. The result would be reliable uncertainties for the first three sources of error affecting Procedure 2.2. If these uncertainties were satisfactorily small, Procedure 2.2 could be adopted as a standard procedure. If not, the commercial development of the flat-plate converters could be encouraged, and Procedure 2.1 and 2.- could be adopted depending upon how accurately the theoretical response of flat-plate pyranometers matched their measured response.

## REFERENCES


1. Geist, J., "The Role of Radiometry in Solar Energy Utilization", Proceedings of the Smithsonian - Eppley Symposium on Solar Radiation Measurements and Instrumentation, November, 1973 (in press).

2. Riesz, F., and B. Sz.-Nagy, Functional Analysis, Frederick Ungar, New York, 1955.

3. Born, M., and E. Wolf, Principles of Optics, Third Edition, Pergamon Press, New York, 1965.

4. Latimer, J.R., "Radiation Measurement, Technical Manual Series No. 2", Canadian National Committee for the International Hydrological Decade, Building No. 8, Carling Avenue, Ottawa, Canada, 1971.

5. Yellott, J.I., and K. Selcuk, "Measurement of Direct, Diffuse and Total Solar Radiation with Silicon Photovoltaic Cells", Solar Energy, Vol. 6, No. 4, 1962.

6. Robinson, N., Solar Radiation, American Elsevier, New York, 1966.

7. Frohlich, C., Geist, J., Kendall, J., and R.M. Marchgraber, "The Third International Comparisons of Pyrheliometers and a Comparison of Radiometric Scales", Solar Energy, Vol. 14, pp. 157-166, 1973.

8. Frohlich, C., "The Relation Between the IPS Now in Use, Smithsonian Scale 1913, Angstrom Scale, and Absolute Scale", Proceedings of the Smithsonian - Eppley Symposium on Solar Radiation Measurements and Instrumentation, November, 1973 (in press).

TABLE C1

Estimates of the percent contribution from directions greater than 40° to the collector normal divided by the time averaged effective irradiance for collectors with different directional response functions, expressed as a percent.

| TYPE OF RESPONSE FUNCTION | $R_a$ (%) |
|---|---|
| Pyranometer[a] | 38 ± 2 |
| Flat-Plate Collector | 28 ± 4 |
| Sol-a-Meter | 27 ± 1 |

[a] response function #3 of Figure C1 was not used in this calculation.

The surface S contains the point p, the normal to S at p is n, and the solid angle Ω surrounds the direction m which makes an angle θ with n. The flux is assumed to be flowing in the opposite direction of m.

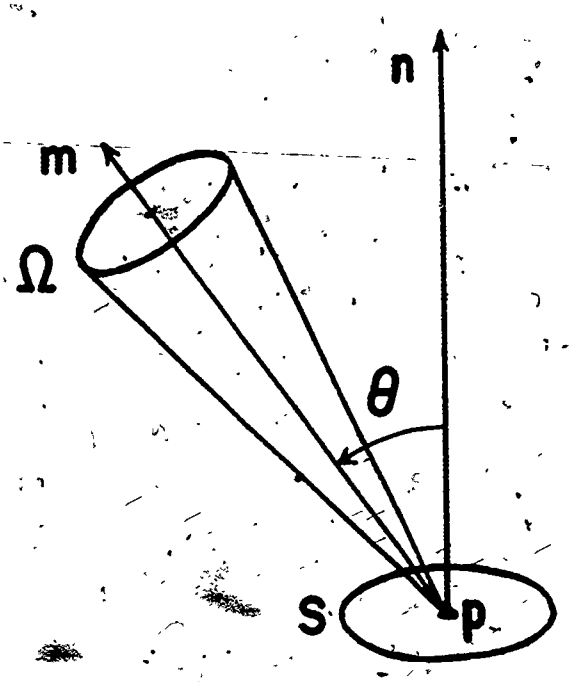


Figure C1. The Geometry for the Definition of Spectral Radiance.

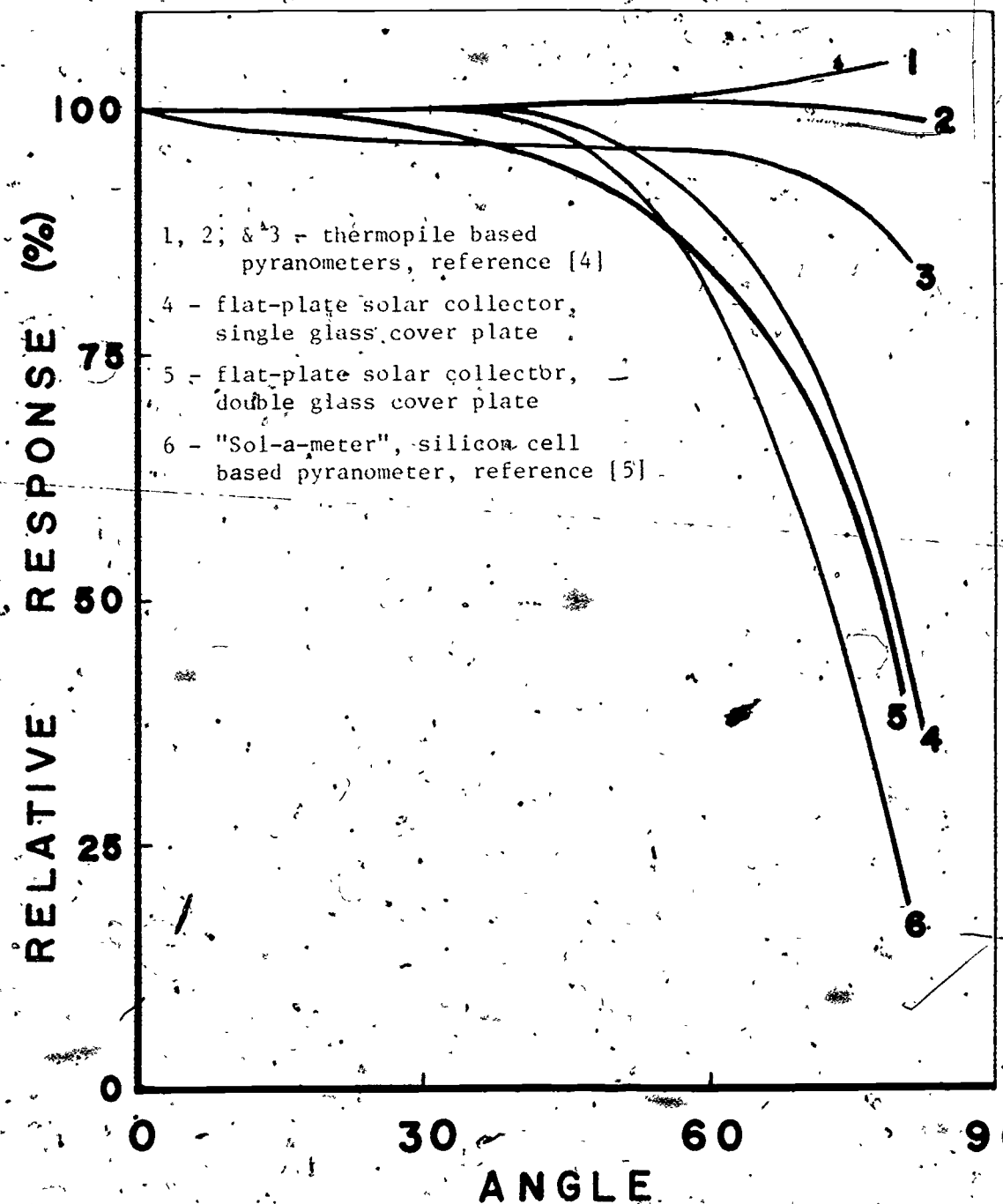


Figure C2. The Relative Directional Response of Commercially Available Pyranometers.

Upper Curve - winter solstice

Middle curve - equinoxes

Lower curve - summer solstice

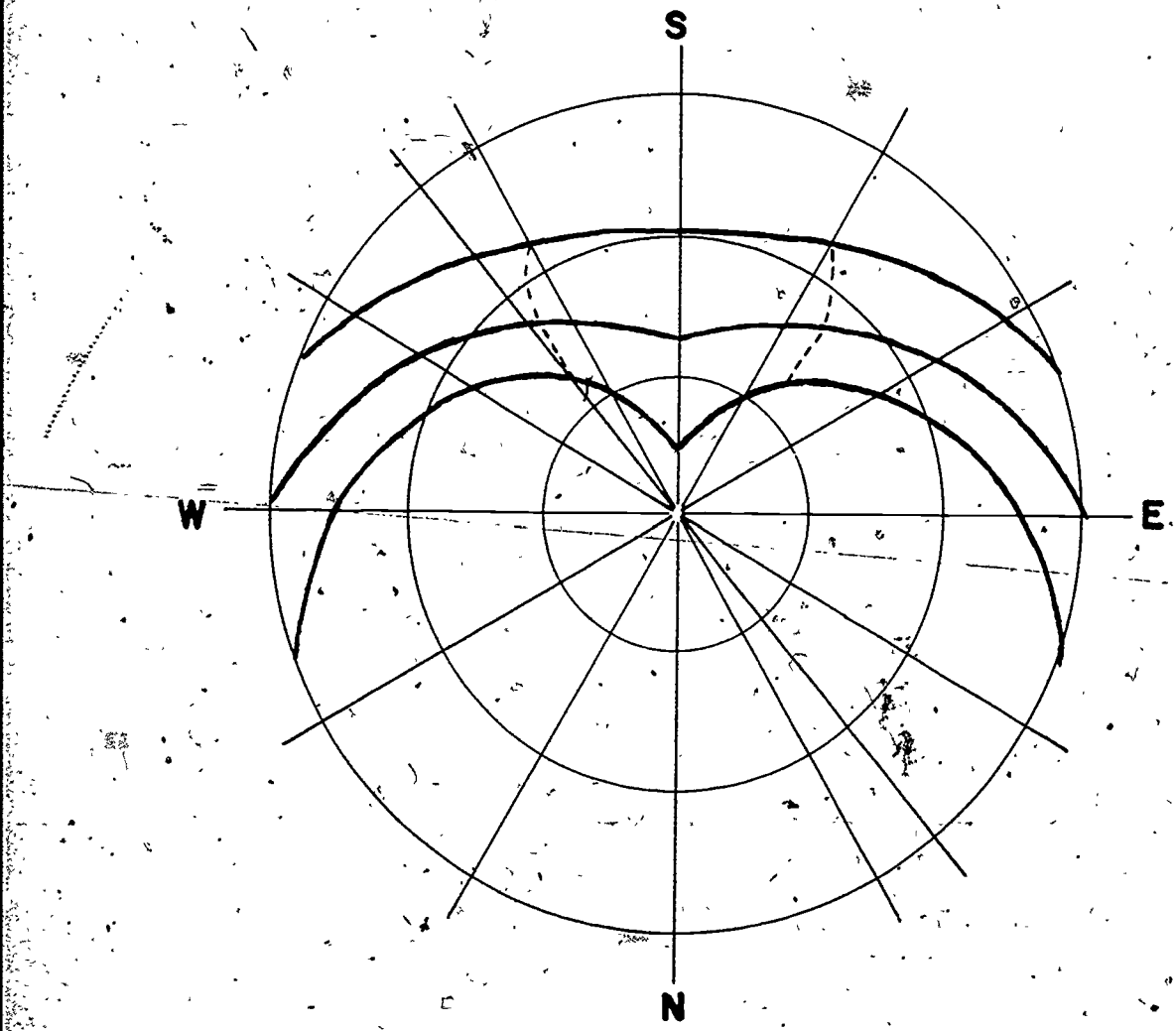


Figure C3. The Projection of the Path of the Sun through a Hemisphere Whose Polar Axis is Perpendicular to the Surface of the Earth at a Latitude of 37°.

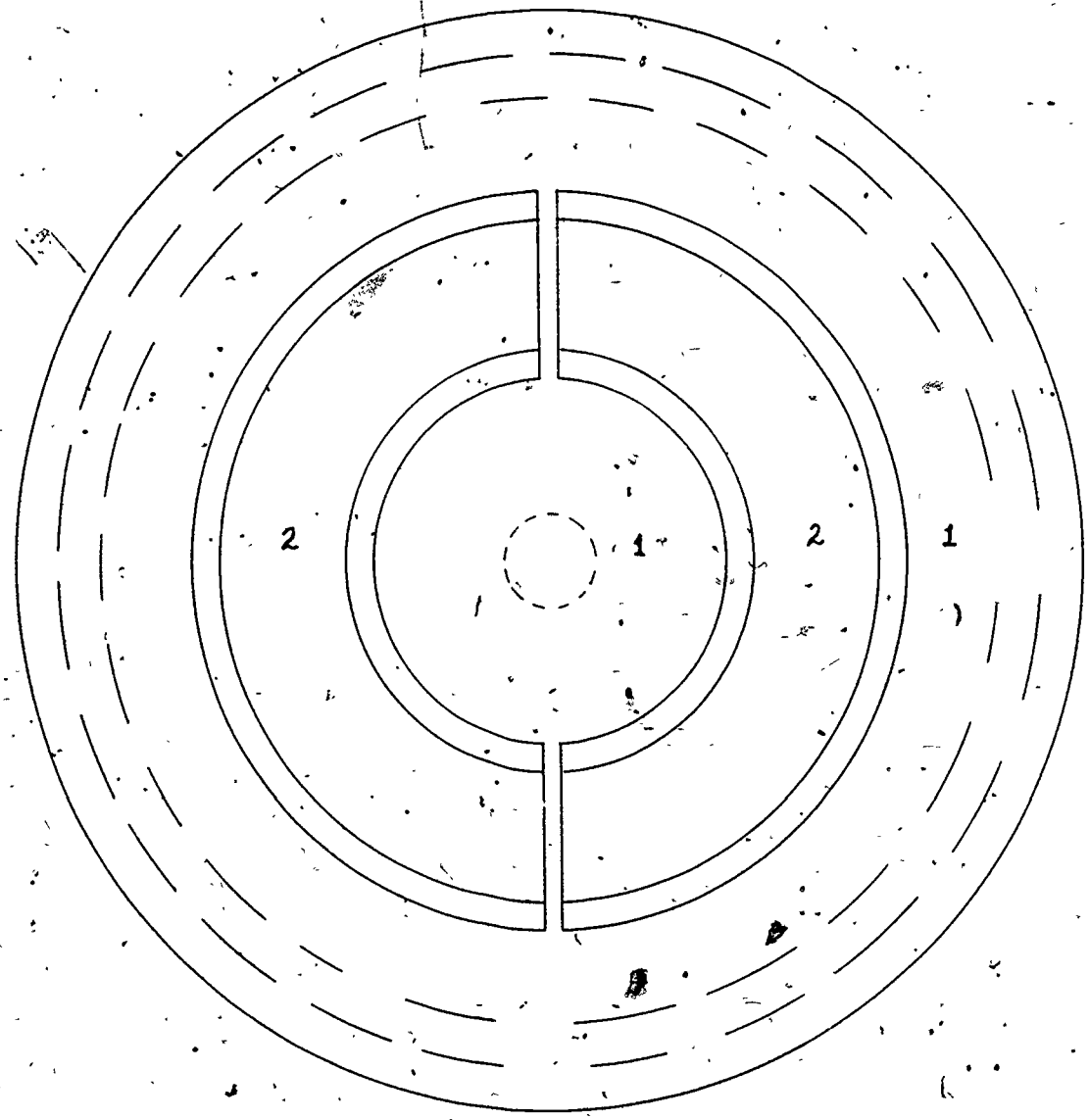


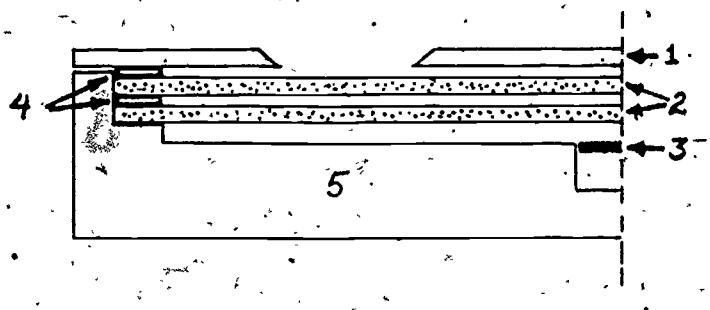


1. View limiting aperture
2. Glass windows
3. Receiver
4. Spacers
5. Case

Figure C4. Proposed Design for an Electrically Calibrated Flat-Plate Pyranometer.

9. Appendix D

Reviewers of Testing Procedures

NSF/RANN Workshop on the NBS Draft
Standards for Testing Solar Collectors and
Thermal Energy Storage Devices
Fort Collins, Colorado
August 23, 1974

Attendence List

Redfield Allen
Department of Mechanical Engineering
University of Maryland
College Park, MD 20742

J. Marx Ayres
Ayres & Hayakawa
1180 S. Beverly Drive
Los Angeles, California 90035

William L. Bailey
Motorola, Inc.
4039 E. Raymond Street
Phoenix, Arizona 85040

Chandler M. Baldwin
University of California
6532 Boelter Hall
Los Angeles, California 90024

Everett M. Barber, Jr.
School of Architecture
Yale University
New Haven, Conn. 06510

William Beverly
Boeing Aerospace Corporation
P.O. Box 3999, MS 88-06
Seattle, Washington 98124

W. Howard Card
Syracuse University
111 Link Hall
Syracuse, NY 13210

R.R. Davison
Chemical Engineering Department
Texas A & M University
College Station, Texas 77843

W. Hurlebaus
General Electric Corporation
P.O. Box 8661
Philadelphia, PA 19101

Mike Keeling
Motorola, Inc.
4039 E. Raymond Street
Phoenix, Arizona 85040

Don L. Kirkpatrick
General Electric Corporation
Energy Systems Division
RD 2, Box 447A
Glen Moore, PA 19343

Francis de Winter
2950 Thorndike Road
Pasadena, California 91107

J.A. Duffie
University of Wisconsin
1500 Johnson Drive
Madison, Wisconsin 53706

Guy Ervin, Jr.
Atomics International
8900 De Soto Avenue
Canoga Park, California 91304

Roger Gillette
Boeing Aerospace Corporation
P.O. Box 3999, MS 88-06
Seattle, Washington 98124

W.B. Harris
Chemical Engineering Department
Texas A. & M University
College Station, Texas 77843

David L. Hartmen
Dubin, Mindell, Bloome, and
Associates
42 W. 39th Street
New York, New York 10018

Harold Horowitz
National Science Foundation
1800 G Street, N.W.
Washington, D.C. 20550

John R. Howell
University of Houston
3801 Cullen Blvd.
Houston, Texas 77004

K.N. Marshall
Lockheed Research Center
3251 Hanover Street
Palo Alto, California 94304

John H. Martin
Chemical Engineering Department
Texas A & M University
College Station, Texas 77843

Robert R. Miley
National Science Foundation
1800 G Street, N.W.
Washington, D.C. 20550

John Kopecky
Honeywell, Inc.
2600 Ridgeway Road
Minneapolis, Minn. 55110

George A. Lane
Dow Chemical
Larkin Laboratory
Midland, Mi. 48640

Fikry Lansing
Syracuse University
250 Small Road
Syracuse, New York 13210

George Löf
Colorado State University
Engineering Research Center
Fort Collins, Colorado 80521

Paul O. McCormick
Lockheed Corporation
4800 Bradford
Huntsville, Alabama 35807

E.R. McLaughlin
Penn State University
101 Engineering Avenue
University Park, PA 16802

Teuvo Santala
Texas Instruments, Inc.
34 Forest Street
Attleboro, Mass 02703

Stephen L. Sargent
Department of Mechanical Engineering
University of Maryland
College Park, MD 20742

Bob Schlesinger
5108 Melvin Avenue
Tarzana, California 91356

Roger W. Schmidt
Honeywell, Inc.
2600 Ridgeway Parkway
Minneapolis, Minn. 55413

John Schnebly
Grassy Brook Village Inc.
Box 121
Townshend, Vermont 05353

W. Shannon
Lockheed Research Center
3251 Hanover Street
Palo Alto, California 94304

Dale R. Simpson
Department of Geology
Lehigh University
Bethlehem, PA 18015

G.E. Szego
Intertechnology Corporation
P.O. Box 340
Warrenton, Virginia 22186

Stanley W. Moore
Los Alamos Scientific Laboratory
P.O. Box 1663
Los Alamos, New Mexico 85744

Alwin B. Newton
136 Shelbourne Drive
York, PA 17403

Willard Oberdick
University of Michigan
1503 Ottawa
Ann Arbor, Michigan 48105

Ellis E. Pickering
Stanford Research Institute
333 Ravenswood Avenue
Menlo Park, California 94025

Jeff Rauch
Motorola, Inc.
4039 E. Raymond Street
Phoenix, Arizona 85040

Charles Rieck
Motorola, Inc.
4039 E. Raymond Street
Phoenix, Arizona 85040

D.I. Tchernev
Department of Electrical Engineering
University of Texas
Austin, Texas 78712

T.E. Unny
University of Waterloo
Waterloo, Ontario, Canada, W2L3G1

Richard Vernon
NASA Lewis Research Center
21000 Brookpark Road
Cleveland, Ohio 44135

Gary C. Vliet
Mechanical Engineering Department
University of Texas
Austin, Texas 78712

Michael Wahlig
Energy and Environmental Division
Lawrence Berkeley Laboratory
Berkeley, California 94720

John C. Ward
Solar Energy Applications
Laboratory
Colorado State University
Fort Collins, Colorado 80521

Jerome Weingart
International Institute for
Applied Systems Analysis
Laxenburg, Austria

John Yellott
Arizona State University
Tempe, Arizona 85281

NBS Consultants
for the Development of
Interim Performance Criteria for
Solar Heating and Combined
Heating/Cooling Systems and Dwellings
November-December 1974

Frank H. Bridgers,
Bridgers and Paxton Consulting Engineers, Inc.
213 Truman Street, N.E.
Albuquerque, New Mexico 87108

James C. Burke
Arthur D. Little, Inc.
Acorn Park
Cambridge, Mass. 02140

James A. Eibling
Battelle Columbus Laboratories
505 King Avenue
Columbus, Ohio 43201

Ralph J. Johnson
NAHB Research Foundation, Inc.
P.O. Box 1627
Rockville, Maryland 20850

George O.G. Löf
Solar Energy Application Laboratory
Engineering Research Center
Colorado State University
Fort Collins, Colorado 80521

Alwin B. Newton
136 Shelbourne Drive
York, PA 17403

P. Richard Rittelmann
Burt, Hill & Associates - Architects
610 Mellon Bank Building
Butler, PA 16001

George C. Szego
Intertechnology Corporation
Box 340
Warrenton, Virginia 22186

Richard A. Tybout
Department of Economics
1775 South College Avenue
Ohio State University
Columbus, Ohio 43210

John I. Yellott
John Yellott Engineering Associates
901 West El Caminito
Phoenix, Arizona 85021

NBS-114A (REV. 7-73)

| U.S. DEPT. OF COMM. BIBLIOGRAPHIC DATA SHEET | 1. PUBLICATION OR REPORT NO. NBS-TN-899 | 2. Gov't. Accession No. | 3. Recipient's Accession No. |
|---|---|---|---|
| 4. TITLE AND SUBTITLE "Development of Proposed Standards for Testing Solar Collectors and Thermal Storage Devices" | | | 5. Publication Date February 1976<br>6. Performing Organization Code |
| 7. AUTHOR(S) James E. Hill, Elmer R. Streed, George E. Kelly, Jon C. Geist, Tamami Kusuda | | | 8. Performing Organ. Report No. NBS-TN-899 |
| 9. PERFORMING ORGANIZATION NAME AND ADDRESS NATIONAL BUREAU OF STANDARDS DEPARTMENT OF COMMERCE WASHINGTON, D.C. 20234 | | | 10. Project/Task/Work Unit No.<br>11. Contract/Grant No. AG 493 |
| 12. Sponsoring Organization Name and Complete Address (Street, City, State, ZIP) Energy, Research, and Development Administration Division of Solar Energy Washington, D.C. 20545 | | | 13. Type of Report & Period Covered Interim - Calendar Year 1974<br>14. Sponsoring Agency Code |
| 15. SUPPLEMENTARY NOTES | | | |

16. ABSTRACT (*A 200-word or less factual summary of most significant information. If document includes a significant bibliography or literature survey, mention it here.*)

A study has been made at the National Bureau of Standards of the different techniques that are or could be used for testing solar collectors and thermal storage devices that are used in solar heating and cooling systems. This report reviews the various testing methods and outlines a recommended test procedure, including apparatus and instrumentation, for both components. The recommended procedures have been written in the format of a standard of the American Society of Heating, Refrigerating, and Air Conditioning Engineers and have been submitted to that organization for consideration.

17. KEY WORDS (*six to twelve entries, alphabetical order, capitalize only the first letter of the first key word unless a proper name; separated by semicolons*)

Solar collector, solar energy, solar radiation, standard, standard test, thermal performance; thermal storage.

| 18. AVAILABILITY | 19. SECURITY CLASS (THIS REPORT) | 21. NO. OF PAGES |
|---|---|---|
| [X] Unlimited<br>[ ] For Official Distribution. Do Not Release to NTIS<br>[X] Order From Sup. of Doc., U.S. Government Printing Office Washington, D.C. 20402, SD Cat. No. C13.46:899<br>[ ] Order From National Technical Information Service (NTIS) Springfield, Virginia 22151 | UNCLASSIFIED | 265 |
| | 20. SECURITY CLASS (THIS PAGE) UNCLASSIFIED | 22. Price |

USCOMM-DC 29042-P74

*U.S. GOVERNMENT PRINTING OFFICE: 1976 210-801/169 1-3

# NBS TECHNICAL PUBLICATIONS

## PERIODICALS

JOURNAL OF RESEARCH—reports National Bureau of Standards research and development in physics, mathematics, and chemistry. It is published in two sections, available separately:

• Physics and Chemistry (Section A)

Papers of interest primarily to scientists working in these fields. This section covers a broad range of physical and chemical research, with major emphasis on standards of physical measurement, fundamental constants, and properties of matter. Issued six times a year. Annual subscription: Domestic, $17.00; Foreign, $21.25.

• Mathematical Sciences (Section B)

Studies and compilations designed mainly for the mathematician and theoretical physicist. Topics in mathematical statistics, theory of experiment design, numerical analysis, theoretical physics and chemistry, logical design and programming of computers and computer systems. Short numerical tables. Issued quarterly. Annual subscription: Domestic, $9.00, Foreign, $11.25.

DIMENSIONS/NBS (formerly Technical News Bulletin)—This monthly magazine is published to inform scientists, engineers, businessmen, industry, teachers, students, and consumers of the latest advances in science and technology, with primary emphasis on the work at NBS. The magazine highlights and reviews such issues as energy research, fire protection, building technology, metric conversion, pollution abatement, health and safety, and consumer product performance. In addition, it reports the results of Bureau programs in measurement standards and techniques, properties of matter and materials, engineering standards and services, instrumentation, and automatic data processing.

Annual subscription: Domestic, $9.45; Foreign, $11.85.

## NONPERIODICALS

Monographs—Major contributions to the technical literature on various subjects related to the Bureau's scientific and technical activities.

Handbooks—Recommended codes of engineering and industrial practice (including safety codes) developed in cooperation with interested industries, professional organizations, and regulatory bodies.

Special Publications—Include proceedings of conferences sponsored by NBS, NBS annual reports, and other special publications appropriate to this grouping such as wall charts, pocket cards, and bibliographies.

Applied Mathematics Series—Mathematical tables, manuals, and studies of special interest to physicists, engineers, chemists, biologists, mathematicians, computer programmers, and others engaged in scientific and technical work.

National Standard Reference Data Series—Provides quantitative data on the physical and chemical properties of materials, compiled from the world's literature and critically evaluated. Developed under a world-wide program coordinated by NBS. Program under authority of National Standard Data Act (Public Law 90-396).

NOTE. At present the principal publication outlet for these data is the Journal of Physical and Chemical Reference Data (JPCRD) published quarterly for NBS by the American Chemical Society (ACS) and the American Institute of Physics (AIP). Subscriptions, reprints, and supplements available from ACS, 1155 Sixteenth St. N. W., Wash. D. C. 20056.

Building Science Series—Disseminates technical information developed at the Bureau on building materials, components, systems, and whole structures. The series presents research results, test methods, and performance criteria related to the structural and environmental functions and the durability and safety characteristics of building elements and systems.

Technical Notes—Studies or reports which are complete in themselves but restrictive in their treatment of a subject. Analogous to monographs but not so comprehensive in scope or definitive in treatment of the subject area. Often serve as a vehicle for final reports of work performed at NBS under the sponsorship of other government agencies.

Voluntary Product Standards—Developed under procedures published by the Department of Commerce in Part 10, Title 15, of the Code of Federal Regulations. The purpose of the standards is to establish nationally recognized requirements for products, and to provide all concerned interests with a basis for common understanding of the characteristics of the products. NBS administers this program as a supplement to the activities of the private sector standardizing organizations.

Federal Information Processing Standards Publications (FIPS PUBS)—Publications in this series collectively constitute the Federal Information Processing Standards Register. Register serves as the official source of information in the Federal Government regarding standards issued by NBS pursuant to the Federal Property and Administrative Services Act of 1949 as amended, Public Law 89-306 (79 Stat. 1127), and as implemented by Executive Order 11717 (38 FR 12315, dated May 11, 1973) and Part 6 of Title 15 CFR (Code of Federal Regulations).

Consumer Information Series—Practical information, based on NBS research and experience, covering areas of interest to the consumer. Easily understandable language and illustrations provide useful background knowledge for shopping in today's technological marketplace.

NBS Interagency Reports (NBSIR)—A special series of interim or final reports on work performed by NBS for outside sponsors (both government and non-government). In general, initial distribution is handled by the sponsor; public distribution is by the National Technical Information Service (Springfield, Va. 22161) in paper copy or microfiche form.

Order NBS publications (except NBSIR's and Bibliographic Subscription Services) from Superintendent of Documents, Government Printing Office, Washington, D.C. 20402.

## BIBLIOGRAPHIC SUBSCRIPTION SERVICES

The following current-awareness and literature-survey bibliographies are issued periodically by the Bureau:

Cryogenic Data Center Current Awareness Service. A literature survey issued biweekly. Annual subscription: Domestic, $20.00; foreign, $25.00.

Liquefied Natural Gas. A literature survey issued quarterly. Annual subscription: $20.00.

Superconducting Devices and Materials. A literature survey issued quarterly. Annual subscription. $20.00. Send subscription orders and remittances for the preceding bibliographic services to National Bureau of Standards, Cryogenic Data Center (275.02) Boulder, Colorado 80302.

Electromagnetic Metrology Current Awareness Service. Issued monthly. Annual subscription: $24.00. Send subscription order and remittance to Electromagnetics Division, National Bureau of Standards, Boulder, Colo. 80302.